MRI investigations into the pilocarpine model of status epilepticus

ManKin Choy

Thesis submitted for the Degree of Doctor in Philosophy

November 2007

Royal College of Surgeons Unit of Biophysics
& Neurosciences Unit
UCL-Institute of Child Health
University of London

ProQuest LLC
789 East Eisenhower Parkway
P.O. Box 1346
Ann Arbor, MI 48106-1346

DECLARATION

I, ManKin Choy, confirm that the work presented in this thesis is my own. Where information has been derived from other sources, I confirm that this has been indicated in the thesis. The work presented in chapter 7 was in collaboration with Dr. Nick Greene and colleagues at the Neural Development Unit, UCL-Institute of Child Health. The 2-DE, western blot and mass spectrometry experiments were conducted by Dr. Greene and colleagues. All other experiments were conducted by me.

ABSTRACT

Status epilepticus (SE) is a medical neurological emergency and may cause brain injury associated with epilepsy and cognitive decline. Evidence suggests that the hippocampus is particularly vulnerable to injury from SE and that the resulting hippocampal injury has been hypothesised to continue to evolve on to mesial temporal sclerosis associated temporal lobe epilepsy (MTS-TLE). This form of epilepsy is particularly difficult to treat with current medical therapies, and thus it is the most common epilepsy that requires surgical intervention. Therefore understanding the relationships between SE, hippocampal injury and MTS-TLE may provide the basis for development of novel therapies for treating post-SE injury.

Clinical magnetic resonance imaging (MRI) studies have indicated that the hippocampus is injured following SE, but whether this injury will progress on to MTS-TLE remains unclear. To facilitate research, experimental models have been developed for investigating SE and its sequelae. Therefore, this study used the pilocarpine rat model for investigating SE and its related injury with multi-parametric MRI.

The first part of this work investigated post-SE pathology with MRI and results indicate a characteristic injury profile for various brain regions injured by SE. Analysis of the hippocampus indicated a peak response 2 days following the insult showed a striking relationship to the degree of later injury, suggesting that imaging during the early period may predict later outcome. To investigate this response further, a combination of MRI and proteomic analysis was used and protein changes were identified. The second part of this study consisted of developing a method for imaging the onset and evolution of SE, and results suggest that limited perfusion may contribute to the hippocampal vulnerability to prolonged seizures.

This work has identified an early MRI biomarker of later injury, and possible protein substrates for interventional therapy. Furthermore, evidence for the selective vulnerability to SE was found.

TABLE OF CONTENTS

INDEX OF ILLUSTRATIONS

Chapter 1

Chapter 2

Chapter 4

Chapter 5

Chapter 6

Chapter 7

Chapter 8

Publications arising from this thesis

Greene NDE, Bamidele A, Choy M, de Castro SCP, Wait R, Leung K-Y, Begum S, Gadian DG, Scott RC, Lythgoe MF (2007). Proteome changes associated with hippocampal MRI abnormalities in the lithium pilocarpine-induced model of convulsive status epilepticus, *Proteomics*, 7(8):1336-44.

Published abstracts

Choy M, Lythgoe MF, Thomas DL, Gadian DG, Scott RC (2007). MRI characteristics of status epilepticus-induced early hippocampal injury and the association with subsequent brain injury in the lithium-pilocarpine rat model, *61st American Epilepsy Society (AES) annual meeting*, Philadelphia, USA

Choy M, , Scott RC, Thomas DL, Gadian DG, Greene NDE, Wait R, Leung K-Y, Lythgoe MF (2007). MR measurements of diffusion, perfusion and T_2 with proteomic analysis in the rat hippocampus following status epilepticus, *British Neuroscience Association*, Harrogate, UK

Choy M, Scott RC, Thomas DL, Gadian DG, Greene NDE, Lythgoe MF (2007). MR measurements of diffusion, perfusion and T2 with proteomic analysis in the hippocampus following status epilepticus in the rat lithium-pilocarpine model, *15th International society of magnetic resonance in medicine (ISMRM) annual meeting*, Berlin, Germany

Choy M, Lythgoe MF, Thomas DL, Gadian DG, Scott RC (2007). MR measurements of diffusion, perfusion and T_2 in the hippocampus following status epilepticus in the lithium-pilocarpine model, *British Paediatric Neurological Association*, Edinburgh, UK platform presentation

Choy M, , Scott RC, Thomas DL, Gadian DG, Greene NDE, Wait R, Leung K-Y, Lythgoe MF (2007). MR measurements of diffusion, perfusion and T_2 with proteomic analysis in the rat hippocampus following status epilepticus, *16th NMR Symposium*, Oxford, UK platform presentation

Choy M, Greene NDE, Scott RC, Bamidele A, Thomas DL, Wait R, Begum S, Leung K-Y, Gadian DG, Lythgoe MF (2006). Investigation of acute hippocampal injury following status epilepticus using MRI and proteome analysis, *15th NMR Symposium*, Cambridge, UK platform presentation

Choy M, Lythgoe MF, Greene NDE, Bamidele A, Thomas DL, Wait R, Begum S, Leung K-Y, Gadian DG, Scott RC (2006). Investigation of acute hippocampal injury following status epilepticus using MRI and proteome analysis, *7th European Congress on Epileptology*, Helsinki, Finland platform presentation

Choy M, Lythgoe MF, Greene NDE, Bamidele A, Thomas DL, Wait R, Begum S, Leung K-Y, Gadian DG, Scott RC (2006). Investigation of acute hippocampal injury following status epilepticus using MRI and proteome analysis, *British Chapter of ISMRM*, Surrey, UK platform presentation

Choy M, Lythgoe MF, Greene NDE, Bamidele A, Thomas DL, Wait R, Begum S, Leung K-Y, Gadian DG, Scott RC (2006). Investigation of acute hippocampal injury following status epilepticus using MRI and proteome analysis, *ILAE UK Chapter*, Newcastle, UK platform presentation

Choy M, Scott RC, Thomas DL, Gadian DG, Lythgoe MF (2005). Longitudinal MRI measurements of T_2 and CBF in the lithium- pilocarpine model of status epilepticus, *British Chapter of ISMRM*, Oxford, UK. platform presentation

Choy M, Lythgoe MF, Thomas DL, Gadian DG, Scott RC (2005). Magnetic resonance characteristics of the evolution of brain injury following status epilepticus in the lithium-pilocarpine rat model, *59th AES annual meeting*, Washington DC, USA.

ABBREVIATIONS

2-DE.....two-dimensional gel electrophoresis

ADC.....apparent diffusion coefficient

AMPA.....α-amino-3-hydroxy-5-methyllisoxazole-4-propionate

ANOVA..... analysis of variance

ASL.....arterial spin labelling

ATP.....adenosine triphosphate

BBB.....blood brain barrier

BOLD.....blood oxygenation level dependent

Ca.....calcium

CA.....cornu amonis

CASL.....continuous arterial spin labelling

CBF.....cerebral blood flow

CLP.....control imaging lithium-pilocarpine

CLS.....control imaging lithium-saline

CNS.....central nervous system

COX.....cyclooxygenase

CSF.....cerebral spinal fluid

DWI.....diffusion-weighted imaging

DNA.....deoxyribonucleic acid

DRP-2.....dihydropyrimidinase related protein-2

ECG.....electrocardiogram

EDHF.....endothelium-derived hyperpolarizing factor

EEG.....electroencephalogram

EPI.....echo-planar imaging

FLP.....full lithium-pilocarpine

FLS.....full lithium-saline

GABA.....γ-aminobutyric acid

HSP27.....heat shock protein 27

Il-1.....interleukin-1

KA.....kainic acid

LC MS/MS.....liquid chromatography coupled to tandem electrospray mass spectrometry

MASAGE-IEPI.....multiple acquisition of spin and gradient echoes using interleaved EPI

MRI.....magnetic resonance imaging

MTS.....mesial temporal sclerosis

NMDA.....N-methyl-D-aspartate

NMR.....nuclear magnetic resonance

NO.....nitric oxide

NOS.....nitric oxide synthase

PFA.....paraformaldehyde

PGI_2.....prostacyclin

PN.....post natal

PWI.....perfusion-weighted imaging

RF.....radio frequency

ROI.....region of interest

ROS.....reactive oxygen species

SE.....status epilepticus

s.e.m.....standard error of the mean

SRS.....spontaneous recurrent seizures

SDS-PAGE.....sodium dodecyl sulfate polyacrylamide gel electrophoresis

TD.....delay time

TE.....echo time

TI.....inversion time

TLE.....temporal lobe epilepsy

TNF.....tumour necrosis factor

TR.....repetition time

ACKNOWLEDGEMENTS

I would like to thank my PhD supervisors, Rod Scott and Mark Lythgoe, and also David Gadian, who has been a supervisor in all but name, for their continual support and invaluable advice throughout the course of my studies. A special mention goes to Rod, who has been my personal encyclopaedia for all things epilepsy, for always having the time and patience for my relentless questioning, and for listening to my whimsical and meandering theories. His encouragement, drive and enthusiasm for science have been an inspiration to me. Rod, Mark and David have all made this an unforgettable and truly educational experience that I will forever look back with fondness and gratitude.

I owe thanks to everyone in the department of Biophysics for their kindness and understanding that has made my PhD a hugely enjoyable experience. In particular, Martin King, without whom I would not have been able to complete this project, for being an absolute hero; Ted Proctor, for his advice and contagious passion for science; Sally Dowsett, for her invaluable help; and Romina Aron-Badin, for knowing an intimidating number of languages and her sense of humour. Also Kate Riney, Ken Cheung, Rachael Dobson, Jack Wells, Panos Kyrtatos and Jon Cleary for being great company and for listening to my thoughts on epilepsy as well as anything else that happen to pop into my head. I am also grateful to Dave Thomas, John Thornton, Louise van der Weerd, Dan Cuthill, Nick Greene, Gena Raivich, and Matthew Walker for their help and advice during the course of my studies.

I would also like to thank my family and friends who have encouraged and supported me throughout this challenging and rewarding chapter of my life. For being an example of stoicism, character and dignity, and for teaching me to never give up on my dreams; this work is dedicated to the memory of my nan.

THE VALUE OF HAVING FOR A TIME RIGOROUSLY PURSUED A RIGOROUS SCIENCE DOES NOT REST ESPECIALLY IN ITS RESULTS: FOR IN RELATION TO THE SEA OF WORTHY KNOWLEDGE, THESE WILL BE BUT A NEGLIGIBLE LITTLE DROP. BUT IT BRINGS FORTH AN INCREASE OF ENERGY, OF DEDUCTIVE ABILITY, OF PERSISTENCE; ONE HAS LEARNED TO GAIN ONE'S PURPOSE PURPOSEFULLY. TO THIS EXTENT, IN RESPECT TO ALL ONE DOES LATER, IT IS VERY VALUABLE TO HAVE ONCE BEEN A SCIENTIFIC MAN

FRIEDRICH NIETZSCHE

THESIS OUTLINE

This project focuses on the use of MRI to investigate the hypothesis that status epilepticus can cause hippocampal injury that evolves into mesial temporal sclerosis associated temporal lobe epilepsy in the pilocarpine rat model.

Chapters 1 to 4 provide the background information for the MRI investigations into this hypothesis. In chapter 1, a brief history of the evolution of ideas that underlie SE is described, also SE is contextualised from the perspective of a clinical problem, and a discussion as to how the hypothesis developed from clinical observations. Chapter 2 describes the basic theories and physiological mechanisms that are thought to underlie SE, brain injury and epileptogenesis, and discusses some of their proposed roles in brain injury and the epileptogenic process. Chapter 3 details the use of animal models in epilepsy and describes their relevance to epilepsy research, with a particular focus on the status epilepticus models. In addition, the rationale for using the pilocarpine model for this project is presented. Chapter 4 provides an introduction to the basic concepts that underlie MR imaging, including diffusion and perfusion, as well as a review of experimental MRI studies on SE, brain injury and epileptogenesis.

The fifth chapter details the methodological developments that were necessary for conducting the subsequent MRI studies and begins with establishing the pilocarpine model at the department. Chapter 6 presents MRI investigations on post-SE pathology. The work in chapter 7 is derived from chapter 6 and examines the molecular alterations that parallel the multi-parametric MRI changes reported in chapter 6. Chapter 8 describes the findings from the MRI investigations during SE.

Finally, chapter 9 contains a general discussion of the implications of the work and outlines future avenues of research that have emerged from this project.

CHAPTER 1: A HISTORICAL AND CLINICAL PERSPECTIVE OF STATUS EPILEPTICUS

True science is the imitation of nature in concepts

Friedrich Nietzsche

1.1. A HISTORY OF STATUS EPILEPTICUS

Status epilepticus (SE) and epilepsy are both terms derived from the Greek word "epilamvanein", which means "to take hold of" or "to attack" (Gross, 1992), and reflects the very nature of these conditions. Thus, it is of no great surprise that the study of SE has been invariably intertwined with the study of epilepsy. It is now clear that SE has its own pathology distinct from seizures and may even lead on to epilepsy. Seizures have always generated much curiosity and the journey to our current state of knowledge can be traced back to the earliest beginnings of recorded human history.

An epileptic seizure can be a visually striking phenomenon. As such, it is not surprising that widespread accounts of epilepsy can be found throughout human history, and that epilepsy has often been attributed to the work of the supernatural. This was certainly recognised by Hippocrates in his ironically entitled work on epilepsy "On the sacred disease". In this work, he dismissed the supernatural origins of epilepsy, but the term "sacred disease" reflects much of what many cultures ascribe to its causes. This association with the supernatural has meant that sufferers have been often stigmatised because they were considered to be unclean or evil (Gross, 1992). An example of attributing mystical causes to epileptic seizures can be found in one of the earliest known medical references to epilepsy, the Sakkiku cuneiform.

The Sakkiku cuneiform is a Babylonian medical text which dates from around 718-612 BC and within this ancient tome is an entire section devoted to epilepsy (Wilson and Reynolds, 1990). This text details many different forms of epileptic seizures and attributes their causes to the actions of ghosts and demons. Intriguingly the Sakkiku cuneiform also contains the first known description of status epilepticus:

> "If the possessing demon possesses him many times during the middle of the night, and at the time of his possession his hands and feet are cold, he is much darkened, keeps opening and shutting his mouth, is brown and yellow as to the eyes and... It may go on for some time, but he will die"

Even though epilepsy has inspired a lot of interest through the ages, none more so than the classical works by Hippocrates in 500 BC and Galen in the second century, descriptions of conditions resembling SE have been surprisingly few (Shorvon, 1994).

The first step that marked the separation of the study of SE from that of epileptic seizures was taken in the 19th Century, when the term "*État de mal épileptique*" first appeared in Louis Calmeil's university dissertation (1824), a term coined by the patients he was working with at the Salpêtrière hospital. However, it was only in 1868 that the more familiar latinised English expression, *status epilepticus*, was first introduced in Bazires' translation of Trousseau's lectures on clinical medicine.

Early research into SE proceeded primarily by clinical observation and histological evaluation, and seminal studies include work by Trousseau and Bourneville. In 1903 Clark and Prout provided the first systematic analysis of the clinical and pathological features of SE. In this paper, they described SE as the "the maximum expression of epilepsy", although it is worth noting that their definition of SE incorporated only the generalised convulsive form.

The year 1924 marked the discovery of the electroencephalogram by Berger and this signalled a revolution in epilepsy and SE research. This discovery meant that it was now possible to probe the electrophysiological basis of seizures.

In 1962, at the tenth European conference on epileptology and clinical neurophysiology in Marseilles, the first systematic classification of SE was formulated. This was the first meeting to be entirely devoted to the study of SE and, based on clinical and electrophysiological data, the definition of SE was extended from the generalised convulsive variety to incorporate all types of seizures. From this meeting the term SE was used to define "a seizure [that] persists for a sufficient length of time or is repeated frequently enough to produce a fixed or enduring epileptic condition" and this definition remains widely used today (Shorvon, 1994).

1.2. DEFINITIONS OF STATUS EPILEPTICUS

The 1962 definition of status epilepticus by Gastaut and colleagues remains widely accepted and has been updated by the global authority on epilepsy research: the International League Against Epilepsy (ILAE). The current ILAE definition of status epilepticus is:

> 'A seizure which shows no clinical signs of arresting after a duration encompassing the great majority of seizures of that type in most patients or recurrent seizures without resumption of baseline central nervous system function interictally'

Although this definition captures the prolonged and/or iterative nature of SE and also implies that it can occur in different types of seizures, the question of duration is not addressed. This is because the definition of SE will depend on the specific context that it is used in.

There are at least two definitions for the threshold between seizure and SE. If the purpose of the definition was to investigate the effect of SE, such as for epidemiological studies investigating the morbidity or mortality following SE, then the 30 minutes threshold first proposed by Gastaut is the appropriate definition for SE. This was in light of evidence that demonstrated neuropathological changes after a 30 min seizure but not in shorter seizures (see chapter 2) (Meldrum and Brierley, 1973; Klitgaard *et al.*, 2002).

The second definition is in the emergency treatment of patients. If a patient has a seizure that is likely to continue then it would be unethical to wait for SE to be established before beginning therapy, as injury is associated with prolonged seizure activity. In a paper on a new classification of SE, Rona and colleagues have proposed a threshold of 10 minutes (Rona *et al.*, 2005). This threshold was proposed in the light of a number of studies which indicate that self-limiting seizures rarely last longer than a few minutes, and the seizures that do last longer tend to continue for more than 30 minutes (Theodore *et al.*, 1994; Rona *et al.*, 2005). This is further underlined in studies that have demonstrated an associated

time-dependent development of pharmacoresistance to first line anti-convulsant drugs such as diazepam (Lowenstein, 1999).

For the purposes of this thesis, SE is defined as 90 minutes of continuous seizure activity, as earlier studies have demonstrateed that this duration was associated with all animals progressing on to epilepsy (Cavalheiro *et al.*, 2006), and in the tradition of Clark and Prout, will be restricted to the generalised convulsive variety.

1.3. THE EPIDEMIOLOGY OF STATUS EPILEPTICUS

The epidemiology of status epilepticus has been reviewed systematically by Chin and colleagues (Chin *et al.*, 2004). Their review has incorporated data from various population-based studies that included key studies based from Richmond, Virginia and Rochester, Minnesota (Delorenzo *et al.*, 1996; Hesdorffer *et al.*, 1998; Chin *et al.*, 2004) and this section is based primarily on their review.

1.3.1. Incidence of status epilepticus

The incidence of SE has been measured at 6.8 – 41 per 100,000 individuals per year, varying across different age-groups. The cases of SE followed a bimodal distribution with peak frequencies occurring in children under the age of 1 and in patients over the age of 60. Overall, patients with a history of epilepsy accounted for less than 50%, with 16-38% of children and 42-59% of adults having a history of epilepsy. This is a key point as SE has been hypothesised to be one of the causes of epilepsy, which is the focus of this thesis.

1.3.2. Aetiologies of status epilepticus

The aetiologies of SE include cerebrovascular accidents, fever, hypoxia, alcohol-related, metabolic disorders and withdrawal or low levels of anti-epileptic drugs (Delorenzo *et al.*,

1996). However, there is an age effect in that the main causes of SE in adults were cerebrovascular accidents, and withdrawal or low levels of anti-epileptic drugs which accounts for 34% of the cases (Chin *et al.*, 2004). In children, on the other hand, fever was the predominant factor (33-35%) and also low levels of anti-epileptic drug (21%) (Chin *et al.*, 2004).

1.3.3. Mortality associated with status epilepticus

A number of studies have concluded that age and aetiology are the main determining factors of mortality associated with SE (Delorenzo *et al.*, 1996; Hesdorffer *et al.*, 1998; Chin *et al.*, 2004). Deaths across all age groups were between 7.6-22% within 30 days of an episode of SE and 43% within ten years. In children, the group with the highest incidence of SE, mortality was 2-9% in the first 30 days and 7% within the first ten years compared to 22-38% in the acute period and 82% in the longer term for the elderly. However, the highest mortality in the first 30 days was observed in children under the age of 1 (17-18%) and this finding may be due more to the mortality associated with the underlying cause of SE rather than SE itself. This is perhaps emphasised in that no deaths in the short-term occurred in children who had had an episode of fever-induced SE.

1.3.4. Morbidity associated with status epilepticus

SE has been associated with neurological, cognitive, and behavioural impairments. For example, case studies of severe impairment in anterograde memory have been reported following SE (Cendes *et al.*, 1995). Also, other impairments include speech deficits in children following SE, and a low intelligence quotient associated with patients that have a history of SE (Raspall-Chaure *et al.*, 2006). However, clinical evidence for these impairments as a direct result of SE remains unclear because of the difficulties that arise in dissociating the effect of SE from its underlying cause. As such, aetiology, along with seizure duration, has been shown to be the major determining factors for outcome (Raspall-Chaure *et al.*, 2006). Nevertheless, clinical observations have led to a hypothesis that proposes that one particular outcome of SE is the subsequent development of mesial

temporal sclerosis associated with temporal lobe epilepsy, evidence for which is discussed in the next section (Cavanagh and Meyer, 1956; Scott *et al.*, 2003).

1.4. THE RELATIONSHIPS BETWEEN STATUS EPILEPTICUS, HIPPOCAMPAL INJURY AND MESIAL TEMPORAL SCLEROSIS ASSOCIATED WITH TEMPORAL LOBE EPILEPSY

The relationship between SE and the subsequent development of TLE was first proposed by Cavanagh and Meyer in their seminal paper on MTS associated with TLE (Cavanagh and Meyer, 1956). They described a histological study on the resected tissue of patients who had undergone surgical treatment for TLE, and intriguingly, they noted a striking association with an earlier episode of SE in their medical history:

"Closer examination [of the temporal lobe specimens] shows that [Ammon's horn sclerosis] is due to the remarkably high incidence of status epilepticus at or preceding the onset of the epileptic history"

As a result of this observation, the hypothesis was born that SE can cause hippocampal injury that in turn leads on to the development of MTS associated with TLE. In order to test this hypothesis, a series of questions needs to be addressed. Does MTS play a role in TLE? Can SE cause hippocampal injury? And if SE can cause hippocampal injury then can this injury evolve into MTS and TLE?

1.4.1. The role of mesial temporal sclerosis in temporal lobe epilepsy

MTS is the most common pathology associated with TLE, and it is characterised by selective cell loss in the CA1 and CA3 subfields of the hippocampus (fig. 1.1) (Engel, Jr., 1996; Sloviter, 2005). This form of the disease is one of the most resistant to current medical therapies and therefore it is the most common type of epilepsy that requires surgery (Sloviter, 2005). The effectiveness of this surgery suggests that the MTS plays a key

role in TLE, and observations of abnormal electrical activity in these patients further support this hypothesis that MTS plays a central role in seizure generation (Sloviter, 2005).

Figure 1.1. *Human mesial temporal sclerosis compared to normal hippocampus. (**A**) Autopsy control specimen showing normal human hippocampus. (**B**) Mesial temporal sclerosis in a surgical specimen. Note extensive neuron loss in the dentate hilus (h) and in areas CA3 and CA1, and survival of CA2 and subicular (sub) neurons. Sg denotes straight gyrus. Stained with 1% cresyl violet and magnifications at 8×. (adapted from Sloviter 2005).*

1.4.2. Status epilepticus and hippocampal injury

The causal link between SE and hippocampal injury has a long pedigree and dates back to the studies by Bourneville (1876) and Pfleger (1880) (Shorvon, 1994). Since then, post mortem studies of patients who die due either to SE or to an underlying cause have repeatedly shown that the hippocampus is damaged (DeGiorgio *et al.*, 1992). However, the question still remained as to whether a non-fatal episode of SE can cause hippocampal injury. The advent of imaging modalities such as magnetic resonance imaging (MRI) can provide an answer to this question by providing the means to investigate the hippocampus following SE *in vivo*.

The first MRI study that provided evidence for this process was conducted by vanLandingham and colleagues. T_2-weighted scans were performed on children shortly after prolonged febrile convulsions (PFCs), the most common form of SE seen in children, and revealed hyperintensities in the hippocampus, which is indicative of acute oedema (VanLandingham *et al.*, 1998).

In another study, Scott and colleagues also imaged patients after PFCs and identified enlarged hippocampal volumes and elevated T_2 relaxation times in patients imaged within 2 days but these changes were not detected in the patients imaged between 2 and 5 days. Taken together, these results suggest that oedema formation occurs in the hippocampus shortly after PFC (Scott *et al.*, 2002).

1.4.3. The relationship between SE-induced hippocampal injury and mesial temporal sclerosis

It is clear that SE can induce acute hippocampal injury but whether this injury will evolve into MTS still needs to be clarified. Scott and colleagues attempted to explore this further with a follow up study (Scott *et al.*, 2003). The patients imaged shortly after PFC were scanned again around 4-8 months after PFC. They reported that hippocampal volumes and T_2 relaxation times were no different from those of controls at the later time point and suggest that the oedema has resolved by the later time point. Although these patients did not meet the criteria for MTS on MRI, it was suggested that the injury may still be evolving at this still relatively early time and, in fact, may eventually progress onto MTS. An additional finding was that there were increasing hippocampal asymmetries in the follow-up scan, but the underlying basis for these asymmetries is not clear because PFC induce hippocampal changes that are bilateral in nature (Scott *et al.*, 2003).

One possible reason for the hippocampal asymmetries is that PFC causes injury to both hippocampi but one is selectively more vulnerable to damage or one is more resistant. Alternatively, these children may have had pre-existing abnormalities prior to the occurrence of PFC. A combination of both explanations is also plausible, that is the patients have a pre-existing unilateral hippocampal abnormality that is either more susceptible or less vulnerable to PFC damage (Scott *et al.*, 2003). Whatever the reason, most patients present with unilateral MTS and it is clear that longer term studies will help to clarify whether children following PFCs will eventually develop MTS.

So far, there have been a few case reports that have suggested that this SE-induced injury will eventually develop into MTS. These include a case study by Nohria and colleagues on a

young child who presented with SE. They imaged this patient with MRI and observed hippocampal abnormalities shortly after SE. The child later developed mesial temporal sclerosis with temporal lobe epilepsy, and subsequently required epilepsy surgery (Nohria *et al.*, 1994). Also, there was an interesting case reported by Cendes and colleagues in which a patient was poisoned by the excitotoxic glutamate analogue, domoic acid, and later developed bilateral hippocampal sclerosis with temporal lobe epilepsy (Cendes *et al.*, 1995) (for more detail please refer to section 3.3.).

A systematic characterisation of this process, from SE through to the development of TLE is still required. For such a characterisation, the serial imaging as well as obtaining samples for histological analysis precludes such a study in humans, but this can be done in animal models. Another advantage of using animal models is that a relatively homogenous population can be investigated, and, considering these advantages together, it may be possible to identify molecular substrates that could be important for the development of therapies for treating brain injury and also preventing the development of medically intractable temporal lobe epilepsy.

1.5. SUMMARY

The visual impact of epileptic seizures has ensured that epilepsy has generated scholarly interest since the earliest days of recorded human history. However, it was not until comparatively recently that status epilepticus, the most extreme form of seizures, was considered to warrant a distinct entity for study. Since then, SE has been suggested to cause brain injury that may be associated with cognitive decline. Moreover evidence is also mounting which suggests that this injury may evolve into medically intractable epilepsy.

Although the clinical data remain inconclusive with respect to SE due to the dependency on aetiology, animal models have so far provided the most compelling evidence for the progression from SE-induced brain injury on to MTS-TLE. Thus understanding the nature of this progression may provide the basis for developing diagnostic and therapeutic strategies for injury and epilepsy.

CHAPTER 2: THE PHYSIOLOGY OF STATUS EPILEPTICUS, BRAIN INJURY AND EPILEPTOGENESIS

It is a mistake to try to look too far ahead. The chain of destiny can only be grasped one link at a time

Winston Churchill

2.1. INTRODUCTION

Seizures can be described as cell-signalling dysfunction within the CNS leading to mass synchronous firing, and status epilepticus is an unremitting form of this condition. Although controversy remains as to whether short seizures cause brain injury, there is overwhelming evidence that supports the damaging effect of prolonged seizures. This injury caused by SE is associated with cognitive decline and has been hypothesised to lead on to the development of medically intractable MTS-TLE. The relationships between SE, brain injury and TLE in humans remain contentious but work on animal models support this hypothesis. From this work, many physiological mechanisms have been identified and have been suggested to underlie the transition from the normal state to seizure and SE, as well as injury through to the development of TLE. This chapter will review some of these physiological mechanisms in this particular context.

2.1. STATUS EPILEPTICUS AND SEIZURES

2.1.1. Seizure initiation, propagation and termination

Initiation, propagation and termination are three distinct stages of seizures. The initiation stage is characterised by the transition from neuronal activity that is sparse, asynchronous, and local to activity that is dense, synchronous and outwardly spreading. Propagation can be described roughly as a pulse of synchronous activity transmitted from one neuronal population to the next. And finally the termination phase that can be understood, in space, in terms of propagation failure and, in time, in terms of secondary activity patterns following in the wake of an initial wave of seizure activity and ultimately a return to rest (Pinto *et al.*, 2005). Electrophysiological evidence suggests that although short and prolonged seizures share similar characteristics for the initiation and propagation stages, it is, by definition, the failure of the termination stage that distinguishes seizures from SE (Shorvon, 1994).

2.1.1.1. Initiation

For a seizure to begin, three factors are required: the presence of cells with intrinsic burst-generating properties, loss of postsynaptic inhibitory control around these cells and also the synchronisation of the epileptic discharges (Shorvon, 1994). Burst-generating cells are thought to be the key initiators of a seizure and examples of cells with burst-generating properties include the hippocampal pyramidal cells in the CA1 and CA3 layers, and in neocortical cells, especially in layers IV and V (Shorvon, 1994). These cells can be made to burst by a variety of changes in their microenvironment and these have been demonstrated both *in vitro* and *in vivo*. Examples of these changes include increases in the extracellular concentration of either K^+ or pH, and also decreases in extracellular Ca^{2+} (Yaari and Beck, 2002).

A number of mechanisms have been suggested to underlie the synchronisation of epileptic discharges. One hypothesis is that gap junctions could be central to this process. This followed the observation that very high frequency EEG activity (>80Hz) often precedes epileptiform activity and these high frequency oscillations are too fast to be accounted for by synaptic transmission, and thus gap junctions may underlie this fast activity by facilitating diffusion of ions between cells (Traub *et al.*, 2005). Intriguingly, there is an abundance of gap junctions on glutamatergic neurons, the activation of which is critical for seizure generation (Avoli *et al.*, 2002; Traub *et al.*, 2005), but the contribution of gap junctions to this process requires further study.

2.1.1.2. Propagation

Propagation occurs primarily along existing neuronal pathways (Shorvon, 1994) but changes in the extracellular environment can also facilitate the recruitment of other brain regions (Traub *et al.*, 2005). One study that demonstrates the importance of existing neuronal pathways in seizure propagation was conducted using a rat model of cortical dysplasia (Setkowicz *et al.*, 2006). In this study, cortical dysplasia was induced in rats at different gestational periods with gamma radiation, and when the animals had reached adulthood, SE was induced with pilocarpine. SE caused clear differences in patterns of

injury and the pattern depended on when cortical dysplasia was induced, thereby suggesting that altering neuronal pathways will alter the propagation of seizure activity and thus injury.

Changes in the extracellular environment can also influence propagation. These alterations include changes in ion concentration of the extracellular fluid, and volume transmission. Volume transmission is the accumulation of neurotransmitters in the synaptic cleft, which may result from the repeated firing of action potentials, and these molecules can diffuse out of the cleft resulting in activation of neighbouring cells.

The speed of seizure propagation can vary quite substantially, ranging from <200 μm/s to >10 mm/s (Trevelyan *et al.*, 2007). Trevelyan and colleagues have demonstrated, using hippocampal slices, that the speed of seizure propagation is modulated by a feedforward inhibition mechanism (Trevelyan *et al.*, 2006). However, this feedforward mechanism becomes less effective after repeated stimulation (Trevelyan *et al.*, 2007). The researchers therefore suggested that this mechanism may account for the range of propagation velocities seen in seizures.

Some seizures only remain focal whereas some seizures generalise, but the mechanisms that facilitate seizure generalisation are not known. This is possibly due to sufficient inhibitory activity outside of the epileptic focus that prevents seizure activity from propagating to other brain regions. One hypothesis is that rapid generalisation occurs through recruitment of the thalamus, but studies have been, as yet, unable to substantiate this theory (Timofeev and Steriade, 2004).

2.1.1.3. Termination

It has been postulated that the termination mechanisms fail in SE and that this failure is the primary distinction between short and prolonged seizures (Shorvon, 1994). However, the nature of these mechanisms is still incompletely understood. One of the mechanisms proposed to play a primary role involves the Na^+/K^+ ATPase pump, which is critical for repolarisation of the membrane potential by actively resetting the ionic concentration gradient following neuronal firing (Heinemann and Jones 1990). This pump requires energy and has been estimated to consume around 60% of total cerebral ATP. However, it is the

by-products of ATP metabolism that could be important for seizure termination. Repeated seizure activity leads to more metabolism of ATP which in turn leads to an increase in the levels of adenosine (fig. 2.1) and adenosine, acting through A_1 receptors, has been shown to have an anti-convulsant effect (Ribeiro *et al.*, 2002). Furthermore, *in vitro* experiments have shown that A_1 receptors are critical for the transition from short seizures to SE (Avsar and Empson, 2004) (see section 2.1.2.3 for more details). Taken together, it can be hypothesised that seizures are inherently self-limiting. A seizure starts and propagates, then as the seizure continues, more ATP is used leading to increases in adenosine; following a sustained period of seizure activity adenosine accumulates, and this therefore exerts an anti-convulsant effect thereby stopping the seizure.

Figure 2.1. *Major pathways of adenosine production, metabolism and transport through the cell membranes (Adapted from Yuzlenko, 2006) (Yuzlenko and Kiec-Kononowicz, 2006)*

Evidence for a role of adenosine in seizures include findings that elevated adenosine levels during seizure activity have been identified in the epileptic foci of MTS-TLE patients using microdialysis probes (During and Spencer, 1992; Boison, 2005). Furthermore, an increase in adenosine of between a 6-31 fold was measured in these patients and this rise was suggested to be sufficient to terminate seizures (During and Spencer, 1992).

Other mechanisms may also contribute to seizure termination, for example a reduction in pH, which can occur due to increased respiration (i.e. increased CO_2) or during anaerobic respiration (i.e. increased lactic acid) (Dulla *et al.*, 2005). Interestingly, the inhibitory neurotransmitter GABA can be metabolised for ATP production (Heinemann *et al.*, 2002), but whether this has any implications for persistent seizure activity is unclear.

Termination mechanisms fail in SE, but the mechanisms that underlie this remain unclear. Presumably in certain situations a combination of various factors come together to override termination mechanisms such as those involving adenosine. For example, consider prolonged febrile convulsions.

Prolonged febrile convulsions are the most common form of status epilepticus in children and are seen almost exclusively within a specific age-range, between 6 months and 1 year, and this suggests a seizure-susceptibility period in development. Also, fever, as the name implies, is a defining characteristic of PFCs and the fact that increases in temperature cause a lowering of seizure threshold in neurons suggests an additional seizure-susceptibility factor. Therefore this would suggest that these two factors - age and fever - would favour seizure initiation, and seizure prolongation may possibly reflect the reduction in seizure threshold to an extent that the inherent termination mechanisms become ineffective.

The failure of termination mechanisms is likely to be dependent on aetiology and the mode of initiation. Whatever the mechanism for termination, the failure to do so can lead to disruption of autoregulatory processes within the brain as well as activation of potentially harmful mechanisms such as excitotoxicity, which can have important implications for the sequelae to SE.

2.1.2. Neurochemical changes associated with status epilepticus

The modulation of brain neurochemistry forms the basis of many of the anti-convulsant drugs used for the treatment or prevention of seizures and SE. Brain chemistry changes considerably from the moment a seizure begins, and these changes have led to the hypothesis that a seizure starts when there is a disruption in the balance between excitatory and inhibitory neurotransmission, with a net increase in excitation (Shorvon, 1994; Urbanska *et al.*, 1998; Morimoto *et al.*, 2004; Boison, 2005). This is further emphasised in chemoconvulsant models of seizures and SE in which chemicals are used to induce a net increase in excitation. These chemicals, when applied, can induce seizure-like or seizure activity in *in vitro* and *in vivo* models respectively. The *in vitro* experiments are typically electrophysiological, using brain slice preparations and modulation of physiological mechanisms. Examples include low magnesium solutions that removes the magnesium block and voltage dependence of NMDA receptors; K-channel blockers such as 4-aminopyridine (4AP), which prolongs and enhances synaptic potentials; and low calcium solutions, which increase membrane excitability while blocking chemical synaptic transmission. Similarly, *in vivo* administration of chemicals such as pilocarpine, which acts on cholinergic muscarinic receptors; kainic acid, a glutamate analogue; bicuculline, a $GABA_A$ antagonist, and 4AP have been used to induce seizures in animal models. This section will review the neurochemistry of glutamate and γ-amino butyric acid (GABA), the two most abundant and extensively studied CNS neurotransmitters, and also adenosine, which has been implicated in intrinsic anti-seizure mechanisms (see section 2.1.1.3).

2.1.2.1. Glutamate

Glutamate is the most prevalent excitatory neurotransmitter in the central nervous system (Nicholls *et al.*, 2001) and exerts its effect through the activation of various receptors, which are ionotropic or metabotropic receptors.

Enhancement of excitatory neurotransmitter mechanisms has been proposed to have a central role in epilepsy. Indeed, in the CNS, facilitation of transmitters acting on the cholinergic system (pilocarpine, soman) or glutamatergic system (kainic acid) can result in seizures. The glutamatergic system has attracted the most attention in epilepsy research

because of its abundance in the brain and association with excitotoxicity. Evidence that supports a role for glutamate in seizures include elevated levels of glutamate that have been found *in vivo* both in animal models and in patients (Urbanska *et al.*, 1998; Ueda *et al.*, 2002).

There are three types of ionotropic glutamate receptors: N-methyl-D-aspartate (NMDA), α-amino-3-hydroxy-5-methyllisoxazole-4-propionate (AMPA), and 2-carboxy-3-carboxymethyl-4-isopropenylpyrrolidine (kainate) receptors.

AMPA and kainate receptor activation leads to the influx of Na^+ and the efflux of K^+. The NMDA receptor has a different pharmacology to that of the AMPA and kainate receptors. Mg^{2+} acts to block the receptor in the resting state and partial depolarisation is required to remove Mg^{2+} before glutamate and glycine can bind to activate this channel. This receptor, when activated, allows the influx of Na^+ and Ca^{2+} and the efflux of K^+. The NMDA receptor has received a lot of attention due to its central role in a number of processes in neurons. It has crucial roles in synaptic transmission, regulation of gene expression, dendritic sprouting, synaptic remodelling, long-term potentiation and long-term depression (Waxman and Lynch, 2005) which may all have roles to play in injury and epileptogenesis. Not surprisingly, drugs acting on NMDA receptors have received widespread interest, and studies have indicated that NMDA antagonists, such as ketamine, can produce substantial neuroprotection when given after the onset of SE (Fujikawa, 1995). However when the NMDA antagonists (e.g. MK-801, remacemide) were tested in clinical trials, these drugs were effective for reducing seizure frequency, but this effect did not last, and the accompanying adverse effects, such as psychoses, have thus limited their clinical application (Urbanska *et al.*, 1998).

The metabotropic glutamate receptors are G-protein linked and thus have an indirect influence on neurotransmission via modulation of secondary messenger mechanisms such as IP_3 and cAMP (Ure *et al.*, 2006). Presently, 8 different receptor subtypes are known ($mGlu_1$-$mGlu_8$) and these are subdivided into three groups depending on their pharmacological profile and sequence homology: Group I, II and III. Their pharmacology is beyond the scope of this thesis but Group I and III agonists and Group II antagonists are thought to have anti-convulsant properties (Moldrich *et al.*, 2003). As such there is increasing interest in these receptors as potential targets for anti-epileptic drugs.

Group I mGluRs are especially prominent in the CA3 region of the hippocampus. Activation of these receptors enhances neuronal excitability and this has been shown to facilitate long-term potentiation induction and provoke long-term depression, as well as internalisation of AMPA receptors. These receptors may also have a role in prolonging seizure activity. Using guinea pig hippocampal slices, Merlin and Wong demonstrated that selective agonists of Group I mGluRs converted picrotoxin-induced brief discharges into prolonged discharges lasting several seconds, and these prolonged discharges induced by the agonists continued for hours even after the agonist was removed (Merlin and Wong, 1997)., which supports the hypothesis that these receptors have a role in seizures.

2.1.2.2. γ-amino butyric acid

γ-aminobutyric acid (GABA) is the major inhibitory neurotransmitter in the brain (Nicholls *et al.*, 2001), and alterations in GABAergic transmission have been implicated in epilepsy. There are three types of GABA receptors that have been classified: $GABA_A$, $GABA_B$ and $GABA_C$. Both $GABA_A$ and $GABA_C$ are ionotropic receptors that modulate the passage of Cl^-, whereas $GABA_B$ is a metabotropic G-protein-linked receptor. Although epilepsy research has focussed mainly on the $GABA_A$ receptor, increasing evidence suggests $GABA_B$ also plays a role (Sperk *et al.*, 2004; Enna and Bowery, 2004; Bettler *et al.*, 2004). $GABA_C$ has only recently been identified in the developing rat hippocampus and it remains to be seen whether this receptor type is important in the epileptic brain (Alakuijala *et al.*, 2005).

One of the reasons for the interest in $GABA_A$ receptor is the anti-convulsant properties of barbiturates and benzodiazepines that act to enhance its function (Nicholls *et al.*, 2001). The benzodiazepines are commonly used clinically and they are the first line drugs for the treatment of SE. However, studies suggest that both barbiturates and benzodiazepines gradually lose their efficacy as SE continues and this partly underpins the need to treat SE quickly and effectively. This loss of efficacy is known as pharmacoresistance and functional modulation of $GABA_A$ receptors has been hypothesised to underlie this decrease in effectiveness (Jones *et al.*, 2002).

Both short and long-term changes in GABA receptors have been demonstrated in animal models and patients (Morimoto *et al.*, 2004), and these changes may be relevant to epileptogenesis. Studies have suggested that the ionotropic GABA receptors can shift from an inhibitory to an excitatory action in pathological conditions (Cossart *et al.*, 2005) and this has been identified in the resected hippocampi of patients with TLE (Cohen *et al.*, 2002). This implies that the major inhibitory neurotransmitter could actually facilitate seizure activity in these patients and could be important for understanding their medically intractable condition. Also GABAergic transmission has a major role in the synchronisation of neuronal networks such as in non-REM sleep and thus could be an important mechanism for seizure synchronisation (Cossart *et al.*, 2005).

2.1.2.3. Adenosine

Adenosine has been suggested to be an endogenous cerebral anticonvulsant and may play a primary role in seizure termination mechanisms (Shorvon, 1994; Boison, 2005) (see section 2.1.1.3). A 6-31 fold increase in adenosine has been detected in the epileptogenic focus of intractable MTS-TLE patients during seizures and this increase has been suggested to be sufficient to suppress seizure activity (During and Spencer, 1992). Adenosine is not a classical neurotransmitter, like glutamate and GABA, in the sense that it is not stored in synaptic vesicles but is released from the cytoplasm to the extracellular space via a nucleoside transporter (Ribeiro *et al.*, 2002).

There are four types of adenosine receptor- A_1, A_{2A}, A_{2B} and A_3- which are all G-protein linked (Ribeiro *et al.*, 2002), and it is the A_1 receptor that has generated the most interest in epilepsy research. The hippocampus possesses high levels of A_1 receptors, which are found both pre- and post-synaptically. The activation of A_1 reduces excitatory neurotransmitter release pre-synaptically and stabilises membrane potential post-synaptically. This action is through the inhibition of adenylate cyclase and activation of phospholipase C (Boison, 2005).

Evidence for the role of A_1 receptors in seizures has been shown, *in vitro*, to be critical for the transition from seizure to SE (Avsar and Empson, 2004). Furthermore, A_1 knockout mice develop lethal SE shortly after traumatic brain injury when compared to wild-type mice, which suggests that A_1 receptors are critical for modulation of seizure-induced injury

(Kochanek *et al.*, 2006). Although the precise function of A_1 receptors in epilepsy is not known, it is notable that a reduction in A_1 receptors and altered A_1 function have also been reported in epilepsy patients and in animal models of chronic epilepsy (Boison, 2005).

Adenosine agonists have been shown to be effective for seizure suppression, while antagonists facilitate seizures (Boison, 2005). However, adenosine agonists in therapy have had limited success due to the associated peripheral and central side effects, such as sedation (Ribeiro *et al.*, 2002). Nevertheless adenosine-based medications remain an attractive avenue for development of novel therapies for intractable epilepsy.

2.1.2.4. Other neurochemical changes

Although glutamate, GABA and adenosine are altered in seizures, a considerable range of neurotransmitters and neuromodulators and their respective receptors are also modulated. A detailed discussion of all of these molecules is beyond the scope of this thesis; however, changes in acetylcholine, dopamine, noradrenaline, serotonin, taurine, glycine, aspartate, opioid as well as neuropeptides such as substance P, neuropeptide Y and galanin have all been identified (Shorvon, 1994; Wasterlain *et al.*, 2002). This list is not completely exhaustive and other neurochemicals, perhaps as yet unidentified, may also play major roles in seizures and SE.

2.1.3. The pathophysiology of status epilepticus

The pathophysiology of SE is summarised in figure 2.2. These physiological changes can be divided into two phases: compensation and decompensation (Lothman, 1990). The first to occur is compensation and this is the period when various physiological mechanisms are recruited to match the increases in energy demand from seizing neurons. Short seizures are confined to this period. The second stage, decompensation, begins after around 30mins of continuous seizure activity and this is the point when the compensatory mechanisms begin to fail (Lothman, 1990).

During the compensation phase of SE, tachycardia and blood pressure increase, and raised plasma levels of lactate and glucose can be detected. The pH begins to fall, due to increases in CO_2 and lactate, and changes in brain metabolism occur with measurable increases in CBF and also in glucose and oxygen utilisation.

Figure 2.2. *Summary of systemic alterations and brain metabolism in SE. Various events are aligned with respect to a time line. Note discontinuities in the time line and the designation of a critical transition period after 30 minutes of SE. (1) loss of reactivity of brain oxygen tension later in SE, (2) postulated mismatch between the sustained increase in oxygen and glucose utilisation and a fall in CBF, (3) depletion of brain glucose and glycogen, (4) decline in the brain energy state. PEDs = paroxysmal epileptiform discharges. (Adapted from Lothman, 1990).*

After a period of approximately 30 minutes of continuous seizure activity, the mechanisms recruited to meet demand begin to fail. At this point cerebral autoregulation begins to fail,

and CBF becomes wholly reliant on systemic blood flow, which falls gradually. As the seizure continues, respiratory and metabolic acidosis, electrolyte imbalance and hyperthermia develop, and all can contribute to SE-associated injury (Shorvon, 1994). Although neuronal death can be detected after around 30mins, it is still not understood at which stage epileptogenesis begins or whether it is independent of these phenomena.

2.2. MECHANISMS OF BRAIN INJURY

2.2.1. Ischaemia

Ischaemia, defined as restriction of blood supply, had been hypothesised to be the underlying mechanism for SE-induced injury, but has since been discredited as the primary mechanism for SE-induced injury following the work by Meldrum and colleagues. The ischaemia hypothesis was suggested following observations that the hippocampus was a particularly vulnerable structure to both global ischaemia and SE, and that there were striking histological similarities between hippocampal cells following these injuries (Siesjo and Wieloch, 1986). However, Meldrum and colleagues demonstrated that the primary mechanism of injury was through seizure activity. In their seminal study, they avoided SE associated systemic complications by paralysing and ventilating their experimental animals, adolescent baboons, and thereby maintained a constant blood supply (Meldrum and Brierley, 1973), they therefore demonstrated that, independent of systemic complications, prolonged seizure activity alone can cause neuronal death. Subsequent studies have suggested that the likely mechanism responsible for this neuronal injury is excitotoxicity, and that this mechanism of cell injury underlies injury in SE, ischaemia and hypoglycaemia, therefore explaining the histological similarities following each of these insults (Siesjo and Wieloch, 1986). Nonetheless, it should be acknowledged that ischaemia may contribute to SE-induced injury through systemic complications commonly associated with SE (see section 2.1.3).

2.2.2. Excitotoxicity and Ca^+

Excitotoxicity is the main mechanism that underlies seizure-induced neuronal injury, mediated primarily through the influx of extracellular Ca^{2+} via glutamatergic NMDA receptors (Chen and Wasterlain, 2006). The damaging effect of glutamate was first described by Lucas and Newhouse who demonstrated that administering monosodium glutamate systemically caused retinal damage in rat pups, which they attributed to a direct effect of glutamate (Lucas and Newhouse, 1957). Subsequently, the role of NMDA receptors in cell injury was revealed by Olney and colleagues when they used selective glutamate analogues to demonstrate that neuronal cell death was due to the activation of these receptors (Olney *et al.*, 1974; Olney and de Gubareff, 1978).

Clinical and experimental studies have demonstrated that SE is associated with increased levels of extracellular glutamate during seizure initiation and maintenance (During and Spencer, 1993; Ueda *et al.*, 2002). The persistent activation of NMDA receptors in SE causes a toxic accumulation of intracellular levels of Ca^{2+} by activating intracellular pathways that can lead to cell death. These include the activation of proteases, phospholipases, endonucleases, kinases and nitric oxide synthases. Activation of these systems can lead to degeneration of cell membranes, DNA destruction, and mitochondrial dysfunction, which in turn can lead to the production of toxic levels of highly reactive free radicals that causes membrane and DNA destruction and can ultimately lead to cell death.

2.2.2.1. A hypothesised role of Ca^+ and the development of epilepsy

Ca^{2+} is a ubiquitous intracellular second messenger and has a central role in many physiological processes including neurotransmitter release, cell growth and differentiation and gene expression (Delorenzo *et al.*, 2005). However, there is increasing evidence which suggests that Ca^{2+} may be a potential marker for SE, epileptogenesis and epilepsy (Delorenzo *et al.*, 2005). Raza and colleagues reported that, in a time-course study using the pilocarpine model of SE, elevated levels of intracellular Ca^{2+} were seen in hippocampal neurons from immediately after SE until 1 year later (Raza *et al.*, 2004). Furthermore, they

demonstrated that inhibition of the NMDA receptor, using MK-801, prevented both the increases in Ca^{2+} and the development of spontaneous recurrent seizures (Raza *et al.*, 2004).

Although some cells do die after SE, it is the surviving population of cells which is of interest as dead cells cannot elicit any seizure activity. Delorenzo has suggested that, following SE, the neurons that survive have a compromised Ca^{2+} homeostasis due to the seizure activity, and as Ca^{2+} is involved in processes such as neurotransmitter release, consistently elevated levels of intracellular Ca^{2+} can lead to a perennial hyper-excitable state, and therefore contribute to the development of epilepsy (Delorenzo *et al.*, 2005). This Ca^{2+} hypothesis is intriguing as it is the first to suggest and have evidence for a link between SE, brain injury, epileptogenesis and epilepsy.

2.3. PATHOPHYSIOLOGY FOLLOWING STATUS EPILEPTICUS

2.3.1. Cell death

There remains little doubt that prolonged seizures can cause cell death, the main mechanism underlying this being excitotoxicity. Specific brain regions are particularly susceptible to convulsive SE, the most studied of which is the hippocampus; however neuronal injury also occurs in extra-hippocampal regions. Convulsive SE causes a selective destruction of the hippocampal CA1, CA3 and CA4 subfields, whereas CA2 is relatively spared. This is thought to be due to the connections between these regions. Also, it has been hypothesised that this pattern of cell loss, which is a defining characteristic of MTS, may reflect the progression of SE-induced injury that can lead on to the development of MTS-TLE.

2.3.1.1. Selective vulnerability of the hippocampus

The selective vulnerability of the CA1, CA3 and CA4 subfields of the hippocampus is thought to reflect the physical circuitry of the hippocampus that provides the pathway for

seizure propagation, and the relative sparing of CA2 reflects the lack of major connections within the hippocampal network (Paxinos, 1995)(fig. 2.3). This has been supported in animal models in which electrical stimulation of areas such as the entorhinal cortex, the perforant pathway or the hippocampus can generate seizures with injury to the vulnerable subregions (White, 2002). Furthermore, electrophysiological experiments on brain slices have demonstrated that cutting the Schaffer collaterals prevents seizure activity in CA1 and cutting the perforant pathway prevents abnormal activity propagating to the hippocampus (Avoli *et al.*, 2002). In addition, the vulnerable subfields may also reflect the low levels of calcium-binding proteins and the relative abundance of NMDA receptors and KA receptors found in these regions (Shorvon, 1994; Cendes, 2004).

Figure 2.3. *Major intrinsic connections of the rat hippocampal formation. Arrows indicate the directionality of the connections. EC, entorhinal cortex; DG, dentate gyrus; S, subiculum; PrS, presubiculum; PaS, parasubiculum. (Adapted from Paxinos et al., 1995)*

2.3.1.2. Other regions of brain injury

Although the hippocampus is the region that has received the most attention in epilepsy research, as it is the most commonly and severely affected region of the brain, other areas are also injured by SE. These include the thalamus, cortex, amygdala and the cerebellum in which cell loss and gliosis have also been observed (Shorvon, 1994)

2.3.1.3. Cell loss continues long after status epilepticus

The duration and severity of SE determine the degree of subsequent injury, and a period of between forty to sixty minutes of continuous seizure activity is required before neuronal death is observed (Fujikawa, 1995). However, even though cell death can be seen immediately after SE, cell loss continues after this period. The temporal evolution of cell death following SE has been described by Fujikawa using the pilocarpine model, with cell death being more severe at 24h than immediately after SE (Fujikawa, 1996). In addition, MRI studies have also shown that there is a progressive and ongoing cell death after SE. Roch and colleagues imaged rats following pilocarpine-induced SE and reported progressive brain atrophy (Roch *et al.*, 2002a), and Pitkanen and Sutula have reported neuronal damage to continue for up to 2 months after SE (Pitkanen *et al.*, 2002). Clinical studies have also indicated a progressive cell loss following SE. In a longitudinal MRI study by Scott and colleagues, an increasingly asymmetry in hippocampal volumes as observed in patients following SE and it was suggested that this injury may progress onto MTS (Scott *et al.*, 2003). Taken together, these studies indicate that cell loss continues for a substantial period after SE. However, whether subsequent epileptic seizures contribute to this cell loss remains unclear.

2.3.1.4. Cell death mechanisms

The terms apoptosis and necrosis have been suggested to cause confusion due to the ambiguities in their definition (Sloviter, 2002) and therefore cell death will be used as a term that encompasses both descriptions. Cell death mechanisms can occur via two distinct

pathways: extrinsic or intrinsic. The extrinsic pathway is activated by extracellular stimuli via the cell-surface ligand-gated death receptor family (Delhalle *et al.*, 2003). Members of this family include TNFR1, Fas/CD95, DR3, DR4, DR5, and DR6 and can be activated by members of the tumour necrosis factor family of cytokines. The intrinsic pathway is induced by intracellular signals and the mitochondria play a central role in this cell death pathway. The initiating step is DNA damage and this leads to the release of cytochrome *c* from the intermembrane space. Both pathways lead to the activation of caspases and, ultimately, cell death.

Up-regulation of caspases has been identified following SE in experimental studies and in the epileptic human temporal cortex (Becker *et al.*, 1999; Henshall *et al.*, 2000; Narkilahti and Pitkanen, 2005). Furthermore, there is evidence which suggests that cell death pathways are active beyond the period after the initial injury and into the epileptogenic period (Henshall and Simon, 2005). This is further supported by the fact that cell loss has been observed to continue up to two months following SE (Pitkanen *et al.*, 2002). However, the role of caspases in epileptogenesis has yet to be fully elucidated. In a study by Narkilahti and colleagues (Narkilahti *et al.*, 2003), the administration of a caspase-3 inhibitor during and after SE did not influence the severity of the acquired epilepsy in the amygdala-kindled rat. Moreover, the animals had a reduction in neuronal damage when compared to controls, and also a reduction in mossy fibre sprouting and thus Narkilahti and colleagues suggested that prevention of cell death may not be the best focus for development of anti-epileptogenic compounds.

Although injury, by definition, is required for epileptogenesis in acquired epilepsy, the notion that cell death may not be has also been demonstrated by drugs that are effective at preventing cell death but had little effect on subsequent epilepsy. Examples include the use of NMDA antagonists, and also the anti-convulsant, valproate (Brandt *et al.*, 2003; Brandt *et al.*, 2006). However, although these drugs do not influence the acquired epilepsy, the effectiveness of these agents may become an important part of post-SE therapy as cell loss is associated with cognitive decline.

2.3.2. Inflammation

The role of inflammation in the pathogenesis of SE has received increasing interest following studies which indicate that the immune response is the most prominent process that is modulated post-SE, and this has been found in patients and also in experimental models of SE (Gorter *et al.*, 2006). Although inflammation has been implicated in a wide range of CNS pathologies including traumatic brain injury, multiple sclerosis and cerebral ischaemia, its role in post-SE pathology remains unclear. Recently, it has been suggested that inflammation may have a key role in epileptogenesis, as up-regulation of inflammatory genes have been found that seemed to be independent of aetiology (Lukasiuk and Pitkanen, 2007).

Inflammation is the body's first line of defence against tissue injury and invasion by foreign pathogens, and it is characterised by the presence of a host of molecules that are not or barely detectable in physiological conditions (Vezzani and Granata, 2005). These molecules include cytokines and various established mediators of inflammation, and they are associated with the recruitment of phagocytic cells, including monocytes/macrophages and microglia. It is notable that the regional and cellular patterns of induction of these inflammatory molecules, and their time course of activation, appear to depend on the nature and severity of the injury (Vezzani and Granata, 2005).

It is still not clear whether it is cell death or continuous seizure activity that initiates the inflammatory response, but various inflammatory mediators have been associated with SE (Vezzani, 2005). These include tumour necrosis factor-α (TNF- α), interleukin-1β (Il-1β), and cyclooxygenase-2 (COX-2) (Jankowsky and Patterson, 2001; Voutsinos-Porche *et al.*, 2004; Turrin and Rivest, 2004; Iosif *et al.*, 2006). TNF- α and Il-1β can exacerbate seizure activity (Vezzani and Granata, 2005) and their expression is rapidly increased (<30mins) after the induction of seizures (De Simoni *et al.*, 2000). Although the mechanisms that underlie this enhancement of seizure activity are not completely clear, cytokines have been shown to modulate neurotransmitter systems. For example, Il-1β enhances NMDA receptor-mediated increases in intracellular calcium (Viviani *et al.*, 2003), which may have implications for seizure-induced injury. Taken together, these studies indicate that cytokines may have a role in the pathogenesis of SE.

SE is associated with selective damage to the limbic system, and if inflammation is determined by the nature and severity of the injury, then the time course and distribution of inflammatory mediators may provide a clue as to the degree of injury and the processes that are modulated. Il-1β and TNF-α levels are increased across the entire brain following SE and this suggests that there is a CNS-wide inflammatory response. However, the increased expression of COX-2 has been shown to be localised almost exclusively in the hippocampus and the piriform cortex following pilocarpine-induced seizures, areas known to exhibit progressive injury. This suggests that the vascular recruitment of inflammatory cells occurs in these regions (Turrin and Rivest, 2004). A recent study using the lithium-pilocarpine model demonstrated that a selective COX-2 inhibitor administered following SE can reduce the severity of subsequent epilepsy (Jung *et al.*, 2006), and may indicate an important role for COX-2 in epileptogenesis.

These studies indicate that the inflammatory process may have a key role to play in brain injury and the development of epilepsy. It is likely that certain inflammatory pathways are beneficial for brain injury following SE while, perhaps, certain ones are exacerbating the situation. Its effect on epileptogenesis requires further study and may be an interesting avenue for the development of novel post-SE therapies.

2.3.3. Neurogenesis

Although it is now widely accepted that SE can result in an increase in neurogenesis - the birth of newborn neurons - the functional consequences of this phenomenon in injury and epileptogenesis remain unclear, and constitute an active area of research. However, whether this process is beneficial or deleterious is still a matter of debate.

The dentate gyrus of the hippocampus is one of only two regions in the mammalian brain in which neurogenesis is known to occur throughout adulthood, and SE has been shown to induce an increase in neurogenesis in this area. This has been repeatedly demonstrated in various animal models of SE including chemoconvulsant and electrical stimulation models (Parent *et al.*, 1997; Bengzon *et al.*, 1997; Gray and Sundstrom, 1998; Parent *et al.*, 1998).

However, it is not just persistent seizure activity that can increase neurogenesis; a single after-discharge, induced by stimulation of the hippocampus, can lead to an increase which can still be detected 2 weeks later (Bengzon *et al.*, 1997). This suggests that neurogenesis could be modulated not just in SE but also by short seizures. Further evidence for this includes a study by Cha and colleagues, in which they induced spontaneous recurrent seizures using the lithium-pilocarpine method, and they found that these spontaneous seizures could also lead to elevated levels of neurogenesis (Cha *et al.*, 2004).

The molecular signals that orchestrate physiological neurogenesis and seizure-induced neurogenesis have only begun to be elucidated. These include hormones, growth factors, neurotrophins and extracellular matrix molecules, which have all been found to be modulated following seizures, and also alterations in neurotransmitter and neuromodulatory systems including glutamate, serotonin, nitric oxide and glucocorticoids (see Abrous for a comprehensive review) (Parent, 2002; Abrous *et al.*, 2005). Glucocorticoids have historically been one of the first factors studied for their influence on adult neurogenesis (Abrous *et al.*, 2005). These steroids increase during physiological stress and have been shown to inhibit neurogenesis, and also cause neuronal atrophy in the rat hippocampus (Woolley *et al.*, 1990; Kim *et al.*, 2004). Elevated glucocorticoid levels have been detected in patients following SE (Calabrese *et al.*, 1993) and have also been shown to potentiate seizures (Lee *et al.*, 1989), but whether they have a role to play in pathology remains to be seen. Moreover, glucocorticoids can also suppress inflammation, which is a mechanism that has also been implicated in post-SE pathology (see section 2.3.2). These data suggest that glucocorticoids have an effect on both neurogenesis and inflammation, and may therefore have a role in SE-induced pathology.

Until recently, it was unclear as to whether electrical activity, cell death, or both lead to the increases in neurogenesis (Parent, 2002). However, it seems that either one of these mechanisms can lead to increases in neurogenesis. Evidence for this has been provided by Smith and colleagues who demonstrated that, in the rapid amygdala kindling model, neurogenesis can be induced without a concomitant increase in cell death (Smith *et al.*, 2005). Also cell death mechanisms have been shown to facilitate neurogenesis (Abrous *et al.*, 2005).

Although evidence shows that an increase in newborn cells can be found after SE, whether these new born cells integrate fully into the existing brain circuitry and function properly is still not completely clear. One important factor in integration of the new cells is the severity of the initial SE. Mohapel and colleagues found that, four weeks after SE, a majority of these new neurons die in fully convulsed animals but not in partially convulsed rats (Mohapel *et al.*, 2004). Also, newly born cells have been shown to migrate to abnormal locations within the hippocampus, such as the CA3 layer, dentate hilus and the inner molecular layer, and have altered physiological characteristics, which suggests a role for neurogenesis in the reorganisation of brain circuitry post-SE (Abrous *et al.*, 2005). Furthermore, it is not just the new born cells that can form aberrant synaptic connections, pre-existing granule cells have also been shown to do so too (Parent *et al.*, 1999).

The hypothesis that alterations in brain circuitry facilitate seizure generation (see section on 2.3.4.) is supported by studies that found SE-induced granule cells have abnormal electrophysiological dynamics, and exhibit hyperexcitability that occurs synchronously with CA3 pyramidal neurons (Scharfman *et al.*, 2000; Jakubs *et al.*, 2006). However, it is notable that neurons are not the only cell type formed following seizures, as gliogenesis - the formation of new astrocytes and oligodendrocytes - has also been identified following SE (Parent *et al.*, 2006b). For example, Hinterkeuser and colleagues have identified immature astrocytes in the CA1 region in patients with TLE and these astrocytes have altered potassium channel function that is thought to favour seizure generation (Hinterkeuser *et al.*, 2000). But the role and function of these new glia cells in brain injury and epileptogenesis require further study.

2.3.3.1. Granule cell dispersion

The precise role of the alteration in neurogenesis in MTS and epileptogenesis is still far from clear. One proposed abnormality in which neurogenesis has been implicated is granule cell dispersion (GCD), which is seen in approximately 40% of MTS patients (Blumcke *et al.*, 2002). GCD is characterised by a widening of the granule cell layer of the dentate gyrus (Fahrner *et al.*, 2007). Studies have identified associations between GCD density and the severity of hippocampal cell loss, and also between GCD and early seizure

onset (Blumcke *et al.*, 2002). However, there are also data that suggest that GCD may be a pre-existing developmental abnormality rather than an abnormality associated specifically with seizures and SE. For example, GCD has been observed without hippocampal cell loss; however these specimens analysed were accompanied by widespread cortical malformations (Blumcke *et al.*, 2002).

2.3.4. Mossy fibre sprouting

Mossy fibre sprouting is the formation of new synaptic contacts on abnormal locations in the supragranular region, the inner molecular layer of the dentate gyrus, and the CA3 region of the hippocampus (Longo *et al.*, 2003), and has been described in human TLE as well as in experimental animal models. Mossy fibre sprouting is one of the hallmarks of MTS (Longo and Mello, 1997; Pitkanen *et al.*, 2000b) and it has been hypothesised that this sprouting occurs following SE and forms a reverberating circuit that facilitates seizure generation, and therefore could be critical in epileptogenesis and the maintenance of epilepsy. Nevertheless, the significance of mossy fibre sprouting in epilepsy remains a controversial issue.

Mossy fibre synapses are an important component of inhibitory circuits in the normal hippocampus, and abnormal and excessive sprouting have been identified in humans with TLE (Frotscher *et al.*, 2006). These mossy fibres in TLE have also been shown to have abnormal electrophysiological dynamics, therefore suggesting a role in the generation of seizures in epilepsy (Wilson *et al.*, 1998; Frotscher *et al.*, 2006; Sloviter *et al.*, 2006).

The role of mossy fibre sprouting in epileptogenesis has been questioned following a series of observations. Experimental studies have demonstrated that recurrent seizures can develop before the appearance of mossy fibre sprouting (Bouilleret *et al.*, 1999). Also, in a study by Longo and Mello mossy fibre sprouting was blocked with cycloheximide, a protein synthesis inhibitor. This drug was investigated in both the pilocarpine model and kainate model, and in both models the animals still progressed on to spontaneous recurrent seizures despite having a reduction in sprouting (Longo and Mello, 1997). Therefore these data suggest that sprouting is not critical to epileptogenesis. However, it should be noted

that subsequent studies have questioned whether cycloheximide does indeed block sprouting (Williams *et al.*, 2002).

There are conflicting reports as to whether mossy fibre sprouting maintains epilepsy via the development of recurrent excitatory circuits. Gorter and colleagues observed that there was an increase in mossy fibre sprouting in rats with progressive epilepsy – animals that had a progressive increase in numbers of seizures – when compared to rats with non-progressive epilepsy (Gorter *et al.*, 2006). However, Pitkanen and colleagues found no association between the densities of mossy fibre sprouting with the total number of lifetime seizures or seizure frequency in experimental models or human TLE (Pitkanen *et al.*, 2000a). Whether this sprouting plays a significant role or is just an epiphenomenon in epilepsy still requires clarification.

2.4. SUMMARY

This chapter has aimed to review the physiological mechanisms that underlie SE, brain injury and epileptogenesis. In short, disruption of neurochemical processes may act as an initiator to seizures. When a seizure begins, a series of physiological changes occur, and, in most cases, inherent mechanisms act to terminate this event. However, when these termination mechanisms prove to be insufficient then injury can occur, and areas such as the hippocampus are particularly vulnerable to such an event. It has been hypothesised that injury to the hippocampus can eventually evolve into an area that acts as a seizure generator.

Following SE, a host of complex physiological mechanisms is activated, and these may have important roles in the evolution of SE-induced injury. In areas such as the hippocampus, cells die due to repeated depolarisation and this continues long after the end of the seizure. Neurogenesis is also increased following continuous seizure activity, and this may be beneficial or detrimental. In the early period following SE, the body's defences are recruited but it is still not known what role inflammation may play. It is possible that it is the interactions between these mechanisms that may play a critical in injury.

Nevertheless, as the injury evolves a number of marked and characteristic anatomical changes can be found. These include granule cell dispersion and mossy fibre sprouting, which have been hypothesised to play a role in seizure generation. It is likely that other, perhaps unknown, mechanisms also play important roles in SE and the development of epilepsy.

In the context of an evolving injury, the advantages of monitoring the injury over time are apparent and MRI offers the opportunity to do so. Previous MRI studies have already provided novel insights into seizures and epilepsy. However, recent advances in MR technologies have yet to be used to investigate these processes. It is now possible to use MRI to report on changes in energy status, function and morphology, as well as perfusion alterations that may provide clues to underlying pathology. It can be envisaged that the advent of molecular targeting MRI techniques that are currently being developed, may reveal exciting insights into SE, brain injury and epileptogenesis.

CHAPTER 3: ANIMAL MODELS OF STATUS EPILEPTICUS, BRAIN INJURY AND EPILEPTOGENESIS

The best model of a cat is a cat – preferably the same cat

Nobert Weiner

3.1. INTRODUCTION

There are a considerable number of epilepsy syndromes that have been defined by the ILAE, and therefore it is not surprising that a large number of animal models have been developed for investigating these syndromes in epilepsy research. An exhaustive review of which is beyond the scope of this thesis, and the interested reader is referred to "Models of Seizures and Epilepsy" for an in-depth review of epilepsy models (Pitkanen *et al.*, 2006).

There is little doubt that animal models have been a primary research tool for epilepsy research, and the use of these models has led to breakthroughs that provide much of the theory that underlies the current state of knowledge on epilepsy today. Furthermore, in the last century, animal models have also led to therapeutic advances in seizure management. For example, the effectiveness of phenytoin as an anti-convulsant was discovered through animal experiments, and since its introduction in 1939 it remains an important medication for the acute treatment of seizures and SE.

Despite these advances, the search for a therapy that treats the underlying causes of epilepsy remains an elusive goal. However, development of animal models that mimic human epileptogenesis, in parallel with clinical studies, have begun to reveal some of the processes that occur during epileptogenesis, some of which have been outlined in chapter 2. It is hoped that by understanding the role of these processes in epileptogenesis will point to productive avenues for developing preventative therapies.

An initial brain insult leading to brain injury that evolves into acquired epilepsy is the context that epileptogenesis has been most widely studied in. As such, the SE models, in which all of these events occur, have been the subject of intense investigation. This sequence of events is thought to share many similarities with the human condition, and because of the occurrence of spontaneous recurrent seizures, or acquired epilepsy, these models fall into a class of animal models that are thought to be true models of epilepsy.

This chapter will review the most commonly used SE models: kainic acid, pilocarpine (with or without lithium pre-treatment) and the electrical induction models. In addition, an

overview of the hyperthermia model of prolonged seizures in the immature rat will be presented. Furthermore, the choice of an appropriate animal model is critical for answering specific investigative questions, and as such, the rationale for choosing the pilocarpine model for our current studies will also be discussed.

3.2. THE USE OF ANIMAL MODELS IN EPILEPSY RESEARCH

Ideally, research on human epilepsy should be carried out on humans with epilepsy, but human research is not always possible or practical (Engel and Schwartzkroin, 2006). There are obvious ethical problems associated with human epilepsy research, especially when invasive techniques are required. Moreover, it is often difficult to control for clinical variables, such as genetic background, and the economic cost of conducting studies can be prohibitive because typically large populations of patients need to be included. Although new non-invasive technologies offer many exciting opportunities for investigating the human condition, the need for new approaches for diagnosis, treatment and prevention of epilepsy can be facilitated by the use of animal models in parallel with human epilepsy research.

Despite the development of animal models for research into epilepsy, the range of animal models developed does not completely mimic all of the complex aetiologies and varieties of syndromes identified in humans (Ben-Ari and Cossart, 2000). However, the nature of animal models is that they share basic similarities with aspects of human epilepsy, and by investigating these similarities they provide the tools to divulge basic molecular and cellular mechanisms associated with epilepsy and seizures. Furthermore, the relevance of the animal models can be articulated by the key role that they have played since the early half of the 20th century in which animal models have led to the discovery of treatments for epilepsy disorders, some of which are still commonly used today (Sarkisian, 2001). Nevertheless, most of the treatments used in epilepsy are predominantly used for the management of seizures, and therapies that treat the underlying causes of epilepsy are still required.

Since the relationship between SE, brain injury and MTS-TLE was first hypothesised by Cavanagh and Meyer (Cavanagh and Meyer, 1956), animal models have been developed that display a similar sequence of events in which the animals progress on to spontaneous recurrent seizures following an initial brain insult. Moreover, these models share a number of other similarities to the human condition. The most important of these are a latent period that separates the initial insult and the occurrence of the first spontaneous recurrent seizure, the non-convulsive and convulsive seizures lasting 1 to 3 mins are observed in the animals and appear similar to complex partial seizures with secondary generalisation in humans, and once epilepsy had been established there is an increase in seizure frequency. In addition, features such as neuronal loss, reactive gliosis, and axonal sprouting in the hippocampus and several surrounding structures in the animals parallel many of the changes observed in tissue from patients with TLE (Dudek *et al.*, 2006).

So far, evidence from these models suggest that there are differences between the mechanisms underlying epileptogenesis and the mechanisms involved in maintaining the expression of seizures, and therefore suggest that the drugs which prevent epileptogenesis may be different from the drugs that manage seizures (Leite *et al.*, 2002).

Even though epileptogenesis models share many similarities to the human condition, the direct relevance of these models have been questioned, in that whether these events actually occur in humans. However, an incident in Canada, outlined below, offers a human equivalent of the widely used epilepsy models and supports the view that these models are important for investigating epileptogenesis in humans.

3.3. DOMOIC ACID POISONING: A HUMAN MODEL OF ACQUIRED EPILEPSY

In 1987, over 150 people became acutely ill after eating contaminated blue mussels (Jeffery *et al.*, 2004). Of these people, 19 individuals were hospitalised and 4 people died as a result of the poisoning. It was subsequently established that these mussels were contaminated with domoic acid, which is an analogue of kainic acid and has similar actions on the

glutamatergic system. These mussels feed on phytoplankton and the contamination occurred as a result of a bloom of a specific species of phytoplankton, *Pseudonitzschia f. mulitseries*, in the region where the mussels originated from.

One specific case of domoic acid poisoning was in an elderly patient with no previous history of epilepsy, which was reported by Cendes and colleagues (Cendes *et al.*, 1995). This patient developed complex partial SE, which required large doses of phenobarbital to control. After the episode, the patient acquired severe anterograde memory impairment that was consistent with hippocampal injury, but no EEG abnormalities were observed in him over the first 8 months following intoxication. However, one year after the poisoning incident the patient developed complex partial seizures. When he was taken back to the hospital, he had a complex partial seizure with secondary generalisation after which MRI revealed a hyperintense T_2 signal and marked atrophy in both hippocampi. The patient subsequently died from pneumonia, and histology revealed substantial cell loss throughout the hippocampi that was consistent with MTS.

This case report supports the view that associates SE, brain injury and TLE in humans, and therefore supports the use of SE-induced epilepsy models for investigating epileptogenesis.

3.4. MODELS OF STATUS EPILEPTICUS WITH EPILEPTOGENESIS

The most common animal models used to study SE, brain injury and epileptogenesis involve either electrical stimulation or chemical convulsants to initiate SE (Loscher, 2002). The electrical stimulation models require surgical insertion of an electrode in areas such as the hippocampus or the amygdala, followed by the application of an electric current to induce SE. The chemical convulsants can be administered either systemically or focally for generating SE. Alternative methods for generating SE include a hyperthermia model in immature rats that also display SE, brain injury and epileptogenesis. Whatever the induction method, one of the key features of these models is that after the onset of the seizure, the seizure becomes independent of the mode of induction and therefore are self-sustaining (Mazarati *et al.*, 2006).

The decision as to which animal model to use depends on the investigative question that is being asked. As such, it is important to understand the advantages and disadvantages of specific models. The electrical models have a distinct advantage over the chemical models in that the investigator can be sure that the injury that results from stimulation is solely due to electrical activity, and not from the side effects that a persistent chemical agent introduces. However, a disadvantage of the electrical models is that both neuronal and non-neuronal tissue will be stimulated during the induction of SE. A major advantage of the chemical models is that SE induction is a lot less labour intensive than the electrical models, and thus they are comparatively straightforward to set-up.

Regardless of whether electrical or chemical method is used for initiating SE, over 80% of the animals will subsequently develop epilepsy, and therefore the SE models are considered to be the most reliable and robust way to induce chronic epilepsy (Dudek *et al.*, 2006; Mazarati *et al.*, 2006). In contrast, the hyperthermia model induces epilepsy in around 35% of the animals, although these data are from animals that had seizures lasting for less than 30 minutes (Dube *et al.*, 2006). It has been suggested that it is the identification of common mechanisms between the different models that will provide valuable insights into the fundamental mechanisms of brain injury and epileptogenesis (Dudek *et al.*, 2006).

3.4.1. Electrically-induced status epilepticus models

Electrical stimulation can be used to induce self sustaining SE in a variety of locations in the limbic system, such as the perforant pathway or the amygdala. These methods require surgical implantation of the electrodes into the relevant stimulation site, and also a stimulator and EEG recording equipment for assessing the success of seizure generation and activity.

The localised activation of the limbic regions offers a number of advantages over the chemoconvulsant models. As previously mentioned, the investigator can be sure that it is the propagation of electrical activity that is inducing injury and not the systemic effects of an initiating drug. It is perhaps because of this that there are lower mortality rates

associated with these methods with a reported survival rate of nearly 100% (Mazarati *et al.*, 2006).

The neuropathology following electrically-induced SE is very much dependent on the protocol in which the duration of SE and the area of induction are key factors in determining outcome. The injury observed following SE is typically less than that found in the chemoconvulsant models, with varying degrees of cell loss in the hippocampus, amygdala, entorhinal and piriform cortices, as well as the thalamus (Mazarati *et al.*, 2006).

An additional advantage of these models is that EEG is recorded during SE. Treiman and colleagues have characterised five different stages of EEG activity during SE, and noted an association between periodic epileptiform discharges and subsequent development of epilepsy (Treiman, 1995). Therefore, if periodic epileptiform discharges are observed during the seizure then this could be used as a good predictor of which animals will progress on to spontaneous recurrent seizures (Bertram and Cornett, 1993).

3.4.2. Chemically-induced status epilepticus

Status epilepticus and seizures can be induced with a variety of chemicals with many different mechanisms of action (Velisek, 2006). These include bicuculline, a $GABA_A$ antagonist; flurothyl, a convulsant; and the selective glutamatergic agonist NMDA. However, not all of these chemicals will elicit subsequent development of epilepsy following SE, an example of which is flurothyl. Therefore the selection of an appropriate model is required if SE and epileptogenesis are to be investigated.

The most widely used models for investigating SE, brain injury and epileptogenesis are the pilocarpine model and the kainic acid model (Sarkisian, 2001), which act on the cholinergic and the glutamatergic neurotransmitter systems respectively. Other drugs that act on these systems can also be used to study brain injury and epileptogenesis; for example, soman, a cholinesterase inhibitor, and domoic acid, a selective kainate agonist, have also been used (Bhagat *et al.*, 2001; Velisek, 2006).

Whether using pilocarpine or kainic acid, either drug is most commonly administered by via the intraperitoneal route. Alternatively, these drugs can be given subcutaneous, intravenous, intracerebroventricular, and intrahippocampal. In either model, a single systemic injection is associated with higher mortality than with multiple low doses, and not all animals will experience SE with the single dose (Velisek, 2006).

For the pilocarpine model, pre-treatment with lithium can substantially reduce the pilocarpine dose needed for inducing SE, although the precise mechanism of lithium is not known, hypotheses include the ability of lithium to prevent the desensitisation of the muscarinic receptor (Clifford *et al.*, 1987; Pontzer and Crews, 1990). In a study that compared the single dose pilocarpine with the lithium-pilocarpine models, Clifford and colleagues did not observe any behavioural, electrographic, metabolic or histopathological differences between the two (Clifford *et al.*, 1987). However, a possible disadvantage of lithium pre-treatment is that its mechanism of action has not been fully defined, but this may be out-weighed by its advantages in that this model is associated with higher reproducibility of SE and lower mortality, which may be a reflection of reduced systemic cholinergic effects when compared to high doses of pilocarpine.

With action on different neurotransmitter systems, it is not surprising that there are several differences between the kainic acid and the pilocarpine models. In the kainic acid model, EEG changes are first detected in the hippocampus, whereas in the pilocarpine model these are found first in the ventral forebrain (Clifford *et al.*, 1987). Furthermore, although metabolic activation was detected in the forebrain of the pilocarpine animals, this was not found in the kainic acid rats. In terms of the injury observed following SE, kainic acid was reported to cause slightly more damage in the hippocampus than in the pilocarpine model, but pilocarpine induced greater neocortical changes following SE.

Similarly to the electrical models, both the kainic acid and pilocarpine models (with or without lithium pre-treatment) induce neuronal injury in a variety of regions in the brain. These include the hippocampus, piriform cortex, entorhinal cortex and the amygdala (Dudek *et al.*, 2006; Cavalheiro *et al.*, 2006; Mazarati *et al.*, 2006). It should also be noted that although a vast majority of animals in either model will progress on to spontaneous recurrent seizures, these animals display different pharmacological responses to drug

therapy. For example, valproate is effective at preventing epilepsy and reducing neurodegeneration in the kainic acid model, which is in contrast to the pilocarpine model (Loscher, 2002). The differences between the effectiveness of drugs in various models are perhaps not surprising given that the SE induction chemicals have distinct mechanisms of actions, and that systemic effects may play a role.

3.4.3. Experimental prolonged febrile seizures

Prolonged febrile convulsions are the most common type of SE in humans and are characterised by fever and seizures in a specific age range (Chin *et al.*, 2004). These characteristics have been incorporated and developed into an animal model of experimental prolonged febrile seizures (Dube *et al.*, 2006). These seizures are induced by hyperthermia in rats aged between postnatal day (PN) 7 – 14 and which, in terms of hippocampal development, are thought to be equivalent to the first year of human life (Avishai-Eliner *et al.*, 2002).

In this rat model, seizures are generated by raising and maintaining the core temperature to 40-42C for 30 minutes, and these rats will have a seizure that lasts for around 24mins (Dube *et al.*, 2006). EEG data indicate that these seizures are limbic in origin and involve the hippocampal formation. Furthermore, this model, in which seizures last for less than 30 minutes, does not lead to acute or long term neuronal death, but a transient neuronal injury in limbic structures including the hippocampus, amygdala and perirhinal cortex. Acute T_2 changes have also been reported in the hippocampus, amygdala, piriform cortex and medial thalamus, which are consistent with other models of SE (Dube *et al.*, 2004). Around 88% of these experimental animals that have undergone early prolonged febrile seizures have been reported to show interictal discharges, and approximately 35% of these animals developed spontaneous recurrent seizures (Dube *et al.*, 2006).

It is unclear how this model compares with the other prevailing models of SE. The duration of and the severity of SE have been shown to be critical in SE sequelae (Fujikawa, 1996), and therefore most studies have used a seizure duration significantly greater than 30 minutes compared to the 24 minutes in this model. It may be argued that the prolonged

febrile seizure model is focussing on injury and epileptogenesis in the absence of neuronal death, and therefore this model indicates that neuronal death is not critical for epileptogenesis. However, it remains to be seen whether longer seizures that will result in cell death facilitate the development of epilepsy.

3.5. OTHER MODELS OF EPILEPTOGENESIS

The main characteristic of the chronic epilepsy models is the expression of spontaneous recurrent seizures (SRS) some time after a precipitating brain insult (White, 2002). Although the SE models are the most widely used for investigations into epileptogenesis, there are other models that also display this phenomenon. These include stroke, cerebral infection or traumatic brain injury as an initiating brain insult.

3.6. RATIONALE FOR USE OF THE LITHIUM-PILOCARPINE/ PILOCARPINE MODEL IN THIS STUDY

The pilocarpine model was chosen for this thesis for a variety of reasons. The most important reason is that SE, brain injury and epileptogenesis can both be investigated using this one model. Additional benefits of the pilocarpine model are that this model is highly reproducible, with a majority of the animals entering SE, and depending on the duration of SE, most of these will also progress on to spontaneous recurrent seizures.

Furthermore, we decided to use an animal model that was well-established in the epilepsy research field because this was the first experimental epilepsy project to be conducted in our laboratory. An example of the widespread use of pilocarpine can be shown with a search on PubMed with the parameters: status epilepticus, animal, journal article in the last 5 years with either one of electrical, kainic acid or pilocarpine. This search returned 41, 143 and 237 articles respectively. This may reflect that the pilocarpine model is, compared to the electrical stimulation models, relatively simple to set up, and the cost of the drugs used

in this model is not prohibitive with 1 gram costing £12.76 (Sigma-Aldrich, UK), unlike kainic acid in which an equivalent amount costs £9,880.00 (Sigma-Aldrich, UK). For these reasons the lithium-pilocarpine/pilocarpine model was chosen for our investigations.

3.7. SUMMARY

There have been many advances in identifying the underlying mechanisms of epilepsy and epileptogenesis in recent times that have been underpinned by the use of animal models. These have helped in the development of anti-convulsant therapies that have been effective for the management of seizures, and we have moved away from primitive and ineffective treatments such as those used in the 19th century that included mistletoe, turpentine and even castration (Gross, 1992). However, the goal of providing a therapy that will prevent epilepsy remains elusive.

The development of animal models of acquired epilepsy, such as the SE models outlined in this chapter, can provide the necessary tools for elucidating the underlying mechanisms of brain injury and epileptogenesis, which may provide the basis for therapy. However, there is a multitude of ways for inducing brain injury and epileptogenesis, and differences even exist between the SE models. But, as Dudek had suggested (Dudek *et al.*, 2006), the most valuable aspects of these models are likely to be in identifying mechanisms that are common across the models, and these are likely to be associated with the fundamental mechanisms of brain injury and epileptogenesis rather than a model-specific phenomenon. With this in mind and for the more practical reasons outlined above, we have chosen the pilocarpine rat model for our initial investigations into SE, brain injury and epileptogenesis.

CHAPTER 4: MRI, STATUS EPILEPTICUS AND EPILEPSY

Observe due measure, for right timing is in all things the most important factor

Hesiod

4.1. INTRODUCTION

Magnetic resonance imaging has revolutionised the investigation of pathologies *in vivo*, especially in disorders of the central nervous system, and it is now routinely used for both diagnostic and research purposes. Its non-invasive nature and ability to provide information about anatomical, functional and metabolic processes means that MRI is becoming the medical imaging modality of choice in many diagnostic areas. Furthermore, because of its non-invasive nature, longitudinal studies can be conducted. This means that the natural evolution of pathologies can be monitored in single subjects and here lies the main strength of MRI.

In epilepsy research, and perhaps more pertinently in epileptogenesis research, the ability to follow pathology subsequent to SE on to the development of spontaneous recurrent seizures offers an exciting alternative to traditional methods such as histology. Also a sequence of events occurs from the onset of a seizure through to its termination, but how these events translate into the injury associated with SE remains unclear. Traditional *in vivo* techniques have been employed to measure various physiological phenomena, such as electrical signals during a seizure, but these methods tend to be limited by the lack of either spatial or temporal resolution. The spatial resolution and discrimination of soft tissue that MRI offers is unparalleled by any other modality and the advent of increasingly faster imaging MR techniques offers the possibility for investigating evolution of these phenomena.

Another advantage of MRI is that it can be used to investigate a variety of changes in tissue state by utilising various types of contrast, with each contrast offering unique information. For example, T_1 and T_2 imaging interrogates the local physical micro-environment of tissue water. In addition, more recent developments in MR contrasts, such as diffusion and perfusion imaging, provide the tools to investigate directly the underlying physiological nature of changes in the tissue.

A comprehensive review of the theories that underlie MRI are beyond the scope of this thesis, and interested readers are directed to "NMR and its applications to living systems",

which explores these areas in greater detail (Gadian, 1996). This chapter will review the basic theory of nuclear magnetic resonance (NMR), which underpins MRI, and also the theory behind the associated contrasts that have been used in this thesis. Also previous MRI studies on epilepsy will be reviewed.

4.2. PRINCIPLES OF NUCLEAR MAGNETIC RESONANCE

Nuclear magnetic resonance exploits the magnetic moment generated by the spin of atomic nuclei. The most frequently investigated nucleus in MRI is the proton (^1H) because of its abundance in organic matter, and its relatively high magnetic moment compared with other nuclei. When an object is placed into a magnetic field (B_0), such as the field of an MRI scanner, the nuclear spins take up one of two directions in relation to the field: either parallel or anti-parallel. As one nucleus that is oriented in one direction essentially cancels out another that is oriented in the opposite direction, it is the net difference between the populations of the two directions - known as the longitudinal magnetisation - that can be manipulated for detection in MRI.

The longitudinal magnetisation can only be detected if it is disturbed away from B_0 (z-axis), which can be achieved by applying a radiofrequency (RF) pulse in the plane perpendicular to B_0. This creates an oscillating magnetic field (B_1) that causes the nuclei to rotate away from the z-axis towards the x-y plane. The frequency (ω_0) at which the longitudinal magnetisation can be disturbed is called the Larmor (resonance) frequency and this is determined by the strength of B_0, and the property of a given atomic nucleus known as the gyromagnetic ratio (γ). This relationship is described by the equation:

$$\omega_0 = \gamma B_0$$

If the RF at the Larmor frequency is applied for an appropriate time, all of the net magnetisation for that specific nucleus will tilt into the x-y plane and as such this pulse of RF is called a 90° pulse (figure 4.1). Once the net magnetisation is moved away from B_0, the signal can be detected by a receiver coil. As the nuclei precess in the x-y plane, an

electrical current oscillating at the resonance frequency is generated in the coil and it is this signal that is processed to give the final MR image.

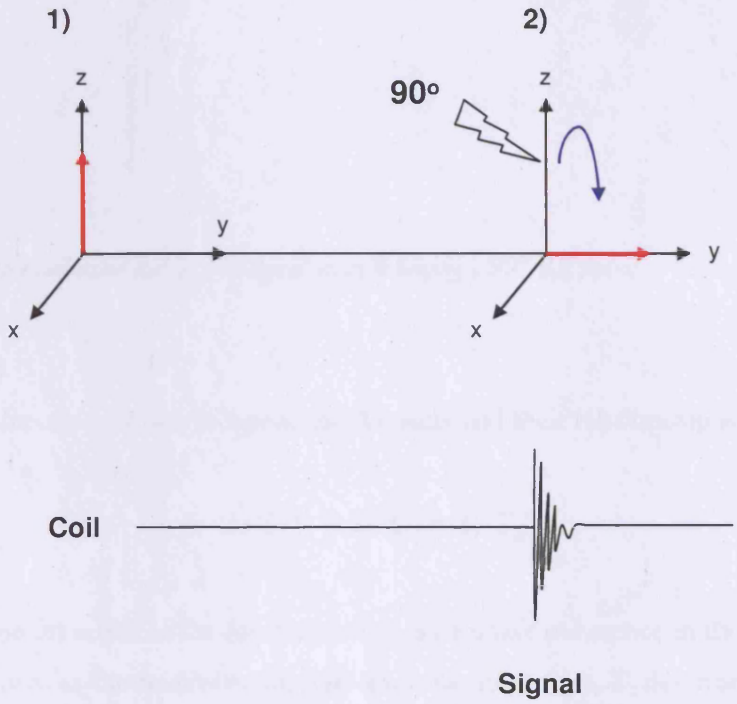

Figure 4.1. *Net magnetisation. 1) Net magnetisation shown in red that resides along the z-axis cannot be detected by the coil. 2) Application of a 90° RF pulse tilts the magnetisation into the x-y plane and signal can now be detected.*

4.3. SEQUENCES: SIGNAL, RELAXATION AND MANOEUVRE

A 90° pulse causes the entire net magnetisation to be tilted into the x-y plane and this generates a signal that can be detected by a receiver coil. However, this signal, known as the free induction decay, disperses at a rate described by the term T_2^* (fig. 4.2).

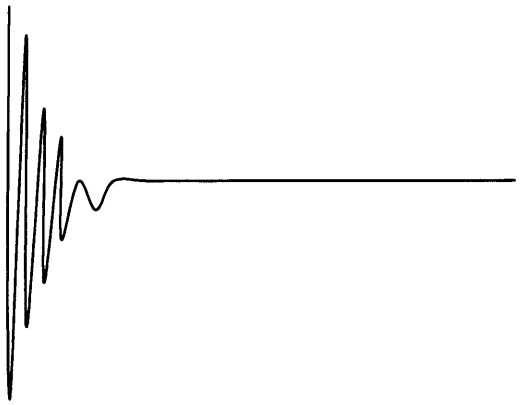

Figure 4.2. *Free induction decay. The signal decay following a 90° RF pulse.*

T_2* relaxation consists of two independent elements and their relationship is defined by:

$$1/T_2^* = 1/T_2 + 1/T_2'$$

The T_2 component refers to the fundamental loss of phase coherence in the x-y plane over time. Also known as the transverse or spin-spin relaxation time, T_2 describes the alteration of the precession rates of the nuclei through interactions with neighbouring nuclei, and this takes place independently of energy exchange with the lattice.

The T_2' component describes the effects of magnetic field inhomogeneities that result in the dephasing of spins. T_2* comprises both of these elements and it is the susceptibility of T_2* to field inhomogeneities that makes it sensitive to the blood oxygenation level dependent, or BOLD, effect, which is widely used in functional MRI studies.

The relaxation times that have been described so far only characterise the processes that occur in the x-y plane. A further relaxation time describes the recovery of net magnetisation along the z-axis, and this is the T_1 relaxation time. Also known as the longitudinal or spin-lattice relaxation time, this time constant describes the rate of energy exchange between the excited hydrogen nuclei and their molecular environment, which may be facilitated by the presence of macromolecules and tissue structures in the immediate surroundings.

T_1 and T_2 describe fundamental processes in NMR, and both can be measured through manipulation of the nuclei with particular sequences of radiofrequency pulses applied at the resonance frequency. T_1 and T_2 are commonly measured using the inversion recovery and the Hahn spin echo sequences respectively. Both will be described in brief below.

4.3.1. The inversion recovery sequence

The inversion recovery sequence is the most well known method for interrogating T_1 (see fig. 4.3). It consists of two RF pulses: a 180° pulse followed by a 90° pulse. The initial 180° pulse flips the net magnetisation from the +z direction to the –z direction and this then gradually relaxes back to the original state. A 90° pulse is then applied before the net magnetisation completely recovers, tilting the net magnetisation into the x-y plane and thus enabling the signal to be detected. A delay time (TD) then allows the magnetisation to return back to equilibrium.

The period between the two pulses is called the inversion time (TI). By scanning at a series of different TI times T_1 can then be determined.

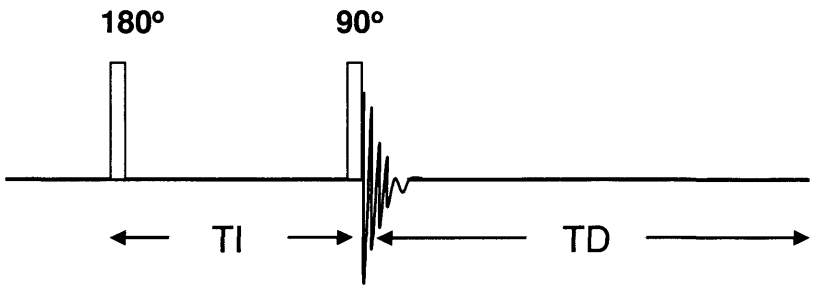

Figure 4.3. *The inversion recovery sequence. TI, or the inversion time, is the time between the initial 180° and the subsequent 90° RF pulse for investigating T_1. The 90°RF pulse tilts the magnetisation along z into the x-y plane whereby the signal can be detected. A delay time, TD, then allows the net magnetisation to recover to equilibrium.*

4.3.2. The Hahn spin echo sequence

The Hahn spin echo sequence involves two RF pulses, 90° and 180°, separated by a time known as TE/2 (fig. 4.4). TE, or echo time, is the time between the initial 90° pulse and the resulting echo signal. The 90° pulse tilts the magnetisation into the x-y plane and, as previously mentioned, the signal decays due to the loss of coherence as the nuclei dephase over time. In essence, the dephasing occurs as a result of some nuclei spinning faster or slower due to T_2* processes.

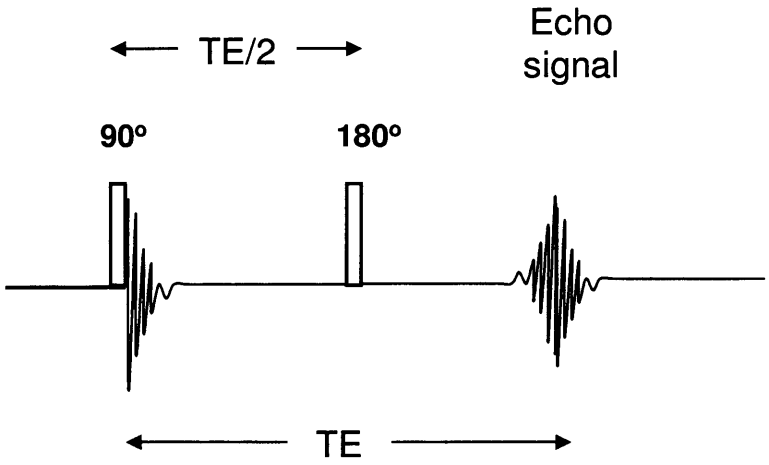

Figure 4.4. *The Hahn spin echo. TE, or echo time, is the period between the initial 90° pulse and the resulting echo signal. Note that the echo signal resembles a reflected image of a free induction decay signal as the nuclei regain and then lose coherence.*

A simple analogy is a clock with an hour hand and a minute hand. If following a 90° RF pulse both hands point at 12 then, following a period of time, the two hands separate as the minute hand moves faster in the clockwise direction, which is akin to losing coherence in the x-y plane. If a 180° RF pulse is applied at time TE/2, then this causes both hands to move in an anti-clockwise direction. At this point, the minute hand is now behind the hour hand and following another period of TE/2, the minute hand reaches back to 12 at the same time as the hour hand. This results in the echo signal. Thus the 180° RF pulse acts as a refocusing pulse. However intrinsic T_2 relaxation processes leads to a loss of signal that cannot be retrieved by this refocusing, and therefore the resulting signal yields information

about T_2. T_2 can be determined by performing experiments using a series of different TE values.

4.4. THE BASIS OF IMAGING USING NMR

In MRI, a series of magnetic gradients are required for spatial localisation of signal from a sample. MR imaging manipulates two components of the signal generated following the application of an RF pulse: the *frequency* at which the spins oscillate, and the *phase* at which this oscillation occurs. This can be achieved by applying three gradients along the x, y and z planes, the timings of which are illustrated for a single-slice spin echo sequence in figure 4.5.

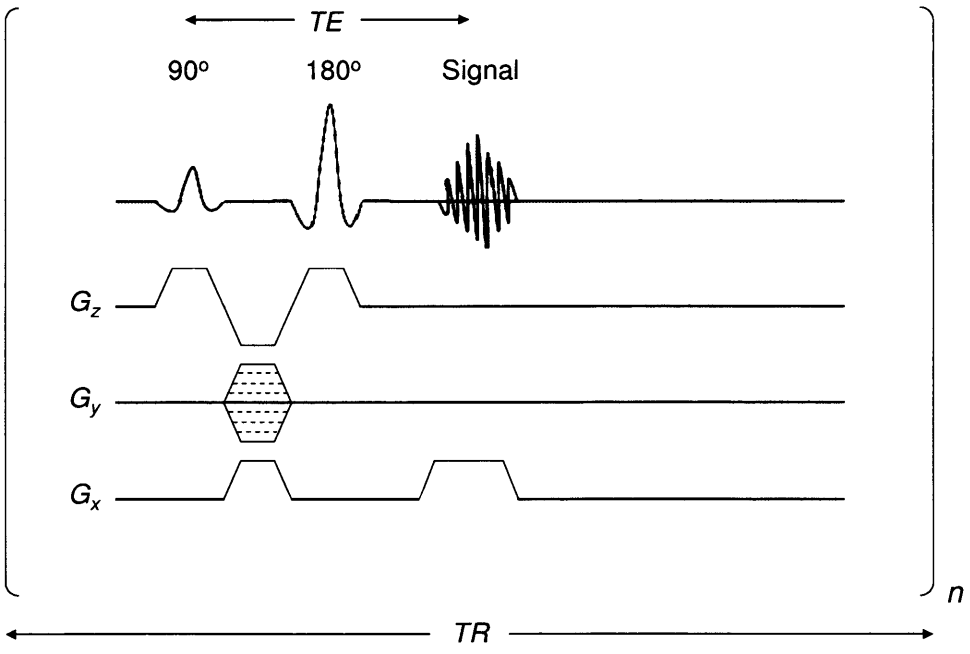

Figure 4.5. *Radiofrequency pulse and gradient timings for a two-dimensional Fourier-transform imaging sequence. G_z is the gradient for slice selection, G_y is the phase-encoding gradient, and G_x is the read gradient. The dashed lines on the G_y gradient indicate that n G_y values are acquired in consecutive scans. TR denotes repetition time and TE denotes echo time.*

The first gradient, G_z, that is applied is along the z-axis and is known as the slice select gradient. When this field gradient is applied, the nuclei experience different fields according to the position along the z-axis, and thus the nuclei at each point along z have a specific Larmor frequency. Therefore if an RF pulse is applied that encompasses only a specific bandwidth of frequencies then this would result in an excitation of the nuclei within a selected slice. However, this gradient causes the nuclei to dephase and thus a negative gradient is applied following excitation to remove these effects. Similarly to the 90° excitation pulse, the G_z gradient is applied again during the 180° pulse to select the region for excitation.

The second gradient, G_y, is applied after RF excitation and is called the phase encoding gradient. Applied along the y-axis, the phase encoding gradient acts to alter the phase of the spins relative to their previous state such that the phase change can be subsequently detected. In order to do this, this gradient is applied after the excitation pulse and before signal acquisition. The amplitude of this gradient is altered in a step-wise fashion following signal acquisition thereby altering the phase of the spins to differing degrees.

The third gradient, G_x, is known as the frequency encoding, or readout, gradient and this is applied along the x-axis during the acquisition of the echo signal. This field gradient causes the spins to experience different fields according to the position along this axis, and therefore to oscillate at correspondingly different frequencies. Similarly to the G_z gradient, the frequency encoding gradient also causes dephasing and therefore a compensatory gradient is also applied before the acquisition of signal.

The matrix of raw data acquired in this way has to be processed to obtain the final image and this is achieved by using the Fourier transform, which defines a relationship between a signal in the time domain and its representation in the frequency domain. The signals undergo a 2 dimensional Fourier transformation to extract the signal intensities as well as the spatial distribution of the spins in the x-y plane. By manipulating the gradients and the RF pulses, different types of image contrast can be generated.

4.5. DIFFUSION AND PERFUSION IMAGING

T_1 and T_2 , which reflect the physical micro-environment of water in tissue, form much of the basis of tissue contrast in MRI and can provide excellent definition of structures in the brain (Gadian, 1996; van der Weerd *et al.*, 2004). This is because water molecules can be free or bound to macromolecules and their state will affect T_1 and T_2; this can be exploited to give the contrast seen in MR images. However, a drawback to these methods is that the precise relationship between these parameters and physiological phenomena is not completely clear.

Diffusion and perfusion imaging are sophisticated techniques for generating tissue contrast and can be directly related to physiological phenomena. For these reasons, diffusion and perfusion imaging, along with T_1 and T_2, were incorporated into our studies. In the following section the theory that underlies these techniques is reviewed.

4.5.1. Diffusion

Free diffusion describes the unrestricted random movement of molecules in space over a given period of time. However, diffusion is restricted in complex biological systems because of the presence of natural barriers such as cell membranes, and therefore it is not truly free (Baird and Warach, 1998). Therefore in biological tissues, self-diffusion of water is referred to as apparent diffusion, and it can be described quantitatively by the apparent diffusion coefficient (ADC), which has units of mm^2sec^{-1}. ADC can be influenced by a variety of factors including temperature, viscosity of the medium and the local microarchitecture of the tissue.

MR imaging can be made sensitive to diffusion by using a pair opposing magnetic field gradient pulses to spatially encode water molecules (Baird and Warach, 1998) (fig,4.6). If the water molecules remain in the same position following the gradient pulses, then they experience the full extent of the opposing pulses and thus will not generate any loss of signal. However, if the water molecules have moved away from their original position then

the second pulse, or rephasing pulse, leads to a loss of signal such that the degree of signal change is inversely related to the degree of diffusion. This is why on diffusion-weighted images the areas of high diffusion will appear hypointense and low diffusion will appear hyperintense, while the opposite is observed in the calculated ADC maps. Additionally, it is also worth noting that diffusion can occur in *any* direction and therefore encoding diffusion along only one axis is not sufficient to measure ADC. Thus a series of encoding gradients in different directions have to be applied for calculating ADC.

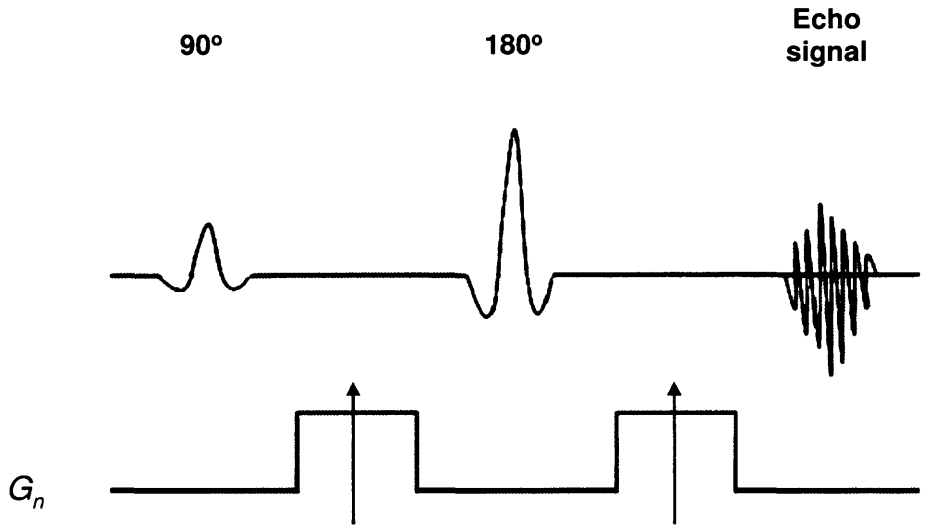

Figure 4.6. *A spin-echo sequence with the incorporation of gradients that generate diffusion weighting. These gradients (G_n) can be applied along any axis, and generally multiple directions are required to ensure no directional bias. Also the amplitude of these gradients can be modulated to change the degree of diffusion-weighting as indicated by the arrows. By performing these steps, ADC can be directly calculated from the resulting set of images.*

4.5.2. Perfusion

Blood provides a constant source of essential nutrients for tissue function and survival. It is delivered to the tissue by the vascular system, but it is only through the capillaries that the exchange of oxygen, nutrients and clearance of waste products between tissue and blood occurs, and this is reflected in perfusion or cerebral blood flow (CBF). This contrasts with bulk flow through major vessels, such as arteries and veins, in which no exchange occurs.

As such, perfusion is defined as the volume of blood delivered to a mass of tissue within a given period of time with units of ml/100g/min (Thomas *et al.*, 2000). For the purposes of the present study, measuring perfusion can identify changes in the haemodynamics of tissue during SE and subsequent injury.

There are two main MRI approaches for measuring CBF: bolus tracking and arterial spin labelling (ASL). The bolus tracking methods are widely used clinically, and require the intravenous injection of an exogenous tracer, a gadolinium-based contrast agent. The ASL techniques also require a tracer, but this tracer is endogenous in the sense that the water protons in blood are magnetically labelled, and because of this, ASL methods allow multiple measurements to be performed without the limitations associated with administrating exogenous substances. This is the main reason that the ASL methods were chosen for our studies on SE.

The ASL methods for perfusion measurement are based on the fact that the magnetisation and relaxation characteristics of tissue water are affected by the inflow of blood water (Thomas *et al.*, 2000). MR imaging can be made sensitive to CBF if the magnetic spin state of blood water is different from that of the tissue. This can be achieved by magnetically labelling the blood water that will flow into the imaging slice. In the current study, a continuous ASL (CASL) method was used for labelling the blood (Detre *et al.*, 1992).

The CASL techniques require the acquisition of two images: a CBF-sensitised image in which the blood has been magnetically labelled, and a control image. In this technique, a radiofrequency pulse is continuously applied to a pre-determined set of blood vessels in order to invert or tag the blood entering the imaging slice. This tagging is typically applied to the neck in which there are four major vessels that supply blood to the brain. When the labelled blood perfuses the brain tissue of the imaging slice, there is an exchange of spins and this alters the magnetisation and relaxation characteristics of the tissue, and thus renders the image sensitive to CBF. A control image is also acquired in which the blood is not labelled. The difference between the two images is directly related to blood flow and therefore CBF can subsequently be calculated.

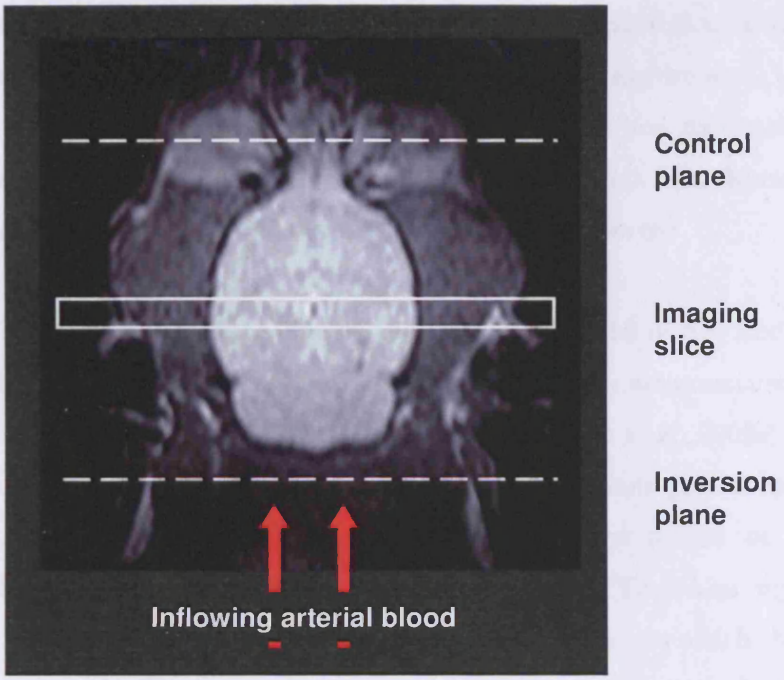

Figure 4.7. *Representation of the continuous arterial labelling (CASL) technique. An axial scan of the rat brain showing the position of the imaging, control and labelling planes. Blood inflowing from the neck is magnetically labelled when passing through the inversion plane. The site of the inversion slice was chosen in each animal by locating the coordinates for the back of the cerebellum. The control plane was chosen by default to be equidistant to the imaging slice in the opposite direction.*

4.6. MRI IN EXPERIMENTAL EPILEPSY

4.6.1. T_1 and T_2 in epilepsy

T_2 increases in the hippocampus have been observed following SE in humans (VanLandingham *et al.*, 1998; Scott *et al.*, 2003) and also in a variety of SE models including both chemically-induced and electrically-induced models (Bhagat *et al.*, 2001; Roch *et al.*, 2002a; Dube *et al.*, 2004; Nairismagi *et al.*, 2004). In all of these MR studies, transient T_2 changes have been reported within the first 7 days after SE and they have been interpreted as reflecting the presence of oedema.

Righini and colleagues performed one of the first studies that followed the progression of brain injury after SE for longer than the initial few hours (Righini *et al.*, 1994). After KA-induced SE, the rats were imaged from 3 hours to 9 days and the investigators noted a hyperintense T_2-weighted signal from 24 hours to 72 hours after kainate injection. An initial decrease in ADC followed by an increase was also observed.

In a study that investigated the lithium-pilocarpine rat model of SE, Roch and colleagues observed T_2-weighted hyperintensities and demonstrated a clear association between these hyperintense regions and areas of neuronal swelling (Roch *et al.*, 2002a). Therefore, they suggested that the T_2 changes that were observed in the acute period are likely to reflect oedema formation and resolution, which parallel interpretations of similar changes observed in stroke research (Baird and Warach, 1998). They also reported an initial transient MRI change in the piriform and entorhinal cortices, in which there was a period of normalisation by 5-9 days and a subsequent hyperintense T_2 signal in the chronic phase (3-9 weeks). The investigators noted that the latter phase appeared to coincide with the onset of spontaneous seizures (Roch *et al.*, 2002a). A similar T_2 change in the limbic areas following electrical stimulation of the amygdala was also reported by Nairsmagi and colleagues (Nairismagi *et al.*, 2004). However, neither of these studies have been able to provide any evidence of a relationship between these early MR changes and subsequent severity of epilepsy (Nairismagi *et al.*, 2004). It is also worth noting that late T_2 increases have been observed in patients and in experimental models which correlated with neuronal loss and the neuropathological features of MTS (Briellmann *et al.*, 2002; Roch *et al.*, 2002a).

In a study by Jupp and colleagues in the amygdala-kindled rat model, T_2 changes were also reported. They reported progressive T_2 increases in focal regions of the hippocampus without any changes in hippocampal volume, which suggests that T_2 can change without any concomitant cell loss (Jupp *et al.*, 2006). A similar phenomenon has also been observed in the experimental febrile seizure rat model (Dube *et al.*, 2004). Dube and colleagues reported a transient T_2 change without any histological evidence of cell death, and they suggested that the T_2 change may indicate pathological cellular processes such as oedema that promote epileptogenesis.

4.6.2. Diffusion in epilepsy

Non-invasive MR imaging of animal models of epilepsy began in the early 1990s (Lythgoe *et al.*, 2002). These early studies used ADC and T_2-weighted imaging to investigate SE and focussed on the acute structural changes following a seizure. These studies reported reductions in ADC, during and shortly after SE, in a variety of seizure models without concomitant T_1 and T_2 changes at early time points (Zhong *et al.*, 1993; Zhong *et al.*, 1995; Prichard *et al.*, 1995; Ebisu *et al.*, 1996).

Since then, ADC changes associated with SE have been described during the acute period with reports of both increases and decreases in ADC (Tokumitsu *et al.*, 1997; Wall *et al.*, 2000; Fabene *et al.*, 2003; Engelhorn *et al.*, 2007). Engelhorn and colleagues investigated ADC changes during SE in the pilocarpine rat model, and reported that ADC values were decreased 90mins after SE onset in all the regions that were analysed, which included the hippocampus, thalamus, piriform cortex and the cortex. However, by 120mins of SE most regions had returned to baseline with the exceptions of the hippocampus and the thalamus. An ADC decrease was also reported by Zhong and colleagues in the flurothyl rat model after 80mins of SE (Zhong *et al.*, 1995). In contrast, van Eijsden and colleagues noted a significant hippocampal ADC increase at 3h of SE, which returned to baseline by 5h of continuous seizure activity in the isoflurane-anaesthetised lithium-pilocarpine rat model (van Eijsden *et al.*, 2004).

Nakasu and colleagues investigated ADC changes over a period of 7 days in the kainic acid rat model (Nakasu *et al.*, 1995). They observed an initial ADC decrease at the 1h time point, with a subsequent dramatic decrease in the amygdala-piriform cortex at 24h. By 3 days, this region had normalised. In contrast, no significant ADC changes were observed in the hippocampus or in the parietal cortex. On the other hand, hippocampal ADC decreases were observed following the induction of SE with the anti-cholinesterase inhibitor, soman, by Bhagat and colleagues (Bhagat *et al.*, 2001).

In another study, Wall and colleagues monitored diffusion changes over a 24h period (Wall *et al.*, 2000). They also observed striking ADC decreases in the piriform cortex. They

imaged at 3, 6, 9, 12 and 24h after pilocarpine-induced seizures, and reported a maximal ADC decrease in the piriform cortex at 12h, which remained low at 24h, while cortical ADC was decreased at 12h but had returned to baseline by 24h. In the hippocampus, ADC was significantly increased by 24h. This hippocampal ADC increase was also observed following pilocarpine-induced SE at 12 h (Fabene *et al.*, 2003). Fabene and colleagues also noted that ADC decreased in the amygdala and the cortex of these rats.

In all of these studies, decreases in ADC have been attributed to cytotoxic oedema, whereas the ADC increases were considered to be due to a breakdown of the blood-brain-barrier leading to vasogenic oedema. ADC changes have been most frequently characterised in stroke, and it is in stroke studies that Moseley and colleagues established that ADC decreases following ischaemia were the result of the formation of cytotoxic oedema and a consequence of the relocation of water from the extracellular to the intracellular compartment (Moseley *et al.*, 1990). This has been subsequently demonstrated in SE, and it has been suggested that this is due to excitotoxic seizure activity, which disrupts ion homeostasis leading to movement of water from extra- to intracellullar space (Baird and Warach, 1998; Roch *et al.*, 2002a). Evidence of cell death and neuronal swelling following SE has been reported at times that coincide with ADC decreases (Wall *et al.*, 2000; Roch *et al.*, 2002a).

The nature of the diffusion changes remains controversial, especially with regards to the hippocampus. Both ADC increases and decreases have been reported in the early period, but these changes may reflect the length of SE or the mode of induction, which can influence outcome (Fujikawa, 1996).

4.6.3. Perfusion in epilepsy

There have only been a few studies that have used MRI to investigate the haemodynamic response related to SE. One of the early studies was by Fabene and colleagues (Fabene *et al.*, 2003), who investigated the effects of pilocarpine-induced SE at 12h by measuring relative cerebral blood volume (rCBV) using an iron-based contrast agent. They observed regional areas of high rCBV, most notably in the hippocampus, cerebral cortex and the

thalamus. They noted concomitant diffusion- and T_2-weighted changes in these regions and attributed these changes to oedema formation. Furthermore, the areas with the most substantial increases in perfusion were areas associated with areas that displayed the greatest neuronal loss. Fabene and colleagues followed up this study with another in which they imaged rats after 4-aminopyridine-induced SE at 2h, 24h and 3 days (Fabene *et al.*, 2005). They reported decreases in ADC and T_2-weighted hyperintensities in the hippocampus, medial thalamus, temporal and parietal cortices that normalised by 3 days. For rCBV, they observed increases that were highest at 2h post-seizure induction in the hippocampus (16%), the parietal cortex (32%) and the medial thalamus (44%), which all normalised by day 3. Their analysis with electron microscopy indicated that these early changes at 2h were associated with astrocytic swelling, which gradually resolved by day 3.

Engelhorn and colleagues used a semi-quantitative approach with a gadolinium-based contrast agent for investigating perfusion changes during pilocarpine-induced SE (Engelhorn *et al.*, 2005). They observed perfusion increases during the early phase of SE and a subsequent decrease as SE progressed up till 2h. They reported that areas with a maximal decrease in perfusion were associated with substantial neuronal loss. These studies indicate that perfusion-imaging is sensitive to various changes in the brain following and during SE. However, perfusion imaging has yet to be used to investigate these processes in a longitudinal fashion, and therefore this type of imaging forms part of the studies that are presented in the later chapters of this thesis.

4.7. SUMMARY

This chapter has aimed to review briefly the basic theories that underlie MRI and also the variety of different imaging techniques that have been used in the current project. In addition, a review of MRI studies on seizures, epileptogenesis and epilepsy demonstrate that these longitudinal and multiparametric investigations can provide important information about the underlying disease processes.

CHAPTER 5: METHODOLOGICAL DEVELOPMENTS

If I find 10,000 ways something won't work, I haven't failed. I am not discouraged, because every wrong attempt discarded is another step forward

Thomas A. Edison

5.1. INTRODUCTION

The main aim of the work presented in this thesis was to use MRI to monitor changes in brain structure and function during SE and the evolution of subsequent injury.

For animal MR imaging, anaesthesia is typically used to reduce stress and to limit motion, as stress can influence physiology and motion can distort the acquired images. However, using anaesthesia for imaging SE and subsequent injury presents a problem in that the effect of anaesthesia on these phenomena are not completely understood.

Although the precise mechanisms of action of anaesthetic agents are unknown, these drugs are known to exert their effect by acting directly on the CNS. This therefore suggests that anaesthesia could potentially influence our investigations into SE. This is supported by the fact that anaesthetic agents are used for the treatment of refractory SE (Shorvon, 1994), which suggests that SE could be modulated by these drugs. Furthermore studies have demonstrated anaesthetic agents can influence pathology in a number of brain insults, including cerebral ischaemia and traumatic brain injury (Warner *et al.*, 1993; Statler *et al.*, 2006), but the neuroprotective effect has also been suggested to delay rather than prevent the evolution of the injury (Kawaguchi *et al.*, 2000). Also halothane, an inhalant anaesthetic, has been shown to confer a neuroprotective effect *during* electrically-induced SE (Walker *et al.*, 1999), and thus indicates that altering SE with anaesthesia can influence post-SE pathology. Taken together, these data suggest that anaesthesia may have an effect on SE and subsequent injury. As the effects of anaesthesia have not been determined, the MRI investigations were divided into two distinct components:

1) MRI of brain injury following SE
2) MRI during SE

For these investigations, a series of preliminary studies were carried out in order to arrive at the final methodologies used in the later chapters of this thesis. In this chapter, the key developments in these methodologies for each of these components are presented, the first of which was to set up an animal model of SE. The developments began with the

experiments for MRI of brain injury following SE as standard techniques were used and the pilot studies conducted were to investigate the most appropriate time points for study. The developments for MRI during SE include investigations into an appropriate anaesthetic for seizure induction, and modifications of the MRI set up for the later investigations.

5.2. SETTING UP THE PILOCARPINE/LITHIUM-PILOCARPINE MODEL

The lithium-pilocarpine model was used for the reasons given in section 3.6. The lithium-pilocarpine model and pilocarpine model have similar patterns of seizure onset and neuronal damage (Clifford *et al.*, 1987). However, for the lithium-pilocarpine model there is an extra step, in that a pre-treatment with lithium chloride is required. As this was the first epilepsy model to be set up in our laboratory, the availability of expertise from the UCL Institute of Neurology, London with the pilocarpine model meant that it was prudent to start with this particular model before moving on to the lithium-pilocarpine model.

5.2.1. The Racine scale: behavioural assessment of SE

One of the requirements of establishing an SE model is that there needed to be a method for assessing the progression on to SE. A convenient and standard method of assessing the progression of seizure activity and SE is by using a stereotypical behaviour scale, which was first developed in experiments by Racine (Racine, 1972). This scale, known as the Racine scale, is presented below in table 5.1 together with the corresponding seizure type; the onset of SE parallels seizure stage 3.

Seizure stage	Animal behaviour	Seizure type
0	Immobility	Partial
1	Facial automatisms	Partial
2	Head nodding	Partial or secondary generalised
3	Unilateral forelimb clonus/bilateral forelimb clonus	Secondary generalised
4	Bilateral forelimb clonus and rearing	Secondary generalised
5	Rearing, falling and generalized convulsions	Secondary generalised

Table 5.1. *The Racine scale for behavioural assessment of seizure progression in the rat with the corresponding seizure type.*

5.2.2. The rationale for a seizure of 90 minutes

It was decided that a 90 minute prolonged seizure was appropriate for the proposed investigations. This was because a persistent pilocarpine-induced SE lasting for 90 minutes has been shown to result in all animals progressing on to spontaneous recurrent seizures (Mello *et al.*, 1993). Also, earlier suppression of SE has been demonstrated to lead to fewer animals developing spontaneous recurrent seizures (Lemos and Cavalheiro, 1995). A longer seizure duration was not considered because a higher mortality rate is associated with longer and more severe episodes of SE (Cavalheiro *et al.*, 2006).

Two pilot studies were undertaken to assess the successful implementation of a seizure that lasts for 90 minutes, first in the pilocarpine model and then in the lithium-pilocarpine model. The outcome measures for both studies were that the animals progressed on to Racine stage 3 and that the seizure had to continue for 90 minutes, at which point diazepam was given to abolish SE. All injections were administered intraperitoneally.

5.2.3. The pilocarpine protocol

The following protocol, courtesy of Dr. Annalisa Scimemi (Department of Clinical and Experimental Epilepsy, UCL-Institute of Neurology), was used to induce and abolish SE:

a) Methylscopolamine 1mg/kg 20 minutes before pilocarpine
b) Pilocarpine hydrochloride 320mg/kg
c) Methylscopolamine 1mg/kg 60 minutes after 1st dose
d) Diazepam 10mg/kg 90 minutes after onset of SE (stage 3 Racine scale)

Seven Sprague-Dawley rats underwent this protocol. One animal died 30 minutes after the administration of pilocarpine. Two rats did not progress onto SE but did display some head nodding behaviour. Four of the animals progressed onto stage 3 of the Racine scale by 40 minutes, and proceeded on to stage 5. All of the rats that progressed on to SE continued to display the stereotypic behaviour until after diazepam administration.

5.2.4. The lithium-pilocarpine protocol

The differences between the pilocarpine model and the lithium-pilocarpine model are that lithium is administered typically between 18-24h before pilocarpine, and also a lower dose of pilocarpine is required for SE. It is notable that pre-treatment with lithium can be given between 2-24h before pilocarpine without affecting the number of animals that will express SE (Chaudhary *et al.*, 1999). Referring to the literature, 3mEq/kg of lithium chloride and 30mg/kg of pilocarpine were the standard dosages used. The following protocol was used:

a) Pre-treatment with lithium chloride, 3mEq/kg, 18-24 hours prior to SE induction
b) Methylscopolamine 1mg/kg 20 minutes prior to pilocarpine
c) Pilocarpine hydrochloride 30mg/kg
d) Methylscopolamine 1mg/kg 60 minutes after 1st dose
e) Diazepam 10mg/kg 90 minutes after the onset of SE (stage 3 Racine scale)

Four rats underwent the protocol. All of the animals progressed onto SE within 40 minutes, and the seizure continued until after diazepam administration.

These pilot studies demonstrated that SE could be successfully induced using either the pilocarpine or the lithium-pilocarpine methods, and that the seizure will last for at least 90 minutes.

5.3. MRI OF BRAIN INJURY FOLLOWING STATUS EPILEPTICUS

The main aim of this study was to use MRI to characterise brain injury following SE and to identify any early predictors of outcome. The main benefits of using MRI are the ability to provide longitudinal multi-parametric information in individuals. As such, an approach was used that incorporated quantitative T_1, T_2, ADC and CBF as well as a high resolution whole brain anatomical scan at a range of time points. However, the chronic MRI monitoring of disease processes is a time-consuming and costly endeavour. Therefore it was crucial to establish the most appropriate time points before beginning such a study.

Two pilot studies were undertaken for this purpose. The first was to evaluate whether there are any significant changes over the initial hours following the termination of SE, and the second study was used to evaluate long term changes following SE.

5.3.1. MRI

Scans were performed on a 2.35T horizontal bore magnet (Oxford Instruments, UK) interfaced to a SMIS console (Guilford, UK). Physiological parameters monitored include electrocardiography (ECG) recordings and rectal temperature, which was maintained at 37±1°C using an air warming system.

All animals were anaesthetised with 1.5% isoflurane in a 60:40 N_2O:O_2 mix delivered via a nose cone and placed on a animal holder with bite and ear bars securing the head to

minimise movement artefacts. Physiological parameters monitored include electrocardiography (ECG) recordings and rectal temperature, which was maintained at 37±1°C using an air warming system.

Images were acquired using a volume transmitter coil and a separate decoupled surface receiver coil. A central coronal imaging slice was selected that included the hippocampus and the piriform cortex (-3.3mm from bregma). The central slice was determined by visual inspection of anatomical landmarks. All sequences were run using a 2mm-thick coronal slice.

T_2 maps were obtained using the multiple acquisition of spin and gradient echoes with an interleaved echo planar imaging (MASAGE-IEPI) sequence (Thomas *et al.*, 2002). The parameters used were: TR=1,500 ms, 16 averages, with TE_1=24 ms, TE_2=65 ms, TE_3=106 ms (for definitions of $TE_{1/2/3}$, see Thomas *et al*, 2002).

Quantitative ADC maps were calculated from trace-weighted single shot spin-echo EPI images. The parameters were as follows: TR = 1500 ms, TE = 56 ms, 48 averages, b= 38 and 872 s/mm^2. Duration of acquisitions: T_2 = 4 mins and ADC = 9 mins.

5.3.1.1. Image processing and data analysis

ADC and T_2 maps were reconstructed using in-house software written in IDL Software Version 5.6 (Research systems Inc., Boulder, CO, USA). The hippocampus was delineated on all processed images and analysed with SMIS Image Display Version 3.7.

5.3.2. MRI within the first 4 hours after SE

The progression of pathological changes during the initial hours following SE was not known, and thus a brief investigation was conducted to provide an indication of whether there are any substantial changes following SE during this early period.

Two animals were used to investigate this initial period following SE and to see whether MRI can be used to detect any notable changes. SE was induced in two animals and serially

imaged using T_2 and diffusion at 30, 60, 120, 150 and 210 minutes following SE (fig. 5.1). The images were assessed and no changes in either ADC or T_2 in the brain were found over this period. This experiment indicated that there were no overt MR changes within the initial 210 minutes following SE, which was important for the purposes of imaging on day 0 after SE.

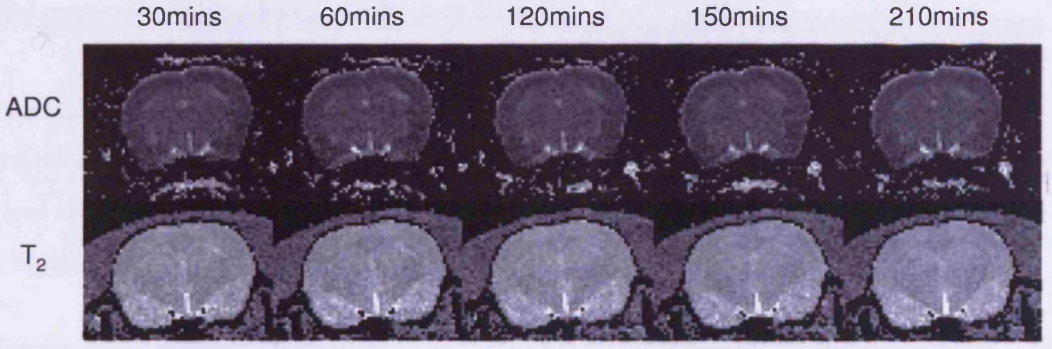

Figure 5.1. *ADC and T_2 maps in the first 210 minutes following SE.*

5.3.3. MRI following SE over 77 days

The aim of this pilot study was to establish that it was possible to image animals following SE for an extended period, and that these animals could survive SE followed by serial anaesthesia. Four adult male Sprague-Dawley rats weighing 200-275g underwent the lithium-pilocarpine protocol (section 5.2.2). The animals were scanned at various time points after SE. Imaging was as follows:

Rat 1: 1, 5, 7, 14, 21, 28, 35, 42, 56, 63, 70 and 77 days
Rat 2: 5, 7, 14, 21, 28, 42, 49, 56, 63, 70 and 77 days
Rat 3: 3, 7, 14, 21, 28, 35, 42, 49, 56, 63 and 70 days
Rat 4: 1, 3, 7, 14, 21, 28, 35, 49, 56, 63 and 70 days

The hippocampal T_2 data are presented in figure 5.2. No overt changes in T_2 or ADC were observed over the initial few days after SE in the hippocampus other than on day 3 for rat 4. This change on day 3 was consistent with experimental and clinical studies in which an

early and transient response has been reported (Nakasu *et al.*, 1995; Scott *et al.*, 2002; Roch *et al.*, 2002a). However, the region associated with the hippocampus at the beginning of the study displayed concomitant high T_2 and increased ADC during the later periods following SE (fig. 5.3), which is consistent with the presence of CSF and an increase in ventricular volume. This suggests that the hippocampus continues to atrophy following the early period, however the hippocampus tissue did not demonstrate any further changes, which parallel previous MRI studies (Nairismagi *et al.*, 2004).

Furthermore, visual inspection of the images suggests that there was little difference between day 21 and day 70 (fig. 5.3). Therefore these data indicate that MRI can detect changes only during the acute phase following SE and that the later periods are associated with hippocampal atrophy and ventricular enlargement, which stabilised by day 21.

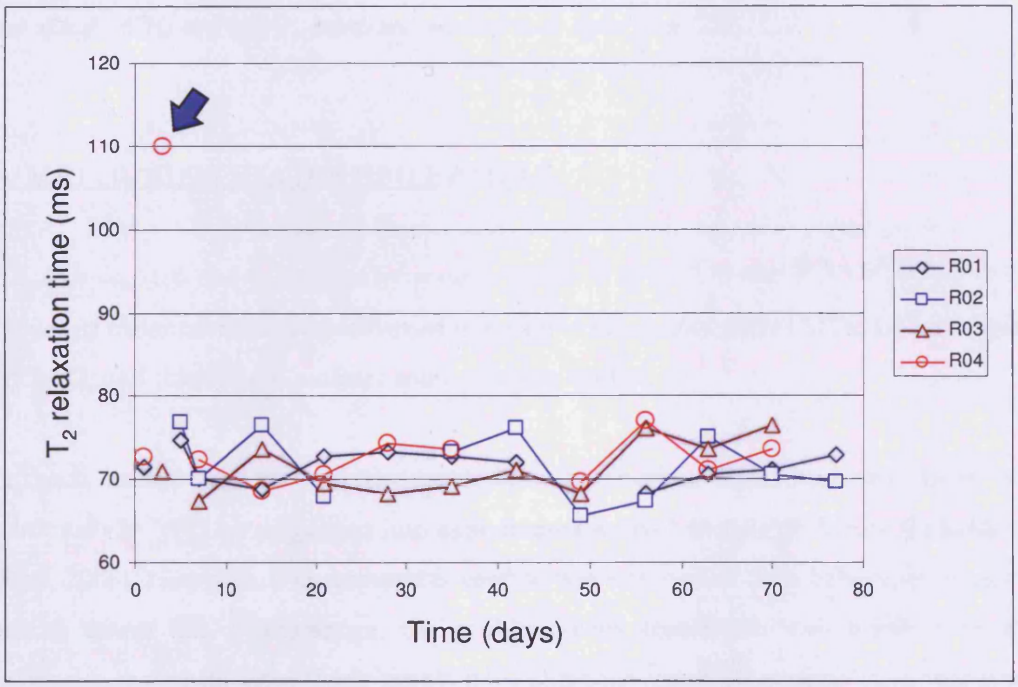

Figure 5.2. *Chronic hippocampal T_2 time course following SE. Four animals were imaged over a variety of times. Blue arrow indicates that there was a high hippocampal T_2 3 days after SE for rat 4 (R04). No other changes were observed.*

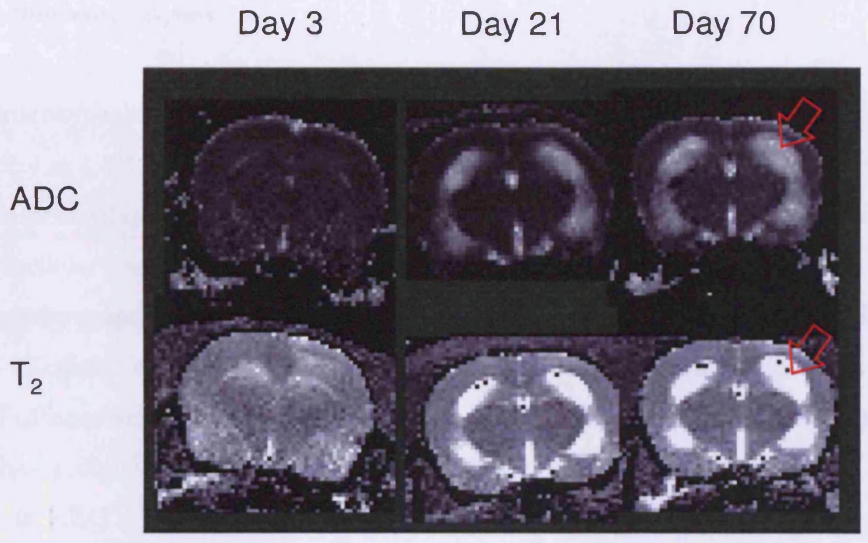

Figure 5.3. *ADC maps and T_2 maps acquired on 3, 21 and 70 days post-SE. Red arrows indicate areas of high ADC and high T_2, which are consistent with signal from CSF.*

5.4. MRI DURING STATUS EPILEPTICUS

A series of experiments were performed to design a set up that allows SE to be investigated with MRI, and this section outlines some of these studies.

For both ethical reasons and the prevention of motion, anaesthesia has been used traditionally in MRI investigations into experimental animal models of disease (Lukasik and Gillies, 2003). However, if anaesthesia is used to prevent motion then behaviour cannot be used to assess SE. Furthermore, the problem with anaesthesia also presents another problem in that many anaesthetic agents have anti-convulsant properties. Therefore it was necessary to use an alternative method for assessing SE, and EEG was set up for this purpose.

5.4.1. The electroencephalogram

The electroencephalogram (EEG) has been the primary tool for investigating epilepsy since its discovery in 1924. EEG measures the extracellular electrical signal that originates in the changes in postsynaptic potentials at neuronal cell bodies and dendrites of pyramidal cells. The extracellular currents that are generated are small, but it is the summation and synchrony of the activity of a large population of neurons that generates a detectable signal for EEG (Teplan, 2002). EEG is the only method that directly measures activity in the brain and offers a very high temporal resolution in the order of milliseconds. On the other hand, it has a disadvantage in that it cannot offer much in spatial information (Teplan, 2002). It is EEG's sensitivity to synchronous neuronal activity that makes it the gold standard tool for investigating and diagnosing epilepsy.

It is notable that MRI offers excellent spatial resolution and that the combination of EEG with MRI techniques has been implemented for investigating brain function (Linden, 2007; Mantini *et al.*, 2007). However, the implementation of these methods in parallel is not trivial. Problems exist in that the EEG electrodes have to be compatible with MRI. Also the action of the MRI gradients can lead to disruption of the EEG signal and therefore sophisticated software is required to extract the EEG information. Thus the simultaneous acquisition of EEG and MRI was not considered for this project.

5.4.2. Investigation into inducing and maintaining SE for 90 minutes under anaesthesia

5.4.2.1. Introduction

In clinical medicine, general anaesthesia is always used as an adjunct to another procedure with the sole exception of the treatment of refractory SE (Campagna *et al.*, 2003). The potentiation of the $GABA_A$ receptor and the inhibition of excitatory ion channels, such as the neuronal nicotinic and glutamate receptors, lead to the reduction in neuronal excitability and underlie the mechanisms of action of the general anaesthetics (Rudolph and Antkowiak, 2004). However, the inhibitory effect of anaesthetics presents a problem in that

one of the aims of this project was to use MRI to investigate the onset and termination of SE, which requires exciting the brain.

Certain anaesthetic agents have been associated with seizure activity. For example, lignocaine at high doses has been shown to induce seizures but on the other hand it is an effective anti-convulsant at lower doses (Shorvon, 1994). Nonetheless, this particular agent cannot be used because if a seizure is to be induced then this would lead to motion artefacts during MRI. As some anaesthetics may have a pro-convulsant effect, the aim of the present experiments was to investigate the induction and maintenance of SE under an anaesthetic regimen. Two were chosen: isoflurane and fentanyl/medetomidine.

5.4.2.1.1. Isoflurane

Isoflurane is a volatile gaseous agent that belongs to a class of drugs known as the inhalant anaesthetics, which include halothane and sevoflurane (Campagna *et al.*, 2003). The precise mechanism of action for isoflurane, like the other drugs of its class, remains unclear; however it has been shown to have action on various neurotransmitter systems including those of GABA, glycine, acetylcholine and glutamate.

Isoflurane is a commonly used anaesthetic in MR studies of small animals (Lukasik and Gillies, 2003). Its main advantage is that, as an inhalant anaesthetic, it is simple to modulate the depth of anaesthesia to maintain homeostasis, and it is cleared rapidly from the body making it particularly suitable for MRI (Flecknell *et al.*, 1996). However, isoflurane is also used for the treatment of refractory SE (Shorvon, 1994) and may therefore prevent the onset of pilocarpine-induced SE. Nevertheless, van Eijsden and colleagues have successfully used inhalant anaesthetics for the induction and maintenance of SE using the lithium-pilocarpine method in rats (van Eijsden *et al.*, 2004). Therefore, the induction and maintenance of SE using pilocarpine under isoflurane anaesthesia was investigated with EEG.

5.4.2.1.2. Fentanyl/medetomidine

The combination of fentanyl and medetomidine can be used to induce surgical anaesthesia in small animals (Meert and De, 1994; Wolfensohn and Lloyd, 1998). However, whether SE can be induced under this anaesthetic regimen has not previously been investigated.

Fentanyl belongs to the family of drugs derived from morphine, and it is approximately one thousand times more effective as an analgesic than morphine (Lukasik and Gillies, 2003). It has a preferential action on the μ-opioid receptor and has been shown to potentiate seizures in a dose-dependent manner (Cherng and Wong, 2005). Medetomidine is an α_2-adrenegic agonist and causes sedation (Wolfensohn and Lloyd, 1998). In relation to SE, the α_2-adrenegic agonists have been shown to modulate seizure activity and have both pro- and anti-convulsant properties (Halonen *et al.*, 1995). Therefore, the induction and maintenance of SE using pilocarpine under fentanyl/medetomidine anaesthesia was investigated with EEG.

5.4.2.2. Methods

All animal care and procedures were carried out in accordance with the UK Animals (Scientific Procedures) 1986 Act.

5.4.2.2.1. Study Design

Thirteen adult male Sprague-Dawley rats (250-300g) were randomly divided into two groups: isoflurane (n=6) or fentanyl/medetomidine (n=7). The animals were anaesthetised and intrahippocampal EEG electrodes were surgically implanted. 20 minutes of baseline EEG was acquired before pilocarpine was administered and then continuously until the end of the experiment. In total, 3 hours of EEG was recorded irrespective of whether or not SE was induced. The experimental design is outlined in figure 5.4.

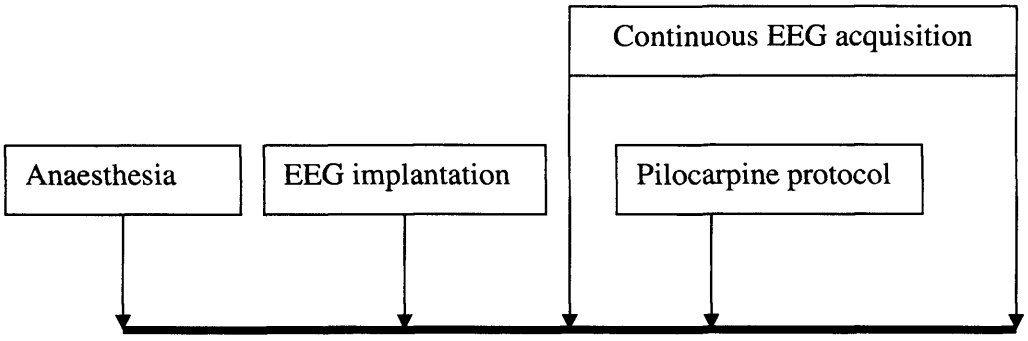

Figure 5.4. *Study design for the investigations into inducing and maintaining SE for 90 minutes under anaesthesia.*

5.4.2.2.2. Surgery

The animals were anaesthetised with either isoflurane (1.5% in a 60/40 N_2O:O_2 mix) or fentanyl (300μg/kg, i.p) and medetomidine (300μg/kg, i.p). Tungsten wire electrodes (50μm diameter, Science Products GMBH, Germany) were implanted bilaterally at symmetrical points in the hippocampus for EEG recording (AP, -4mm from bregma; ML, 2mm, and DV, 3.2mm from the neocortex). The hippocampal electrodes were referenced to a ground electrode attached to the tail of the animal.

5.4.2.2.3. Assessment of anaesthesia: reflex behaviour

There is no literature that describes drug interactions with the pilocarpine protocol and therefore reflex behaviour was used to assess the level of anaesthesia. The paw pinch withdrawal reflex and the corneal reflex are considered to provide a good estimation of the depth of anaesthesia suitable for surgical procedures, and these reflexes were used throughout this study to ensure that the animals were under suitable levels of anaesthesia (Green, 1982). If the animal retained either reflex during any period of the protocol then, for fentanyl, an additional dose of 100μg/kg of was given, or for isoflurane, the level of isoflurane was increased. The depth of anaesthesia was assessed using reflex behaviour every 15mins to ensure the animal remained unconscious throughout the experiment.

5.4.2.2.4. Pilocarpine protocol

Preliminary experiments (n=3, data not shown) indicated that multiple doses of pilocarpine were required to induce SE under anaesthesia using the lithium-pilocarpine protocol. As the doses required for inducing SE were similar to the levels used in the pilocarpine model without lithium, the pre-treatment with lithium was abandoned and the pilocarpine model was used for subsequent studies. The precise reasons for the loss or reduced ability of lithium to sensitise the CNS to pilocarpine is unclear but this result suggests that this effect is blocked or reduced whilst under anaesthesia. Furthermore, the standard dose of 320mg/kg induced SE in only 8/15 animals (see section 5.2.3), and further studies indicated that a dose of 375mg/kg was more efficacious for inducing SE under anaesthesia.

5.4.2.2.5. EEG acquisition

EEG was acquired and recorded continuously using a Bioamp differential amplifier interfaced with a Powerlab data acquisition system (AD Instruments, Australia). Signals were filtered between 1-120Hz and also a 50Hz notch filter was used to reduce noise and a sampling rate of 1024 per second.

5.4.2.2.6. Data Analysis

Analysis of electrophysiological data was carried out off-line on a Pentium computer, using Chart software (AD Insturments, Australia).

5.4.2.3. Results

5.4.2.3.1. Animal behaviour

No reflex behaviour was observed in any animals throughout the duration of the experiments. The isoflurane-anaesthetised animals remained motionless throughout. The fentanyl/medetomidine anaesthetised animals displayed facial automatisms following pilocarpine administration. Also tonic extensions of the forelimbs and hindlimbs, in which the entire body of the rat became outstretched, were observed. These tonic extensions lasted for a few seconds, occurred intermittently, and only during the period of increased EEG activity.

5.4.2.3.2. Desynchronisation after pilocarpine

All animals under either anaesthetic protocol displayed a reduction in EEG amplitude following pilocarpine administration (fig. 5.5b-c). The desynchronisation persisted for the duration of the experiments in the isoflurane-anesthetised animals. In the fentanyl/medetomidine-anaesthetised animals, desynchronisation continued until the onset of SE.

5.4.2.3.3. Time to SE

None of the animals under isoflurane anaesthesia progressed to SE (n = 6). In contrast, 6 out of 7 animals under fentanyl/medetomidine anaesthesia progressed to SE (fig. 5.5d). Of the animals that did progress onto SE, the mean SE onset time following pilocarpine administration was 22.83 ± 1.9 mins (mean ± sem).

5.4.2.3.4. Duration of SE

In the animals that did progress on to SE, seizure activity persisted until the administration of diazepam, at which point the amplitude of the EEG gradually reduced (fig. 5.5e).

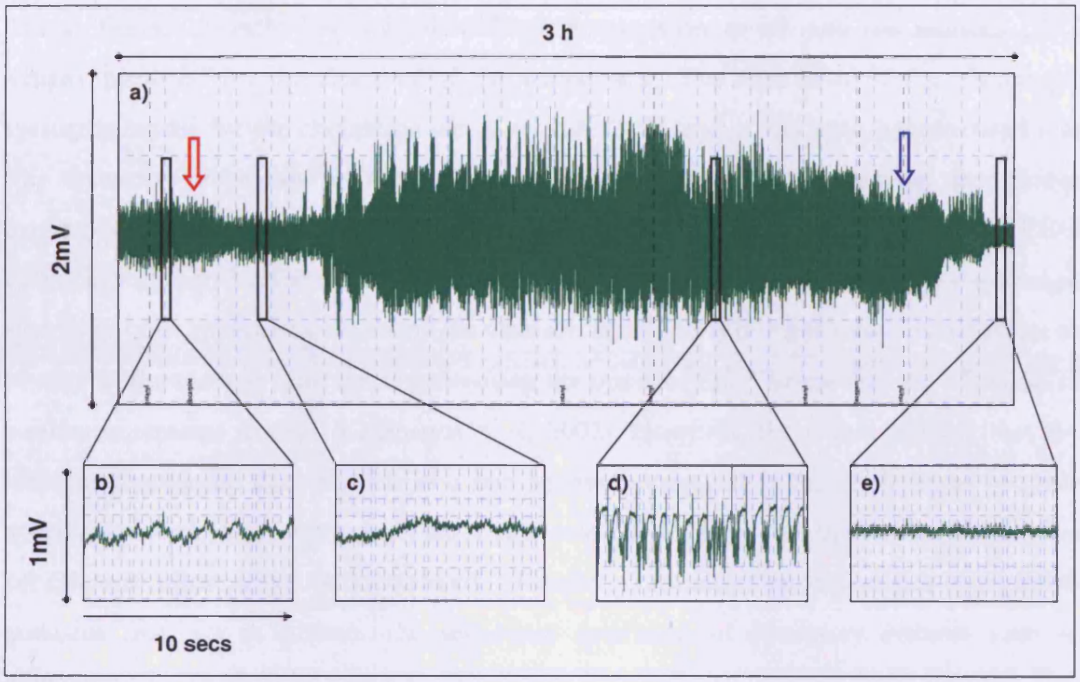

Figure 5.5. *Intrahippocampal EEG recording in a fentanyl/medetomidine anaesthetised rat. a) 3 h EEG acquisition for duration of experiment; b) baseline EEG; c) EEG desynchronisation post-pilocarpine (375mg/kg); d) increase in EEG indicates the rat in SE; e) decrease in EEG following diazepam (10mg/kg). Red arrow denotes pilocarpine administration, blue arrow indicates diazepam administration.*

5.4.2.4. Discussion

All animals remained under anaesthesia for the duration of the experiment. All of the animals in both anaesthetic protocols have a reduction in EEG activity following pilocarpine administration, due to the desynchronisation of neuronal activity. It is likely that this was a result of a sudden mass activation of the muscarinic system by pilocarpine, leading to a disruption of rhythmic neuronal firing, this association between EEG desynchronisation and cholinergic stimulation has been reported previously (Rasmusson *et al.*, 1994)

The isoflurane-anaesthetised animals did not progress on to SE and the reduced EEG activity persisted for the duration of the experiment. The activation of the cholinergic system is crucial for the cholinergic drugs to induce SE, and it has been hypothesised that this system is important in the maintenance of sustained seizure activity that drives excitatory mechanisms responsible for neuronal damage (Cavalheiro *et al.*, 2006). The EEG desynchronisation indicates that pilocarpine was efficacious in activating the cholinergic system in both anaesthetic regimens (Rasmusson *et al.*, 1994) but this raises the question as to why isoflurane was effective at preventing the onset of SE. The mechanism of action of isoflurane remains unclear (Campagna *et al.*, 2003). However, these data indicate that the inhalant anaesthetic does not act as a competitive antagonist at the cholinergic, or more specifically muscarinic, receptors. This is supported by findings that indicate an attenuation on calcium influx, which is downstream of the muscarinic receptor (Corrales *et al.*, 2004) and this may act to prevent the secondary activation of excitatory systems such as glutamate.

It is also notable that van Eijsden and colleagues have reported studies using a similar inhalant anaesthetic to isoflurane, halothane, with fentanyl/fluanisone for anaesthesia induction, in which they successfully induced SE using the lithium-pilocarpine method (van Eijsden *et al.*, 2004). However, our preliminary experiments with either the pilocarpine or lithium-pilocarpine method and halothane yielded similar results to isoflurane, and even with a doubling and tripling of the pilocarpine doses and reductions in the levels of anaesthesia, no signs of seizure activity could be detected (data not shown). This finding is supported by other studies in which the anti-convulsant activity of halothane has also been demonstrated (Murao *et al.*, 2000; Murao *et al.*, 2002). However, it is notable that these studies, as well as the current study, did not use fentanyl/fluanisone for inducing anaesthesia and therefore it may be possible that this method for induction followed by halothane is an effective method for producing SE using the lithium-pilocarpine method, as reported by van Eijsden and colleagues (van Eijsden *et al.*, 2004).

Under the fentanyl/medetomidine regimen, 6 out of 7 animals progressed on to SE and this activity persisted until diazepam was administered. A number of features were identified during seizure activity. Facial automatisms developed and there was also intermittent generalisation of seizures that manifests as tonic extension of the limbs.

Although these animals were still unconscious, these episodes could be problematic for MRI during SE. Recent experiments have used fentanyl by itself and have successfully induced SE with pilocarpine (Engelhorn *et al.*, 2005); however, fentanyl is an analgesic by itself and does not satisfy the criteria for anaesthesia (Wolfensohn and Lloyd, 1998). Furthermore, although their set up had "an especially designed MR-compatible head holder, allowing reliable fixation to avoid seizure-related movements", no details were provided and also it is not clear as to whether these tonic extensions were observed (Engelhorn *et al.*, 2005). Nevertheless, SE was successfully induced with pilocarpine under anaesthesia using fentanyl/medetomidine anaesthesia.

An alternative to using anaesthesia is to use neuromuscular blockade. This class of drugs prevents activation of the neuromuscular junction and thus skeletal muscle contraction. These paralysing agents are, rightly, heavily regulated due to the negation of any reflex action and thus it is not possible to gauge the consciousness of an animal. These regulations were put in place following reports of patients who were paralysed but conscious during surgical operations, and these situations are considered to be among the most traumatic events that can happen to humans or animals. However, there could still be a case of using neuromuscular blockade in investigations such as SE if they are used in combination with anaesthetics. Such a combination would remove the problems associated with motion for MRI and it may be possible to investigate some of the fundamental mechanisms that underlie seizure initiation, maintenance and propagation without affecting the seizure itself, which may be worth pursuing in future studies.

5.4.2.5. Conclusion

In conclusion, this study demonstrates that it is possible to induce SE under fentanyl/medetomidine anaesthesia, but not under isoflurane. However, even though the animals were under anaesthesia, SE was associated with motor events that may be problematic for MRI.

5.4.4. Reduction of motion artefacts: changes to the MRI animal holder

The previous study demonstrates that it is possible to induce SE and maintain the seizure for 90mins whilst the animal is under anaesthesia. This step was critical as the welfare of the animal is paramount and suffering has to be kept to the minimum. However, even though the seizure can be induced, motion remains a problem and this leads to degradation of the MR image quality. As muscle relaxants cannot be used, various alterations to the MRI animal holder were developed to minimise physically the movement of the brain.

The initial step was to induce SE with the animal on the animal holder and to investigate whether it was possible that the existing set-up was sufficient for MRI of SE. The animal holder was designed for anaesthetised animals and the animals lay on their backs with ear bars and a bite bar that act to secure the head in place for imaging (see fig 5.6).

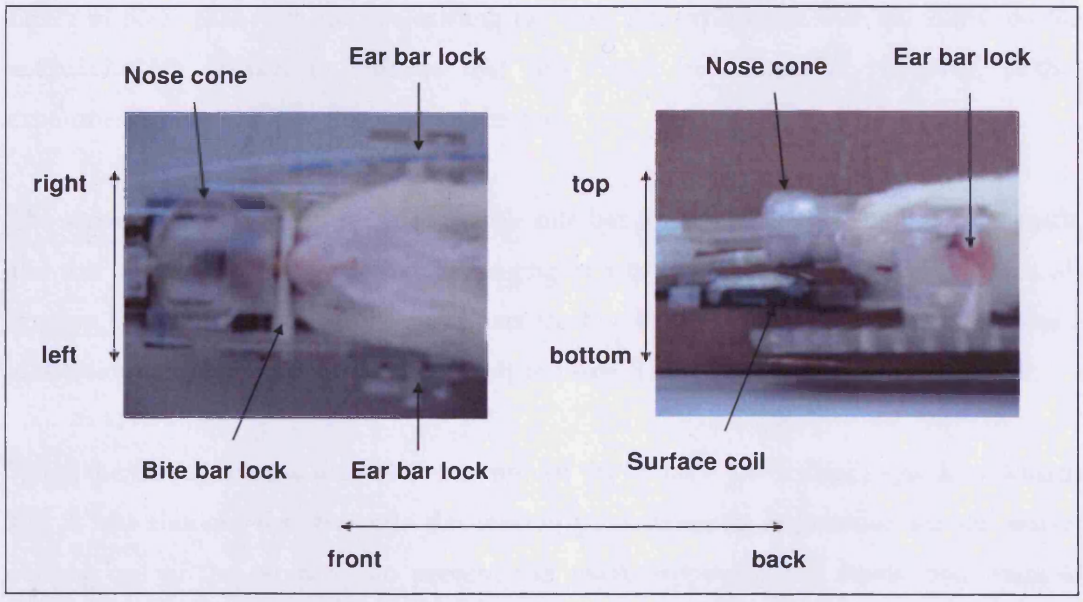

Figure 5.6. *A photograph of the animal holder used for MRI of the rat. Note the animal lies on its back. Also for this probe, ear bars and bite bars are used to hold the head of the anaesthetised animal in place for MRI.*

It quickly became apparent that the set-up was insufficient to prevent motion during SE using this animal holder design. The main problem was the intermittent tonic extension of the forelimbs and hindlimbs that pulled the animal out of the ear bars.

The irregular nature of the tonic extensions meant it was not possible to predict when these would occur and therefore the process of adapting the animal holder was particularly time consuming. A typical experiment required the animal to be anaesthetised and set up on the animal holder, which would take between 40-60 minutes. Once set up, pilocarpine was administered to the animal and seizure activity began in around 30 minutes. After this point the tonic extensions of the limbs could occur at any point thereafter, and it was only after this point that an adaptation could be made to the animal holder.

Various alterations to the animal holder were made and these steps were cumulative. Reducing the size of the ear bars for the animal was tried to try to lock the head more firmly in place than with the pre-existing ear bars. An experiment with an animal on the animal holder seemed to indicate that this could be successful. However, further experiments indicated that this was not the case.

The animal holder design had an adjustable bite bar for the teeth that slid back and forth, and this was sufficient for traditional imaging of anaesthetised animals. However, for SE imaging, as the rat came out of the ear bars the bite bar also slid out of place. Therefore a lock was added to secure the bite bar firmly in place. This also proved to be insufficient.

When the rat experiences the tonic extension of the limbs, it also arches its neck backwards and it was thought that this was the motion predominantly responsible for the animal coming out of the ear bars. To prevent this from happening, the animal was wrapped tightly in a plastic sheet. The plastic sheet limited the movement of the body as the seizure took hold and did seem to reduce the movement of the neck but was also not sufficient for preventing the animal from coming loose. Adaptations were also tried by raising and supporting the base of the head at varying degrees by attempting to limit the neck arching motion.

At this point, it was thought that the main problem was the ear bars and also that the animal was lying on its back. Therefore an alternative animal holder was used that was designed and engineered by Dr. Edward Proctor (fig. 5.7). This animal holder has the animal lying on its front with the nose secured into a nose cone and no ear bars are used. In this set-up, the surface coil is placed directly onto the head of the animal and can provide an additional means of securing the animal. Initial experiments indicated that this MRI animal holder was promising as the animal would not drop out of the field of view if and when the tonic extensions occur; however the rats were still liable to move, although the nose cone did limit lateral movement. The adaptations on the first animal holder were added on to this new probe in a step-wise fashion. A further adaptation was to add a support for the surface coil. This was because it was thought that as the surface coil was placed on the head, then any movement may cause movement to the coil and manifest itself as a loss in signal.

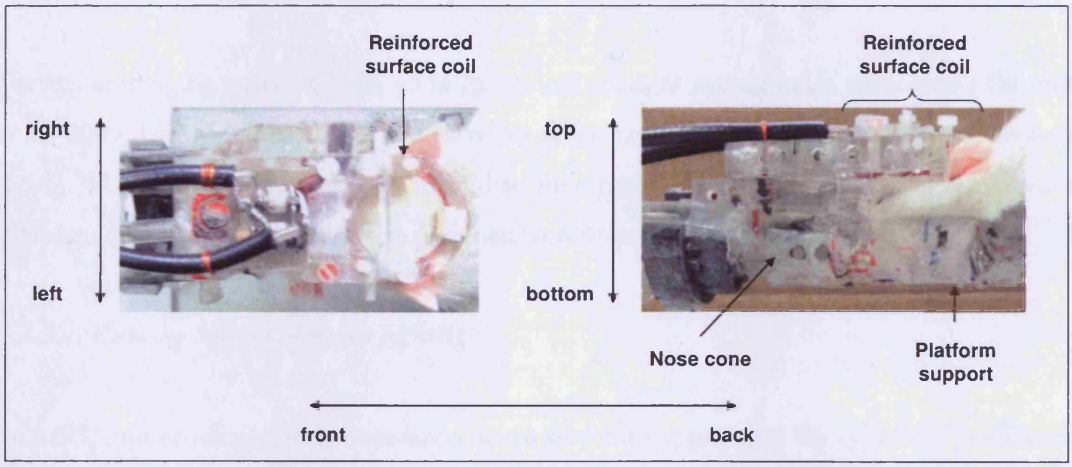

Figure 5.7. *A photograph of the adapted animal holder used for MRI during SE of the rat. Note the animal lies on its front. Also for this probe, no ear bars and bite bars are used, and a nose cone, reinforced surface coil and a platform support were incorporated to limit motion during MRI.*

The addition of the various adaptations appeared to have limited the motion and the tonic extensions did not move the animals to such a great degree. Nevertheless, the main limitation of the bench experiments was that it was not possible to evaluate whether subtle movement still occurred, and whether this motion would produce artefact and if so to what degree.

Early experiments with perfusion MRI indicated that movement was a problem and that the rat can move back or forward. This was in the order of millimetres and was apparent on the MR images as a different slice to the previous acquisition was observed. It was assumed that these movements were due to the tonic extensions as this could not be directly assessed when the rat was in the MR scanner. This seemed logical because the movement was only intermittently observed between contiguously acquired images and also because this was seen at least 30 minutes following pilocarpine administration. However, it was thought that if the movement was only intermittent then it may be possible to scan during SE and then visually assess and remove the images that had motion artefacts. Therefore, a protocol was designed to limit the effect of motion.

5.4.5. MRI of status epilepticus protocol

Perfusion imaging is sensitive to acute functional changes during brain pathology (Thomas *et al.*, 2000; Lythgoe *et al.*, 2002) and provides information about energy supply (see section 4.5-6). Thus, perfusion imaging was used to investigate SE. However, motion remained a problem and an MRI protocol was designed to reduce the influence of movement.

5.4.5.1. Reducing the effect of motion on MRI

In MRI, numerous methods have been developed for suppressing the problems associated with motion (Gadian, 1996). For example, in cardiac imaging successive data acquisitions can be synchronised to a specific phase of the cardiac cycle. However, the irregularity of the motion associated with SE means that imaging cannot be synchronised to any specific physiological phenomena such as those measured with EEG. Another method is to use rapid imaging techniques, such as echo-planar imaging (EPI) or parallel imaging, which are widely used in studies that require fast imaging, for example in functional imaging. Although EPI has been implemented on our current system, the development of additional techniques was beyond the remit of this thesis and therefore this was not pursued any further and so an alternative approach was taken.

For any imaging experiment, the signal-to-noise ratio needs to be sufficient to distinguish tissue from background noise. The simplest way to increase the signal-to-noise is by increasing the number of averages (n) for a given acquisition; this leads to an increase in the signal-to-noise ratio of $\sqrt{n}$ (Gadian, 1996). The current implementation of the perfusion and diffusion techniques on our MRI scanner uses multiple averaging, 88 and 32 averages respectively, and produces one averaged data set at the end of each scan. The problem with imaging SE is that any motion during the acquisition of any one of the averages leads to artefacts for that given data set. However, averaging can also be performed after acquisition and this can be utilised for imaging SE (fig. 5.8).

The prevalent motion that was thought to affect imaging SE with our set up was the intermittent tonic seizures, which last for a few seconds. If the averages for a scan were reduced then the images that have been affected by motion can be identified and omitted from a data set. Therefore a series of low average scans was acquired continuously for imaging SE and averaged together after the end of the experiment.

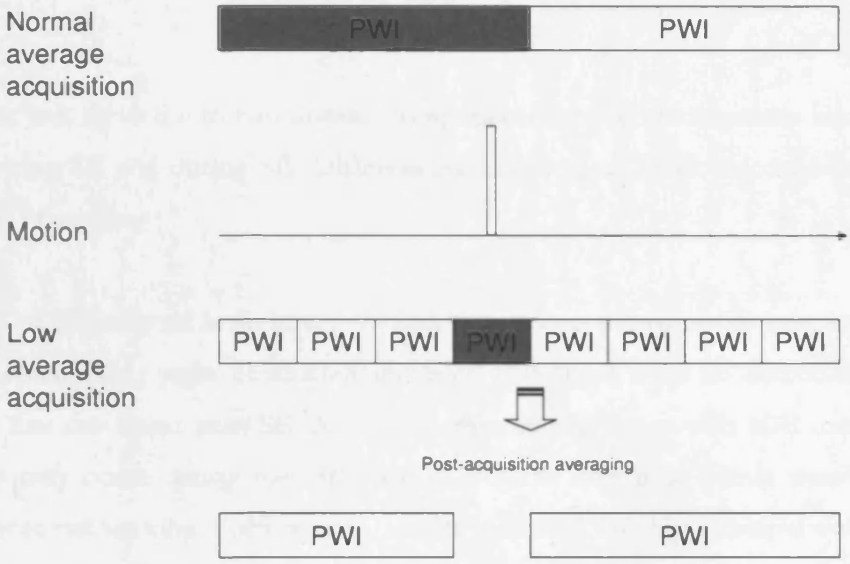

Figure 5.8. *Representation of perfusion-weighted image (PWI) acquisition for SE. The central line indicates motion at a particular point in time. The normal average experiment would result in the loss of data due to motion artefact for that entire period. However, if low average acquisitions were used then that particular experiment can be removed, and although some data would be lost, the rest of the acquisitions over that period can be used. Grey boxes indicate scans that have been affected by motion artefact.*

5.4.6. Conclusion: a final protocol for MRI during SE

In summary, a series of methodological developments was necessary to enable the study of SE with MRI, the first of which was being able to induce SE under fentanyl/medetomidine. Although the animal remained unconscious under this form of anaesthesia for the duration of an experiment, motion was a problem. As such, a number of adaptations were made to the animal holder for additional restraint, and also an MRI protocol, which consisted of low average perfusion acquisitions, was designed to minimise the adverse effects of motion. These developments were all integrated in to the set-up for our MRI studies for monitoring SE.

5.5. SUMMARY

This project was divided into two distinct components for our investigations into SE using MRI: following SE and during SE. Different methodological developments were required for each set of studies.

In the MRI of SE-induced brain injury, various time points following SE were investigated. The pilot studies that were conducted indicated that there were no detectable changes during the first few hours post-SE. Also, the assessment of tissue with MRI indicated that T_2 changes may occur during the early period, but the later time points were associated with hippocampal atrophy. Furthermore, results indicated that hippocampal volume at 21 days after SE was similar to that of volumes on day 70.

In the MRI during SE, the main problems were anaesthesia and motion, and a new anaesthetic regimen with fentanyl/medetomidine was found to be conducive to pilocarpine-induced SE. However, motion still presented a problem, and various methods were tried to reduce the impact of movement. The first method was to develop physical means to limit motion to allow the animal to be imaged. This was followed by changes in the design of the MRI protocol that would allow the omission of degraded images.

These developments provided the basis for the design of the experiments presented in this thesis.

CHAPTER 6: MRI FOLLOWING STATUS EPILEPTICUS

A bad beginning makes a bad ending

Euripides

6.1. INTRODUCTION

As described in the previous chapter, MRI can be used to monitor the temporal events during SE. In a similar manner, MRI can also be used to investigate the period following SE.

SE can cause brain injury that continues to evolve over time, and it has been hypothesised that this injury is associated with temporal lobe epilepsy (Cavanagh and Meyer, 1956; Scott *et al.*, 2006). Following the cessation of SE a host of complex physiological mechanisms are recruited and include cell death, inflammation, neurogenesis and mossy fibre sprouting, which have been implicated in post-SE pathology (Parent, 2002; Walker *et al.*, 2002; Vezzani and Granata, 2005; Pitkanen *et al.*, 2007). The roles that each of these processes may play in post-SE pathologies are beginning to be revealed, and studies have suggested that these mechanisms may contribute to varying degrees in specific aspects post-SE. For example, one possible consequence of SE is cognitive decline, and evidence suggests that cell death as a result of SE may underlie this pathology (Niessen *et al.*, 2005). On the other hand, the contribution of cell death to subsequent epilepsy is less clear as drugs that provide neuroprotection after SE may not influence the expression of later epilepsy (Brandt *et al.*, 2006).

The characterisation of physiological pathways after SE, such as inflammation and cell death, indicates that these processes may be transient or delayed (Fujikawa, 1996; Jankowsky and Patterson, 1999). These data suggest that aspects of post-SE injury may be expressed in a time-dependent manner. However, the temporal relationships between these processes and later outcome have not been fully defined. A number of studies have indicated that various MRI indices are altered during the early phase after SE, and these have been observed in a variety of animal models and also in humans (Roch *et al.*, 2002a; Dube *et al.*, 2004; Nairismagi *et al.*, 2004; Jupp *et al.*, 2006). Although the molecular bases for these changes remain unclear, the temporal relationships between these early changes and the evolution of brain injury have not been fully investigated. Therefore it was the aim of this study to monitor the progression of brain injury following SE with a particular

emphasis on the early period and to investigate the relationships between early injury and later outcome

For the purposes of these investigations, the lithium-pilocarpine model of SE was monitored with multi-parametric MRI over a period of 21 days. The multi-parametric MRI technologies used include quantitative T_1, T_2, diffusion, and, for the first time in studies following SE, perfusion. In addition, a high resolution T_2-weighted anatomical scan was acquired for investigating structural changes following SE.

A further aim was also incorporated into the experimental design to investigate the effect of anaesthesia on the pathophysiology following SE. MR imaging of animals requires the use of anaesthesia to prevent motion, and in this study, animals are serially imaged in order to characterise brain injury following SE. Therefore it is possible that anaesthesia could modify the pathophysiology following SE, and thus control groups were included to investigate the effect of anaesthesia on the pathophysiology following SE.

6.2. MATERIALS AND METHODS

6.2.1. Experimental design

All animal care and procedures were carried out in accordance with the UK Animals (Scientific Procedures) 1986 Act. The study design is outlined in figure 6.1 and the rationale for the design is provided below.

This study involved four groups: full-imaging lithium-pilocarpine (FLP), full-imaging lithium-saline (FLS), control-imaging lithium-pilocarpine (CLP), and control-imaging lithium-saline (CLS) (fig.6.1). The full-imaging groups were used to characterise the progression of brain injury following SE using MR and were imaged at least 24 hours before lithium injection and then subsequently after SE on days 0, 1, 2, 3, 7, 14, and 21. The control-imaging groups were used to investigate the effect of anaesthesia on pathophysiology following SE and were therefore imaged before lithium injection and on day 21. After imaging on day 21, all animals were sacrificed for histological analysis in which neuronal damage was assessed with Nissl stain.

The MRI protocol consisted of a high resolution T_2-weighted spin-echo sequence to identify regions of pathology across the whole brain, and single slice quantitative T_1, T_2, diffusion and perfusion maps. As the quantitative measurements could only be conducted on a single slice, this slice was chosen to include the hippocampus and the piriform cortex, which are regions known to be damaged following SE (Roch *et al.*, 2002a).

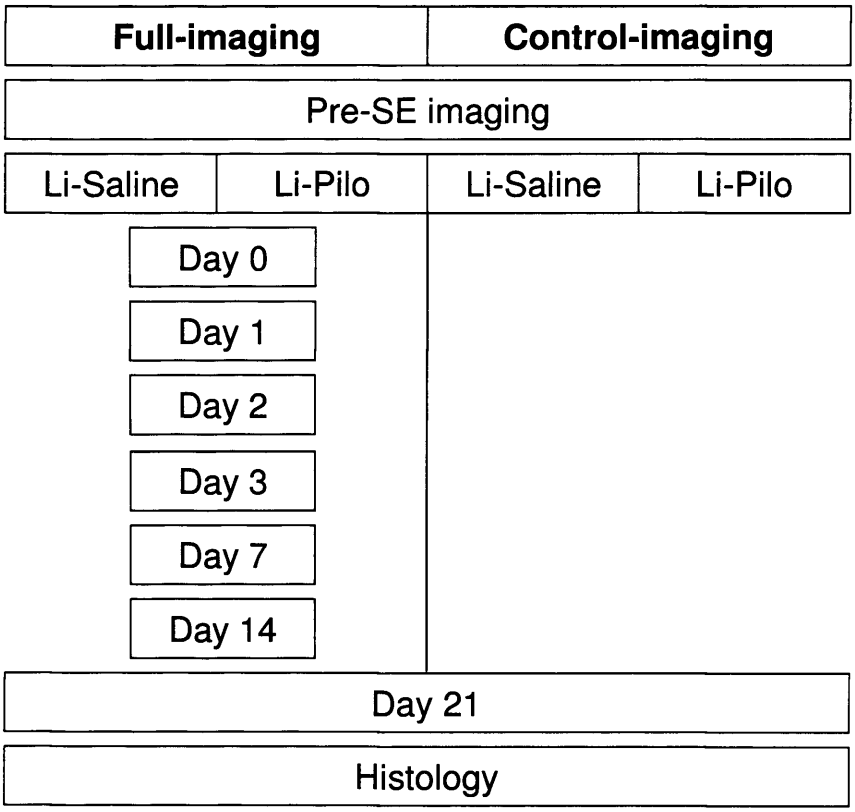

Figure 6.1. *Experimental design. This study involved two main groups, either full-imaging or control imaging. Within each of these groups, the animals were administered either lithium-pilocarpine or lithium-saline. The full imaging groups were imaged before lithium injection (pre-SE) and subsequently after SE on days 0, 1, 2, 3, 7, 14 and 21. The control-imaging groups were imaged only on pre-SE and on day 21. After imaging on day 21, all animals were sacrificed for histology.*

6.2.2. Animal Preparation

26 adult male Sprague-Dawley rats weighing 200-270g at the beginning of the experiment were used (supplied by Charles River, Margate, Kent, UK). The animals were housed with a standard light/dark cycle and with access to food and water *ad libitum*. The animals were housed in groups of three or four before SE induction and housed singly thereafter.

The animals were divided randomly into one of the four groups – FLP (n = 9), FLS (n = 7), CLP (n = 5), CLS (n = 5). All animals were injected with lithium chloride (3 mEq/kg,

i.p., Sigma-Aldrich, Dorset, UK) approximately 18-22 hours before seizure induction. On the following day, the animals were injected with methylscopolamine (1 mg/kg, i.p., Sigma-Aldrich) to reduce the peripheral cholinergic effects of pilocarpine and then following 15-20 minutes with pilocarpine hydrochloride (30 mg/kg, i.p., Sigma-Aldrich) in the lithium-pilocarpine groups or saline in the lithium-saline groups. Diazepam (10 mg/kg, i.p., Phoenix Pharma Ltd, Gloucester, UK) was administered 90 mins after the onset of SE to terminate the seizure. Lithium chloride, pilocarpine hydrochloride and methylscopolamine were freshly prepared prior to administration using 0.9% saline.

6.2.3. Behavioural assessment of seizures: the Racine scale

The Racine scale of limbic patterns of seizure was used to assess the progression to SE (Racine 1972). The Racine scale was described previously in section 5.2.1, and animals were considered to have progressed on to SE when stage 3 was observed.

6.2.4. MRI

Scans were performed on a 2.35T horizontal bore magnet (Oxford Instruments, UK) interfaced to a SMIS console (Guilford, UK). All animals were anaesthetised with 1.5% isoflurane in a 60:40 N_2O:O_2 mix delivered via a nose cone and placed on a probe with bite and ear bars securing the head to minimise movement artefacts. Physiological parameters monitored include electrocardiography (ECG) recordings and rectal temperature, which was maintained at 37 $\pm$ 1°C using an air warming system.

Images were acquired using a volume transmitter coil and a separate decoupled surface receiver coil. A central coronal imaging slice was selected that included the hippocampus and the piriform cortex (-3.3 mm from bregma). The central slice was determined by visual inspection of anatomical landmarks.

A high resolution T_2-weighted spin-echo was used for volumetric analysis. The parameters for this sequence were 1500 ms repetition time (TR), 80 ms echo time (TE), 30 mm field-

of-view (FOV) with a 128 x 128 matrix, a 1 mm slice thickness and 10 averages. The duration of acquisition was 35 mins.

All subsequent sequences were run on a 2 mm-thick coronal slice.

For non-invasive CBF measurement, we used the CASL method (Alsop and Detre, 1996), based on spin-echo echo-planar imaging (EPI) with interleaved adiabatic fast-passage inversion and control measurements. The centre of the inversion plane was situated 2 mm behind the back of the cerebellum in all animals (approximately 10 kHz frequency offset); for the control image the same offset value was used, but with the sign reversed. A post-labelling delay time of 500 ms was used to minimise transit time effects and intravascular artefacts. The echo time (TE) was 36 ms, the repetition time (TR) 1000 secs, and 88 averages were acquired. A non slice selective inversion recovery (IR) EPI sequence was used to obtain the tissue T_1 and the spin density (M_0) parameters necessary for subsequent CBF quantification. Images were acquired with 2000 ms repetition time (TR), 18 ms echo time (TE), an inversion time (TI) array of 284 ms, 434 ms, 634 ms, 834 ms, 1234 ms, 1734 ms, 2734 ms, and 3734 ms and 88 averages were used. The IR data were fitted to obtain T_1, α_0 and M_0 assuming a mono-exponential recovery function. Subsequently, these values were used to calculate CBF from the difference between the labelled and control image (Alsop and Detre, 1996). Assumptions were T_1 of arterial blood = 1.5 secs, blood:brain partition coefficient for water (λ) = 0.9, efficiency of the spin labelling pulse = 0.71 (previous results; data not shown), tissue transit time = 250 ms, arterial transit time = 200 ms. Duration of acquisitions: T_1 = 11 mins and CASL = 16 mins.

Quantitative T_2 and ADC maps were obtained using the methods described in section 5.3.1. Duration of acquisitions: T_2 = 4 mins and ADC = 9 mins.

Total scan time was 75 minutes.

6.2.5. Image processing and data analysis

The high resolution T_2-weighted images were reconstructed using SMIS reconstruction software (SMIS version 6.1). T_1, T_2, ADC and CBF maps were reconstructed using in-

house software written in IDL Software Version 5.6 (Research systems Inc., Boulder, CO, USA) in order to obtain quantitative maps. Four regions of interest (ROI) (see fig. 6.2) - cortex, piriform cortex, hippocampus, thalamus - were delineated on all processed images and analysed with SMIS Image Display Version 3.7.

For the high resolution T_2-weighted anatomical scans, analysis was performed using ImageJ (version 1.38, NIH, USA).

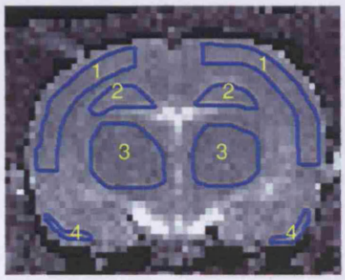

Figure 6.2. *Representative regions of interest drawn to delineate anatomical structures for quantitative analysis. Numbers indicate regions corresponding to: 1, cortex; 2, hippocampus; 3, thalamus; 4, piriform cortex.*

6.2.6. Volumetric assessment of brain structures

Four contiguous high-resolution T_2-weighted anatomical slices (-2.3 to -6.7 from bregma), which covered the hippocampus, were used for volumetric assessment. Regions of interest were drawn by an independent observer who was unaware of the groupings of the animals. The regions drawn were as follows: hippocampus, ventricle and whole brain.

Hippocampal tissue borders were defined using a standard rat brain atlas (Paxinos, 1995) (See fig. 6.3). Ventricular borders were defined by the hyperintense regions on the scans. Volumes were calculated by multiplying the areas of the given region of interest by the slice separation (1.1mm).

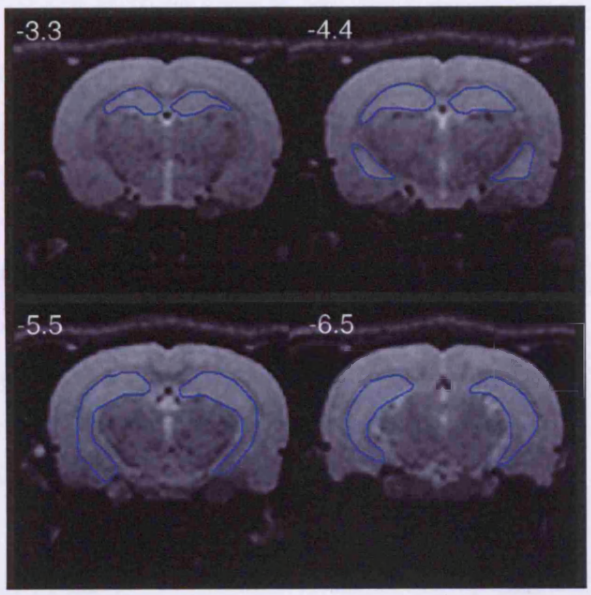

Figure 6.3. *Regions of interest for volumetric analysis. A high-resolution scan from one animal. Highlighted areas are hippocampal regions of interest that were drawn for calculating hippocampal volumes. Numbers show approximate distance from Bregma.*

6.2.7. Statistical analysis

A repeated-measures (degrees of freedom-adjusted mixed-model) two-way ANOVA was conducted on the time courses of the CBF, T_1, T_2 and ADC data for each brain region. The main effects for these analyses were days (-1, 0, 1, 2, 3, 7, 14, 21) and treatment (pilocarpine, saline). Similarly, repeated measures (degrees of freedom-adjusted mixed-model) two-way ANOVA was used to test changes on day 0 with main effects as: days (-1. 0) and treatment (pilocarpine, saline).

For investigating the effect of serial imaging on MR measurements of tissue status, regional differences between day 21 and pre-SE were calculated for the four groups - FLS, FLP, CLS and CLP - a Kruskal-Wallis one-way ANOVA was used.

One-way ANOVA was used to investigate differences in whole brain volumes and hippocampal volumes between the four groups. For cases in which significant differences were found, a *post-hoc* Tukey test was used to identify group differences.

Multiple regression analysis was used to investigate the relationship between hippocampal volumes and ventricular volumes.

Principal component analysis and regression analysis was used to investigate the relationships between early injury and hippocampal volumes on day 21. This was followed by a principal component analysis of the early injury data.

All statistical analyses were performed in SPSS for Windows Version 14.0.

6.2.8. Histopathology

Following the final scan, the animals were deeply anaesthetised with 5% isoflurane in 100% N_2O and were perfused transcardially, using 4% paraformaldehyde in PBS (pH 7.4). The brains were immediately removed and rotated at 4°C in 1% paraformaldehyde in PBS (pH 7.4) for 2 hours. Finally, the brains were put in 30% sucrose in PBS and stored overnight at 4°C for cryoprotection. The brains were then frozen with dry ice and stored at -80°C. 40 μm coronal slices were taken, and sections were stained with Nissl and examined by light microscopy.

6.3. RESULTS

6.3.1. Behaviour

Within 5 min after the injection of pilocarpine, rats developed diarrhoea, piloerection, and other signs of cholinergic stimulation. During the following 15-20 min, they exhibited head bobbing, scratching, masticatory automatisms, and increased exploratory behaviour. Progression to SE started between 25-40 min after pilocarpine administration with bilateral forelimb clonus and episodes of rearing and falling.

6.3.2. Pre-existing brain abnormalities

Pre-existing brain abnormalities were identified during the pre-SE time point in 3 animals (fig. 6.4). In all 3 of these animals, the high-resolution T_2-weighted images revealed unilateral hyperintense regions which indicated an enlarged ventricle. These rats were removed from the study due to these abnormalities, and no further imaging was conducted. In total, 26 rats that did not have abnormalities on the scans were included in the present study.

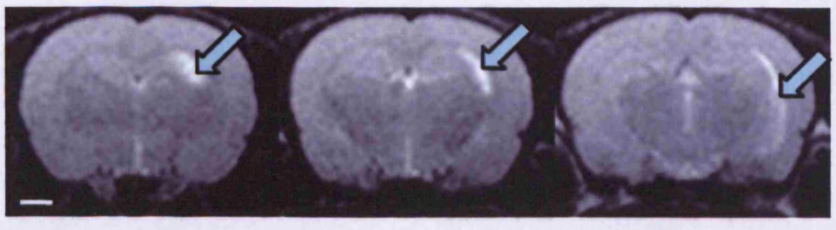

Figure 6.4. *Example of a hyperintense T_2-weighted signal that was identified in this animal during the pre-SE time point (arrow). This animal was subsequently removed from this study. Scale bar equals 2mm.*

6.3.3. MRI over 21 days following SE

The MRI time course for T_2, T_1, CBF and ADC measurements are presented in the following sections. For each of the MRI time courses, the results are given with three sets of data: representative MR maps acquired over the course of 21 days, which indicates the regional nature of the brain injury; the MR measurements for individual animals, which demonstrates the consistency and variability of the regional analysis; and a mean time course for the full imaging lithium-pilocarpine group and the full imaging lithium-saline group, which is presented for the ease of the reader.

6.3.3.1. T_2 changes following SE

Figure 6.5 shows the T_2 maps acquired over the 21 day time course from a single animal. Figure 6.6 shows the measured T_2 relaxation times in individual animals in the FLP and FLS groups, and figure 6.7 shows the mean T_2 time course. Cortical T_2 relaxation times before drug administration were 67.4 ms ± 0.25 and 67.1 ms ± 0.54 (mean ± s.e.m) for the FLP and FLS groups respectively. T_2 in the other regions measured at this time point were: hippocampus (71.5 ms ± 0.9; 69.6 ms ± 0.7), piriform cortex (77.3 ms ± 0.9; 77.0 ms ± 0.8), thalamus (62.4 ms ± 0.4; 61.5 ms ± 0.5).

The following results are expressed as a percentage from baseline measurements measured pre-SE. Comparisons of T_2 values were made between the pre- and day 0 time points and these indicated that T_2 was increased in all of the brain regions analysed. In the cortex, an increase from pre-SE to 103.6% ± 0.65% ($F = 22.80$, $p < 0.001$) was measured (mean ± s.e.m). The hippocampus increased to 105.7% ± 1.75% ($F = 5.11$, $p = 0.042$), the piriform cortex to 104.4% ± 1.84% ($F = 5.34$, $p = 0.038$), and the thalamus to 107.0% ± 1.80% ($F = 13.75$, $p = 0.003$). By day 1, T_2 in the cortex and the thalamus returned to levels observed in pre-SE and the day 1 CLS levels. However, the T_2 increases continued in the hippocampus and the piriform cortex, and reached an observed maximum on day 2 - 115% ± 2.48% and 141% ± 5.06% respectively. By day 7, T_2 returned to baseline levels for both structures.

Statistical analyses on the T_2 time courses indicated that there were significant pilocarpine-induced time-dependent T_2 changes in the cortex ($F = 3.53$, $p = 0.014$), hippocampus ($F = 11.53$, $p < 0.001$), and the piriform cortex ($F = 16.12$, $p < 0.001$). However, no significant pilocarpine-induced time-dependent changes were observed in the thalamus ($F = 2.59$, $p = 0.056$), but a significant pilocarpine effect was detected ($F = 18.56$, $p < 0.001$).

These data indicate an early regional and transient T_2 change following SE.

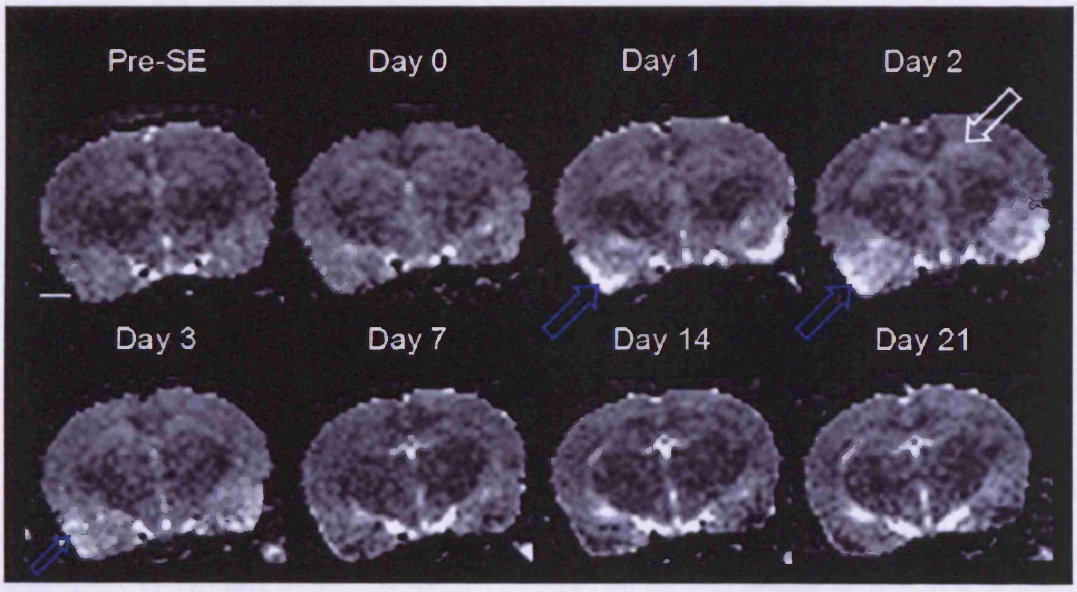

Figure 6.5. *T_2 maps of a single animal from the FLP group. Note the T_2 increase in the piriform cortex on day 1, 2 and 3 (blue arrow). Also hippocampal T_2 was increased on day 2 in this animal (white arrow). Scale bar equals 2mm.*

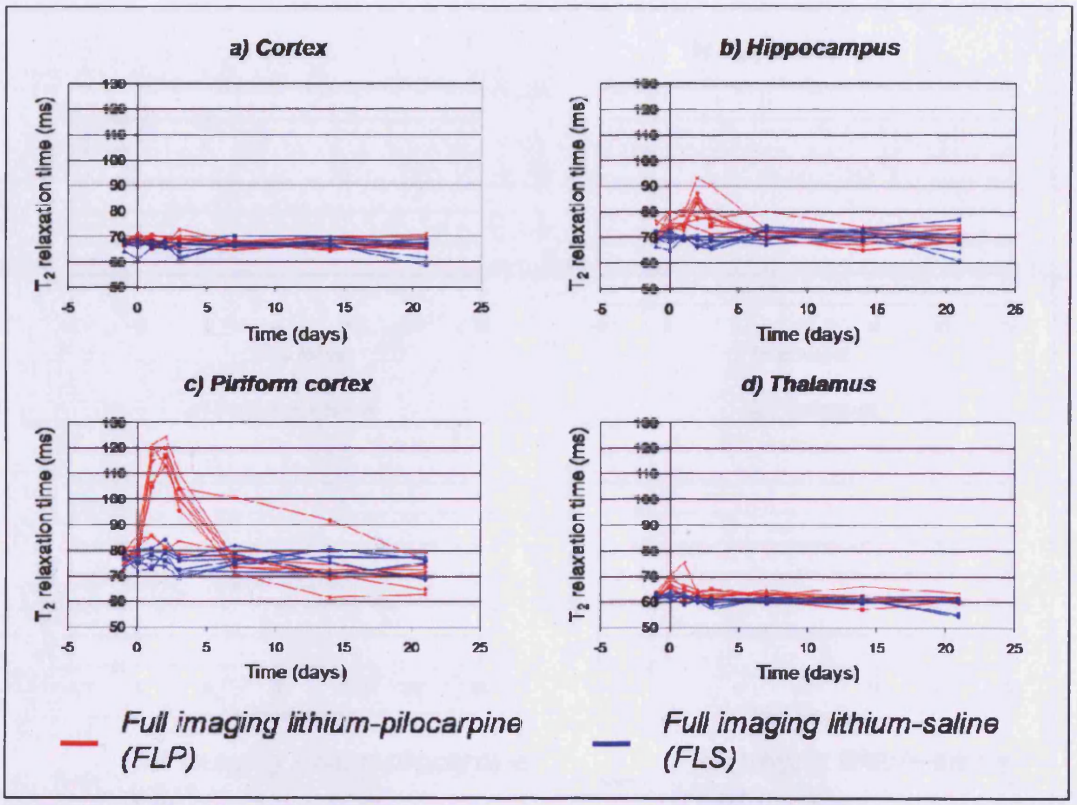

Figure 6.6. *T_2 relaxation times for individual animals in the: a) cortex, b) hippocampus, c) piriform cortex and d) thalamus. T_2 measurements were performed before lithium administration (day -1) and subsequently on days 0, 1, 2, 3, 7, 14 and 21. The red lines are measurements obtained from individual FLP animals and the blue lines from the individual FLS animals.*

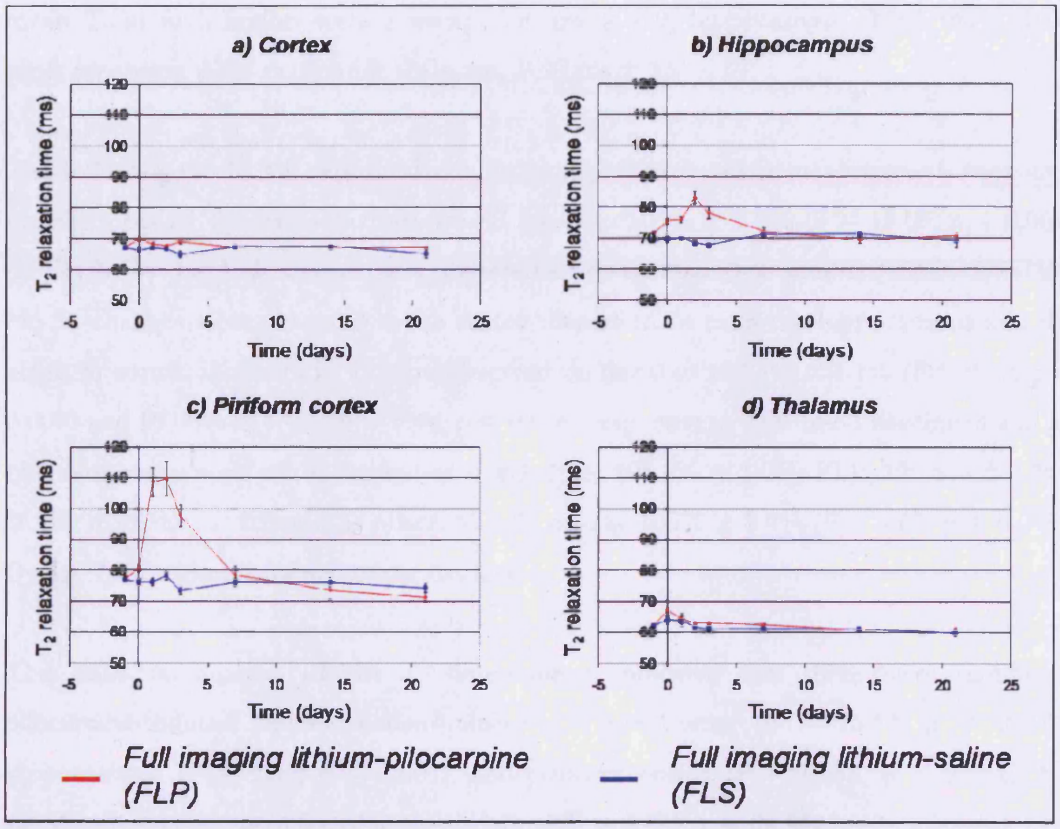

Figure 6.7. *Mean regional T_2 relaxation time courses before and following SE. Mean regional data were measured in the: a) cortex, b) hippocampus, c) piriform cortex, and d) thalamus. T_2 was measured in all animals 1 day before lithium administration (day -1), and subsequently on days 0, 1, 2, 3, 7, 14 and 21 after SE. Data shown as mean ± s.e.m. The red line represents the animals in the full imaging lithium-pilocarpine experimental rats (n = 9), and the blue line depicts the full imaging lithium-saline control animals (n = 7).*

6.3.3.2. T_1 changes following SE

Figure 6.8 shows the T_1 maps acquired from a single animal from the FLP group. Figure 6.9 shows the T_1 time courses in the brain regions of individual animals, and figure 6.10 shows the mean T_1 time course for FLP and CLP groups. Mean pre-SE T_1 measurements in the FLP animals were: cortex, 1280 ms ± 8.1; hippocampus, 1355 ms ± 8.3; piriform cortex, 1387 ms ± 11.5; thalamus, 1085 ms ± 10.7 (mean ± s.e.m). In the FLS group, the

mean T_1 in each region were: cortex, 1256 ms ± 6.9; hippocampus, 1302 ms ± 20.6; piriform cortex, 1384 ms ± 16.7; thalamus, 1097 ms ± 3.9.

The following results are expressed as a percentage from baseline measurements measured pre-SE. Cortical T_1 increased from pre-SE levels to 105% ± 1.1% ($F = 19.09$, $p < 0.001$) on day 0. By day 1, a decrease was observed when compared to pre-SE (95.8% ± 0.7%). No T_1 changes were observed in the cortex thereafter. In both the hippocampus and the piriform cortex, increases in T_1 were observed on day 0 to 103.4% ± 1.1% ($F = 9.39$, $p = 0.009$) and 107.0% ± 1.4% ($F = 5.48$, $p = 0.036$) respectively. This trend continued and an observed mean peak was identified on day 2: FLS, 105.8% ± 1.0%; FLP, 120.6% ± 3.3%. In the thalamus, a change was observed only on day 105% ± 2.4% ($F = 4.69$, $p = 0.049$). By day 7, all regions returned to pre-SE levels.

The statistical analysis of the T_1 time-courses indicated that there were significant pilocarpine-induced time-dependent changes in the cortex ($F = 16.69$, $p < 0.001$), hippocampus ($F = 9.59$, $p < 0.001$), and piriform cortex ($F = 10.55$, $p < 0.001$). No significant changes were found in the thalamus ($F = 0.421$, $p = 0.528$).

These data indicate an early and transient T_1 change following SE across all four regions analysed. All changes in the regions normalised by day 7.

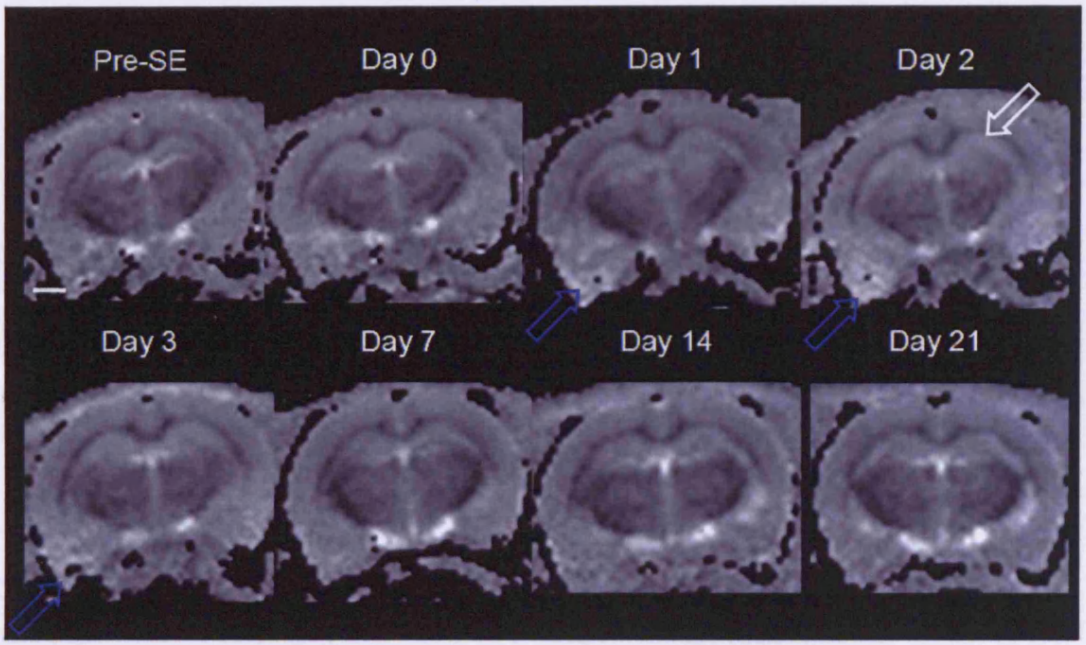

Figure 6.8. *T_1 maps of a single animal from the FLP group. Note the T_1 increase in the piriform cortex on day 1, 2 and 3 (blue arrow). Also hippocampal T_1 was increased on day 2 in this animal (white arrow). Scale bar equals 2mm.*

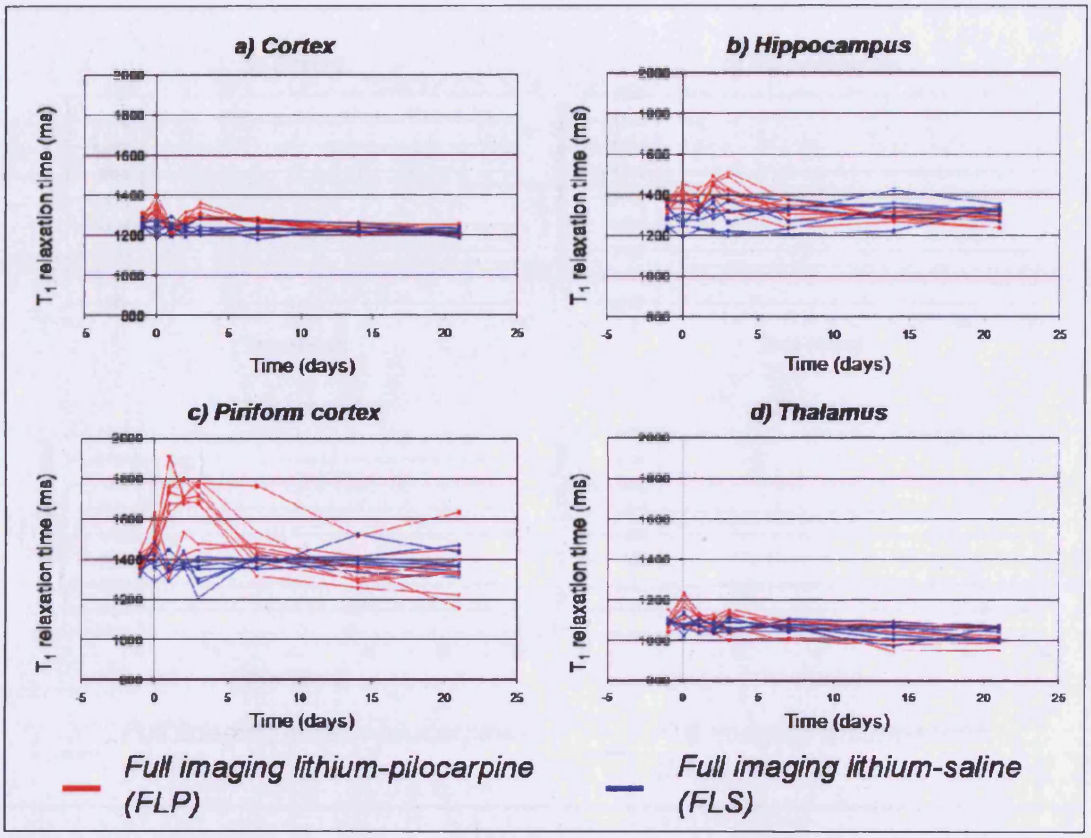

Figure 6.9. *T_1 relaxation time course in the: a) cortex, b) hippocampus, c) piriform cortex and d) thalamus. T_1 measurements were performed before lithium administration (day -1) and subsequently on days 0, 1, 2, 3, 7, 14 and 21. The red lines are measurements obtained from individual FLP animals and the blue lines from the individual FLS animals.*

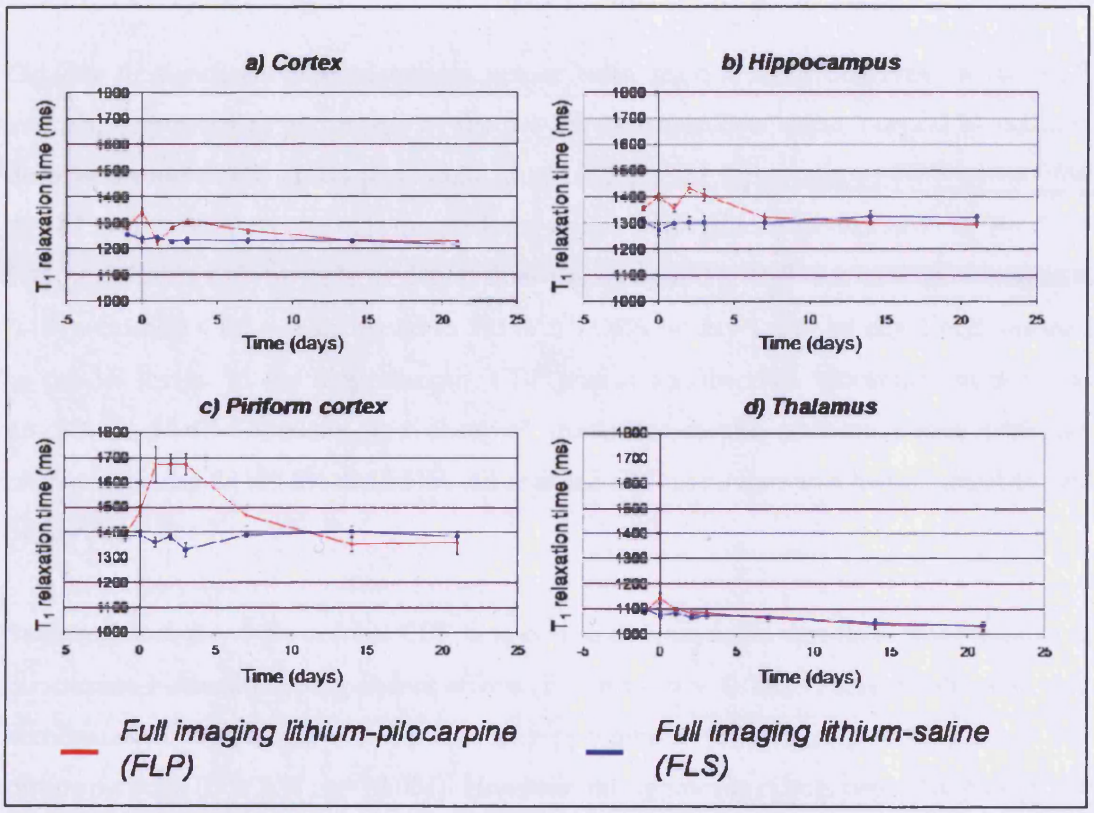

Figure 6.10. *Mean regional T_1 relaxation time courses before and following SE. Mean regional data were measured in the: a) cortex, b) hippocampus, c) piriform cortex, and d) thalamus. T_1 was measured in all animals 1 day before lithium administration (day -1), and subsequently on days 0, 1, 2, 3, 7, 14 and 21 after SE. Data shown as mean ± s.e.m. The red line represents the animals in the full imaging lithium-pilocarpine experimental rats (n = 9), and the blue line depicts the full imaging lithium-saline control animals (n = 7).*

6.3.3.3. CBF changes following SE

Figure 6.11 and 6.12 shows the individual CBF time courses for the brain regions analysed, and figure 6.13 shows the mean CBF time course over 21 days. The mean pre-SE CBF measurements for the FLS and FLP animals respectively were as follows: cortex, 115.6 ml/100g/min ± 8.3, 125.7 ml/100g/min ± 6.8; hippocampus, 87.6 ml/100g/min ± 5.6, 91.4 ml/100g/min ± 8.6; piriform cortex, 133.2 ml/100g/min ± 7.9, 137.5 ml/100g/min ± 8.2 and thalamus, 129.5 ml/100g/min ± 7.9, 130 ml/100g/min ± 7.9 (mean ± s.e.m.).

On day 0, significant CBF decreases across brain regions were observed in the FLP animals. Expressed as percentage of the pre-SE measurements, mean cortical blood flow decreased to 43.0% ± 11.4% ($F = 13.37$, $p = 0.003$), in the hippocampus CBF was at 75% ± 17.7% ($F = 6.73$, $p = 0.02$), the piriform cortex was reduced to 64.0% ± 10.5% ($F = 9.11$, $p = 0.009$) and the thalamic blood flow was measured at 69.7% ± 12% ($F = 1.98$, $p = 0.181$). Cortical CBF was increased to 151% ± 15.6% on day 1, but by day 2 had returned to pre-SE levels. In the hippocampus, CBF was at an observed maximum on day 2 at 164.8% ± 14.8%. Similarly, the observed maximum in the piriform cortex was also observed on day 2 (104.5% ± 15.5%). All regional CBF measurements had returned to pre-SE levels by day 7.

Statistical analysis of the cortical CBF time-course demonstrated that there were significant pilocarpine-induced time-dependent effects ($F = 8.50$, $p < 0.001$). These effects were also demonstrated in the time-courses for the hippocampus ($F = 8.74$, $p < 0.001$) and the piriform cortex ($F = 2.97$, $p = 0.031$). However, no significant effects were observed in the thalamus ($F = 0.137$, $p = 0.717$).

These data indicate that there was a regional and transient CBF change following SE.

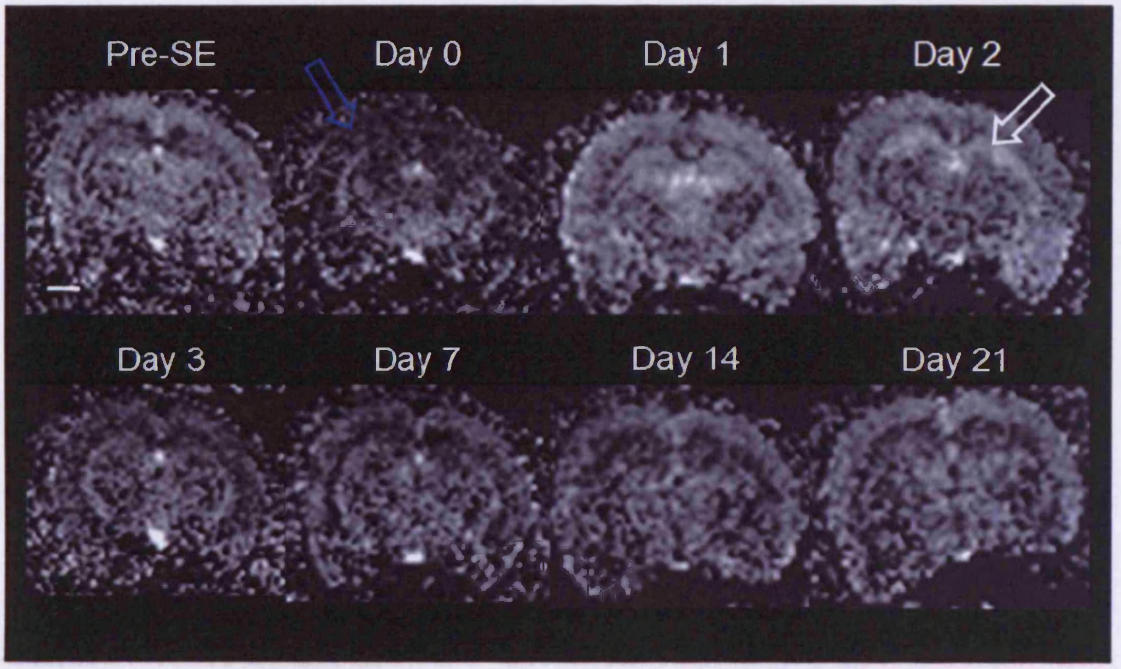

Figure 6.11. *CBF maps of a single animal from the FLP group. Note the decrease in blood flow across the entire brain on day 0 (blue arrow). Also hippocampal CBF increases considerably on the day 2 time point (white arrow). No changes in CBF were noted following day 2 in this animal. Scale bar equals 2mm.*

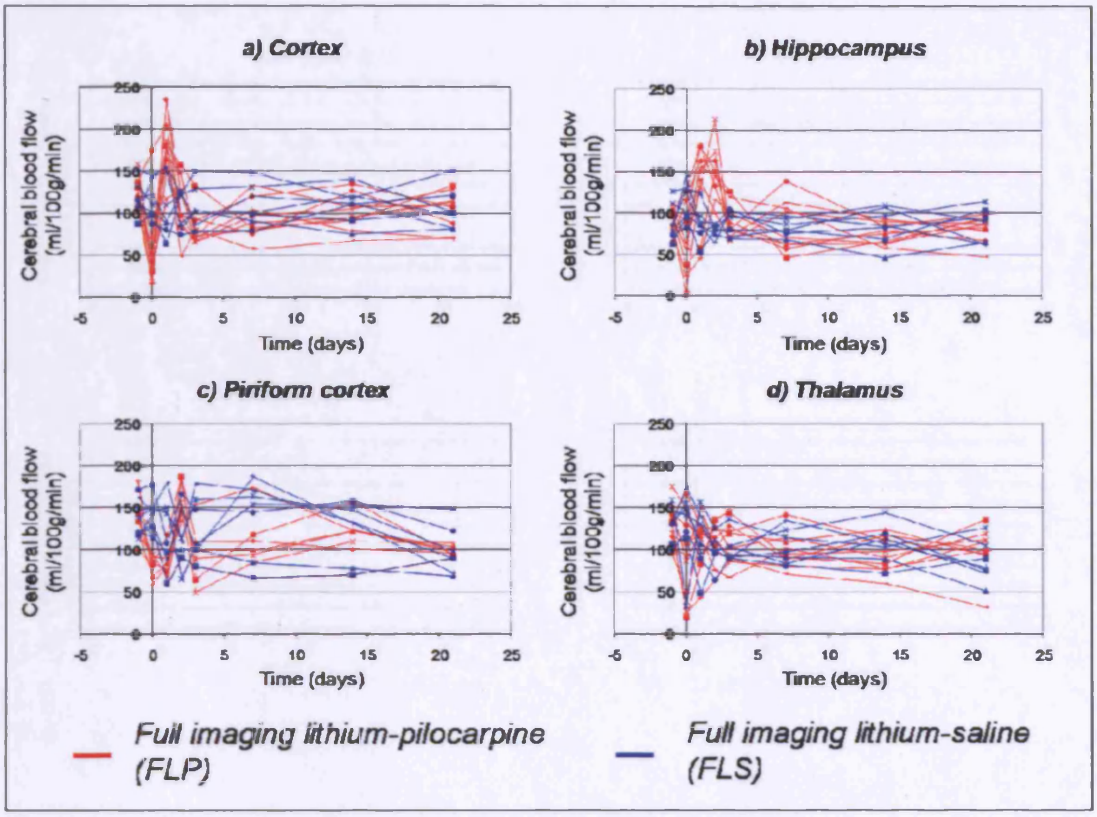

Figure 6.12. *CBF time course in the: a) cortex, b) hippocampus, c) piriform cortex and d) thalamus. CBF measurements were performed before lithium administration (day -1) and subsequently on days 0, 1, 2, 3, 7, 14 and 21. The red lines are measurements obtained from individual FLP animals and the blue lines from the individual FLS animals.*

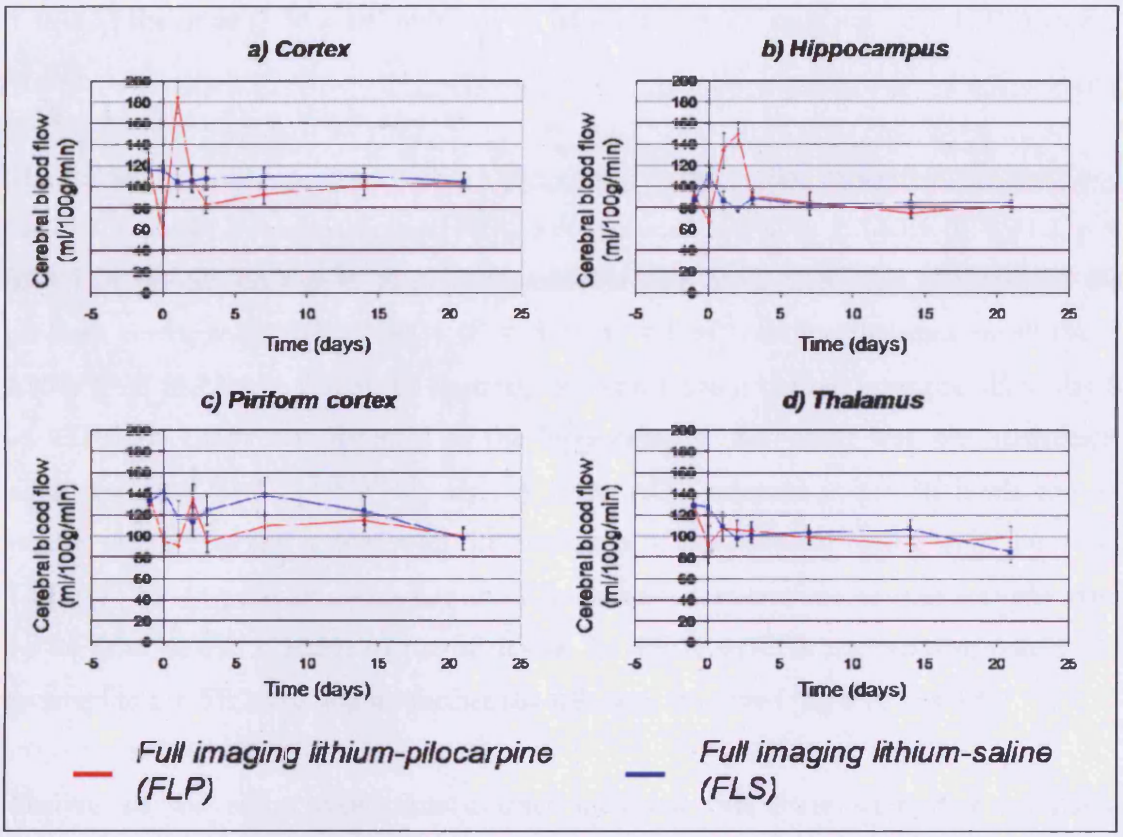

Figure 6.13. *Mean regional cerebral blood flow (CBF) time courses before and following SE. Mean regional data were measured in the: a) cortex, b) hippocampus, c) piriform cortex, and d) thalamus. CBF was measured in all animals 1 day before lithium administration (day -1), and subsequently on days 0, 1, 2, 3, 7, 14 and 21 after SE. Data shown as mean ± s.e.m. The red line represents the animals in the full imaging lithium-pilocarpine experimental rats (n = 9), and the blue line depicts the full imaging lithium-saline control animals (n = 7).*

6.3.3.4. ADC changes following SE

Figure 6.14, 6.15 and 6.16 shows the ADC time courses of the individual regions following SE. However, only ADC data for seven of the nine animals were included for analysis as the data from the remaining two animals were corrupted. The mean ADC measurements before drug administration for FLS and FLP respectively were: cortex ($6.95 \times 10^{-4} mm^2 sec^{-1}$ ± 0.106, $6.70 \times 10^{-4} mm^2 sec^{-1}$ ± 0.198); hippocampus ($7.16 \times 10^{-4} mm^2 sec^{-1}$ ± 0.114, $6.81 \times 10^{-4} mm^2 sec^{-1}$ ± 0.153); piriform cortex ($7.82 \times 10^{-4} mm^2 sec^{-1}$ ± 0.159, $6.81 \times 10^{-4} mm^2 sec^{-1}$

± 0.153); thalamus (7.30 x 10^{-4} mm^2 sec^{-1} ± 0.092, 6.97 x 10^{-4} mm^2 sec^{-1} ± 0.153) (mean ± s.e.m.).

The following results are expressed as a percentage from baseline measurements measured pre-SE. In the FLP animals, cortical ADC were reduced to 90.7% ± 1.63% ($F = 31.2$, $p < 0.001$) of pre-SE on day 0. Significant reductions in ADC were also observed in the piriform cortex to 81.5% ± 3.41% ($F = 5.25$, $p = 0.04$) and the thalamus to 98.1% ± 2.05% ($F = 11.72$, $p = 0.005$). In contrast, although a mean change from pre-SE to day 0 of 93.9% ± 1.15% was detected in the hippocampus, this result was not statistically significant ($F = 2.481$, $p = 0.141$). By day 1, the ADC returned to pre-SE levels and no further changes in any regions with the exception of the piriform cortex were observed. The ADC in the piriform cortex continued to decrease and maximal change was observed on day 1 at 61.6% ± 10.2% of pre-SE levels. By day 7, ADC in the piriform cortex had returned to pre-SE levels and no further changes were observed (fig 6.10 and 6.11).

Analysis of the entire ADC time courses indicated that there were time-dependent pilocarpine effects in the piriform cortex ($F = 10.41$, $p < 0.001$). Significant pilocarpine effects were detected in the cortex ($F = 10.22$, $p = 0.009$) and the thalamus ($F = 11.55$, $p = 0.005$). However, no significant effects were detected in the hippocampus ($F = 2.08$, $p = 0.174$).

Although the quantitative hippocampal ADC data did not demonstrate any significant differences in the FLP animals, visual inspection of the ADC maps showed a decrease within a sub-region of the hippocampus on day 2 (fig 6.10). This region appeared to correspond with the CA1 subfield of the hippocampus. The reason why this decrease in ADC was not detected could be due to the averaging of the ADC across the entire hippocampal region, and thus subtle changes are lost in this form of analysis. In total, 5 of the 7 animals demonstrated a regional ADC decrease in the hippocampus on day 2.

These data indicate that there is a regional and transient ADC change following SE, which normalised by day 7. Furthermore, an ADC increase was also observed on day 14 in the hippocampal region that was due to CSF and confirmed on the high resolution anatomical images.

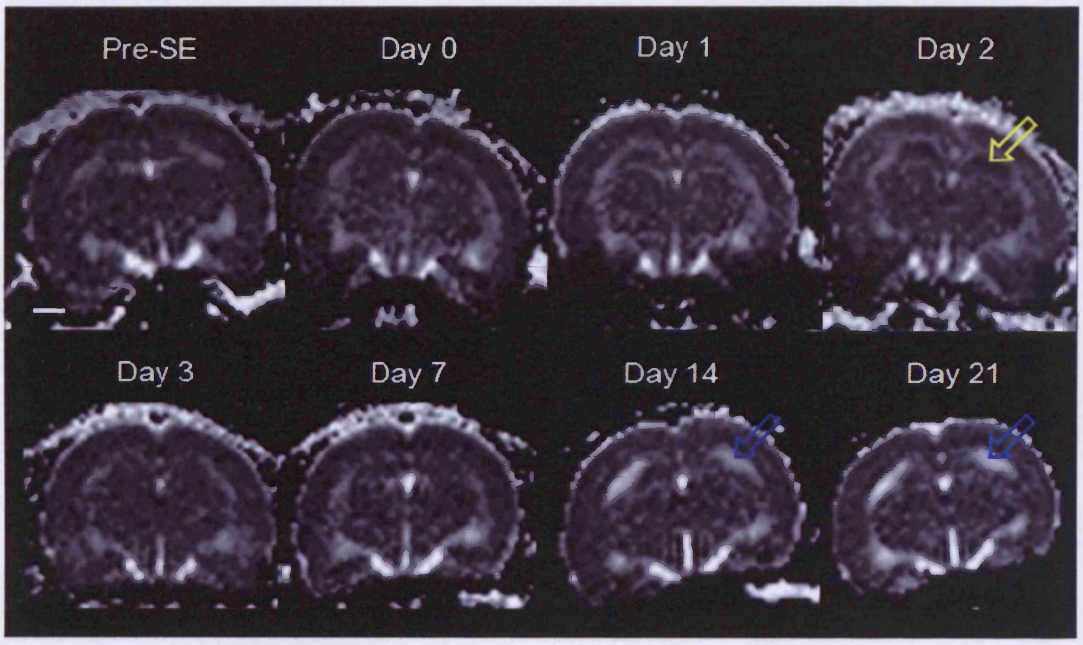

Figure 6.14. *ADC maps from the same animal acquired over 21 days following SE. Note the regional decrease in ADC in the hippocampus as indicated by the yellow arrow. Also the ADC increase – as indicated by the blue arrows - on days 14 and 21 suggests CSF and thus indicating hippocampal atrophy. Scale bar equals 2mm.*

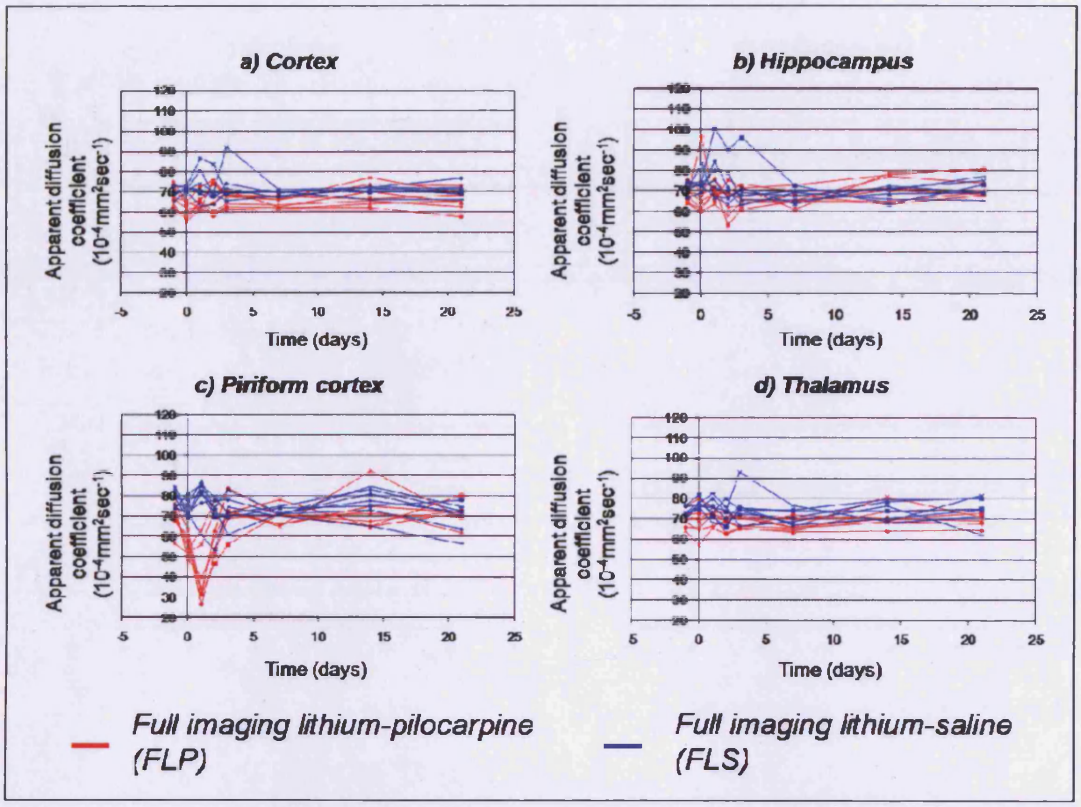

Figure 6.15. *ADC time course in the: cortex, hippocampus, piriform cortex and thalamus. CBF measurements were performed before lithium administration (day -1) and subsequently on days 0, 1, 2, 3, 7, 14 and 21. The red lines are measurements obtained from individual FLP animals and the blue lines from the individual FLS animals.*

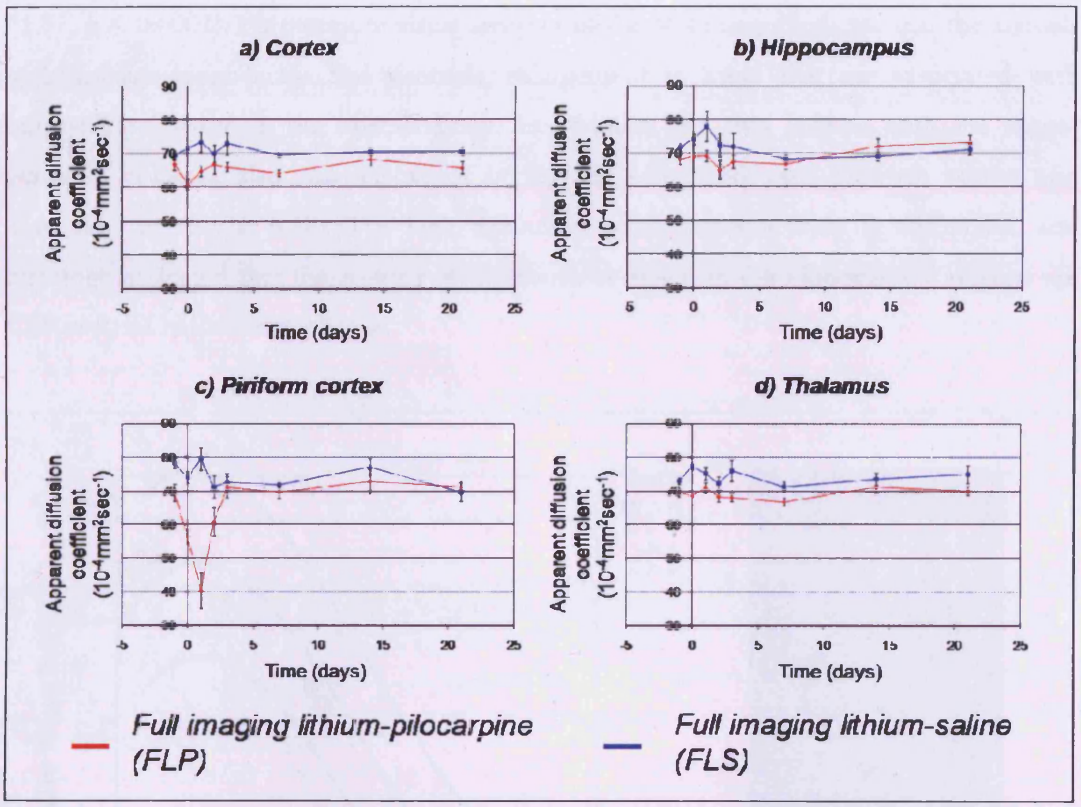

Figure 6.16. *Mean regional apparent diffusion coefficient (ADC) time courses before and following SE. Mean regional data were measured in the: a) cortex, b) hippocampus, c) piriform cortex, and d) thalamus. ADC was measured in all animals 1 day before lithium administration (day -1), and subsequently on days 0, 1, 2, 3, 7, 14 and 21 after SE. Data shown as mean ± s.e.m. The red line represents the animals in the full imaging lithium-pilocarpine experimental rats (n = 7), and the blue line depicts the full imaging lithium-saline control animals (n = 7).*

6.3.4. Volumetrics: hippocampal, ventricular and brain volumes 21 days post-SE

For whole brain volumes, no significant differences were detected between the FLS, FLP, CLS and CLP groups (F = 0.254; p = 0.857).

The relationship between ventricular volumes and hippocampal volumes were investigated (fig. 6.17) with a third order polynomial regression model. This analysis indicated that there was a strong relationship between hippocampal and ventricular volume (R^2 = 0.905, F =

71.77, $p < 0.0001$). Furthermore visual analyses of the MR images indicate that the animals with smaller hippocampi had ventricle enlargement in areas that are associated with hippocampal tissue in the normal brain. In addition, the two animals with the largest ventricle volumes also showed signal in regions associated with piriform cortex and amygdala (fig. 6.17a, 6.18). The high resolution scans together with T_2 and ADC, and histology indicated that the regions of hyperintense signal in the hippocampal regions are CSF and not hippocampal tissue.

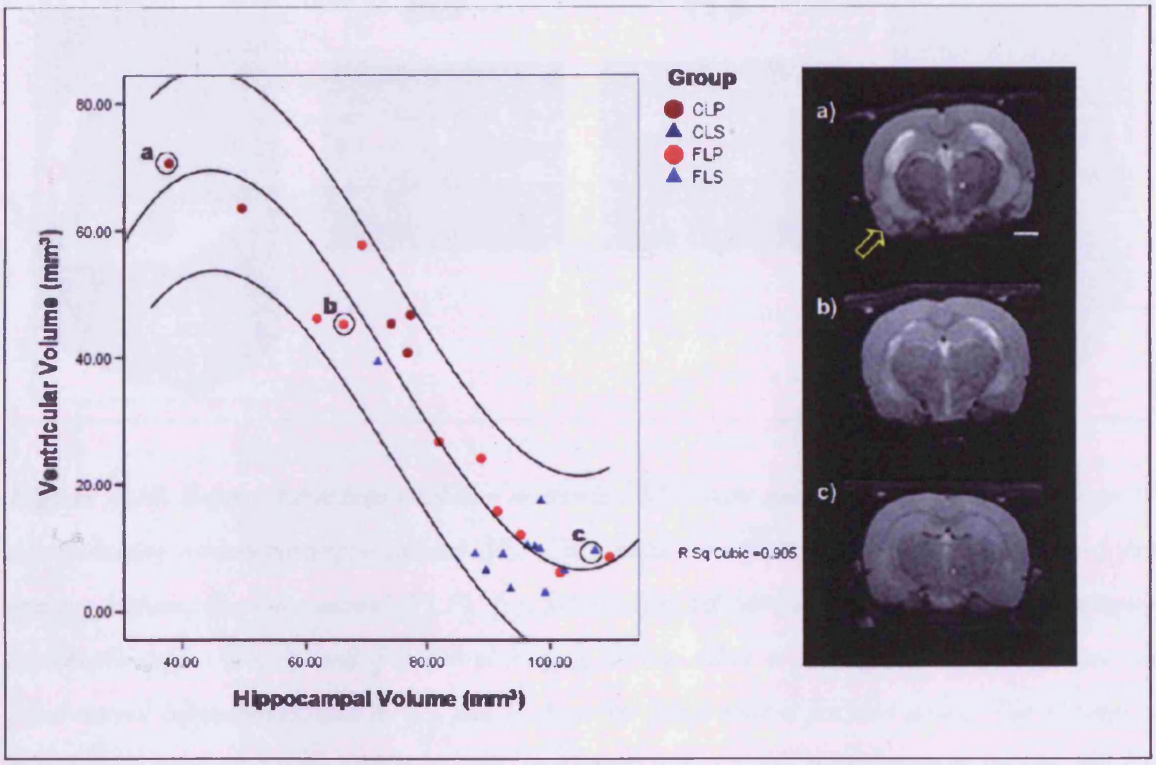

Figure 6.17. *The relationship between hippocampal and ventricular volumes measured on day 21. Regression analysis indicated that a third order polynomial was an appropriate regression model for these data. ($R^2 = 0.905$, $F = 71.77$, $p < 0.0001$). Representative animals (a-c) across the distribution have been highlighted and an anatomical MR image is presented in the right panel. a) shows hyperintense signal and had the lowest hippocampal volume and also revealed signal from areas associated with the piriform cortex; b) shows an animal from the middle of the distribution of hippocampal volumes and signal can be detected from regions that corresponded with the normal hippocampus; c) shows an animal with a non-pathological hippocampal volume. Scale bar in a) equals 2mm.*

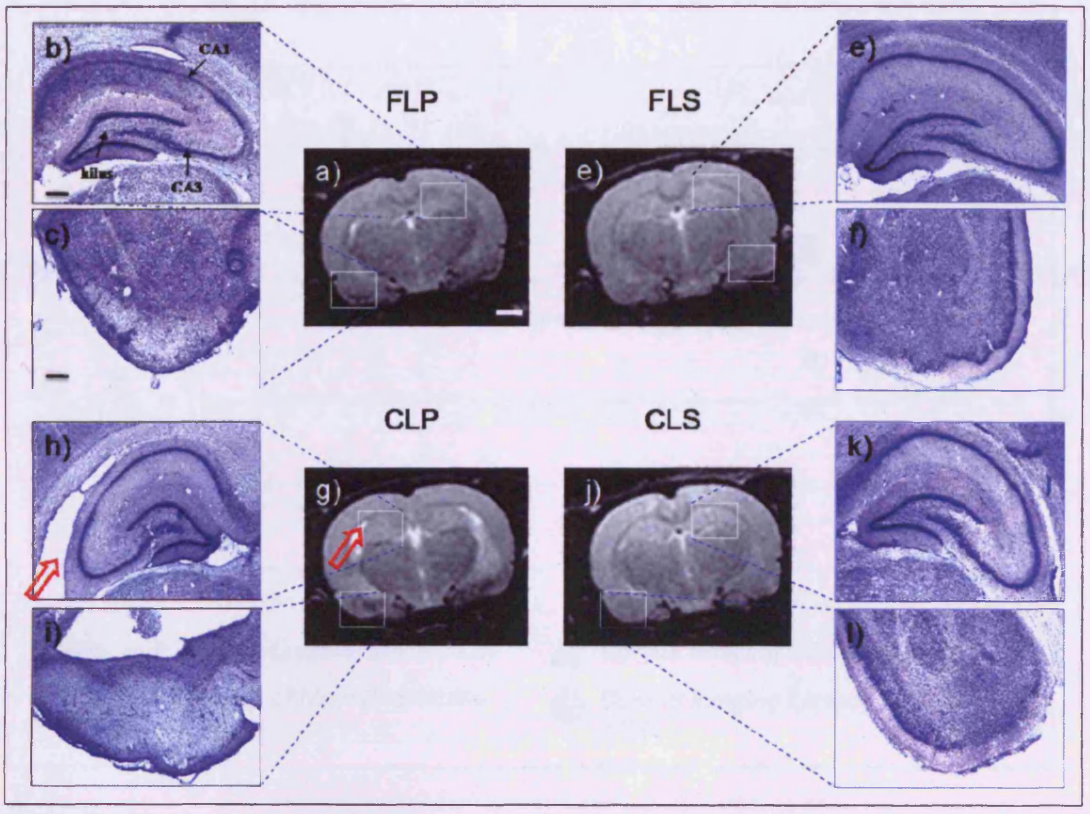

Figure 6.18. *Representative high resolution anatomical MR scans and corresponding histopathology 21 days following lithium-pilocarpine-induced SE. The samples are from the following groups: (a-c) full imaging lithium-pilocarpine animal (FLP), (e-f) full imaging lithium-saline (FLS), (g-i) control imaging lithium-pilocarpine (CLP), and (j-l) control imaging lithium-saline (CLS). (b, e, h and k) shows the Nissl-stained hippocampus, and (c, f, i and l) shows the Nissl-stained piriform cortex. The histological sections were taken at a magnification of x40. Red arrows denote region of hippocampal atrophy, which is confirmed on histology. White scale bar in a) equals 2mm; black scale bar in b) and c) equals 200μm.*

Hippocampal volumes between the four groups were investigated and significant differences were found ($F = 5.84$; $p = 0.004$) (fig. 7.19). Post-hoc analyses indicated that there were no differences between the saline control groups ($p = 0.999$) or between FLS and FLP ($p = 0.589$). However, significant differences were observed between CLS and CLP ($p = 0.008$). In addition differences were found between the two pilocarpine groups ($p = 0.048$).

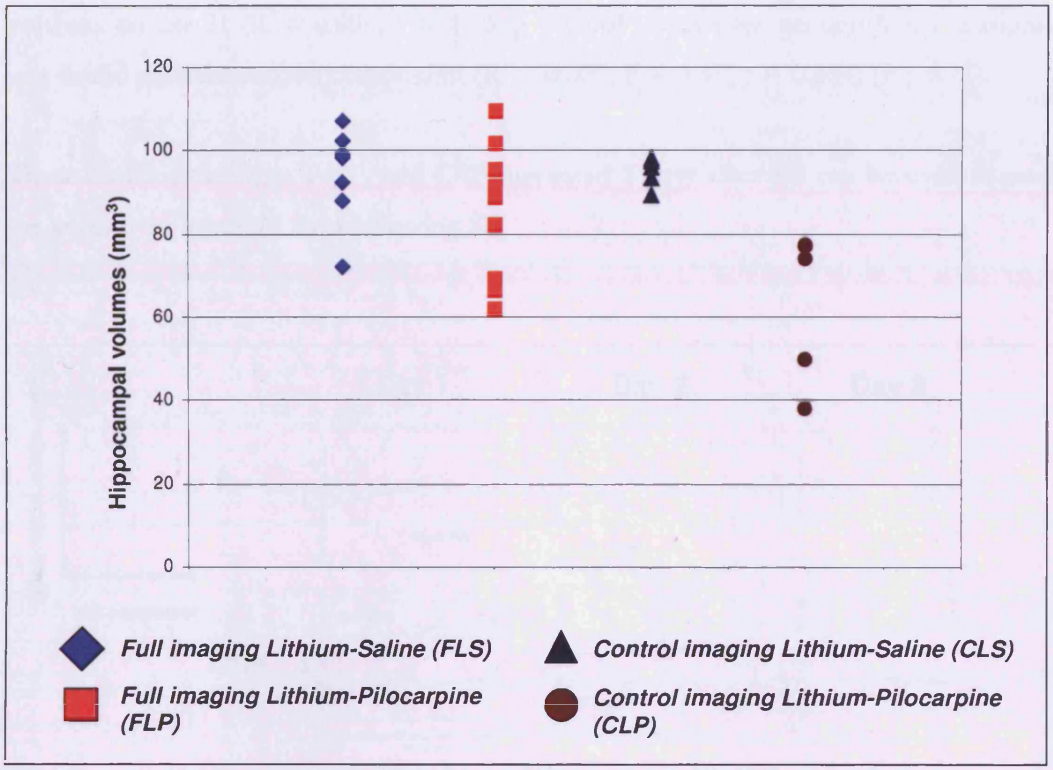

Figure 6.19. *Hippocampal volume 21 days after SE.*

6.3.5. The relationship between acute hippocampal MR changes and hippocampal volumes on day 21

The relationships between hippocampal MR changes on days 1, 2 and 3 and hippocampal volumes on day 21 were investigated in the FLP animals (fig 6.20). Statistical analyses indicated that there were significant relationships between the MR measurements on 2 day after SE with hippocampal volume on day 21 (fig 6.20), but none were found between either days 1 or 3 and hippocampal volume.

A principal component analysis was performed on the day 2 data because of the significant relationships observed. Two components were extracted (fig. 6.21). The first component was highly weighted to T_2, CBF and T_1, whereas the second component was weighted predominantly with ADC. Regression analysis was conducted on these two components and a significant relationship was found between the first component and hippocampal

volumes on day 21 (R^2 = 0.899, F = 44.5, p = 0.001). However, no significant relationship was found with the second component (R^2 = 0.007, F = 0.37, p = 0.854) (fig. 6.21).

These data indicate that T_1, T_2 and CBF measured 2 days after SE can be used to predict the severity of injury 21 days following SE.

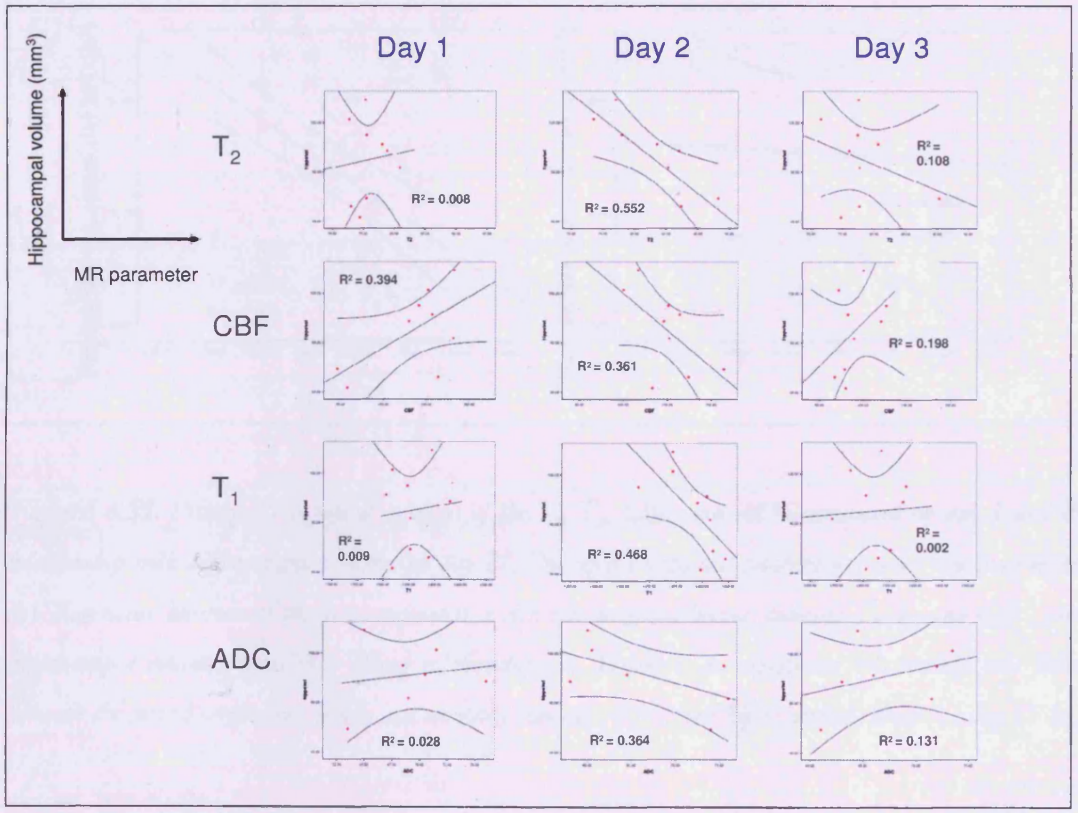

Figure 6.20. *The relationships between the MR measurements during the acute period following SE and hippocampal volume on day 21. Note that relationships can be observed on day 2 only.*

a) Principal component analysis

	Component	
	1	2
T2	.960	-.174
CBF	.944	.177
T1	.739	-.591
ADC	.551	.793

b) Component 1

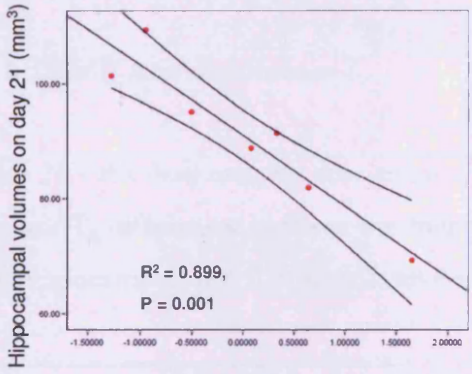

c) Component 2

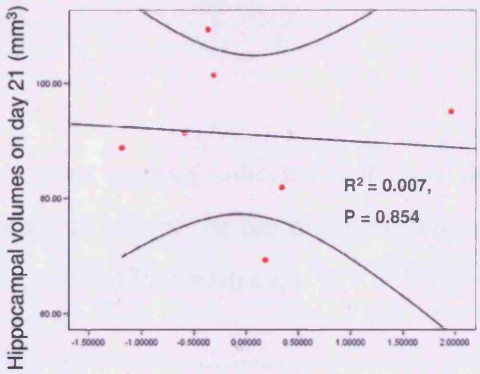

Figure 6.21. *Principal component analysis of the T_1, T_2, CBF and ADC measured on day 2 and the relationship with hippocampal volumes on day 21. Principal component analysis extracted two components (a). Regression analysis of the first component, which was weighted heavily towards T_2, T_1 and CBF, with hippocampal volumes revealed a strong relationship (b). However, no significant relationship was found between the second component, which was weighted towards ADC, and hippocampal volume on day 21 (c).*

6.3.6. Effect of serial isoflurane anaesthesia on brain injury

For investigating the effects of serial anaesthesia, two groups that were imaged before lithium injection and on day 21 (CLS, CLP) were compared against the imaged time course groups (FLS, FLP). The differences between the data acquired on day 21 were subtracted fro the corresponding data before lithium injection for each region to investigate these effects.

6.3.6.1. Effect of serial anaesthesia on T_2

On day 21 - the final imaging time point – statistical analysis indicated that there were no significant T_2 differences between the four groups in any of the brain regions: cortex, p = 0.920; hippocampus, p = 0.218; piriform cortex, p = 0.456; thalamus, p = 0.771 (fig. 6.22)

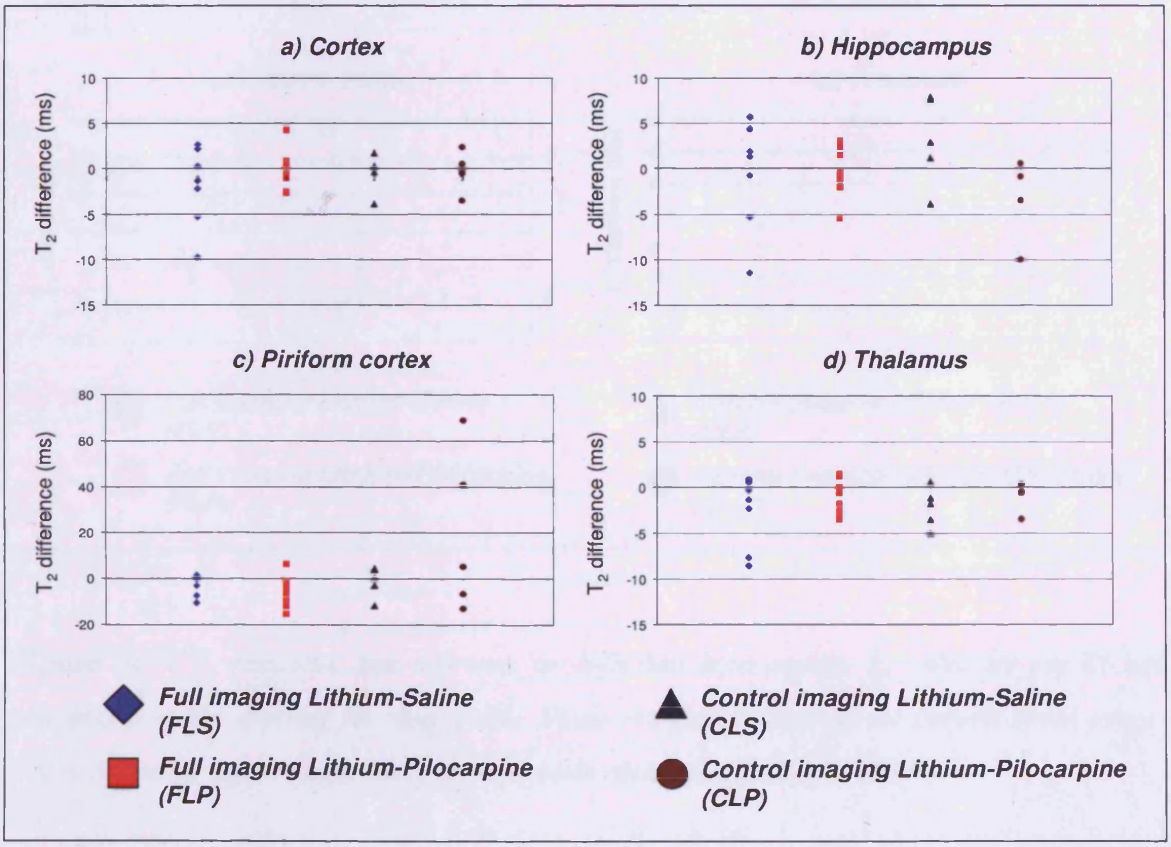

Figure 6.22. *T_2 relaxation times differences for individual brain regions. T_2 values for day 21 were subtracted from corresponding pre-SE values. Please note the range for the piriform cortex (-20 to 80ms) is different to the other brain regions (-15 to 10ms).*

6.3.6.2. Effect of serial anaesthesia on T_1

Figure 6.23 shows the regional data for T_1. The analysis indicated no significant differences in the hippocampus ($p = 0.086$), piriform cortex ($p = 0.461$) or the thalamus ($p = 0.730$). However, cortical T_1 differences were observed ($p = 0.016$). Post-hoc analysis of cortical T_1 demonstrated that there were significant differences between the FLP and CLP groups ($p = 0.029$).

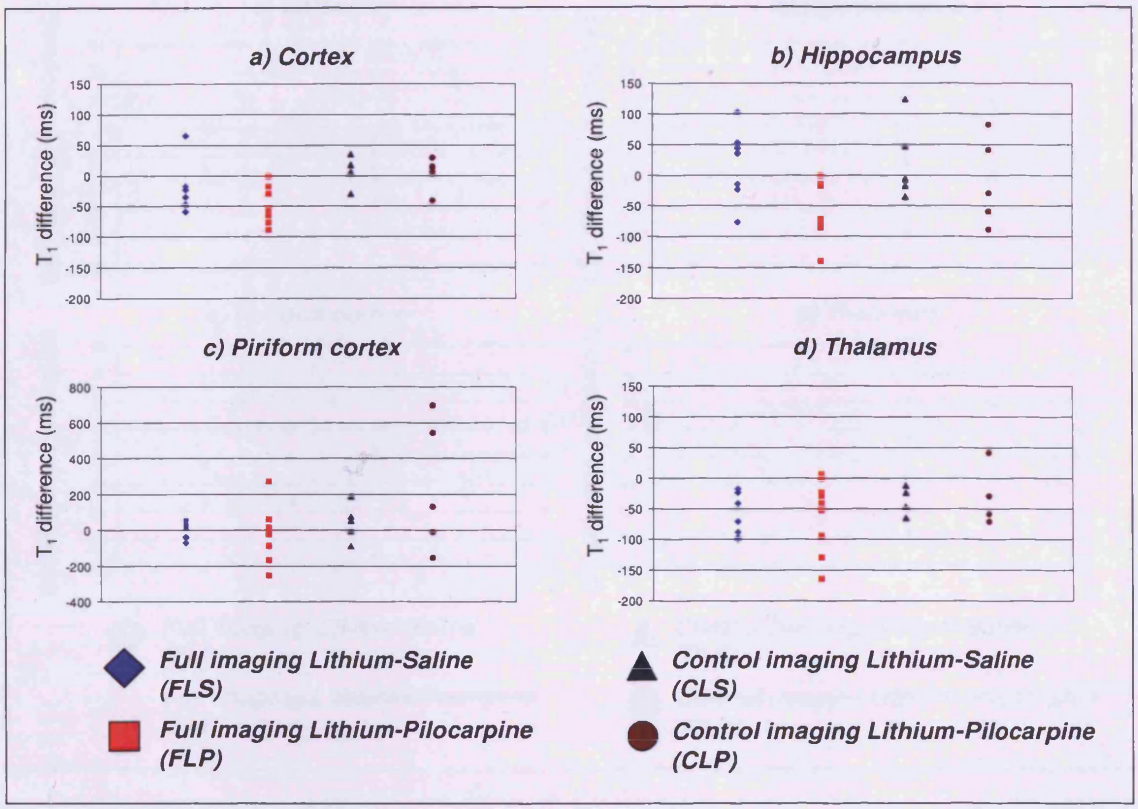

Figure 6.23. *T_1 relaxation time differences for individual brain regions. T_1 values for day 21 were subtracted from corresponding pre-imaging data. Please note that the scale for the piriform cortex (range -400 to 800ms) is different from that of the other brain regions (range -200 to 150ms).*

6.3.6.3. Effect of serial anaesthesia on CBF

Analysis of the four groups was performed to investigate the possible effect of repeated anaesthesia following SE (fig. 6.24). No statistical differences were observed in the cortex ($p = 0.093$), hippocampus ($p = 0.109$), piriform cortex ($p = 0.447$) or the thalamus ($p = 0.838$).

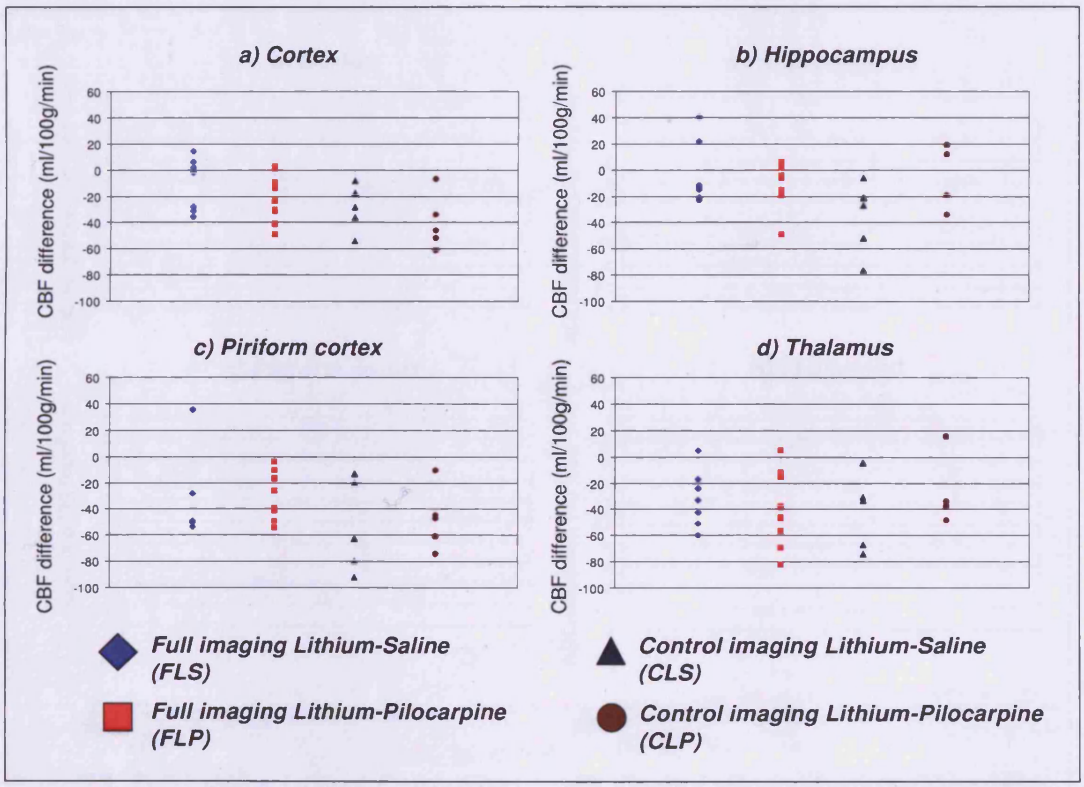

Figure 6.24. *CBF differences for individual brain regions. CBF values for day 21 were subtracted from corresponding pre-SE CBF values.*

6.3.6.4. Effect of serial anaesthesia on ADC

The ADC differences from pre-SE to day 21 were analysed to investigate the effects of repeated imaging following SE (fig. 6.25). No significant differences were observed in the cortex ($p = 0.351$), hippocampus ($p = 0.198$), or the thalamus ($p = 0.516$). A significant difference was observed in the piriform cortex ($p = 0.020$), however a post-hoc analysis indicated there were no significant differences between the pilocarpine groups ($p = 0.088$).

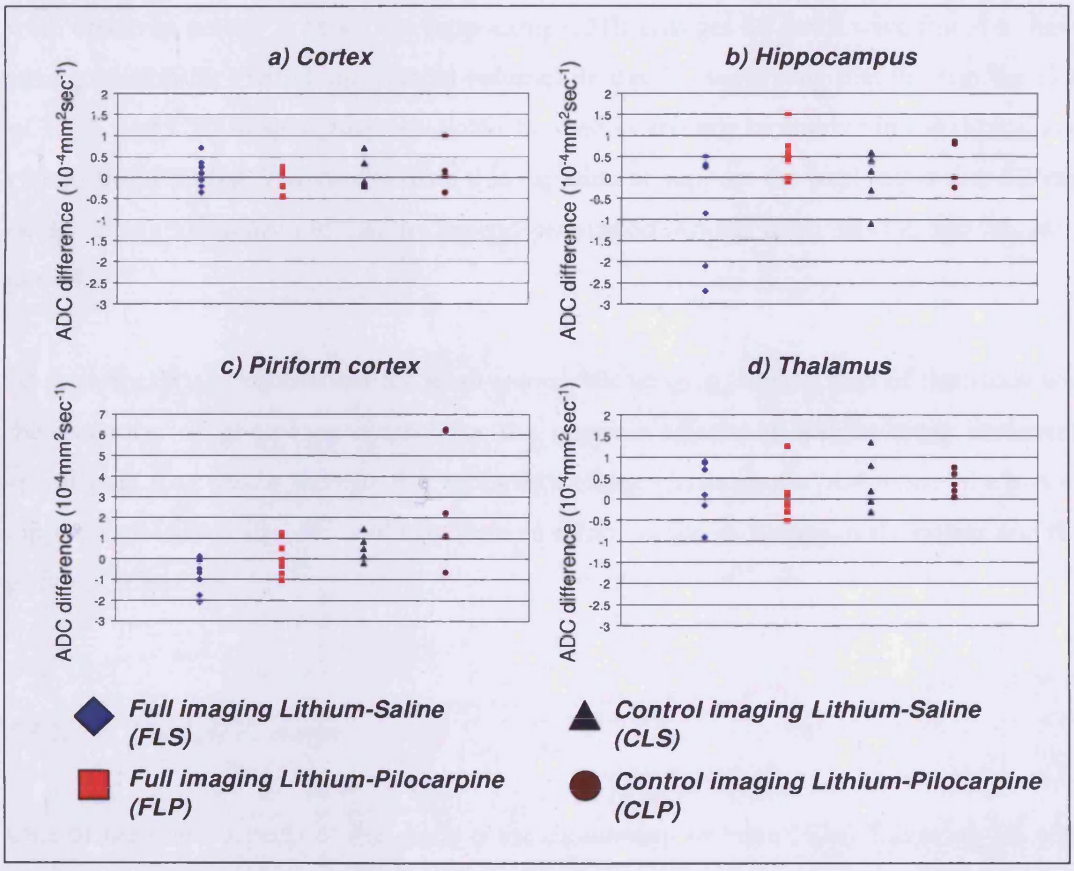

Figure 6.25. *ADC differences for individual brain regions. ADC values for day 21 were subtracted from pre-SE. Please note the range for the piriform cortex (-3 to 7 x 10^{-4} mm^2 sec^{-1}) is different from that of the other brain regions (-3 to 2 x 10^{-4} mm^2 sec^{-1}).*

These data indicate that serial anaesthesia has an effect on brain injury following SE, and differences were observed in cortical T_1 and ADC in the piriform cortex after SE.

6.4. DISCUSSION

The assessment of brain pathology with multiparametric MRI, a novel aspect of which is the inclusion of perfusion imaging, has identified characteristic regional differences during the early phase following SE. The observed changes all normalised by day 7 and remained at baseline levels until the end of the study. In contrast, hippocampal atrophy continued. During the acute period, peak MR changes in the hippocampus and the piriform cortex were observed on day 2. Moreover hippocampal MR changes on day 2 were found to have strong relationships with hippocampal volumes on day 21, suggesting that the combination of T_2, T_1 and CBF imaging may potentially be used as an early biomarker in the clinical and experimental setting. The results from this experiment support the hypothesis that SE can cause acute brain injury and that the neurodegeneration process continues beyond this early period.

As anaesthesia is a requirement for small animal MR imaging, a novel part of this study was the inclusion of groups to control for the possible effects of serially using isoflurane anaesthesia. Our results indicate that repeated isoflurane anaesthesia may reduce the loss of hippocampal tissue after SE, and may have an effect on the pathology in the cortex and the piriform cortex.

6.4.1. T_1, T_2 and ADC changes

One of the novel aspects of this study is the monitoring of brain injury following SE with quantitative T_1 imaging, which showed a similar pattern to T_2 changes. Previous MRI studies have investigated T_2 and ADC changes following SE and have also shown that these parameters change during the early period (Nakasu *et al.*, 1995; Wall *et al.*, 2000; Bhagat *et al.*, 2001; Dube *et al.*, 2004; Nairismagi *et al.*, 2004). Moreover, these changes occur predominantly in the hippocampus and the piriform cortex, which are regions that have been widely shown to be vulnerable to SE, and this has been reported in electrical stimulation as well as chemical induction SE models including the lithium-pilocarpine model (Roch *et al.*, 2002a; Dube *et al.*, 2004; Nairismagi *et al.*, 2004). Our data indicated that

T_2 increases and ADC decreases in these two regions during the first 7 days following SE, and these changes have been widely interpreted as the presence of oedema formation (Nakasu *et al.*, 1995; Bhagat *et al.*, 2001; Roch *et al.*, 2002a; Nairismagi *et al.*, 2004). However, although all these MRI studies have reported piriform cortex changes that follow a similar trend to the data presented in this study, the changes in the hippocampus have been reported to show a different pattern.

Previous studies have shown that various MRI changes occur in the hippocampus. For example, ADC increases during the first week and also T_2-weighted hyperintensities that increase in the first 2 days and continue to be high for up to 9 weeks following SE have been reported, which are in contrast to what we have observed (Wall *et al.*, 2000; Roch *et al.*, 2002a; Fabene *et al.*, 2003). In the current study, hippocampal decreases in ADC were observed, and furthermore, although T_2 increases were also observed, these changes normalised by day 7 after SE, which are consistent to other studies that have reported similar results (Nakasu *et al.*, 1995; Dube *et al.*, 2004; Nairismagi *et al.*, 2004). Model differences are unlikely to underlie these contradictory data as between these studies various modes of SE induction have been used. One possible explanation that may underlie these discrepancies may be due to differences in data processing.

The region of interest for the hippocampus can be drawn can be of one of two different ways and depends on the question that is being investigated. The first is a region of interest that encompasses the traditional outline of the rat hippocampus and this region is maintained throughout the study. However, if the hippocampus atrophies then this region will measure CSF as well as the characteristics from the tissue. Therefore, increases in ADC and T_2 as a result of CSF will be measured, as signal is not solely from the hippocampus. This method for drawing a region of interest that includes the non-pathological borders of the hippocampus can provide information about the progression of hippocampal atrophy (Wall *et al.*, 2000). The second method of drawing a hippocampal region of interest concerns solely the MR changes within the hippocampal tissue, and requires the region of interest to be modified according to the atrophy of the hippocampus. This can be done by using the combination of T_2 and ADC data to evaluate whether CSF is included into the region that is drawn. By using this method, the hippocampal tissue characteristics can be measured, which was the method used in this study. Therefore these two methods of

processing may underlie the contradictory reports, with respect to the hippocampus, in the epilepsy literature.

The present study also reported acute transient T_2 increases in the piriform cortex, and it is interesting to note that Roch and colleagues found that T_2 increases in the piriform cortex are required for the subsequent onset of spontaneous recurrent seizures. Although this finding was reported in 21 day old rats, this may also suggest that the animals in the present study will progress on to epilepsy.

In general, previous studies have shown that neuronal swelling and cell death occur during the first week after SE with parallel changes in ADC and T_2 (Nakasu *et al.*, 1995; Fujikawa, 1996; Roch *et al.*, 2002a) and, therefore our data are likely to indicate that the ADC, T_1 and T_2 changes following SE reflect the formation and resolution of oedema.

6.4.2. Perfusion

Another novel part of this study was the investigation of haemodynamic changes following SE. We measured regional quantitative CBF following SE and observed reductions in CBF at the day 0 time point for all regions. After this time, CBF was increased in the cerebral cortex, hippocampus and the piriform cortex. By day 2 CBF returned to baseline in the cerebral cortex, CBF in the hippocamus and the piriform cortex remained high. Subsequently (day 7) the CBF in all regions returned to baseline, after which no further changes were observed.

In the present study, a significant reduction in CBF was observed in all regions at day 0. A similar finding was reported by Engelhorn and colleagues, although this was observed during the later phase of SE (Engelhorn *et al.*, 2005). Furthermore, they reported that perfusion increased within a few minutes of SE and subsequently decreased as SE progressed. They also observed a relationship between the early blood flow reduction and subsequent cell death, but an underlying mechanism for the CBF decrease was not explored. One possible hypothesis that may explain the observations in the present study is that the CBF decrease reflects a failure of cerebral autoregulation, which has been reported

as a result of prolonged seizure activity (Lothman, 1990). The concept suggests that as cerebral autoregulation fails, the CBF becomes wholly dependent on systemic blood pressure. In the current study, diazepam was administered to stop the seizure and this may explain the finding in this study. Diazepam acts primarily through the potentiation of inhibitory $GABA_A$ receptors leading to a reduction in seizure activity. The reduced seizure activity would thereby result in a concomitant decrease in systemic pressure. A combination of reduced central and systemic activity may in turn lead to an attenuation of CBF.

Following the initial decrease in CBF, blood flow increased in various regions following SE. Elevated levels of cerebral blood volume (CBV) have been reported 12 h after the onset of SE by Fabene and colleagues. They reported various hyperperfused areas that included the hippocampus, cerebral cortex and the thalamus. We observed similar elevated levels of perfusion by day 1 in the cerebral cortex and the hippocampus but did not observe any changes in thalamic perfusion. Moreover, cortical CBF was increased and reached a maximum on day 1, and hippocampal CBF was high on days 1 and 2. There also appeared to be a non-significant but systematic increase in CBF on day 2 in the piriform cortex (see fig. 6.12 and 6.13).

The discrepancy in the thalamus between the Fabene study and our studies may be due to a number of methodological differences between these studies. Fabene and colleagues did not use lithium pre-treatment and also gave the animals a 4 h seizure compared to the 90 minutes used in this study, either of which may exacerbate injury leading to changes in perfusion. Also they measured relative CBV whereas absolute CBF was measured for this study. Nevertheless it is the measurements at different time points that are likely to underlie this discrepancy. It is possible that 12 h perfusion does, in fact, increase in all of these regions in our animals but whereas perfusion remains high in the cerebral cortex and the hippocampus at 24 h, thalamic perfusion may have returned to normal by this period.

Nevertheless, perfusion increases have been observed in a variety of conditions, such as subarachnoid haemorrhage and SE, and have been associated with cell death and inflammation (Rowe *et al.*, 1998; Blamire *et al.*, 2000; Fabene *et al.*, 2003; Engelhorn *et al.*, 2005). However, investigations into the time course for CBF changes after SE has not been

previously reported and therefore the mechanisms that underlie these alterations in CBF following SE remain unclear.

Local blood flow is primarily maintained by the release of paracrine vasodilators from endothelial cells, which can be induced by various mechanisms including neurotransmitters, neuropeptides and physical vascular stimuli, such as shear stress (Scotland *et al.*, 2005). To date, endothelial-derived vasodilatation is thought to occur through three main pathways: nitric oxide (NO), prostacyclin (PGI_2) and endothelium-derived hyperpolarizing factor (EDHF) (Brandes *et al.*, 2000), but the relative contribution of these pathways to the observed CBF changes have not been studied in the current study.

NO is generated by the action of the nitric oxide synthase family of proteins (NOS) and excessive amounts of NO have been shown to cause cell injury and death (Moncada and Bolanos, 2006). Presently, three isoforms of NOS have been identified: endothelial derived NOS (eNOS), neuronal NOS (nNOS), and the inducible form, iNOS (Cuzzocrea and Salvemini, 2007). In CNS injury, two post-injury periods have been defined with reference to high levels of NO production: immediately after injury and several hours-to-days later. The initial period has been associated with nNOS generated by neurons, and the later period with iNOS produced by infiltrating inflammatory cells (Conti *et al.*, 2007). However, whether this trend occurs following SE is not clear, but NOS up-regulation has been shown to play a role in the injury caused by SE (Montecot *et al.*, 1998; Chuang *et al.*, 2007) and seem to parallel the activation of inflammatory cytokines (De Simoni *et al.*, 2000). Moreover, these changes seem to correspond with the period of elevated CBF that we have observed in this study.

PGI_2 is a prostaglandin that is produced by the activation of cyclo-oxygenase (COX) family of proteins. Two forms of COX have been currently identified: COX-1 and COX-2 (Cuzzocrea and Salvemini, 2007). Whereas COX-1 is present in tissues and plays a cytoprotective role in normal physiological function, COX-2 is expressed during inflammation (Vanheel and Van, V, 2000). The increased expression of COX-2 has been identified following SE-induced injury and were found to be localised almost exclusively around the hippocampus and the piriform cortex (Turrin and Rivest, 2004). Furthermore, in these regions the temporal pattern of expression of COX-2 following pilocarpine-

induced seizures parallel the transient nature of the CBF time courses that were observed in this study (Turrin and Rivest, 2004). It is notable that a recent study indicated that celecoxib, a selective COX-2 inhibitor, administered after lithium-pilocarpine-induced SE has been shown to reduce the subsequent severity and frequency of spontaneous recurrent seizures (Jung *et al.*, 2006). This suggests that COX-2 may have a key role to play in the modulation of outcome following SE.

Vasodilatation cannot be fully accounted for by the actions of NO and PGI_2, and there is now strong evidence for the existence of a third pathway, EDHF (Bryan, Jr. *et al.*, 2005). The identity of EDHF remains elusive, but its defining characteristic is that it requires the involvement of potassium channels, which are often calcium-activated (Bryan, Jr. *et al.*, 2005). Although electrolyte imbalance has long been associated with seizures (Shorvon, 1994; Hinterkeuser *et al.*, 2000; Cock *et al.*, 2002), and a persistent elevation of intracellular calcium has been implicated in the pathogenesis of epilepsy (Delorenzo *et al.*, 2005), whether EDHF has a role to play post-SE has not been explored.

Taken together, these data indicate that the observed CBF change may reflect an inflammatory process and also cell death, both of which have been identified during this acute period following SE. However, further studies are required to elucidate the underlying basis for these observed CBF changes and the relationship with later injury. It is possible that an acute inflammatory reaction following SE plays a key role in subsequent brain injury and epileptogenesis.

6.4.3. Volumetric assessment 21 days post-SE

Analysis of the volumetric data indicated that there were no significant brain volume differences between the four groups 21 days after SE. However, hippocampal volume differences were found; these results will be discussed further in section 6.4.5. In addition, regression analysis indicated that there was a strong association between ventricular and hippocampal volumes.

MRI has been previously used to measure hippocampal volumes post-SE in animal models and in humans, and reductions in hippocampal volumes have been reported following the early period post-SE (Scott *et al.*, 2002; Wolf *et al.*, 2002; Niessen *et al.*, 2005). Although multiple areas are known to be injured by SE, the hippocampus appears to be particularly vulnerable to prolonged seizure activity. It is also notable that the reduced hippocampal volumes measured with MRI are related to functional deficits; a relationship that has been widely reported using histological assessment of hippocampal volume with spatial memory tests (Moser *et al.*, 1995; Nunez *et al.*, 2000; Wu *et al.*, 2001). These data suggest that MRI volumetrics are a valid method for assessing of hippocampal volumes.

The finding that brain volume did not change following SE has been reported previously 60 days after SE in the pilocarpine rat model (Niessen *et al.*, 2005), and our results also replicate this finding. In addition, the data from the current study are similar to the results reported by Niessen and colleguaes, in which reductions in hippocampal volumes and enlargement of ventricular volumes were observed. Taken together, these results suggest that neuronal loss after SE occurs predominantly in the hippocampus.

Although the relationship between ventricular volume and hippocampal volume has also been reported (Niessen *et al.*, 2005), in the present study regression analysis indicated that the association between increasing ventricular volumes and atrophy of the hippocampus was only true up to a degree after which the relationship no longer holds. This was observed in two of the animals that showed the most severe hippocampal atrophy and enlarged ventricles, in which signal from CSF could also be seen from the piriform cortex and the amygdala. Whether the injury was caused by a particularly severe form of SE or by some unknown environmental condition remains unclear. The severity of injury caused by SE has been shown to depend on its duration (Fujikawa, 1996), but environmental stresses have also been associated with hippocampal atrophy (Zhao *et al.*, 2007). Also, environmental stress is associated with selective neuronal loss in the CA1 and CA3 regions of the hippocampus, which are also particularly vulnerable to SE-induced injury (Fujikawa, 1996; Zhao *et al.*, 2007). Whether environmental stress has any implications on the progression of cell loss seen in SE-induced injury has yet to be explored.

6.4.4. The serial effect of isoflurane on brain injury after SE

The main purpose of investigating the effects of isoflurane was to see whether the pathophysiology following SE was affected when the animals were serially imaged. The experimental design for this study included additional control groups for investigating such an effect. Significant differences in hippocampal volumes between the full-imaging and control-imaging pilocarpine groups were observed in which the FLP group showed less hippocampal atrophy than the CLP group. Also, when the tissue status was assessed by quantitative MRI, significantly different changes were found in the cortical T_1 and ADC in the piriform cortex. Taken together, these data indicate that the serial use of isoflurane may confer a degree of neuroprotection following SE.

The neuroprotective effect of isoflurane has been demonstrated in experimental models of traumatic brain injury and ischaemia but its effect following SE has not previously been explored (Statler *et al.*, 2006; Koerner and Brambrink, 2006). Similarly to other general anaesthetics, the mechanisms of action of isoflurane remain unclear but it has been shown to act on a host of neurotransmitter systems including those involving GABA, glycine, acetylcholine, serotonin as well as the three types of ionotropic glutamate receptors (Rudolph and Antkowiak, 2004). However, which of these mechanisms are important in neuroprotection is not known.

The long term neuroprotective effect of isoflurane has also been questioned in that this effect dissipates around 2-3 weeks after ischaemia; in contrast, this effect has been shown to persist following traumatic brain injury (Statler *et al.*, 2006). In relation to the current study, whether the neuroprotection persists after the 21 days is not known. Furthermore, as multiple doses of anaesthesia were given for the imaging time course, and thus it was not possible to assess whether it was the cumulative effect of isoflurane or this was due to an early effect after SE. It has been suggested that it is the timing of the anaesthesia that is critical in that this effect is exerted at or very near the time of brain injury, and it is therefore likely that the neuroprotection observed may be due to an early effect of anaesthesia (Statler *et al.*, 2006). Although the neuroprotective effect was investigated in this study, its effect on epileptogenesis was not studied and the change in brain injury following SE may suggest an interesting avenue for further study.

The question remains as to whether the MRI time course has been altered due to the effect of isoflurane. The acute transient response after SE that were observed have been detected following SE in previous MR studies that used other anaesthetics, such as ketamine, and also in humans (Nakasu *et al.*, 1995; Scott *et al.*, 2002; Roch *et al.*, 2002a). Therefore these studies suggest that the acute and transient response that was observed does occur irrespective of the anaesthetic used. However, whether this response has been modulated is not known. Nevertheless, these results indicate that future studies should take the potential effects of anaesthesia into consideration.

6.4.5. The relationships between maximal hippocampal MR changes on day 2 and hippocampal volume on day 21

One of the main findings in this study is that maximal hippocampal MR changes measured 2 days after SE were strongly associated with hippocampal volumes on day 21, which was not observed with either day 1 or day 3 measurements. Further analysis indicated that it was the combination of T_1, T_2 and CBF measurements on day 2 that was highly predictive of hippocampal volumes on day 21 and suggesting an early biomarker for injury.

Although all four of the parameters were found to be altered in the hippocampus over the first 3 days, it is unclear why it was only at 2 days after lithium-pilocarpine induced SE that a relationship with later injury was found and whether this is a model-specific phenomenon. Similarly to this study, T_2 and ADC changes, as well as in $T_{1\rho}$ and rCBV, have been reported acutely post-SE pathology in experimental models and in humans shortly after the seizure (Nakasu *et al.*, 1995; Wall *et al.*, 2000; Roch *et al.*, 2002a; Scott *et al.*, 2003; Nairismagi *et al.*, 2004). However, quantitative measurements at similar intervals over this acute period have not been previously attempted, and thus it is unclear as to whether the peak changes occur specifically at 2 days in other forms of SE. Clarification of this phenomenon in humans may provide a diagnostic tool for identifying patients who may progress on to a poor outcome, and offer an opportunity for early intervention.

During this early period, a variety of processes has been described, including cell death, inflammation and increased neurogenesis (see chapter 2). Each of these processes is likely to be contributing to differing degrees to each of the parameters, and the physiological basis of each of these changes has previously been discussed. One particular physiological process that is consistent with both oedema (T_1 and T_2) and increased CBF is inflammation, which is invariably present following an insult (Blamire *et al.*, 2000; Ambrosini *et al.*, 2005). Inflammation is a process that has been previously implicated in post-SE pathology and inflammatory molecules have been identified during this early period (see section 2.3.2) (Jankowsky and Patterson, 2001; Vezzani and Granata, 2005). However, a direct relationship between early inflammation and later outcome has not, to our knowledge, been previously reported. Due to this relationship, we hypothesise that status epilepticus is associated with acute brain inflammation which modulates brain injury and subsequent epileptogenesis, and thus a reduction in inflammation will reduce the incidence and severity of later epilepsy. A recent study that investigated the post-SE effect of selectively inhibiting COX-2, a key inflammatory pathway, supports this hypothesis (Jung *et al.*, 2006). Clearly, the period around 2 days requires further study, and identifying concomitant molecular changes may elucidate novel pathways for investigating post-SE pathology.

6.5. CONCLUSION

This study supports the hypothesis that SE induces progressive injury that continues to evolve following the acute period. Changes in T_1, T_2, ADC and CBF can be observed during this acute period and may reflect the onset and resolution of inflammation. Moreover, peak changes in T_2 were observed during this early period, 2 days after SE, and our analysis indicates that there is a striking relationship between T_1, T_2 and CBF changes and hippocampal volume measured on day 21. Taken together, these results suggest that we have identified an early biomarker on day 2 for outcome in the lithium-pilocarpine model. This may be an important period following SE-induced injury and may indicate a window of opportunity for early intervention. Further studies are required to elucidate the mechanisms that occur during this period, and this is the basis of investigations reported in the following chapter.

CHAPTER 7: PROTEOME CHANGES ASSOCIATED WITH MAXIMUM HIPPOCAMPAL MRI ABNORMALITIES FOLLOWING STATUS EPILEPTICUS

Do not dwell in the past, do not dream of the future, concentrate the mind on the present moment

Buddha

7.1. INTRODUCTION

Chapter 6 reported on the temporal evolution of brain injury following SE, characterised using multi-parametric MRI. In that study, the hippocampus of the lithium-pilocarpine rat was found to elicit a maximum MRI response at 2 days after SE. Moreover, this response demonstrated a significant relationship with the evolution of injury on day 21. Therefore these data indicated that early hippocampal injury can predict later injury. However, the of the MRI changes is unknown.

Studies have demonstrated that a host of physiological processes are activated during this period following SE. By day 2 these include inflammatory, cell death as well as neurogenic mechanisms (Fujikawa, 1996; Vezzani and Granata, 2005; Parent *et al.*, 2006a) (see chapter 2), as well as alterations in neurotransmitter systems and Ca^{2+} signalling (Raza *et al.*, 2001; McNamara *et al.*, 2006). However, one of the main difficulties of comparisons between studies is that different animal models or implementation of animal models are used. For example, although the duration of the prolonged seizure has been shown to be crucial for the progression of brain injury and the development of spontaneous recurrent seizures, seizures that range from 20 mins to 6 hours can be found throughout epilepsy literature (Mello *et al.*, 1993; van Eijsden *et al.*, 2004; Dube *et al.*, 2006). In MRI studies conflicting reports exist, for example, both ADC increases and decreases have been reported following SE (Nakasu *et al.*, 1995; Wall *et al.*, 2000; Fabene *et al.*, 2003). Thus it is possible that alterations in the temporal profile of the underlying molecular changes may also exist between different studies. Therefore to identify specific molecular changes that parallel the MRI parameters reported in chapter 7 we performed an image guided proteomic study.

In this study, MRI was combined with proteomic analysis to elucidate the protein changes associated with the maximal hippocampal MRI changes 2 days post-SE.

7.1.1. Proteomics

Proteomics encompasses a variety of techniques that are defined by the large-scale characterisation of proteins expressed by the genome (Hoehn and Suffredini, 2005). These techniques include chromatography, electrophoresis, mass spectrometry and protein arrays. Of these techniques, protein separation by two-dimensional gel electrophoresis (2-DE) combined with protein identification by mass spectrometry are currently the most widely used methods for investigating proteome changes. 2-DE is the best established technique that can be routinely applied for parallel quantitative expression profiling of large sets of complex protein mixtures (Gorg *et al.*, 2004). For this reason, 2-DE was selected as the technique to be used to investigate the molecular changes that parallel the MRI changes reported at 2 days post-SE.

A detailed review of these techniques is beyond the scope of this thesis, however an overview of the basic principles that underlie 2-DE and mass spectrometry will be presented. The interested reader is referred to some excellent reviews on these methods and others used in proteomics (Gorg *et al.*, 2004; Hoehn and Suffredini, 2005).

7.1.1.1. Two-dimensional gel electrophoresis (2-DE)

The 2-DE method involves successive separation of proteins on the basis of charge and molecular mass and is capable of resolving more than 5,000 proteins in a mixture (Gorg *et al.*, 2004). A protein sample is first separated by isoelectric focussing on a pH gradient immobilised on a gel strip to which high voltage is applied. Proteins migrate until they reach a point on the pH gradient at which that particular protein carries no net electrical charge, the so called isoelectric point (Greene *et al.*, 2002). After the proteins have reached their isoelectric point, the gel strip is subsequently applied to the top of a sodium dodecyl sulfate polyacrylamide gel, for electrophoresis (SDS-PAGE) in the second dimension which separates proteins on the basis of molecular mass. Protein spots are then visualised by silver staining. The final result is essentially a 2 dimensional protein map of the sample, with each spot on the gel corresponding to a single protein. Imaging software can then be used to analyse the gels, to search for spots that differ in abundance between experimental

samples. Spots of interest can be cut out of the gel for identification using mass spectrometry.

7.1.1.2. Liquid chromatography coupled to tandem electrospray mass spectrometry

Mass spectrometry measures the mass to charge ratio (m/z) of ionised peptides or protein ions based on the flight of the charged particles through an electric or magnetic field (Hoehn and Suffredini, 2005). There are a variety of configurations for a mass spectrometer and their main components are the ionisation source, the mass analyser and the detector. The configuration used in this study was liquid chromatography coupled to tandem electrospray mass spectrometry, or LC-MS/MS. As with any configuration of mass spectrometry, the same fundamental principles apply. In brief, the sample is ionised and then accelerated from the ion source into an analyser, which separates the molecules according to their m/z ratios. The advantage of the LC-MS/MS configuration is that it can provide sequence information which enhances protein identification (Hoehn and Suffredini, 2005).

Following excision of proteins spots from the gel they are digested with the protease, trypsin, to generate peptides which are amenable to LC-MS/MS analysis. Peptides are separated by liquid chromatography which is coupled to the mass spectrometer. Peptides are ionised by electrospray ionisation and the ions enter the tandem mass spectrometer, which incorporates two distinct analysers separated by a collision cell. Peptides are separated and their mass determined in the first analyser. Peptides of selected mass/charge ratio enter the collision cell and are dissociated into fragments of varying lengths owing to collision-induced fragmentation. The fragments of the peptide then pass into the second mass analyser where the masses of these 'product' ions are determined. Analysis of the difference in mass between fragments allows the amino acid sequence of the peptide to be determined. Peptide sequence can then be used to interrogate protein databases to reveal protein identity.

7.2. MATERIALS AND METHODS

The MRI experiments, which were a separate set from those in chapter 6 as the animals had to be sacrificed for tissue sample extraction, and the sample extraction was conducted by me, whereas the protein separation and western blot component was conducted by Dr. Nick Greene, Abiodun Bamidele, Sandra de Castro and the protein identification with mass spectrometry by Drs Robin Wait, Kit-Yi Leung and Shajna Begum.

7.2.1. Experimental Design

All animal care and procedures were carried out in accordance with the UK Animals (Scientific Procedures) 1986 Act. The experimental design for this study is outlined in figure 7.2.1.1.

10 adult male Sprague Dawley rats (200-220 g) were divided into one of two groups: lithium-pilocarpine (n = 6), lithium-saline (n = 4). CBF and T_2 imaging were performed these animals before lithium injection to obtain a baseline measurement and also to verify that the brains of these rats were anatomically normal before inclusion into this study. Following injection of either saline or pilocarpine, the animals underwent further CBF and T_2 imaging on days 0, 1 and 2 days after treatment. After the final imaging time point, the animals were sacrificed and their hippocampi were excised for proteome analysis.

For the purposes of this study, ROI MRI analysis was performed on the hippocampus and also the piriform cortex. Analysis was performed on the piriform cortex because previous studies have indicated that acute T_2 changes in this region are required for the subsequent development of spontaneous recurrent seizures (Roch *et al.*, 2002b).

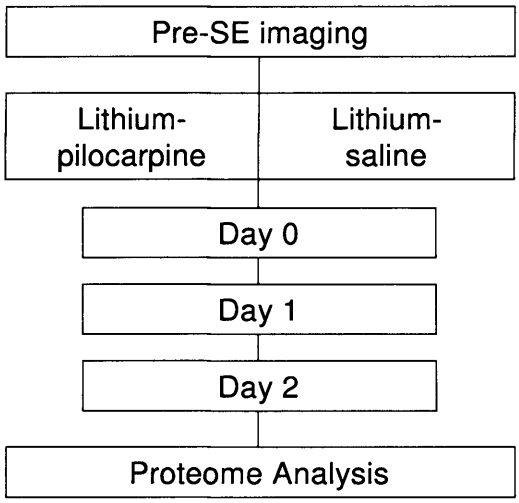

Figure 7.1. *Experimental design. The animals were imaged before and after the induction of SE. Following imaging on day 2, the animals were sacrificed and the hippocampi were removed for proteome analysis.*

7.2.2. Lithium-pilocarpine model

The drug protocol for the lithium-pilocarpine model was identical to the one described in section 6.2.2. In brief, lithium-chloride chloride (3 mEq/kg, i.p., Sigma-Aldrich, Dorset, UK) was injected 18-20 h before pilocarpine treatment. Methylscopolamine (1 mg/kg, i.p., Sigma-Aldrich) was administered 15 mins prior to pilocarpine treatment, and pilocarpine hydrochloride (30 mg/kg, i.p., Sigma-Aldrich) was then injected to induce status epilepticus (n=6 rats). Diazepam (10 mg/kg, i.p., Phoenix Pharma Ltd, Gloucester, UK) was administered 90 mins after the onset of SE to terminate the seizure. Control rats (n=4) received all treatments with the exception of saline instead of pilocarpine.

7.2.3. Magnetic resonance imaging

Animals were anesthetized with 3% isoflurane and maintained on 1.5% isoflurane with 60/40% N_2O/O_2 delivered via a nose cone. Rats were placed on a probe with bite and ear bars securing the head to minimize motion artifacts. Physiological monitoring included

electrocardiography (ECG) recordings and rectal temperature recordings. Temperature was maintained at 37 ± 1 °C using an air warming system.

Imaging was performed 1 day prior to any injections and on day 0, 1 and 2 days after SE. Images were acquired using a volume transmitter coil and a separate decoupled surface receiver coil, using a 2.35 Tesla horizontal bore magnet (Oxford Instruments, Oxford, UK) interfaced to a SMIS console (Guildford, UK). Coronal images were obtained approximately 3.3 mm from bregma.

T_2 and CBF data were acquired using a MASAGE-IEPI sequence (Thomas *et al.*, 2002) and a continuous arterial spin labeling sequence respectively. The sequence parameters were identical to the ones described in section 6.2.4.

All images were reconstructed with IDL Software Version 5.2 (Research Systems Inc., Boulder, CO) in order to obtain quantitative T_2 and CBF maps. CBF and T_2 values were calculated for the hippocampus and piriform cortex. Repeated-measures (degrees of freedom-adjusted mixed-model) two-way ANOVA was performed on the T_2 and CBF data (mean ± sem). The main effects were: treatment (saline, pilocarpine) and individual time-points (pre-SE, day 0, day 1 and day 2).

7.2.4. Sample preparation

Rats (6 pilocarpine-treated and 4 controls) were sacrificed at 2 days after SE following MRI and the hippocampus and forebrain were removed by dissection, immediately frozen on dry ice and stored at -70 °C. Tissue samples were minced using a needle and homogenised by sonication (15 seconds at 15 μm amplitude) in 1 ml lysis buffer containing 9.5 M urea, 2% CHAPS, 0.8% Pharmalyte pH3-10, 1% DTT, with 1x protease inhibitor cocktail (Complete, Roche) and 1 x phosphatase inhibitor cocktail I and II (Sigma, St. Louis, MO, USA). Aliquots of 200 μl were stored at -70 °C prior to 2-DE and protein concentrations were determined using Protein Assay Reagent (Bio-Rad, Richmond, CA).

7.2.5. 2-DE

Protein loadings of 300 µg were used for all gels, samples being diluted to 225 µl with lysis buffer, added to 225 µl rehydration buffer (8 M urea, 2% CHAPS, 0.8% Pharmalyte pH3-10, 0.2% DTT) and loaded by in-gel rehydration onto pH4-7, 18 cm linear IPG strips (GE Healthcare, Amersham, UK). 2-DE was performed as described previously with minor modifications (Leung *et al.*, 2001; Greene *et al.*, 2002). Briefly, strips were focused for 65 kVh using a MultiphorII (GE Healthcare). Prior to the second dimension strips were equilibrated for 15 minutes in equilibration buffer (6 M urea, 30% glycerol, 2% SDS, 0.05 M Tris/HCl pH8.8) containing 1% DTT and 25 minutes in equilibration buffer containing 2.5% iodoacetamide. The second dimension separation was carried out on 12% SDS-PAGE gels, with modification of the running buffer to contain 1.5% SDS. Gels were fixed and silver-stained using PlusOne stain (GE Healthcare).

7.2.6. Gel image analysis

Gels were scanned using a GS800 calibrated densitometer (Bio-Rad,) and analysed using PDQUEST (Version 7.0, Bio-Rad) and Progenesis PG220 with TT900S2S (Non-Linear Dynamics, Newcastle-Upon-Tyne, UK) software. A set of 32 gels comprising 15 control and 17 pilocarpine-treated samples (2 or 3 gels from each animal) were selected for analysis. Quantitative comparisons were made between these replicate groups. Spots on the edge of gels that were not detected in all the gels for an individual sample were excluded from further analysis. Quantitation was based on the normalised volume of spots and statistical comparison was by student's t-test, with $p<0.05$ considered significant.

7.2.7. Mass spectrometry

Protein spots were excised manually from a minimum of three different gels and subjected to in gel digestion with trypsin as described previously (Leung *et al.*, 2001). Samples were analysed by liquid chromatography coupled to tandem electrospray mass spectrometry (LC-ESI-MS/MS). Spectra were recorded using a Q-Tof spectrometer (Micromass,

Manchester, UK) interfaced to a Micromass CapLC capillary chromatograph. Samples were dissolved in 0.1% formic acid and aliquots were injected onto a 300 μm x 5 mm Pepmap C18 column (LC Packings, Amsterdam, NL) and eluted with an acetonitrile/0.1% formic acid gradient. The capillary voltage was set to 3,500 V. A survey scan over the m/z range 400-1300 was used to identify protonated peptides with charge states of 2, 3 or 4, which were automatically selected for data-dependent MS/MS analysis, and fragmented by collision with argon. The resulting product ion spectra were transformed onto a singly charged m/z axis using a maximum entropy method (MaxEnt3, Waters) and proteins were identified by correlation of uninterpreted spectra to entries in SwissProt/TrEMBL, using ProteinLynx Global Server (Version 1.1, Waters) (Wait *et al.*, 2005). The database was created by merging the FASTA format files of SwissProt, TrEMBL and their associated splice variants (1,768,175 entries at the time of writing). No taxonomic or protein mass and *pI* constraints were applied. One missed cleavage per peptide was allowed, and the initial mass tolerance window was set to 100 ppm. In parallel the spectra were also searched against the NCBI non-redundant database (3,879,234 sequences as of August 2006) using the Mascot search algorithm (www.matrixscience.com). For an identification to be considered valid we required that two or more peptides independently matched the same protein sequence, that the peptide score was significant (typically greater than 55; $P < 0.05$), and that manual interpretation confirmed agreement between spectra and peptide sequence. In addition Mascot searches of all spectra were performed against a randomised version of the NCBI database using the same parameters as in the main search. In no case did this search retrieve more than a single peptide, and in all instances the peptide score was below the 0.05 significance level.

7.2.8. Western blot

Protein samples containing 1 μg total protein (in lysis buffer as above) were diluted in Laemmli sample buffer (Bio-Rad), resolved on 10% Nu-PAGE gels (Invitrogen, Paisley, UK) and transferred to Immobilon-P (Millipore, Watford, UK). Equal loading of lanes (based on assay of total protein) was confirmed by silver staining of parallel lanes, supported by equal intensity of bands on the β-tubulin blots. Blots were incubated with antibodies to Hsp27 (1:1000, StressGen/Nventa, San Diego, CA), CRMP-2/DRP-2

(1:4000, CovalAb, Cambridge, UK), α-tubulin or β-tubulin (both 1:10,000, Santa Cruz Biotechnology, Inc.). Proteins were detected using horseradish peroxidise-conjugated secondary antibodies (DAKO, Ely, UK), with development using ECL+ Western blotting Detection System (GE Healthcare). Experiments were performed in triplicate, in each case using three saline-treated and three pilocarpine-treated samples. Quantity One software (Bio-Rad) was used for quantification of protein bands.

7.3. RESULTS

7.3.1. Animal behaviour

For each pilocarpine-treated animal, clinical signs of seizure activity were noted. All rats exhibited a well-defined pattern of behaviour following the injection of the convulsant. Around 5 mins after pilocarpine, the animals developed piloerection, diarrhoea and other signs of cholinergic stimulation. In the following 15-20 mins, head-bobbing, chewing and increased exploratory behaviour were observed. The rats then progressed to SE with episodes of head and bilateral forelimb clonus and rearing and falling around 25-35 mins after injection of pilocarpine.

7.3.2. T_2

MRI revealed a marked T_2 increase in the piriform cortex of pilocarpine-treated animals, which was evident at days 1 and 2 (Fig. 7.2) and a significant time-dependent difference was found between the pilocarpine and saline groups ($F=13.28$, $p=0.0017$). On day 2, the mean T_2 values were 110 ± 7.2 ms (mean ± sem) for pilocarpine-treated animals and 75 ± 1.9 ms for the saline-treated controls.

In the hippocampus, a time-dependent difference was also found ($F=13.364$, $p=0.006$). As expected, this was to a lesser degree (T_2 (mean ± sem): pilocarpine group 88 ± 5 ms; saline group 72 ± 0.3 ms) at day 2, than for the piriform cortex.

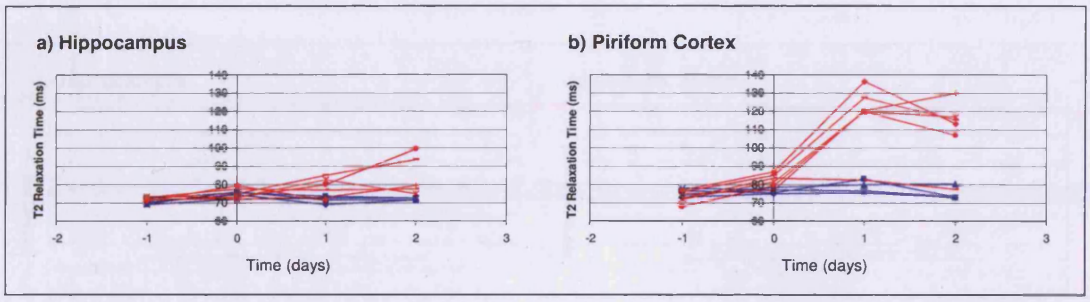

Figure 7.2. *T_2 relaxation times for individual animals in the: a) hippocampus, b) piriform cortex. T_2 measurements were performed before lithium administration (day -1) and subsequently on days 0, 1 and 2. The red lines are measurements obtained from individual lithium-pilocarpine treated animals and the blue lines from the individual saline treated animals.*

7.3.3. CBF

CASL measurements demonstrated significant time-dependent differences in hippocampal CBF of the pilocarpine-injected animals when compared to the saline-injected rats ($F = 6.18$, $p = 0.014$). Over the period of imaging, the greatest degree of hippocampal CBF change was observed on day 2 (fig. 7.3), with mean hippocampal CBF for the pilocarpine-injected group at 185.7 ± 33.6 ml/100g/min, and for the saline-injected animals, 72 ± 0.3 ml/100g/min (mean ± sem). In contrast, no significant CBF differences were observed in the piriform cortex ($F = 1.03$, $p = 0.344$). On day 2, the mean CBF values in the piriform cortex were 127.5 ± 38.0 ml/100g/min and 73.0 ± 1.04 ml/100g/min for the pilocarpine and saline groups respectively.

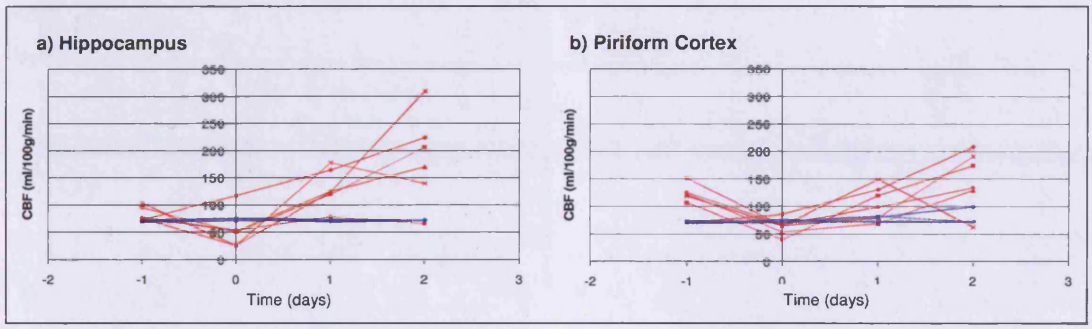

Figure 7.3. *CBF time course in the: a) hippocampus, and b) piriform cortex. CBF measurements were performed before lithium administration (day -1) and subsequently on days 0, 1 and 2. The red lines are measurements obtained from individual lithium-pilocarpine treated animals and the blue lines from the individual saline treated animals.*

7.3.4. 2-DE of hippocampus protein samples

In line with the experiments reported in chapter 6, MRI of the pilocarpine-treated rat brain confirmed that there were pathological changes in the hippocampus by 2 days, which is a region known to be associated with the subsequent epilepsy. Therefore this region, based on the spatial and temporal MRI T_2 and CBF changes, was isolated for further 2-DE analysis. Among detectable protein species, approximately 800 spots were matched on pH4-7 gels generated using hippocampal protein samples. A representative gel is shown in figure 7.4. A set of 32 gels comprising 15 pilocarpine-treated (SE) samples (2 or 3 gels from each of 6 animals) and 17 control samples (from 8 animals) was selected for analysis. Protein spots were excised from gels and subjected to tryptic digestion followed by LC-MS/MS for identification (fig 7.4, Table 1). Proteins that were present with equal abundance in SE and control samples included α-enolase (fig 7.4; spot 2), ubiquitin carboxyl-terminal hydrolase (spot 3) and peroxiredoxin 6 (spot 1; confirmed by MS analysis of spots from 4 separate gels).

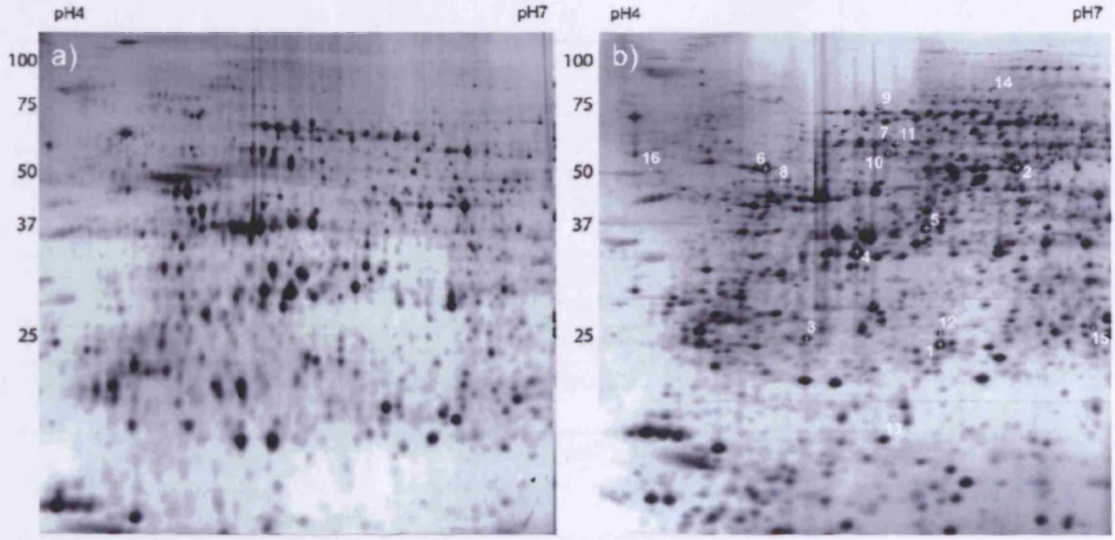

Figure 7.4. *Typical 2D protein profile for adult rat hippocampus 2 days following SE from a) Lithium-saline injected rat; b) Lithium-pilocarpine-injected rat. Proteins were separated on the basis of pI (pH4-7 on the x-axis) and Mr (molecular mass kDa is indicated on y-axis). Numbered spots were identified by LC-MS/MS (see Table 1).*

Spot no.	Protein	Accession no.	Theoretical Mr/pI	No. Matched peptides
1	Peroxiredoxin 6	O35244	24.67/5.8	6
2	Alpha enolase	P04764	46.98/6.5	8
3	Ubiquitin carboxyl-terminal hydrolase isozyme L1	Q00981	24.82/5.1	6
4	Tubulin beta chain	P04691 P69897	49.93/4.79	14
5	Tubulin beta chain	P04691	49.93/4.79	5
6	ATP synthase beta chain, mitochondrial precursor	P10719	56.33/5.3	2
7	Chaperonin containing T-complex protein 1, epsilon subunit	Q68FQ0	59.59/5.72	6
8	Gamma-enolase	P07323	46.98/5.03	18
9	Stress-70 protein (GRP75)	P48721	73.80/5.97	4
10	Vacuolar ATP synthase subunit B, brain isoform	P62815	56.52/5.57	6
	Spots that are up-regulated in pilocarpine-treated hippocampus ($p<0.01$)			
11	Dihydropyrimidinase related protein-2	P47942	62.24/5.9	11
12	Heat-shock protein beta-1 (HspB1) Heat 27kDa Protein (HSP 27)	P42930	22.87/6.5	7
13	Tubulin alpha chain	P68370	50.10/4.94	3
14	Ezrin (p81, Cytovillin)	P31977	69.22/5.83	18
15	Dihydropteridine reductase	P11348	25.54/7.67	2
	Spots that are down-regulated in pilocarpine-treated hippocampus ($p<0.01$)			
16	Histone-lysine N-methyltransferase (mouse)	XP_00105 6302	40.48/4.53	1

Table 7.1. *Protein identities determined by LC-MS/MS analysis of gel spots.*

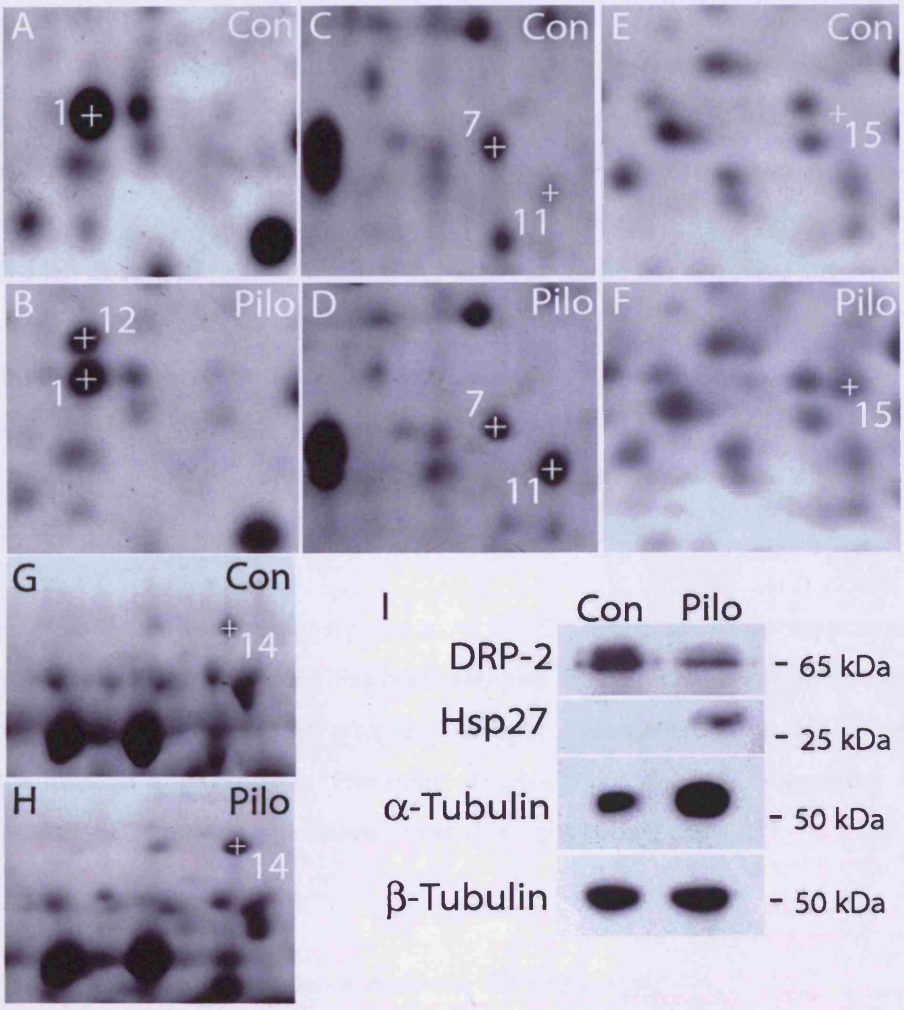

Figure 7.5. *Examples of differentially expressed spots in enlarged regions of representative 2D gels from control (Con; A, C, E, G) and lithium pilocarpine-treated (Pilo; B, D, F, H) samples. Gels show increased abundance of HSP27 (A-B; Spot 12), DRP-2 (C-D; Spot 11), Dihydropteridine reductase (E-F; Spot 15) and Ezrin (G-H; Spot 14) in hippocampus samples from lithium pilocarpine-treated rats compared to controls. Western blots (I) show increased total abundance of HSP27 and a-tubulin and reduced abundance of DRP-2 in lithium pilocarpine-treated rats, whereas β-tubulin shows no apparent difference. Molecular weight is indicated.*

7.3.5. Differential expression of heat shock 27 kDa protein

Computer-assisted image analysis was used to detect protein spots that differed in abundance on gels generated from hippocampus of control and pilocarpine-treated (SE) rats. This analysis did not reveal any spots in control samples that were absent from all treated samples. In contrast, we were able to identify a protein species that was present at relatively high abundance (Spot 12; figs. 7.4 and 7.5) in all SE samples, but was virtually undetectable by silver staining on the control gels (more then 9-fold difference ($p<0.001$)). This protein was isolated from five separate gels and in each case was identified by LC-MS/MS as heat-shock protein beta-1 (HspB1), commonly known as heat shock 27 kDa protein (HSP27). Increased expression of Hsp27 in SE samples was confirmed by western blot (fig 7.5).

In order to determine whether up-regulation of HSP27 is specific to the hippocampus, we generated additional 2D gels using forebrain samples from the SE and control rats ($n = 2$ for each). As for hippocampal samples the spot corresponding to HSP27 was also detectable at high abundance in forebrain samples from SE rats, suggesting that up-regulation of HSP27 may be a global response throughout the brain.

7.3.6. Quantitative changes in abundance of proteins in SE hippocampus

Among statistically significant differences between gels, visual verification confirmed that in addition to HSP27, 5 other spots were present at greater abundance in SE samples, whereas 4 spots were decreased in abundance. Using LC-MS/MS identities were obtained for 5 of the varying spots, whereas the remainder were present at very low abundance and have not been identified to date.

A spot identified as dihydropyrimidinase related protein-2 (DRP-2; spot 11, fig 7.4 and 7.5) showed approximately four-fold up-regulation in SE samples ($p<0.01$). As DRP-2 has previously been reported to show multiple isoforms on 2D gels, western blotting of the same samples as used for 2-DE was carried out, to determine if total abundance also varies. Western blotting for DRP-2 revealed a major band at 65 kDa with a minor band of slightly

higher molecular weight, as expected (fig 7.5I). In contrast to the increased abundance of the DRP-2 spot on 2-DE, the bands on western blots were consistently of lower intensity for hippocampus of pilocarpine-treated rats compared to controls. Thus, while one species is up-regulated following SE, the overall protein abundance of DRP-2 decreases.

Spots 13, 14 and 15 (fig 7.4) were also found to be present at significantly greater abundance on gels generated using SE samples compared to controls (two-fold up-regulation, $p<0.005$, fig 7.5). These spots were identified as α-tubulin, ezrin and dihydropteridine reductase (Table 1). Spot 13, which corresponds to α-tubulin, migrates as a species of approximately 18 kDa, a much lower mass than predicted. The peptides that were identified from this spot by LC-MS/MS (table 7.1) all lie within the N-terminal third of the protein and it appears likely that this spot corresponds to a fragment of the protein. However, western blot analysis also showed an approximate two-fold up-regulation of the 50 kDa band, corresponding to the full length α-tubulin (fig 7.5I).

Among spots that were apparently down-regulated in hippocampus after SE, spot 16 (fig 7.4, Table 1) showed a two-fold reduction in abundance ($p<0.005$), and was identified as corresponding to the predicted rat homologue of histone-lysine N-methyltransferase (H3 lysine-4 specific SET7).

7.4. DISCUSSION

7.4.1. MRI changes following SE parallel our previous MRI observations

MRI demonstrated that significant time-dependent T_2 changes occurred in the hippocampus and the piriform cortex following pilocarpine-induced SE. In addition, this effect was also observed in hippocampal CBF, but no significant CBF effect was observed in the piriform cortex. For the pilocarpine-treated animals, the T_2 and CBF measurements at 2 days after SE from the current study with the corresponding 2 day measurements from chapter 6 are presented in table 7.2.

	Cerebral blood flow (ml/100g/min)		T_2 (ms)	
	Hippocampus	Piriform Cortex	Hippocampus	Piriform Cortex
Results from present study	185 ± 33.6	127 ± 38.0	88 ± 5.0	110 ± 7.2
Results from previous study presented in chapter 6	149 ± 11.1	135 ± 14.2	76 ± 0.91	110 ± 5.5

Table 7.2. *A comparison between the CBF and T_2 measurements at 2 days following lithium pilocarpine-induced SE in the current study and the study presented in chapter 6. Data shown as mean ± s.e.m. These data indicate that there are consistent increases in CBF and T_2 in the hippocampus and the piriform cortex in this study and that of chapter 6.*

These data indicate that the hippocampal T_2 and CBF changes have been observed here are consistent with the changes that were observed at day 2 in the study presented in chapter 6. This is important because it is at this point in time that a significant T_2 relationship was found between early and late injury and it is this period during hippocampal injury that we aimed to investigate. Also, T_2 changes were observed in the piriform cortex. These changes have been suggested to be critical for the subsequent development of spontaneous

recurrent seizures in young lithium-pilocarpine rats (Roch *et al.*, 2002b) and, although it is unclear as to whether this necessarily implies that this is true for adult rats, this may nevertheless indicate that these animals will eventually progress onto epilepsy.

7.4.2. Peroxiredoxin 6

Comparison between the pilocarpine and saline hippocampal samples yielded relatively few proteins that were significantly altered in expression at 2 days following SE. This may be due to the fact that only a subset of proteins, only the most abundant species in the samples, is detected on 2D gels. One protein that was identified was peroxiredoxin 6 (antioxidant protein 2). Although in this study no changes were found, this protein has been reported to be up-regulated in the kainic acid-induced rat model of SE (Krapfenbauer *et al.*, 2001)

Peroxiredoxin 6 functions as an antioxidant and has been proposed to be up-regulated as a response to oxidative stress. However, in our study no detectable change in abundance of this protein was observed and this could reflect a difference between the pilocarpine and kainic acid models. Alternatively, this discrepancy may be due to differences in methodology. In the kainic acid model study, whole brain was analysed compared to just the hippocampus in the present study. Also, their sample was collected at one week after SE whereas our samples were extracted at 2 days. Therefore, it is possible that peroxiredoxin 6 levels may change as a later response to tissue damage and oxidative stress.

7.4.3. Heat shock protein-27

The most striking difference between the pilocarpine-treated and control samples was the dramatic up-regulation of heat shock protein-27 (HSP27), which was observed in both hippocampus and forebrain.

HSP27 is a member of the heat-shock family of proteins that function as cellular chaperones that help in the folding of nascent polypeptides or proteins that have been

denatured by environmental stress (Hirsch *et al.*, 2006). These proteins have been shown to be induced in response to a variety of stresses including seizures, heat injury and hypoxia and because of this are considered to be markers of cellular stress (Hirsch *et al.*, 2006). Although up-regulation of the members of the heat-shock protein family - HSP70 and HSP72 - has previously been described following pilocarpine-induced SE, this is the first time that induction of HSP27 has been reported in this model (Lian *et al.*, 2005; Tetich *et al.*, 2005).

High levels of HSP27 have previously been identified in brain resected from patients with pharmacoresistant temporal lobe epilepsy (Bidmon *et al.*, 2004), and other CNS disorders such as Alzheimer's disease and stroke (Franklin *et al.*, 2005). Moreover, HSP27 was previously found to be up-regulated in other experimental models of status epilepticus, such as the kainic acid model (Akbar *et al.*, 2001; Krapfenbauer *et al.*, 2001).

The finding in this study of increased HSP27 levels within 2 days after pilocarpine-induced SE, support the hypothesis that this protein is an early marker of seizure-induced cellular stress. The functional effect of HSP27 up-regulation following SE is unclear, but it may represent a neuroprotective response. Direct evidence for an *in vivo* neuroprotective role has been provided by expression of HSP27 using viral vectors in experimental models of stroke, associated with reduced lesion size (Badin *et al.*, 2006). It is also interesting to note that HSP27 has been suggested to play a role in reducing seizure severity, which was observed in the HSP27 over-expressing transgenic mouse following administration of seizure-inducing levels of kainic acid (Akbar *et al.*, 2003).

In the present study, the fact that HSP27 was detected at high abundance in both the hippocampus, which exhibited T_2 and CBF changes, as well as other regions of the brain, suggests that the selective vulnerability experienced by the hippocampus may not be accounted for by a local deficiency in HSP27. Nevertheless this does not exclude the possibility that overexpression of HSP27 would provide some protective role in this animal model (Akbar *et al.*, 2003). In addition, whether HSP27 has a role to play in epileptogenesis has yet to be explored.

7.4.4. Dihydropyrimidinase related protein-2

After HSP27, the protein species that was most significantly up-regulated in hippocampus after SE was dihydropyrimidinase related protein-2 (DRP-2), also known as collapsin response mediating protein-2 (CRMP-2) or turned on after division, 64 kDa protein (TOAD-64). However, the overall abundance of DRP-2, as revealed by western blot, was lower in pilocarpine-treated samples. Multiple spots corresponding to DRP-2, and assumed to be post-translational variants (eg, differentially phosphorylated forms), have been detected in a 2D gel study of human hippocampus (Yang *et al.*, 2004).

As multiple forms are also likely to be present in the rat hippocampus this may suggest that while the overall abundance of protein is reduced following pilocarpine treatment, one particular post-translational variant accumulates. In support of this idea, three of the multiple spots detected in human hippocampus were present at lower intensity in samples from patients with epilepsy, whereas one spot was increased in intensity (Yang *et al.*, 2004). Presumably, certain DRP-2 species must also decrease in abundance in the present study, but these may not be represented on our gels, or each individually do not exhibit sufficient reduction in levels to be detected as significantly different.

DRP-2 is not expressed in neuronal progenitors but is one of the first markers of newborn neurons (Minturn *et al.*, 1995). Widespread expression can be found in the developing nervous system but it is down-regulated post-natally with the notable exception of the hippocampus (Uchida *et al.*, 2005). This correlates with its presence on 2D gels of control hippocampus in this study. DRP-2 is enriched in neuronal axons and is thought to function in axonal growth and pathfinding during development of the nervous system (Arimura *et al.*, 2004). For example, overexpression of DRP-2 can induce the formation of supernumerary axons (Inagaki *et al.*, 2001). Also this protein appears to play a key role in the mediation of signals from extracellular stimuli including guidance molecules such as Semaphorin 3A (Arimura *et al.*, 2004). It is also notable that expression of truncated DRP-2 mutants suppressed the formation of primary axons (Inagaki *et al.*, 2001).

Given that an increase in hippocampal neurogenesis has been widely reported following SE in a variety of animal models (Parent *et al.*, 1997; Bengzon *et al.*, 1997; Gray and Sundstrom,

1998; Parent *et al.*, 1998) and, more pertinent to this study, within 2 days following lithium-pilocarpine induced SE (Ekdahl *et al.*, 2001), it would seem unlikely that the reduction in overall DRP-2 reflects a reduction in hippocampal neurogenesis. This finding may in fact indicate that neurogenic mechanisms are altered following SE and may have implications for the pathogenic mechanisms of epilepsy such as mossy fibre sprouting. Although controversial, mossy fibre sprouting has been suggested to play a key role in the initiation of epilepsy (see section 2.3.4.). Whether alterations in the various DRP-2 isoforms contributes to mossy fibre sprouting remains to be seen, and further studies will be required to determine the functional effects of changes in the levels of individual variants.

7.4.5. α-tubulin

Another protein, α-tubulin, which is required for axon outgrowth, was also found to be up-regulated after SE. Heterodimers of α- and β-tubulin make up the principal component of microtubules, which have multiple cellular functions (Fukata *et al.*, 2002). Synthesis of microtubule proteins is known to occur during growth of axons and dendrites and, like DRP-2, tubulin function is required for formation and guidance of axon growth cones (Baas, 1997; Arimura *et al.*, 2004). In fact a possible functional link between DRP-2 and tubulin is suggested by the fact that DRP-2 can bind to tubulin heterodimers and promote microtubule assembly (Fukata *et al.*, 2002). Thus, altered levels of DRP-2 and α-tubulin may be associated with axonal outgrowth, perhaps of newborn neurons. However, increased abundance of α-tubulin could also relate to one of the many other functions of microtubules.

Elevated levels of α-tubulin mRNA have been reported in the kainic acid model of SE and in a rat kindling model of epilepsy (Krapfenbauer *et al.*, 2001; Sato and Abe, 2001; Hendriksen *et al.*, 2001). Increased abundance of a specific α-tubulin protein spot in the mitochondrial fraction was also noted in the kainic acid model (Hendriksen *et al.*, 2001). In contrast, 2-DE analysis of hippocampi from patients with mesial temporal lobe epilepsy revealed reduced levels of both α and β-tubulin compared to controls (Yang *et al.*, 2004).

In the present study (at 2 days post-SE), increased levels of a low molecular weight form of α-tubulin that may correspond to a breakdown product were detected, which could be suggestive of increased degradation, as in patients. However, similarly to the kainic acid model, our western blot analysis showed that the main full length form of α-tubulin is also present at increased levels following pilocarpine-induced SE (while β-tubulin is unaffected). We did not detect a 50 kDa α-tubulin spot with altered abundance by 2DE, but as this protein is present as multiple spots on 2D gels (Greene *et al.*, 2002; Yang *et al.*, 2004), it is likely that the variation in individual spots was insufficient to be detected in this study or that additional altered species (eg, post-translational variants) are present but with pI values outside the range used in our gels.

Although differences exist between human patients and the rat models (see section 3.1 and 3.2), the more likely explanation for the discrepancy between our findings and in human patients is that this comparison relates to different stages of the disease process (Yang *et al.*, 2004). The human study was performed using samples resected from patients with epilepsy, whereas our study is performed on rats before the occurrence of spontaneous recurrent seizures.

Overall, alterations in abundance of tubulin and DRP-2 suggest that there may be considerable synthesis and/or remodelling of the microtubule-based cytoskeleton early in the pathogenic process and that, at late stages of disease, cytoskeletal proteins may be degraded as hippocampal damage progresses.

7.4.6. Ezrin

Another cytoskeleton-associated protein found to be up-regulated following SE was ezrin, a member of the ezrin-radixin-moesin (ERM) family of proteins. These proteins act as linkers between integral membrane proteins and the actin cytoskeleton and as signal transduction molecules in RhoGTPase signalling to the cytoskeleton (Tsukita and Yonemura, 1997; Ivetic and Ridley, 2004). They are thought to be involved in regulation of cytoskeletal dynamics required for maintenance of cellular morphology, cell-cell adhesion and formation of membrane structures such as ruffles and microvilli (Ivetic and Ridley,

2004). Interestingly, ezrin was previously found at increased abundance in 2DE analysis of mesial temporal lobe epilepsy (Yang *et al.*, 2004).

The observation of increased levels of ezrin both in human patients (Yang *et al.*, 2004) and in the rat only 2 days after SE (this study), suggests that this may be a relatively early and long-lasting change. Although, like tubulins, ezrin is present in multiple post-translationally modified forms (Tsukita and Yonemura, 1997; Yang *et al.*, 2004), increased levels of ezrin have been found in epilepsy patients, in contrast to tubulin. Therefore the time-course and functional consequences of changes in the levels of specific forms of cytoskeletal components may be an interesting avenue for future studies on the pathogenesis of epilepsy.

7.4.7. Dihydropteridine reductase

Dihydropteridine reductase (DHPR) catalyses the production of 5,6,7,8-tetrahydrobiopterin (BH_4) from quinonoid-dihydrobiopterin. This is a key metabolic reaction as BH_4 has numerous cellular functions including acting as co-factor in degradation of phenylalanine, tyrosine and tryptophan by aromatic amino acid hydroxylases, and as an essential co-factor for nitric oxide synthase (NOS) (Ponzone *et al.*, 2004).

Deficiency of DHPR results in BH_4 deficiency whose major pathogenic features are hyperphenylalaninemia and reduced synthesis of dopamine and serotonin (Ponzone *et al.*, 2004). In contrast we observe increased abundance of DHPR in the pilocarpine-treated hippocampus that would suggest that this would lead to an elevation in BH_4 levels. Moreover, as BH_4 is a co-factor for NOS, which produces nitric oxide, it may be hypothesised that this increase in BH_4 may relate to the concomitant increase in hippocampal CBF that was observed with MRI.

The relationships between DHPR, BH_4 and NOS may also suggest a role in SE-induced hippocampal injury. Firstly, increased levels of BH_4 have been proposed to contribute to neuronal cell death, via its role in NOS production, after forebrain ischemia in the rat (Cho

et al., 1999). In addition, NOS has been shown to be up-regulated within this early period following SE and directly contributes to neuronal death (Chuang *et al.*, 2007). On the other hand, BH_4 has also been suggested to possess a capacity for protection against NO toxicity (Koshimura *et al.*, 2000). It is also notable that BH_4 may contribute to neuronal death directly as this protein can increase Ca^{2+} channel currents (Koshimura *et al.*, 2000). Nevertheless the relationships between these proteins require further study in SE-induced pathology.

It is interesting to note that new pharmacological approaches that directly modulate the levels of BH_4 have been proved to be effective for certain clinical conditions such as hypertension (Forstermann, 2006) and also new agents that act on the BH_4 binding site on NOS have been proposed as a novel approach for conditions such as inflammation, sepsis and stroke (Matter and Kotsonis, 2004). Whether these agents can be used to modulate hippocampal injury after SE and epileptogenesis remains to be seen, but the association with inflammation and cell death mechanisms, which have been implicated in SE-induced pathology, means that these agents are an attractive avenue for research and therapy development.

7.4.8. Down-regulation of protein species

Among very few spots that were significantly down-regulated following SE, we identified a histone-lysine N-methyltransferase (H3 lysine-4 specific SET7), which methylates lysine 4 of histone H3. Assembly of methylated histones at gene promoters influences regulation of transcription through interaction with different effector proteins (Sims, III and Reinberg, 2006). In general, methylation at lysine 4 is associated with active transcription at a locus, although some interacting proteins may also be repressive (Sims, III and Reinberg, 2006). Thus, if pilocarpine treatment leads to reduced levels and activity of the histone-lysine N-methyltransferase that is specific for lysine-4, a downstream consequence could be altered transcription of specific genes, which could contribute to the subsequent pathogenesis.

7.5. CONCLUSION

In summary, during the period in which a maximum MRI-detected response in the hippocampus is observed following SE, there are concomitant changes in the levels of various proteins. Although the precise functions of these proteins, in the context of SE, are not completely understood, these proteins have been associated with pathogenic, neuroprotective and neurogenic responses and may therefore have an important role to play in the progression of brain injury and the development of epilepsy.

As only a subset of proteins were investigated in this study, further studies are required to address the later time-course of proteome changes and to examine more acidic and basic subsets of proteins than examined here. The identification of relevant proteins in the pathogenic process may allow the development of strategies for manipulation of protein expression that will reduce hippocampal injury and subsequent epileptogenesis.

This study demonstrates that MRI and proteomics can be used as complementary technologies to identify and examine regions vulnerable to pathological change, and that this can lead to potentially important testable hypotheses. This approach should be pursued in future studies.

CHAPTER 8: MRI DURING STATUS EPILEPTICUS

From a little spark may burst a flame

Dante Alighieri

8.1. INTRODUCTION

The nature of the onset and progression of seizures have been associated with various physiological phenomena in which alterations in blood flow, pH and glucose utilisation have been reported (Lothman, 1990). These alterations in physiology in response to seizures have been hypothesised to fall into two distinct periods: compensation and decompensation, which have been described in section 2.1.3 (Lothman, 1990; Shorvon, 1994). In brief, the compensation phase describes the early period of SE in which various physiological processes are recruited to meet the extra demands from continuous seizure activity, whereas the decompensation phase occurs around 30 minutes of continuous activity and parallels the failure of these physiological processes and the appearance of neuronal injury. One process that fails during the decompensation period is cerebral autoregulation, defined as the capacity of the cerebral circulation to maintain blood flow at a relatively constant level, and at this point blood flow becomes wholly dependent on systemic flow, which consequently may exacerbate injury (Meldrum and Nilsson, 1976).

It is widely accepted that the increase in global CBF more than compensates for the increase in O_2 demand during the early compensation period (Meldrum and Nilsson, 1976; Kreisman *et al.*, 1991; Shorvon, 1994) and that the magnitude of the increase in CBF becomes progressively smaller as the seizure continues, while the cerebral metabolic rate of oxygen ($CMRO_2$) remains elevated (Meldrum and Nilsson, 1976). As a consequence of this gradual reduction, CBF would eventually approach a critical level for supplying adequate O_2 to the brain (Meldrum and Nilsson, 1976). Thus a mismatch between the supply of nutrients from the blood and the enhanced energy demand from the seizing neurons may contribute to injury in the vulnerable regions of the brain.

The hippocampus is an area that displays a selective vulnerability to SE and it is has been hypothesised that the resulting injury caused by SE predisposes to epilepsy. The selective vulnerability to SE is supported by the studies described in chapter 6 and 7 as well as reports that neuronal injury occurs almost exclusively in the hippocampus with seizures of shorter duration, and also that this region shows a progressive and pronounced atrophy following SE (Fujikawa, 1996; Roch *et al.*, 2002a; Nairismagi *et al.*, 2004). Furthermore, the

specific hippocampal subfields injured by SE resemble the characteristic selective cell loss seen in patients with MTS-TLE, which suggests a causative relationship between SE-induced hippocampal injury and subsequent epilepsy (Shorvon, 1994). However, the precise mechanisms that underlie this selectivity to injury remain unclear.

A hypoxic/ischaemic mechanism was initially proposed as the main mechanism for SE-induced injury due to the histological similarities observed between the hippocampal injury induced by SE and by global ischaemia (Siesjo and Wieloch, 1986; Shorvon, 1994). However, it is now widely considered that excitotoxicity, as a result of excessive neuronal activation, is the primary mechanism for seizure-induced injury (Meldrum and Brierley, 1973; Olney *et al.*, 1974; Lothman, 1990). This emerged from studies demonstrating teat the hippocampus can sustain injury in the absence of hypoxia (Pinard *et al.*, 1987; Shorvon, 1994). Nevertheless it has also been hypothesised that a localised failure in the vascular system may act to exacerbate injury, and as yet the regional contribution of this phenomenon has yet to be fully determined (Meldrum and Nilsson, 1976; Kreisman *et al.*, 1991).

The regional CBF response to SE in animal models has been reported to be dependent on the specific actions of the particular agent used for seizure induction. Bicuculline, a selective $GABA_A$ antagonist, induces a similar CBF response in the neocortex and the hippocampus. In contrast, kainic acid produces CBF changes in which the hippocampal CBF is much greater than neocortical blood flow (Pinard *et al.*, 1984). However, contradictory reports exist in that a relative ischaemia in the hippocampus has also been reported following kainic acid-induced SE (Tanaka *et al.*, 1990). The regional CBF changes during pilocarpine-induced SE have not been widely investigated.

MRI can be used to investigate the processes that occur during SE and can provide information about the regional nature of SE (King *et al.*, 1991; Zhong *et al.*, 1993; Prichard *et al.*, 1995; Engelhorn *et al.*, 2005). Perfusion MRI has been widely used to investigate cerebral ischaemia, and the arterial spin labelling technique can be used for the non-invasive *in-vivo* measurement of cerebral blood flow (CBF), which is unparalleled within medical imaging (Alsop and Detre, 1996; Thomas *et al.*, 2000; Lythgoe *et al.*, 2002). This technique also offers good spatial and temporal resolution, and therefore makes it an

increasingly popular technique for investigating the delivery of blood water to tissue. However, only one previous study has investigated perfusion changes during SE with MRI, from which the authors suggested that there is a regional relationship between the maximum decrease in perfusion and subsequent neuronal loss, although this study only investigated relative CBF (Engelhorn *et al.*, 2005). The study reported in this chapter aimed to use MRI to investigate quantitative regional perfusion changes during the course of pilocarpine-induced SE. In order to do this, a number of methodological developments were first required, as outline in section 5.3.

8.2. METHODS

8.2.1. Experimental design

All animal care and procedures were carried out in accordance with the UK Animals (Scientific Procedures) 1986 Act.

16 adult male Sprague-Dawley rats (300-400g, Charles Rivers) were divided into two groups: pilocarpine (n = 13) or saline (n = 3). Once the animals had been prepared for imaging, the animals were given scopolamine (1mg/kg). T_1 images were acquired at the beginning of the experiment for the purposes of CASL calculations. Thereafter perfusion imaging was performed for the duration of the experiment.

The experimental design is outlined in figure 8.1. The first 30 minutes of MRI were acquired for baseline measurements after which the animals were administered either pilocarpine (375mg/kg) or saline. Bench experiments (see section 5.3) indicated that SE began approximately 30 minutes following pilocarpine administration; therefore the animals were imaged for 150 minutes before diazepam (10mg/kg) was given. After diazepam the rats were imaged for up to a further 1 hour. The animals were visually assessed for seizure activity following each set of diffusion and perfusion acquisitions.

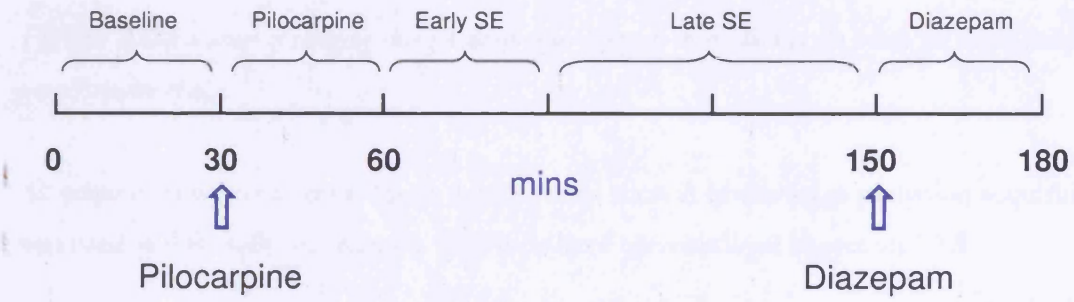

Figure 8.1. *Experimental design for MRI during SE. The key events that occur over the course of MR imaging: pilocarpine at 30mins, SE starts at 60mins and diazepam was given at 150mins.*

8.2.2. MRI

Animals were anesthetized with intraperitoneal injections of fentanyl citrate (300μg/kg) and medetomidine (300μg/kg). 1 h following the initial dose of fentanyl, a bolus of fentanyl (100μg/kg) was given every 30mins to maintain anaesthesia. O_2 was delivered continuously via a nose cone. Rats were placed on a probe with a nose cone and secured using the various adaptations outlined in section 5.3.4 to minimize motion artifacts. Physiological monitoring included electrocardiography (ECG) recordings and rectal temperature recordings. Temperature was maintained at 37 ± 2 °C using an air warming system.

Images were acquired using a volume transmitter coil and a separate decoupled surface receiver coil. A central coronal imaging slice was selected that included the hippocampus (fig 8.2) (-4.8mm from bregma). The central slice was determined by visual inspection of anatomical landmarks.

Figure 8.2. *Location of imaging slice (-4.8mm from bregma) in relation to the whole rat brain (adapted from Paxinos et al.).*

All sequences were run on a 2 mm-thick coronal slice. A low average perfusion acquisition was used in this study, the reasons for which have been outlined in section 5.3.5.

T_1 images were acquired with parameters as previously described (section 6.2.4), which were required for the calculation of CBF, and these scans were acquired at the beginning of each study. Following the acquisition of T_1 images, perfusion experiments were conducted contiguously. For perfusion-weighted imaging, the CASL method was used and all

parameters remained the same as previously described (section 6.2.4) with the exception of the number of averages that were reduced from 88 averages to 22 averages for this study.

Duration of acquisitions: T_1 = 11 mins and CASL = 4 mins. Each animal was scanned for a total time of 3h.

8.2.3. Data processing

8.2.3.1. Regional perfusion-weighted signal intensity ratios and CBF quantitation

T_1 maps, the base images acquired for the CASL acquisition and perfusion-weighted images were reconstructed using in-house software written in Matlab version 6.5 (MathWorks, Massachusetts, USA) in order to obtain quantitative T_1 and perfusion-weighted signal intensities for CBF quantitation.

Motion during image acquisition can cause variation in signal intensity of the image that can result in error in the calculation of CBF. This error leads to a modulation of signal across the entire image and thus across all regions. Therefore to minimise the effects of motion, ratios were calculated to determine regional changes during SE.

8.2.3.2. Criteria for inclusion of data for analysis

The following criteria were used to identify and exclude images with motion artefacts, and therefore to determine which images could be included for analysis. The criteria were first applied to the control images (i.e. prior to subtraction) to identify motion affected images, and then for perfusion-weighted images to account for systematic errors introduced by the instrumentation:

1) All base images from a single experiment were visually assessed using MRIcro software (version 1.40). The software provides a facility to view the experiments along the time domain (fig. 8.3a), and therefore images that have been corrupted by

motion, which would result in a change in signal intensity, can be identified and thus excluded from the analysis (fig. 8.3).

2) Motion can also lead to a shift in the position of the imaging slice, and averaging images from different positions can cause error in the analysis. Therefore for every animal, each image was compared visually to the previous acquisition to determine which images could be averaged together for analysis. If the animal moved, the regions of interest were redrawn to ensure that they corresponded to the correct anatomical regions. Finally, if the hippocampus could not be identified in the imaging slice, the complete data set was excluded from the analysis.

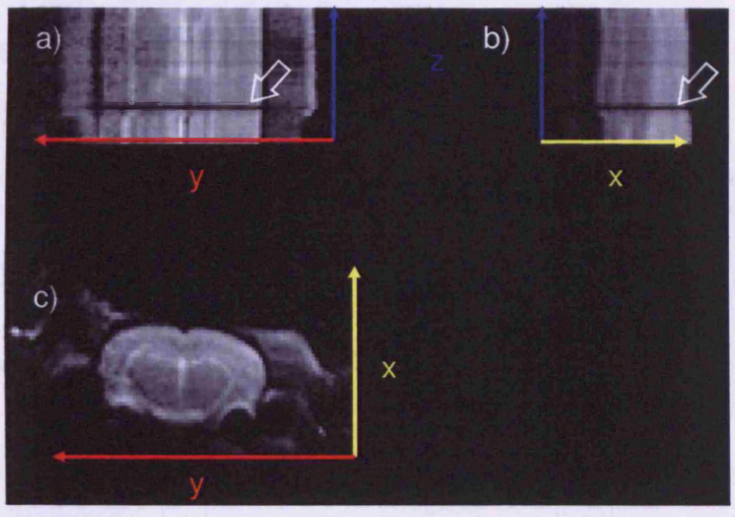

Figure 8.3. *MR data set in an anaesthetised pilocarpine-injected animal. Visual assessment using MRIcro software displayed the data for the duration of the entire experiment. a) denotes view along the z and y-axis; b) along the z and x-axis; and c) along the y and x-axis. Blue lines correspond to the z-axis (time domain), yellow for x (read), and red for y (phase-encoding). The white arrow indicates an acquisition in which there was a reduction in signal and therefore was removed from the analysis.*

8.2.3.3. Post-process averaging

The images that met the inclusion criteria (section 8.2.3.2) were averaged across 5 distinct periods, which were determined by the EEG experiments described in section 5.4 and the previous studies reviewed by Lothman (Lothman, 1990). These were:

1) Baseline
2) Within the first 30mins following pilocarpine administration. This is the period before SE occurs.
3) 30-60mins after pilocarpine. From our previous experiments, this period coincides with the first 30mins of SE and has been associated with the compensation phase of SE.
4) 60-150mins after pilocarpine. This period is associated with the latter stages of SE and this is considered to be the decompensation phase.
5) After approximately 150mins, diazepam was administered to the animal, and this period should reflect the gradual cessation of epileptic activity.

8.2.3.4. Regions of interest

Three regions of interest - cortex, hippocampus, thalamus - were delineated on all processed images and analysed with in-house Matlab software and ImageJ version 1.38x (National Institutes if Health, USA).

8.2.3.5. Statistical Analysis

For CBF measurements, a repeated measures (degrees of freedom-adjusted mixed-model) ANOVA with contrasts to the baseline scans and the hippocampus was conducted. The main effects were as follows: group (pilocarpine, saline); time (pre, pilocarpine, SE, SE late, diazepam); anatomy (cortex, hippocampus, thalamus).

Similarly, for perfusion-weighted ratios relative to the hippocampus, a repeated measures (degrees of freedom-adjusted mixed-model) ANOVA with contrasts to the baseline scans and the hippocampus were conducted. The main effects were as follows: group (pilocarpine, saline); time (pre, pilocarpine, SE, SE late, diazepam); anatomy ratios (cortex:hippocampus, thalamus:hippocampus).

8.3. RESULTS

8.3.1. CBF measurements

In total, 7 animals were included for analysis from the pilocarpine group. Figure 8.4 and table 8.1 show the CBF measurements in the cortex, hippocampus and the thalamus over the course of the experiment. For comparison, the saline-injected animals showed no systematic effects (see fig. 8.4 a) prior to administration of diazepam.

	Pilocarpine CBF (ml/100g/min)		
	Cortex	Hippocampus	Thalamus
Baseline	122 ± 11.0	96 ± 13.9	109 ± 15.0
Pilocarpine	234 ± 32.1	118 ± 21.0	155 ± 24.4
Early Se	121 ± 24.4	65 ± 18.7	108 ± 12.2
Late Se	132 ± 31.6	105 ± 14.6	153 ± 30.2
Diazepam	165 ± 24.2	90 ± 27.2	150 ± 28.4

Table 8.1. *Mean regional CBF measurements before, during, and after SE. Regions include the cortex, hippocampus and the thalamus. CBF expressed as mean ± s.e.m.*

Statistical analyses indicated a regional pilocarpine effect on CBF ($F = 5.06$, $p = 0.031$) (see fig. 8.4b). No significant difference was found between the CBF in the hippocampus and in the thalamus ($F = 0.766$. $p = 0.407$). In contrast, significant differences were found between the hippocampus and the cortex ($F = 14.73$, $p = 0.005$). Analyses indicated that the CBF in the hippocampus and the cortex changed significantly with time. Comparisons between the magnitude of CBF change from baseline of the pilocarpine-injected animals and the saline-injected controls indicated that there were significant differences between the hippocampus and the cortex following pilocarpine injection ($F = 9.45$, $p = 0.014$) and during early SE ($F = 6.87$, $p = 0.031$), but no significant differences were observed for the late SE period ($F = 1.76$, $p = 0.221$) or following diazepam injection ($F = 0.162$, $p = 0.698$).

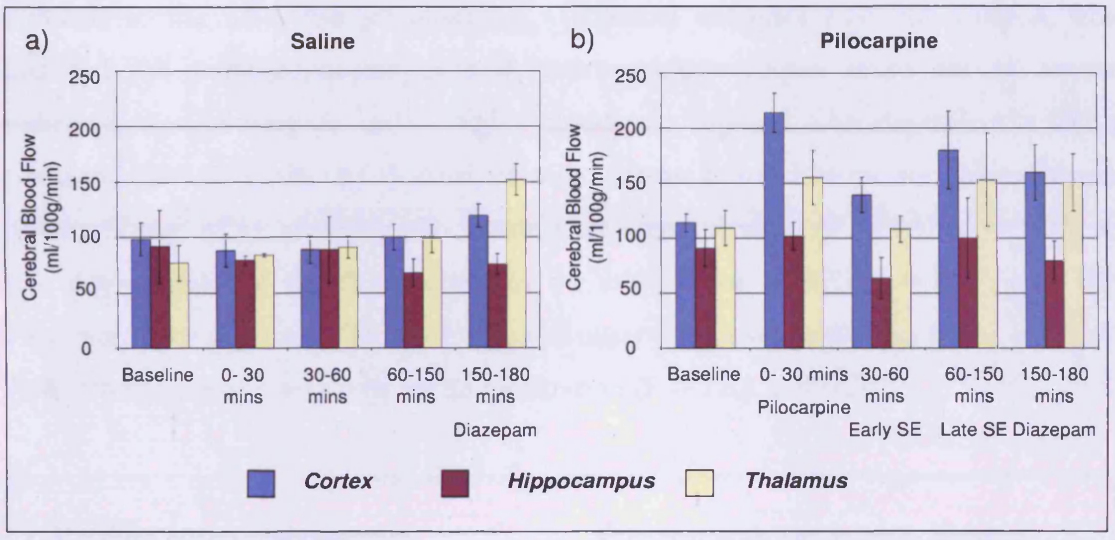

Figure 8.4. *CBF measurements over the course of SE in the cortex, hippocampus, and the thalamus. a) Saline treated rats (n = 3), b) Pilocarpine treated rats (n = 7). Data expressed as mean ± s.e.m.*

8.3.2. Regional perfusion-weighted signal intensities and CBF measurements relative to the hippocampus

Figure 8.5 and table 8.2 shows the changes in perfusion-weighted signal intensity and CBF in the cortex and the thalamus relative to the hippocampus for the pilocarpine-injected animals. These data demonstrated that regional changes occur following either saline or pilocarpine administration that were independent of uniform signal change due to motion. Figure 8.6 shows representative perfusion-weighted images after injection of either saline or pilocarpine in which the perfusion changes in the hippocampus relative to the cortex can be observed.

	Pilocarpine perfusion-weighted signal intensity ratio	
	Cortex:Hippocampus	Thalamus:Hippocampus
Baseline	1.44 ± 0.17	0.73 ± 0.06
Pilocarpine	2.07 ± 0.26	0.87 ± 0.1
Early Se	2.88 ± 0.48	1.55 ± 0.47
Late Se	2.27 ± 0.35	0.96 ± 0.15
Diazepam	2.16 ± 0.46	1.09 ± 0.14

Table 8.2. *Mean regional perfusion-weighted signal intensity ratios relative to the hippocampus before, during, and after SE. Regional ratios include cortex, and thalamus. CBF ratios expressed as mean ± s.e.m.*

Similarly to the CBF changes observed, a repeated measures ANOVA analysis, which included the cortex:hippocampus and thalamus:hippocampus ratios for all animals, indicated that pilocarpine had a highly significant regional time-dependent effect on perfusion ($F = 28.8$, $p = 0.001$). Analysis with contrast to baseline measurements provided weak evidence of an effect by pilocarpine after administration ($F = 4.32$, $p = 0.07$), and also demonstrated a significant effect in the early phase of SE ($F = 6.87$, $p = 0.03$). However, these regional differences were not observed subsequently: late phase of SE ($F = 1.48$, $p = 0.26$); and after diazepam administration ($F = 1.63$, $p = 0.24$).

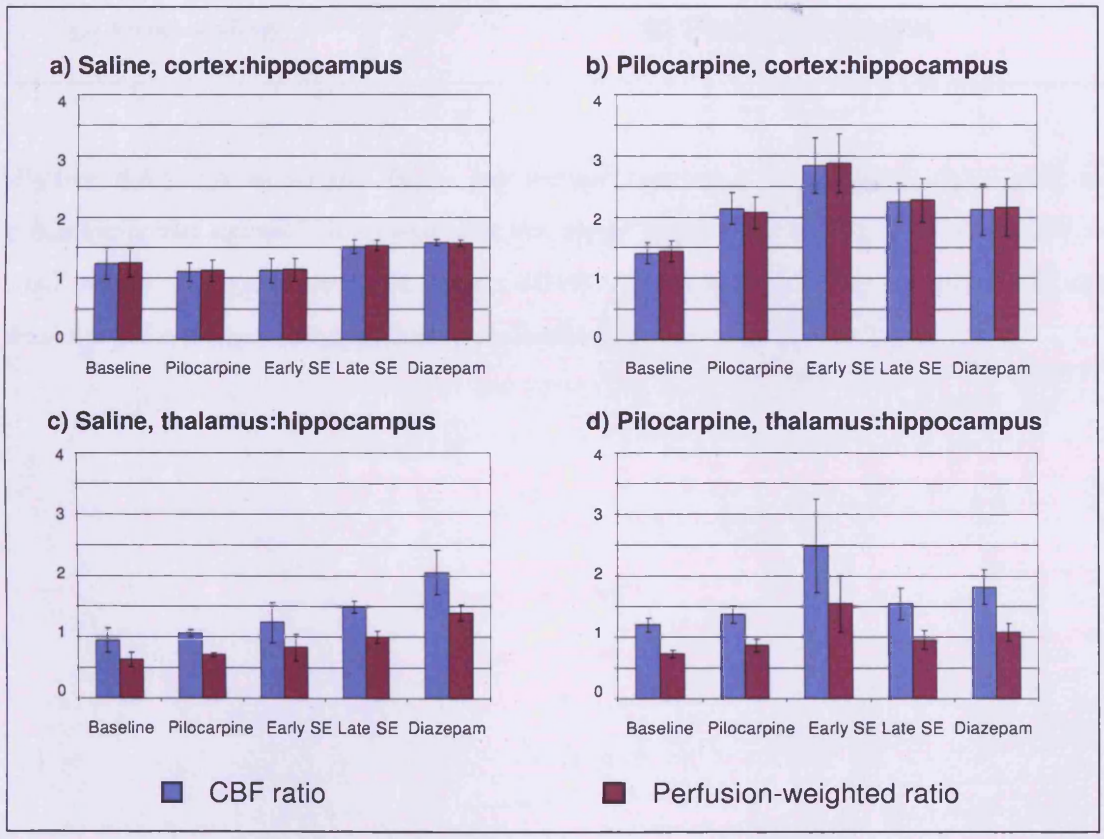

Figure 8.5. *Mean regional changes relative to the hippocampus for CBF measurements and for the perfusion-weighted signal intensities. a) saline-injected, cortex:hippocampus; b) pilocarpine-injected, cortex:hippocampus; c) saline-injected, thalamus:hippocampus; d) pilocarpine-injected, thalamus:hippocampus. Data expressed as mean ± s.e.m.*

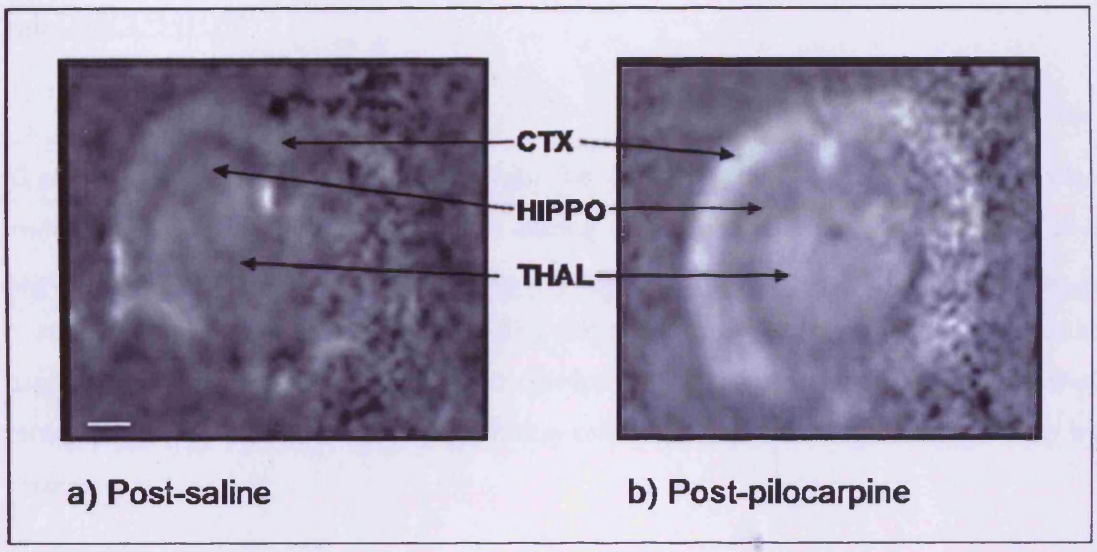

Figure 8.6. *Perfusion-weighted images post-injection from a) a saline-injected animal and b) a pilocarpine-injected animal. These images were the average of all perfusion data following injection from single animals. The regions are: CTX, cortex; HIPPO, hippocampus; and THAL, thalamus. Note the limited perfusion change in the hippocampus compared to the cortex. Scale bar in a) equals 2mm.*

8.4. DISCUSSION

These results demonstrate that MRI can be used to investigate SE and provides information about regional CBF changes during the course of a prolonged seizure. The experiments required methodological developments that were described in chapter 5. Results indicate that, over the course of SE, cortical perfusion changes occur to a greater degree than hippocampal perfusion. After diazepam administration there was an observed return to baseline across all regions, which may reflect the suppression of seizure activity by diazepam.

8.4.1. Absolute CBF, regional CBF ratios, and regional perfusion-weighted signal intensity ratios

CBF measurements can be influenced by motion that may result in variation, which may lead to errors in the calculation of CBF. For this reason, the analysis and interpretation of the data was based not just on absolute CBF, but also on CBF ratios between different regions. Together, these data indicate that cortical perfusion changes to a greater degree than hippocampal perfusion following pilocarpine injection.

8.4.2. Perfusion changes during SE

Seizure-associated increases in CBF have been demonstrated in animal models (Meldrum and Nilsson, 1976; Tanaka *et al.*, 1990; Kreisman *et al.*, 1991; Shih and Scremin, 1992; Andre *et al.*, 2002; Nersesyan *et al.*, 2004); however, the regional profile of seizure associated CBF changes remain unclear.

In the experiments reported here, regional CBF changes were observed over the course of SE indicating that there was a greater increase in the cortex than in the hippocampus after pilocarpine administration and during early SE. A similar pattern was also observed in the thalamus relative to the hippocampus. However, the degree of perfusion change in the cortex tended to be greater than the thalamus, which suggests that the regions respond in a

different manner following pilocarpine injection. Furthermore, the ratios of perfusion changes relative to the hippocampus indicate that both the cortex and the thalamus have consistently higher flows than the hippocampus following pilocarpine administration.

The increases in cortical and thalamic CBF are consistent with previous studies of CBF changes during seizures, and accompanying increases in glucose utilisation and increased $CMRO_2$ have also been reported (Pinard *et al.*, 1984; Tanaka *et al.*, 1990; Kreisman *et al.*, 1991; Shih and Scremin, 1992; Andre *et al.*, 2002). These data suggests that increases in CBF act to compensate for the increase in nutrient demand that the seizing neurons require in the early phase of seizures. However, during the late SE period, the perfusion data indicate a decline in the magnitude of signal change that may reflect the hypothesised failure of cerebral autoregulation. This decline of the cerebral vascular system due to persistent and prolonged seizure activity may eventually lead to a mismatch in energy supply and demand (Meldrum and Nilsson, 1976; Kreisman *et al.*, 1991).

In summary, the results from the current study indicate that CBF in the hippocampus does not increase to the same degree as the cortex. The differences between cortical and hippocampal CBF responses has been previously noted by Pinard and colleagues (Pinard *et al.*, 1987). In contrast to the present study, they reported a substantial increase in hippocampal CBF compared to the cortex following kainic acid induced SE. However, they also noted that there were no apparent differences in cortical and hippocampal CBF when the bicuculline method of SE induction was used (Pinard *et al.*, 1987). Therefore, these data suggest that the CBF response depends on the induction method. It is also noteworthy that intra-amygdala seizure induction with kainic acid has also been shown to demonstrate a limited CBF response that could not account for the concomitant glucose requirement in the hippocampus (Tanaka *et al.*, 1990).

The study detailed in section 5.4.2 demonstrated that pilocarpine can be used to induce prolonged seizure activity under fentanyl/medetomidine anaesthesia, and previous studies have also demonstrated a concomitant increase in glucose utilisation in the hippocampus using the pilocarpine method of seizure induction (Handforth and Treiman, 1995). These data therefore suggest that there is an increase in energy demand in the seizing hippocampus. However, the relatively limited CBF change in the hippocampus may

therefore suggest that in the current set up there may be a regional mismatch between nutrient demand and supply that may contribute to pilocarpine-induced injury.

Pilocarpine acts preferentially on the muscarinic component of the cholinergic system, whereas soman is a cholinesterase inhibitor that, in effect, acts on both the muscarinic and nicotinic systems (Shih and Scremin, 1992; Cavalheiro, 1995). This is in contrast with kainic acid model, which acts on the glutamatergic system, and bicuculline, which acts on the $GABA_A$ network (Meldrum and Nilsson, 1976; Pinard *et al.*, 1987; Tanaka *et al.*, 1990). Therefore the physiological changes associated with SE induction with pilocarpine and soman can be compared as both agents act on the cholinergic neurotransmitter system. CBF with glucose utilisation was investigated in soman-induced SE by Shih and colleagues who observed a lower proportional increase of CBF relative to glucose utilisation in the hippocampus (Shih and Scremin, 1992). Taken together with the results from the present study, these data support the hypothesis that a relative ischaemia occurs in the hippocampus during cholinergic induction of SE through an uncoupling of CBF and metabolism.

There is only one previous paper that has investigated perfusion changes during SE with MRI (Engelhorn *et al.*, 2005). However, significant methodological differences exist between this study and that of Engelhorn and colleagues, including perfusion imaging technique, as well as SE assessment, and regional assessment of perfusion changes. Therefore it is not possible to compare between the two studies.

As previously noted, excitotoxicity is widely accepted as the main mechanism of seizure-induced injury (Lothman, 1990; Shorvon, 1994; Chen and Wasterlain, 2006). Studies that have demonstrated seizure-induced cell death in the absence of a hypoxic/ischaemic mechanism support this hypothesis (Pinard *et al.*, 1984; Shih and Scremin, 1992). Further evidence includes observations of neocortical damage occurring despite CBF matching glucose demand, which was not found in the hippocampus (Shih and Scremin, 1992). However, the regional selectivity of SE-induced injury may indicate that specific regions, such as the hippocampus, have additional factors that underlie their vulnerability. Low levels of calcium-binding proteins as well as the relative abundance of NMDA receptors and KA receptors found in this region have been proposed to underlie this vulnerability

(Cendes, 2004). Also the contribution of hyperpyrexia, as well as a decrease in pH, increase in intracellular calcium, and excessive activity of excitatory neurotransmitters may play key roles. The current study supports the view that a relative ischaemia may contribute to hippocampal injury resulting from pilocarpine-induced SE.

8.4.3. Selective population of animals

The main limitation in this study was that the periods associated with motion were omitted from the current analysis due to the resulting degradation of the images, therefore only a selective population of animals were included in the study. The study described in section 5.4.2 reported that the tonic limb extensions were likely to cause motion problems because of the movement of the head, but this could not be confirmed directly as it is not possible to observe the animals during image acquisition. It was therefore by inference that the images omitted included these periods of tonic motion. These movements are associated with generalised tonic-clonic seizures (Mares and Kubova, 2006) and reflect the tonic component of the seizure. However, tonic seizures have been associated with activation of the brainstem network, whereas the clonic stage is associated with forebrain networks, which include the hippocampus (Andre *et al.*, 2002). Although it is unclear whether these periods play a role in hippocampal injury, the omission of the tonic seizures should be considered in the interpretation of these results in that further perfusion changes may be expected during these seizures. Therefore, one of the limitations of the current study was that a possible contributory mechanism to SE-induced brain injury could not be investigated with the current set-up.

Future studies should consider the use of neuromuscular blocking agents that would allow the inclusion of all aspects of seizure-associated CBF changes. Furthermore, particularly motion sensitive techniques, such as diffusion imaging, may be investigated in parallel with perfusion changes. Diffusion imaging is thought to provide an indication of cytotoxic oedema as a result of energy failure (Gass *et al.*, 2001): as the energy-requiring pumps, such as the Na^+/K^+ ATPase, that maintain the electrochemical gradient across the cell membrane fail, which leads to cell swelling. Therefore diffusion interleaved with perfusion

acquisitions may indicate the point at which energy failure begins with respect to CBF changes in pilocarpine-induced SE.

8.5. CONCLUSION

In conclusion, this study indicates that regional CBF changes occur *in vivo* during pilocarpine-induced SE under fentanyl/medetomidine anaesthesia. Cortical perfusion increased significantly more than hippocampal perfusion and these data support a hypothesis that a relative ischaemia may play a role in the selective vulnerability of the hippocampus to SE.

CHAPTER 9: DISCUSSION

A journey of a thousand miles begins with a single step

Lao-Tzu

The overall aim of the work presented in this thesis was to investigate the hypothesis that status epilepticus, acute hippocampal injury, mesial temporal sclerosis and temporal lobe epilepsy are causally related. Clinical studies have indicated that these events occur in humans, and provide the basis for the hypothesis that SE may cause brain injury which may progress on to MTS associated with epilepsy and cognitive dysfunction. Furthermore as MTS associated epilepsy is particularly difficult to treat with conventional medical therapies, it is the most common type of epilepsy that requires surgical intervention. Therefore, there is a real clinical need to understand the sequence of events from the onset of SE to hippocampal oedema, through to hippocampal sclerosis and associated epilepsy as this may facilitate the development of neuroprotective and anti-epileptogenic strategies. However, as ethical and practical considerations preclude a comprehensive characterisation of these events in patients, an alternative can be to use animal models to investigate these processes. Thus, the pilocarpine rat model was chosen in which SE, brain injury, and mesial temporal sclerosis with epilepsy occur that are hypothesised to be key characteristics that mimic SE associated pathologies in humans.

For this work, MRI was used to investigate these processes as this technology offers a non-invasive multi-parametric quantitative monitoring of brain events, and therefore provided a means to investigate the temporal characteristics of SE associated phenomena. Moreover as MRI is routinely used in the clinical setting due to its non-invasive nature, this provides a possibility of research directly translatable from bench to clinic.

The work in this thesis followed two distinct themes due to divergent methodological needs: MRI for monitoring the evolution of brain injury following SE, and MRI during SE. Chapter 5 describes some of the methodological developments that were required for both themes. For the MRI after SE, preliminary studies were performed to establish the feasibility of imaging the pilocarpine-treated animals over a prolonged period and to provide an indication of appropriate time points for the final study. For MRI during SE, a new method for inducing SE under fentanyl/medetomidine anaesthesia was developed for these purposes, but this set-up presented problems with movement that affected the MRI scanning. Thus, changes were made to the design of the MRI animal holder, and a low

average perfusion acquisition was developed to minimise the problems associated with motion.

Chapter 6 deals with the evolution of brain injury following a 90 minute seizure. The novel aspects of this study were the inclusion of *in vivo* CBF and T_1 measurements in combination with quantitative T_2 and ADC, with a focus on the early changes following SE. In addition, this was the first study that included control groups for investigating the possible effects of a long term exposure to isoflurane anaesthesia.

The monitoring with multi-parametric MRI demonstrated that a transient event occurs following SE, which normalises within 7 days; however hippocampal atrophy continues after this period. These findings are consistent with previous studies that have reported similar changes in humans and also in experimental models (Roch *et al.*, 2002a; Scott *et al.*, 2003; Nairismagi *et al.*, 2004). In addition, peak hippocampal changes in T_1, T_2 and CBF were observed 2 days following SE during this transient period and were found to be predictive of hippocampal volumes measured on day 21, which therefore suggests that a biomarker for injury has been identified. Previous MRI studies following SE have not identified such a biomarker. The present experimental design differed from previous studies due to the emphasis on the characterisation of early injury and continued monitoring into the medium term. Also, quantitative multi-parametric MR measurements were used which included CBF and T_1. It is these elements in the experimental design that provided the basis for identifying the MRI biomarker at the day 2 time point. This study demonstrated that, for the first time, early non-invasive imaging can be used to reveal the evolution of hippocampal injury following SE.

In chapter 3 the role of animal models in medical research was commented on. It was emphasised that it is not ethical or practical to image patients for the characterisation of brain injury in such a sustained manner as this experiment, and this underlies the need for animal models. One of the possible consequences of this study in an animal model is that these findings may be directly translated back in to the clinical domain. Previous clinical studies have identified T_2 increases during this early period in the hippocampus, suggesting that similar processes may occur in humans and animals (Scott *et al.*, 2003). Whether this type of multi-parametric imaging 2 days after SE could be used to identify humans that

may progress on to a poor outcome remains unclear. However, T_1, T_2 and perfusion imaging are clinically approved MRI techniques that are already widely used for diagnostic purposes, and with the identification of a critical predictive period on day 2, it should now be possible to conduct such a study in humans. This may then help to identify patients whose hippocampi will atrophy following SE and thus offer an opportunity for interventional strategies.

In the context of the physiological mechanisms that underlie the MR changes detected on day 2, as with much of the MR literature, the precise processes remain unclear. Previous studies have reported that T_1 and T_2 increases are related to oedema (Nakasu *et al.*, 1995; Roch *et al.*, 2002a; Nairismagi *et al.*, 2004), and blood flow related increases have been identified in regions vulnerable to SE (Fabene *et al.*, 2003), and our findings are in agreement with this work. In addition, histologically- and molecular- based studies have provided evidence for modulation of various processes during the early period in the hippocampus. As described in chapter 2, these processes include cell death, neurogenesis and inflammation. It is possible that all of these processes, as well as perhaps others that have yet been identified, all contribute to the MR changes on day 2. However, these MR changes seem to display key characteristics that are consistent with an inflammatory response.

Among the four "cardinal signs" of inflammation that were first described by Celsus in the 1st century AD are *rubor* (redness), *tumor* (swelling) and *calor* (heat); *dolor* (pain) being the fourth. Swelling is consistent with oedema, and both heat and redness can be generated by increases in blood flow to injured regions. Inflammatory markers, such as COX-2 and iNOS, have been identified in the hippocampus during the early period following SE and the temporal profile of these markers are also consistent with the transient nature of the MR changes (Jankowsky and Patterson, 1999; Voutsinos-Porche *et al.*, 2004; Turrin and Rivest, 2004). Thus, this supports the hypothesis that inflammation underlies the MR changes on day 2. If inflammation does indeed underlie these changes on day 2 then there may be implications for reducing the progression of SE-induced injury in that these early changes can be modulated with pharmaceuticals.

While the current findings do not provide direct evidence for inflammation as the main contributor to the MR changes, it is possible to investigate such an effect *in vivo* by using pharmacological tools: anti-inflammatory drugs are widely used clinically and experimentally. By using these drugs, it may prove possible to elucidate the nature of the biomarker. Furthermore, the relationship with early inflammation and post-SE outcome has not been previously investigated and such an experiment can assess the possibility of anti-inflammatory drugs in relation to post-SE injury. Consistent with the work presented in this thesis, it can be hypothesised that SE induces injury in the hippocampus and that the tissue responds with an inflammatory reaction. The degree of inflammation may reflect the severity of the initial injury, and that, as a consequence, the extent of inflammation measured following SE is in turn predictive of subsequent hippocampal atrophy.

Investigations were also conducted on the role of serial isoflurane anaesthesia, by comparing rats that were only imaged before SE and on day 21 with those imaged throughout the time course. Analysis of hippocampal volumes on day 21 revealed that there was significantly less atrophy than in the group that had serial isoflurane, suggesting that the serial use of isoflurane confers a degree of neuroprotection, which has not been previously reported following SE. Although this neuroprotective effect was found, it remains unclear as to whether it was the repeated nature of the anaesthesia that produced this effect or whether this effect was a result of anaesthesia during the early period following SE. While it may also be possible that isoflurane was more efficacious at stopping SE than diazepam alone and therefore the imaged animals underwent a shorter seizure. Furthermore, as it was not possible to assess the anaesthetic in relation to the severity of epilepsy, the effect of isoflurane on epileptogenesis needs clarification and future studies should be designed to investigate this phenomenon as isoflurane may have therapeutic implications for post-SE pathology. Also, these data suggest that future studies that require the serial use of anaesthesia, such as MR studies, should consider the possible effect of these drugs on outcome.

Chapter 7 describes novel combined MRI and proteomic studies of the hippocampal changes 2 days after SE aimed at to investigating the physiological basis of these changes. MRI was used to monitor these early changes until day 2, at which time point the 2-DE

and mass spectrometry methods were used to identify the concomitant protein changes. The MRI results indicate hippocampal changes similar to those of the study in chapter 6, and a number of proteins were found to be up-regulated in the hippocampus.

HSP27, which is considered to be a marker of cellular stress, showed the highest level of change. Up-regulation of this protein has been shown to confer a degree of protection in SE (Kalwy *et al.*, 2003). A post-translational variant of DRP-2 was also identified but the overall amount of DRP-2 was reduced. This protein has been implicated in neurogenesis and axonal guidance, and therefore modulation of this protein may have a role to play in the eventual development of the epileptic circuitry. Ezrin and α-tubulin, which are both cytoskeletal proteins, were also found to be increased, and this may indicate the widespread neuronal death or remodelling that has been widely reported following SE (Fujikawa, 1996; Krapfenbauer *et al.*, 2001; Nairismagi *et al.*, 2004). DHPR was also found to be up-regulated in the hippocampus on day 2, and this may have a direct relationship with the increased hippocampal CBF. The main action of DHPR is catalysing the formation of BH_4, which is an essential co-factor in the production of NOS (Sims, III and Reinberg, 2006). The role of NO in SE-induced injury remains unclear but it has been suggested to play a role in neuronal injury and may facilitate inflammation (Montecot *et al.*, 1998; Conti *et al.*, 2007). Another protein, histone-lysine N-methyltransferase, was found to be reduced and, although its role is unclear, a possible downstream consequence could be altered transcription of specific genes.

It should be noted that the proteomic approach that has been undertaken remains an initial early step and represents only a small proportion of the entire population of proteins in the hippocampus, and future studies may consider examining more basic or acidic proteins. In addition, the entire hippocampus was used for the work presented in this thesis and future studies may consider a more refined regional approach and isolate regions such as the CA1 and CA3 subfields of the hippocampus that are particularly susceptible to SE-induced injury. Nevertheless, this study demonstrated that a combined MRI and proteomics method provided the means for targeting an interesting period for study. This approach has led to the identification of proteins that offer alternative avenues for investigations into hippocampal injury and, perhaps, epileptogenesis.

Chapter 8 details the experiments in which perfusion imaging was used to investigate SE. Regional perfusion changes were identified, and these results indicated that, unlike the cortex, the hippocampus may not be receiving a sustained and increased perfusion to match the increase in neuronal activity, which is contrary to some studies in the literature (Meldrum and Horton, 1973; Shorvon, 1994). These data support the hypothesis that a relative ischaemia in the hippocampus may contribute to its selective vulnerability to SE.

Future studies should consider a pharmacological approach addressing the problem of motion associated with SE. The use of neuromuscular blockers with fentanyl/medetomidine would serve to completely remove the motion problem and also, as ventilation would be necessary, the role of excessive seizure activity could be investigated without possible confounding factors from systemic effects (Meldrum and Brierley, 1973). The development of such a model to investigate SE could allow new ways to investigate fundamental processes that occur during seizure initiation, propagation and termination, which are the three components of seizure evolution.

In this thesis, MRI was the main tool that was used. Its non-invasive nature and the spatial information that it offers made it an ideal instrument to monitor the progression of SE and the associated injury over time, although it is limited by the lack of specificity in that the processes that underlie T_1, T_2 and ADC are not completely understood. Nonetheless, the multi-parametric quantitative approach used has provided a biomarker that may be translatable to clinical practice, as presently a conventional clinical scanner (1.5T) has a similar field strength to the one used for the work presented in this thesis (2.35T). Advances in MRI technology have moved progressively towards MRI scanners at higher fields, the principal advantage of which is an increase in signal to noise ratio, which can be used to improve anatomic detail and reduce scan time while maintaining image quality. Furthermore, the development of MRI contrast agents can offer the molecular specificity that the methods used in the current work lack. Therefore future studies into SE should consider using of high field MRI scanners and also selective contrast agents.

9.1. FUTURE DIRECTIONS

From the outset of these experiments, it was stated that an understanding of the processes from SE onset through to the development of epilepsy may provide a clue to the development of novel preventative therapies. In light of the identification of the early MRI hippocampal biomarker that can be used to predict the severity of hippocampal injury following SE, and the interpretation that this biomarker relates to a time point in inflammation, a hypothesis was generated that reducing SE-induced inflammation would attenuate brain injury and subsequent epileptogenesis. We have recently received funding for investigating this hypothesis from the Epilepsy Research UK (ERUK), who also funded the work presented in this thesis.

The role of inflammation following SE has been receiving increasing attention in the epilepsy literature, and it has been suggested to play a critical role in the development of epilepsy. For example, a recent study has indicated that a selective COX-2 inhibitor, which is a key inflammatory pathway, can reduce the severity and frequency of subsequent seizures. However, previous studies have not been able to monitor inflammation *in vivo*. Therefore, the methodologies developed in this project will be used to assess the acute efficacy of anti-inflammatory agents during this early period, and their relationship with later epilepsy. One of the limitations of the work presented in this thesis was that epilepsy was not evaluated in the animals. However, for the next study a combination of non-invasive imaging, video-EEG monitoring and histology will be used to assess the efficacy of anti-inflammatory drugs on the development of epilepsy, the relationship between reduction of inflammation, as assessed by MRI, and the severity of epilepsy, and we shall evaluate the use of early MRI as a biomarker for the evaluation of the development of epilepsy and subsequent drug therapy.

9.2. CONCLUSION

This study has attempted to advance the understanding of status epilepticus and its pathological sequelae. MRI was the primary tool used in these investigations and the results indicate the suitability and potential of using MRI for studies into status epilepticus. For the first time, quantitative perfusion imaging was used to investigate the pathological sequelae of status epilepticus, together with traditional imaging methods, and a period during early injury was identified that was predictive of later injury. This suggests that MRI might be used to identify patients who may progress on to a poor outcome, and may be used to investigate neuroprotective strategies. As an animal model was used in this study, a combined approach with MRI and proteomics could be taken to investigate the tissue injury during this early period, and results indicate that during this early period a series of proteins are altered in the hippocampus. These proteins have a multitude of functions and may provide clues for alternative strategies for investigating brain injury and epileptogenesis.

In addition, this work in an animal model allowed the processes that occur during SE to be investigated with MRI. The pilot data suggest that an ischaemic mechanism may contribute to the vulnerability of the hippocampus to prolonged seizure activity.

REFERENCES

Abrous DN, Koehl M, Le MM (2005). Adult neurogenesis: from precursors to network and physiology. Physiol Rev 85:523-569.

Akbar MT, Lundberg AM, Liu K, Vidyadaran S, Wells KE, Dolatshad H, Wynn S, Wells DJ, Latchman DS, de Belleroche J (2003). The neuroprotective effects of heat shocprotein 27 overexpression in transgenic animals against kainate-induced seizures and hippocampal cell death. J Biol Chem 278:19956-19965.

Akbar MT, Wells DJ, Latchman DS, de Belleroche J (2001). Heat shock protein 27 shows a distinctive widespread spatial and temporal pattern of induction in CNS glial and neuronal cells compared to heat shock protein 70 and caspase 3 following kainate administration. Brain Res Mol Brain Res 93:148-163.

Alakuijala A, Palgi M, Wegelius K, Schmidt M, Enz R, Paulin L, Saarma M, Pasternack M (2005). GABA receptor rho subunit expression in the developing rat brain. Brain Res Dev Brain Res 154:15-23.

Alsop DC, Detre JA (1996). Reduced transit-time sensitivity in noninvasive magnetic resonance imaging of human cerebral blood flow. J Cereb Blood Flow Metab 16:1236-1249.

Ambrosini A, Louin G, Croci N, Plotkine M, Jafarian-Tehrani M (2005). Characterization of a rat model to study acute neuroinflammation on histopathological, biochemical and functional outcomes. J Neurosci Methods 144:183-191.

Andre V, Henry D, Nehlig A (2002). Dynamic variations of local cerebral blood flow in maximal electroshock seizures in the rat. Epilepsia 43:1120-1128.

Arimura N, Menager C, Fukata Y, Kaibuchi K (2004). Role of CRMP-2 in neuronal polarity. J Neurobiol 58:34-47.

Avishai-Eliner S, Brunson KL, Sandman CA, Baram TZ (2002). Stressed-out, or in (utero)? Trends Neurosci 25:518-524.

Avoli M, D'Antuono M, Louvel J, Kohling R, Biagini G, Pumain R, D'Arcangelo G, Tancredi V (2002). Network and pharmacological mechanisms leading to epileptiform synchronization in the limbic system in vitro. Prog Neurobiol 68:167-207.

Avsar E, Empson RM (2004). Adenosine acting via A1 receptors, controls the transition to status epilepticus-like behaviour in an in vitro model of epilepsy. Neuropharmacology 47:427-437.

Baas PW (1997). Microtubules and axonal growth. Curr Opin Cell Biol 9:29-36.

Badin RA, Lythgoe MF, van der WL, Thomas DL, Gadian DG, Latchman DS (2006). Neuroprotective effects of virally delivered HSPs in experimental stroke. J Cereb Blood Flow Metab 26:371-381.

Baird AE, Warach S (1998). Magnetic resonance imaging of acute stroke. J Cereb Blood Flow Metab 18:583-609.

Becker AJ, Gillardon F, Blumcke I, Langendorfer D, Beck H, Wiestler OD (1999). Differential regulation of apoptosis-related genes in resistant and vulnerable subfields of the rat epileptic hippocampus. Brain Res Mol Brain Res 67:172-176.

Ben-Ari Y, Cossart R (2000). Kainate, a double agent that generates seizures: two decades of progress. Trends Neurosci 23:580-587.

Bengzon J, Kokaia Z, Elmer E, Nanobashvili A, Kokaia M, Lindvall O (1997). Apoptosis and proliferation of dentate gyrus neurons after single and intermittent limbic seizures. Proc Natl Acad Sci U S A 94:10432-10437.

Bertram EH, Cornett J (1993). The ontogeny of seizures in a rat model of limbic epilepsy: evidence for a kindling process in the development of chronic spontaneous seizures. Brain Res 625:295-300.

Bettler B, Kaupmann K, Mosbacher J, Gassmann M (2004). Molecular structure and physiological functions of GABA(B) receptors. Physiol Rev 84:835-867.

Bhagat YA, Obenaus A, Hamilton MG, Kendall EJ (2001). Magnetic resonance imaging predicts neuropathology from soman-mediated seizures in the rodent. Neuroreport 12:1481-1487.

Bidmon HJ, Gorg B, Palomero-Gallagher N, Behne F, Lahl R, Pannek HW, Speckmann EJ, Zilles K (2004). Heat shock protein-27 is upregulated in the temporal cortex of patients with epilepsy. Epilepsia 45:1549-1559.

Blamire AM, Anthony DC, Rajagopalan B, Sibson NR, Perry VH, Styles P (2000). Interleukin-1beta -induced changes in blood-brain barrier permeability, apparent diffusion coefficient, and cerebral blood volume in the rat brain: a magnetic resonance study. J Neurosci 20:8153-8159.

Blumcke I, Thom M, Wiestler OD (2002). Ammon's horn sclerosis: a maldevelopmental disorder associated with temporal lobe epilepsy. Brain Pathol 12:199-211.

Boison D (2005). Adenosine and epilepsy: from therapeutic rationale to new therapeutic strategies. Neuroscientist 11:25-36.

Bouilleret V, Ridoux V, Depaulis A, Marescaux C, Nehlig A, Le Gal La SG (1999). Recurrent seizures and hippocampal sclerosis following intrahippocampal kainate injection in adult mice: electroencephalography, histopathology and synaptic reorganization similar to mesial temporal lobe epilepsy. Neuroscience 89:717-729.

Brandes RP, Schmitz-Winnenthal FH, Feletou M, Godecke A, Huang PL, Vanhoutte PM, Fleming I, Busse R (2000). An endothelium-derived hyperpolarizing factor distinct from

NO and prostacyclin is a major endothelium-dependent vasodilator in resistance vessels of wild-type and endothelial NO synthase knockout mice. Proc Natl Acad Sci U S A 97:9747-9752.

Brandt C, Gastens AM, Sun MZ, Hausknecht M, Loscher W (2006). Treatment with valproate after status epilepticus: Effect on neuronal damage, epileptogenesis, and behavioral alterations in rats. Neuropharmacology 51:789-804.

Brandt C, Potschka H, Loscher W, Ebert U (2003). N-methyl-D-aspartate receptor blockade after status epilepticus protects against limbic brain damage but not against epilepsy in the kainate model of temporal lobe epilepsy. Neuroscience 118:727-740.

Briellmann RS, Kalnins RM, Berkovic SF, Jackson GD (2002). Hippocampal pathology in refractory temporal lobe epilepsy: T2-weighted signal change reflects dentate gliosis. Neurology 58:265-271.

Bryan RM, Jr., You J, Golding EM, Marrelli SP (2005). Endothelium-derived hyperpolarizing factor: a cousin to nitric oxide and prostacyclin. Anesthesiology 102:1261-1277.

Calabrese VP, Gruemer HD, Tripathi HL, Dewey W, Fortner CA, Delorenzo RJ (1993). Serum cortisol and cerebrospinal fluid beta-endorphins in status epilepticus. Their possible relation to prognosis. Arch Neurol 50:689-693.

Campagna JA, Miller KW, Forman SA (2003). Mechanisms of actions of inhaled anesthetics. N Engl J Med 348:2110-2124.

Cavalheiro EA (1995). The pilocarpine model of epilepsy. Ital J Neurol Sci 16:33-37.

Cavalheiro EA, Naffah-Mazzacoratti MG, Mello LE, Leite JP (2006). The Pilocarpine Model of Seizures. Models of Seizures and Epilepsy. p. 433-448.

Cavanagh JB, Meyer A (1956). Aetiological aspects of Ammon's horn sclerosis associated with temporal lobe epilepsy. Br Med J 44:1403-1407.

Cendes F (2004). Febrile seizures and mesial temporal sclerosis. Curr Opin Neurol 17:161-164.

Cendes F, Andermann F, Carpenter S, Zatorre RJ, Cashman NR (1995). Temporal lobe epilepsy caused by domoic acid intoxication: evidence for glutamate receptor-mediated excitotoxicity in humans. Ann Neurol 37:123-126.

Cha BH, Akman C, Silveira DC, Liu X, Holmes GL (2004). Spontaneous recurrent seizure following status epilepticus enhances dentate gyrus neurogenesis. Brain Dev 26:394-397.

Chaudhary G, Malhotra J, Chaudhari JD, Gopinath G, Gupta YK (1999). Effect of different lithium priming schedule on pilocarpine-induced status epilepticus in rats. Methods Find Exp Clin Pharmacol 21:21-24.

Chen JW, Wasterlain CG (2006). Status epilepticus: pathophysiology and management in adults. Lancet Neurol 5:246-256.

Cherng CH, Wong CS (2005). Effect of fentanyl on lidocaine-induced convulsions in mice. Pharmacology 75:1-4.

Chin RF, Neville BG, Scott RC (2004). A systematic review of the epidemiology of status epilepticus. Eur J Neurol 11:800-810.

Cho S, Volpe BT, Bae Y, Hwang O, Choi HJ, Gal J, Park LC, Chu CK, Du J, Joh TH (1999). Blockade of tetrahydrobiopterin synthesis protects neurons after transient forebrain ischemia in rat: a novel role for the cofactor. J Neurosci 19:878-889.

Chuang YC, Chen SD, Lin TK, Liou CW, Chang WN, Chan SH, Chang AY (2007). Upregulation of nitric oxide synthase II contributes to apoptotic cell death in the hippocampal CA3 subfield via a cytochrome c/caspase-3 signaling cascade following induction of experimental temporal lobe status epilepticus in the rat. Neuropharmacology 52:1263-1273.

Clifford DB, Olney JW, Maniotis A, Collins RC, Zorumski CF (1987). The functional anatomy and pathology of lithium-pilocarpine and high-dose pilocarpine seizures. Neuroscience 23:953-968.

Cock HR, Tong X, Hargreaves IP, Heales SJ, Clark JB, Patsalos PN, Thom M, Groves M, Schapira AH, Shorvon SD, Walker MC (2002). Mitochondrial dysfunction associated with neuronal death following status epilepticus in rat. Epilepsy Res 48:157-168.

Cohen I, Navarro V, Clemenceau S, Baulac M, Miles R (2002). On the origin of interictal activity in human temporal lobe epilepsy in vitro. Science 298:1418-1421.

Conti A, Miscusi M, Cardali S, Germano A, Suzuki H, Cuzzocrea S, Tomasello F (2007). Nitric oxide in the injured spinal cord: synthases cross-talk, oxidative stress and inflammation. Brain Res Rev 54:205-218.

Corrales A, Xu F, Garavito-Aguilar ZV, Blanck TJ, Recio-Pinto E (2004). Isoflurane reduces the carbachol-evoked Ca2+ influx in neuronal cells. Anesthesiology 101:895-901.

Cossart R, Bernard C, Ben Ari Y (2005). Multiple facets of GABAergic neurons and synapses: multiple fates of GABA signalling in epilepsies. Trends Neurosci 28:108-115.

Cuzzocrea S, Salvemini D (2007). Molecular mechanisms involved in the reciprocal regulation of cyclooxygenase and nitric oxide synthase enzymes. Kidney Int 71:290-297.

De Simoni MG, Perego C, Ravizza T, Moneta D, Conti M, Marchesi F, De Luigi A, Garattini S, Vezzani A (2000). Inflammatory cytokines and related genes are induced in the rat hippocampus by limbic status epilepticus. Eur J Neurosci 12:2623-2633.

DeGiorgio CM, Tomiyasu U, Gott PS, Treiman DM (1992). Hippocampal pyramidal cell loss in human status epilepticus. Epilepsia 33:23-27.

Delhalle S, Duvoix A, Schnekenburger M, Morceau F, Dicato M, Diederich M (2003). An introduction to the molecular mechanisms of apoptosis. Ann N Y Acad Sci 1010:1-8.:1-8.

Delorenzo RJ, Hauser WA, Towne AR, Boggs JG, Pellock JM, Penberthy L, Garnett L, Fortner CA, Ko D (1996). A prospective, population-based epidemiologic study of status epilepticus in Richmond, Virginia. Neurology 46:1029-1035.

Delorenzo RJ, Sun DA, Deshpande LS (2005). Cellular mechanisms underlying acquired epilepsy: the calcium hypothesis of the induction and maintainance of epilepsy. Pharmacol Ther 105:229-266.

Detre JA, Leigh JS, Williams DS, Koretsky AP (1992). Perfusion imaging. Magn Reson Med 23:37-45.

Dube C, Richichi C, Bender RA, Chung G, Litt B, Baram TZ (2006). Temporal lobe epilepsy after experimental prolonged febrile seizures: prospective analysis. Brain 129:911-922.

Dube C, Yu H, Nalcioglu O, Baram TZ (2004). Serial MRI after experimental febrile seizures: altered T2 signal without neuronal death. Ann Neurol 56:709-714.

Dudek FE, Clark S, Williams PA, Grace J, Grabenstatter HE (2006). Kainate-Induced Status Epilepticus: a Chronic Model of Acquired Epilepsy. Models of Seizures and Epilepsy. p. 415-432.

Dulla CG, Dobelis P, Pearson T, Frenguelli BG, Staley KJ, Masino SA (2005). Adenosine and ATP link PCO2 to cortical excitability via pH. Neuron 48:1011-1023.

During MJ, Spencer DD (1992). Adenosine: a potential mediator of seizure arrest and postictal refractoriness. Ann Neurol 32:618-624.

During MJ, Spencer DD (1993). Extracellular hippocampal glutamate and spontaneous seizure in the conscious human brain. Lancet 341:1607-1610.

Ebisu T, Rooney WD, Graham SH, Mancuso A, Weiner MW, Maudsley AA (1996). MR spectroscopic imaging and diffusion-weighted MRI for early detection of kainate-induced status epilepticus in the rat. Magn Reson Med 36:821-828.

Ekdahl CT, Mohapel P, Elmer E, Lindvall O (2001). Caspase inhibitors increase short-term survival of progenitor-cell progeny in the adult rat dentate gyrus following status epilepticus. Eur J Neurosci 14:937-945.

Engel J, Jr. (1996). Introduction to temporal lobe epilepsy. Epilepsy Res 26:141-150.

Engel J, Schwartzkroin PA (2006). What Should Be Modelled? Models of Seizures and Epilepsy. p. 1-14.

Engelhorn T, Doerfler A, Weise J, Baehr M, Forsting M, Hufnagel A (2005). Cerebral perfusion alterations during the acute phase of experimental generalized status epilepticus: prediction of survival by using perfusion-weighted MR imaging and histopathology. AJNR Am J Neuroradiol 26:1563-1570.

Engelhorn T, Weise J, Hammen T, Bluemcke I, Hufnagel A, Doerfler A (2007). Early diffusion-weighted MRI predicts regional neuronal damage in generalized status epilepticus in rats treated with diazepam. Neurosci Lett 417:275-280.

Enna SJ, Bowery NG (2004). GABA(B) receptor alterations as indicators of physiological and pharmacological function. Biochem Pharmacol 68:1541-1548.

Fabene PF, Marzola P, Sbarbati A, Bentivoglio M (2003). Magnetic resonance imaging of changes elicited by status epilepticus in the rat brain: diffusion-weighted and T2-weighted images, regional blood volume maps, and direct correlation with tissue and cell damage. Neuroimage 18:375-389.

Fabene PF, Weiczner R, Marzola P, Nicolato E, Calderan L, Andrioli A, Farkas E, Sule Z, Mihaly A, Sbarbati A (2005). Structural and functional MRI following 4-aminopyridine-induced seizures: A comparative imaging and anatomical study. Neurobiol Dis.

Fahrner A, Kann G, Flubacher A, Heinrich C, Freiman TM, Zentner J, Frotscher M, Haas CA (2007). Granule cell dispersion is not accompanied by enhanced neurogenesis in temporal lobe epilepsy patients. Exp Neurol 203:320-332.

Flecknell PA, Cruz IJ, Liles JH, Whelan G (1996). Induction of anaesthesia with halothane and isoflurane in the rabbit: a comparison of the use of a face-mask or an anaesthetic chamber. Lab Anim 30:67-74.

Forstermann U (2006). Janus-faced role of endothelial NO synthase in vascular disease: uncoupling of oxygen reduction from NO synthesis and its pharmacological reversal. Biol Chem 387:1521-1533.

Franklin TB, Krueger-Naug AM, Clarke DB, Arrigo AP, Currie RW (2005). The role of heat shock proteins Hsp70 and Hsp27 in cellular protection of the central nervous system. Int J Hyperthermia 21:379-392.

Frotscher M, Jonas P, Sloviter RS (2006). Synapses formed by normal and abnormal hippocampal mossy fibers. Cell Tissue Res 326:361-367.

Fujikawa DG (1995). Neuroprotective effect of ketamine administered after status epilepticus onset. Epilepsia 36:186-195.

Fujikawa DG (1996). The temporal evolution of neuronal damage from pilocarpine-induced status epilepticus. Brain Res 725:11-22.

Fukata Y, Itoh TJ, Kimura T, Menager C, Nishimura T, Shiromizu T, Watanabe H, Inagaki N, Iwamatsu A, Hotani H, Kaibuchi K (2002). CRMP-2 binds to tubulin heterodimers to promote microtubule assembly. Nat Cell Biol 4:583-591.

Gadian DG (1996) NMR and Its Applications in Living Systems.Oxford University Press.

Gass A, Niendorf T, Hirsch JG (2001). Acute and chronic changes of the apparent diffusion coefficient in neurological disorders--biophysical mechanisms and possible underlying histopathology. J Neurol Sci 186 Suppl 1:S15-S23.

Gorg A, Weiss W, Dunn MJ (2004). Current two-dimensional electrophoresis technology for proteomics. Proteomics 4:3665-3685.

Gorter JA, van Vliet EA, Aronica E, Breit T, Rauwerda H, Lopes da Silva FH, Wadman WJ (2006). Potential new antiepileptogenic targets indicated by microarray analysis in a rat model for temporal lobe epilepsy. J Neurosci 26:11083-11110.

Gray WP, Sundstrom LE (1998). Kainic acid increases the proliferation of granule cell progenitors in the dentate gyrus of the adult rat. Brain Res 790:52-59.

Green CJ (1982) Animal anaesthesia. Laboratory Animals Ltd.

Greene ND, Leung KY, Wait R, Begum S, Dunn MJ, Copp AJ (2002). Differential protein expression at the stage of neural tube closure in the mouse embryo. J Biol Chem 277:41645-41651.

Gross RA (1992). A brief history of epilepsy and its therapy in the Western Hemisphere. Epilepsy Res 12:65-74.

Halonen T, Kotti T, Tuunanen J, Toppinen A, Miettinen R, Riekkinen PJ (1995). Alpha 2-adrenoceptor agonist, dexmedetomidine, protects against kainic acid-induced convulsions and neuronal damage. Brain Res 693:217-224.

Handforth A, Treiman DM (1995). Functional mapping of the early stages of status epilepticus: a 14C-2-deoxyglucose study in the lithium-pilocarpine model in rat. Neuroscience 64:1057-1073.

Heinemann U, Buchheim K, Gabriel S, Kann O, Kovacs R, Schuchmann S (2002). Coupling of electrical and metabolic activity during epileptiform discharges. Epilepsia 43 Suppl 5:168-173.

Hendriksen H, Datson NA, Ghijsen WE, van Vliet EA, da Silva FH, Gorter JA, Vreugdenhil E (2001). Altered hippocampal gene expression prior to the onset of spontaneous seizures in the rat post-status epilepticus model. Eur J Neurosci 14:1475-1484.

Henshall DC, Chen J, Simon RP (2000). Involvement of caspase-3-like protease in the mechanism of cell death following focally evoked limbic seizures. J Neurochem 74:1215-1223.

Henshall DC, Simon RP (2005). Epilepsy and apoptosis pathways. J Cereb Blood Flow Metab 25:1557-1572.

Hesdorffer DC, Logroscino G, Cascino G, Annegers JF, Hauser WA (1998). Incidence of status epilepticus in Rochester, Minnesota, 1965-1984. Neurology 50:735-741.

Hinterkeuser S, Schroder W, Hager G, Seifert G, Blumcke I, Elger CE, Schramm J, Steinhauser C (2000). Astrocytes in the hippocampus of patients with temporal lobe epilepsy display changes in potassium conductances. Eur J Neurosci 12:2087-2096.

Hirsch C, Gauss R, Sommer T (2006). Coping with stress: cellular relaxation techniques. Trends Cell Biol 16:657-663.

Hoehn GT, Suffredini AF (2005). Proteomics. Crit Care Med 33:S444-S448.

Inagaki N, Chihara K, Arimura N, Menager C, Kawano Y, Matsuo N, Nishimura T, Amano M, Kaibuchi K (2001). CRMP-2 induces axons in cultured hippocampal neurons. Nat Neurosci 4:781-782.

Iosif RE, Ekdahl CT, Ahlenius H, Pronk CJ, Bonde S, Kokaia Z, Jacobsen SE, Lindvall O (2006). Tumor necrosis factor receptor 1 is a negative regulator of progenitor proliferation in adult hippocampal neurogenesis. J Neurosci 26:9703-9712.

Ivetic A, Ridley AJ (2004). Ezrin/radixin/moesin proteins and Rho GTPase signalling in leucocytes. Immunology 112:165-176.

Jakubs K, Nanobashvili A, Bonde S, Ekdahl CT, Kokaia Z, Kokaia M, Lindvall O (2006). Environment matters: synaptic properties of neurons born in the epileptic adult brain develop to reduce excitability. Neuron 52:1047-1059.

Jankowsky JL, Patterson PH (1999). Differential regulation of cytokine expression following pilocarpine-induced seizure. Exp Neurol 159:333-346.

Jankowsky JL, Patterson PH (2001). The role of cytokines and growth factors in seizures and their sequelae. Prog Neurobiol 63:125-149.

Jeffery B, Barlow T, Moizer K, Paul S, Boyle C (2004). Amnesic shellfish poison. Food Chem Toxicol 42:545-557.

Jones DM, Esmaeil N, Maren S, Macdonald RL (2002). Characterization of pharmacoresistance to benzodiazepines in the rat Li-pilocarpine model of status epilepticus. Epilepsy Res 50:301-312.

Jung KH, Chu K, Lee ST, Kim J, Sinn DI, Kim JM, Park DK, Lee JJ, Kim SU, Kim M, Lee SK, Roh JK (2006). Cyclooxygenase-2 inhibitor, celecoxib, inhibits the altered hippocampal neurogenesis with attenuation of spontaneous recurrent seizures following pilocarpine-induced status epilepticus. Neurobiol Dis 23:237-246.

Jupp B, Williams JP, Tesiram YA, Vosmansky M, O'Brien TJ (2006). Hippocampal T2 signal change during amygdala kindling epileptogenesis. Epilepsia 47:41-46.

Kalwy SA, Akbar MT, Coffin RS, de Belleroche J, Latchman DS (2003). Heat shock protein 27 delivered via a herpes simplex virus vector can protect neurons of the hippocampus against kainic-acid-induced cell loss. Brain Res Mol Brain Res 111:91-103.

Kawaguchi M, Kimbro JR, Drummond JC, Cole DJ, Kelly PJ, Patel PM (2000). Isoflurane delays but does not prevent cerebral infarction in rats subjected to focal ischemia. Anesthesiology 92:1335-1342.

Kim JB, Ju JY, Kim JH, Kim TY, Yang BH, Lee YS, Son H (2004). Dexamethasone inhibits proliferation of adult hippocampal neurogenesis in vivo and in vitro. Brain Res 1027:1-10.

King MD, van Bruggen N, Ahier RG, Cremer JE, Hajnal JV, Williams SR, Doran M (1991). Diffusion-weighted imaging of kainic acid lesions in the rat brain. Magn Reson Med 20:158-164.

Klitgaard H, Matagne A, Vanneste-Goemaere J, Margineanu DG (2002). Pilocarpine-induced epileptogenesis in the rat: impact of initial duration of status epilepticus on electrophysiological and neuropathological alterations. Epilepsy Res 51:93-107.

Kochanek PM, Vagni VA, Janesko KL, Washington CB, Crumrine PK, Garman RH, Jenkins LW, Clark RS, Homanics GE, Dixon CE, Schnermann J, Jackson EK (2006). Adenosine A1 receptor knockout mice develop lethal status epilepticus after experimental traumatic brain injury. J Cereb Blood Flow Metab 26:565-575.

Koerner IP, Brambrink AM (2006). Brain protection by anesthetic agents. Curr Opin Anaesthesiol 19:481-486.

Koshimura K, Murakami Y, Tanaka J, Kato Y (2000). The role of 6R-tetrahydrobiopterin in the nervous system. Prog Neurobiol 61:415-438.

Krapfenbauer K, Berger M, Lubec G, Fountoulakis M (2001). Changes in the brain protein levels following administration of kainic acid. Electrophoresis 22:2086-2091.

Kreisman NR, Magee JC, Brizzee BL (1991). Relative hypoperfusion in rat cerebral cortex during recurrent seizures. J Cereb Blood Flow Metab 11:77-87.

Lee PH, Grimes L, Hong JS (1989). Glucocorticoids potentiate kainic acid-induced seizures and wet dog shakes. Brain Res 480:322-325.

Leite JP, Garcia-Cairasco N, Cavalheiro EA (2002). New insights from the use of pilocarpine and kainate models. Epilepsy Res 50:93-103.

Lemos T, Cavalheiro EA (1995). Suppression of pilocarpine-induced status epilepticus and the late development of epilepsy in rats. Exp Brain Res 102:423-428.

Leung KY, Wait R, Welson SY, Yan JX, Abraham DJ, Black CM, Pearson JD, Dunn MJ (2001). A reference map of human lung MRC-5 fibroblast proteins using immobilized pH gradient-isoelectric focusing-based two-dimensional electrophoresis. Proteomics 1:787-794.

Lian XY, Zhang ZZ, Stringer JL (2005). Anticonvulsant activity of ginseng on seizures induced by chemical convulsants. Epilepsia 46:15-22.

Linden DE (2007). What, when, where in the brain? Exploring mental chronometry with brain imaging and electrophysiology. Rev Neurosci 18:159-171.

Longo B, Covolan L, Chadi G, Mello LE (2003). Sprouting of mossy fibers and the vacating of postsynaptic targets in the inner molecular layer of the dentate gyrus. Exp Neurol 181:57-67.

Longo BM, Mello LE (1997). Blockade of pilocarpine- or kainate-induced mossy fiber sprouting by cycloheximide does not prevent subsequent epileptogenesis in rats. Neurosci Lett 226:163-166.

Loscher W (2002). Animal models of epilepsy for the development of antiepileptogenic and disease-modifying drugs. A comparison of the pharmacology of kindling and post-status epilepticus models of temporal lobe epilepsy. Epilepsy Res 50:105-123.

Lothman E (1990). The biochemical basis and pathophysiology of status epilepticus. Neurology 40:13-23.

Lowenstein DH (1999). Status epilepticus: an overview of the clinical problem. Epilepsia 40 Suppl 1:S3-S8.

Lucas DR, Newhouse JP (1957). The toxic effect of sodium L-glutamate on the inner layers of the retina. AMA Arch Ophthalmol 58:193-201.

Lukasik VM, Gillies RJ (2003). Animal anaesthesia for in vivo magnetic resonance. NMR Biomed 16:459-467.

Lukasiuk K, Pitkanen A (2007). Gene and protein expression in experimental status epilepticus. Epilepsia 48 Suppl 8:28-32.:28-32.

Lythgoe MF, Thomas DL, Calamante F (2002). MRI measurement of cerebral perfusion and the application to experimental neuroscience. In: van-Bruggen N, Roberts TP, editors. Biomedical Imaging in Experimental Neuroscience.Boca Raton, Florida:CRC Press.

Mantini D, Perrucci MG, Del GC, Romani GL, Corbetta M (2007). Electrophysiological signatures of resting state networks in the human brain. Proc Natl Acad Sci U S A 104:13170-13175.

Mares P, Kubova H (2006). Electrical Stimulation-Induced Models of Seizures. Models of Seizures and Epilepsy. p. 153-160.

Matter H, Kotsonis P (2004). Biology and chemistry of the inhibition of nitric oxide synthases by pteridine-derivatives as therapeutic agents. Med Res Rev 24:662-684.

Mazarati A, Thompson KW, Suchomelova L, Sankar R, Shirasaka Y, Nissinen J, Pitkanen A, Bertram EH, Wasterlain C (2006). Status Epilepticus: Electrical Stimulation Models. Models of Seizures and Epilepsy. p. 449-464.

McNamara JO, Huang YZ, Leonard AS (2006). Molecular signaling mechanisms underlying epileptogenesis. Sci STKE 2006:re12.

Meert TF, De KM (1994). Potentiation of the analgesic properties of fentanyl-like opioids with alpha 2-adrenoceptor agonists in rats. Anesthesiology 81:677-688.

Meldrum BS, Brierley JB (1973). Prolonged epileptic seizures in primates. Ischemic cell change and its relation to ictal physiological events. Arch Neurol 28:10-17.

Meldrum BS, Horton RW (1973). Physiology of status epilepticus in primates. Arch Neurol 28:1-9.

Meldrum BS, Nilsson B (1976). Cerebral blood flow and metabolic rate early and late in prolonged epileptic seizures induced in rats by bicuculline. Brain 99:523-542.

Mello LE, Cavalheiro EA, Tan AM, Kupfer WR, Pretorius JK, Babb TL, Finch DM (1993). Circuit mechanisms of seizures in the pilocarpine model of chronic epilepsy: cell loss and mossy fiber sprouting. Epilepsia 34:985-995.

Merlin LR, Wong RK (1997). Role of group I metabotropic glutamate receptors in the patterning of epileptiform activities in vitro. J Neurophysiol 78:539-544.

Minturn JE, Fryer HJ, Geschwind DH, Hockfield S (1995). TOAD-64, a gene expressed early in neuronal differentiation in the rat, is related to unc-33, a C. elegans gene involved in axon outgrowth. J Neurosci 15:6757-6766.

Mohapel P, Ekdahl CT, Lindvall O (2004). Status epilepticus severity influences the long-term outcome of neurogenesis in the adult dentate gyrus. Neurobiol Dis 15:196-205.

Moldrich RX, Chapman AG, De Sarro G, Meldrum BS (2003). Glutamate metabotropic receptors as targets for drug therapy in epilepsy. Eur J Pharmacol 476:3-16.

Moncada S, Bolanos JP (2006). Nitric oxide, cell bioenergetics and neurodegeneration. J Neurochem 97:1676-1689.

Montecot C, Rondi-Reig L, Springhetti V, Seylaz J, Pinard E (1998). Inhibition of neuronal (type 1) nitric oxide synthase prevents hyperaemia and hippocampal lesions resulting from kainate-induced seizures. Neuroscience 84:791-800.

Morimoto K, Fahnestock M, Racine RJ (2004). Kindling and status epilepticus models of epilepsy: rewiring the brain. Prog Neurobiol 73:1-60.

Moseley ME, Kucharczyk J, Mintorovitch J, Cohen Y, Kurhanewicz J, Derugin N, Asgari H, Norman D (1990). Diffusion-weighted MR imaging of acute stroke: correlation with T2-weighted and magnetic susceptibility-enhanced MR imaging in cats. AJNR Am J Neuroradiol 11:423-429.

Moser MB, Moser EI, Forrest E, Andersen P, Morris RG (1995). Spatial learning with a minislab in the dorsal hippocampus. Proc Natl Acad Sci U S A 92:9697-9701.

Murao K, Shingu K, Miyamoto E, Ikeda S, Nakao S, Masuzawa M, Yamada M (2002). Anticonvulsant effects of sevoflurane on amygdaloid kindling and bicuculline-induced seizures in cats: comparison with isoflurane and halothane. J Anesth 16:34-43.

Murao K, Shingu K, Tsushima K, Takahira K, Ikeda S, Matsumoto H, Nakao S, Asai T (2000). The anticonvulsant effects of volatile anesthetics on penicillin-induced status epilepticus in cats. Anesth Analg 90:142-147.

Nairismagi J, Grohn OH, Kettunen MI, Nissinen J, Kauppinen RA, Pitkanen A (2004). Progression of brain damage after status epilepticus and its association with epileptogenesis: a quantitative MRI study in a rat model of temporal lobe epilepsy. Epilepsia 45:1024-1034.

Nakasu Y, Nakasu S, Morikawa S, Uemura S, Inubushi T, Handa J (1995). Diffusion-weighted MR in experimental sustained seizures elicited with kainic acid. AJNR Am J Neuroradiol 16:1185-1192.

Narkilahti S, Nissinen J, Pitkanen A (2003). Administration of caspase 3 inhibitor during and after status epilepticus in rat: effect on neuronal damage and epileptogenesis. Neuropharmacology 44:1068-1088.

Narkilahti S, Pitkanen A (2005). Caspase 6 expression in the rat hippocampus during epileptogenesis and epilepsy. Neuroscience 131:887-897.

Nersesyan H, Herman P, Erdogan E, Hyder F, Blumenfeld H (2004). Relative changes in cerebral blood flow and neuronal activity in local microdomains during generalized seizures. J Cereb Blood Flow Metab 24:1057-1068.

Nicholls JG, Martin AR, Wallace BG, Fuchs PA (2001) From Neuron to Brain.Sinauer Associates.

Niessen HG, Angenstein F, Vielhaber S, Frisch C, Kudin A, Elger CE, Heinze HJ, Scheich H, Kunz WS (2005). Volumetric magnetic resonance imaging of functionally relevant structural alterations in chronic epilepsy after pilocarpine-induced status epilepticus in rats. Epilepsia 46:1021-1026.

Nohria V, Lee N, Tien RD, Heinz ER, Smith JS, DeLong GR, Skeen MB, Resnick TJ, Crain B, Lewis DV (1994). Magnetic resonance imaging evidence of hippocampal sclerosis in progression: a case report. Epilepsia 35:1332-1336.

Nunez JL, Koss WA, Juraska JM (2000). Hippocampal anatomy and water maze performance are affected by neonatal cryoanesthesia in rats of both sexes. Horm Behav 37:169-178.

Olney JW, de Gubareff T (1978). Glutamate neurotoxicity and Huntington's chorea. Nature 271:557-559.

Olney JW, Rhee V, Ho OL (1974). Kainic acid: a powerful neurotoxic analogue of glutamate. Brain Res 77:507-512.

Parent JM (2002). The role of seizure-induced neurogenesis in epileptogenesis and brain repair. Epilepsy Res 50:179-189.

Parent JM, Elliott RC, Pleasure SJ, Barbaro NM, Lowenstein DH (2006a). Aberrant seizure-induced neurogenesis in experimental temporal lobe epilepsy. Ann Neurol 59:81-91.

Parent JM, Janumpalli S, McNamara JO, Lowenstein DH (1998). Increased dentate granule cell neurogenesis following amygdala kindling in the adult rat. Neurosci Lett 247:9-12.

Parent JM, von dem BN, Lowenstein DH (2006b). Prolonged seizures recruit caudal subventricular zone glial progenitors into the injured hippocampus. Hippocampus 16:321-328.

Parent JM, Yu TW, Leibowitz RT, Geschwind DH, Sloviter RS, Lowenstein DH (1997). Dentate granule cell neurogenesis is increased by seizures and contributes to aberrant network reorganization in the adult rat hippocampus. J Neurosci 17:3727-3738.

Paxinos G (1995) The Rat Nervous System.

Pinard E, Rigaud AS, Riche D, Naquet R, Seylaz J (1987). Continuous determination of the cerebrovascular changes induced by bicuculline and kainic acid in unanaesthetized spontaneously breathing rats. Neuroscience 23:943-952.

Pinard E, Tremblay E, Ben-Ari Y, Seylaz J (1984). Blood flow compensates oxygen demand in the vulnerable CA3 region of the hippocampus during kainate-induced seizures. Neuroscience 13:1039-1049.

Pinto DJ, Patrick SL, Huang WC, Connors BW (2005). Initiation, propagation, and termination of epileptiform activity in rodent neocortex in vitro involve distinct mechanisms. J Neurosci 25:8131-8140.

Pitkanen A, Kharatishvili I, Karhunen H, Lukasiuk K, Immonen R, Nairismagi J, Grohn O, Nissinen J (2007). Epileptogenesis in experimental models. Epilepsia 48 Suppl 2:13-20.:13-20.

Pitkanen A, Nissinen J, Lukasiuk K, Jutila L, Paljarvi L, Salmenpera T, Karkola K, Vapalahti M, Ylinen A (2000a). Association between the density of mossy fiber sprouting and seizure frequency in experimental and human temporal lobe epilepsy. Epilepsia 41 Suppl 6:S24-9.:S24-S29.

Pitkanen A, Nissinen J, Nairismagi J, Lukasiuk K, Grohn OH, Miettinen R, Kauppinen R (2002). Progression of neuronal damage after status epilepticus and during spontaneous seizures in a rat model of temporal lobe epilepsy. Prog Brain Res 135:67-83.

Pitkanen A, Pikkarainen M, Nurminen N, Ylinen A (2000b). Reciprocal connections between the amygdala and the hippocampal formation, perirhinal cortex, and postrhinal cortex in rat. A review. Ann N Y Acad Sci 911:369-391.

Pitkanen A, Schwartzkroin PA, Moshe SL (2006) Models of Seizures and Epilepsy.

Pontzer NJ, Crews FT (1990). Desensitization of muscarinic stimulated hippocampal cell firing is related to phosphoinositide hydrolysis and inhibited by lithium. J Pharmacol Exp Ther 253:921-929.

Ponzone A, Spada M, Ferraris S, Dianzani I, de SL (2004). Dihydropteridine reductase deficiency in man: from biology to treatment. Med Res Rev 24:127-150.

Prichard JW, Zhong J, Petroff OA, Gore JC (1995). Diffusion-weighted NMR imaging changes caused by electrical activation of the brain. NMR Biomed 8:359-364.

Racine RJ (1972). Modification of seizure activity by electrical stimulation. II. Motor seizure. Electroencephalogr Clin Neurophysiol 32:281-294.

Rasmusson DD, Clow K, Szerb JC (1994). Modification of neocortical acetylcholine release and electroencephalogram desynchronization due to brainstem stimulation by drugs applied to the basal forebrain. Neuroscience 60:665-677.

Raspall-Chaure M, Chin RF, Neville BG, Scott RC (2006). Outcome of paediatric convulsive status epilepticus: a systematic review. Lancet Neurol 5:769-779.

Raza M, Blair RE, Sombati S, Carter DS, Deshpande LS, Delorenzo RJ (2004). Evidence that injury-induced changes in hippocampal neuronal calcium dynamics during epileptogenesis cause acquired epilepsy. Proc Natl Acad Sci U S A 101:17522-17527.

Raza M, Pal S, Rafiq A, Delorenzo RJ (2001). Long-term alteration of calcium homeostatic mechanisms in the pilocarpine model of temporal lobe epilepsy. Brain Res 903:1-12.

Ribeiro JA, Sebastiao AM, de MA (2002). Adenosine receptors in the nervous system: pathophysiological implications. Prog Neurobiol 68:377-392.

Righini A, Pierpaoli C, Alger JR, Di Chiro G (1994). Brain parenchyma apparent diffusion coefficient alterations associated with experimental complex partial status epilepticus. Magn Reson Imaging 12:865-871.

Roch C, Leroy C, Nehlig A, Namer IJ (2002a). Magnetic resonance imaging in the study of the lithium-pilocarpine model of temporal lobe epilepsy in adult rats. Epilepsia 43:325-335.

Roch C, Leroy C, Nehlig A, Namer IJ (2002b). Predictive value of cortical injury for the development of temporal lobe epilepsy in 21-day-old rats: an MRI approach using the lithium-pilocarpine model. Epilepsia 43:1129-1136.

Rona S, Rosenow F, Arnold S, Carreno M, Diehl B, Ebner A, Fritsch B, Hamer HM, Holthausen H, Knake S, Kruse B, Noachtar S, Pieper T, Tuxhorn I, Luders HO (2005). A semiological classification of status epilepticus. Epileptic Disord 7:5-12.

Rowe J, Blamire AM, Domingo Z, Moody V, Molyneux A, Byrne J, Cadoux-Hudson T, Radda G (1998). Discrepancies between cerebral perfusion and metabolism after subarachnoid haemorrhage: a magnetic resonance approach. J Neurol Neurosurg Psychiatry 64:98-103.

Rudolph U, Antkowiak B (2004). Molecular and neuronal substrates for general anaesthetics. Nat Rev Neurosci 5:709-720.

Sarkisian MR (2001). Overview of the Current Animal Models for Human Seizure and Epileptic Disorders. Epilepsy Behav 2:201-216.

Sato K, Abe K (2001). Increases in mRNA levels for Talpha1-tubulin in the rat kindling model of epilepsy. Brain Res 904:157-160.

Scharfman HE, Goodman JH, Sollas AL (2000). Granule-like neurons at the hilar/CA3 border after status epilepticus and their synchrony with area CA3 pyramidal cells: functional implications of seizure-induced neurogenesis. J Neurosci 20:6144-6158.

Scotland RS, Madhani M, Chauhan S, Moncada S, Andresen J, Nilsson H, Hobbs AJ, Ahluwalia A (2005). Investigation of vascular responses in endothelial nitric oxide synthase/cyclooxygenase-1 double-knockout mice: key role for endothelium-derived hyperpolarizing factor in the regulation of blood pressure in vivo. Circulation 111:796-803.

Scott RC, Gadian DG, King MD, Chong WK, Cox TC, Neville BG, Connelly A (2002). Magnetic resonance imaging findings within 5 days of status epilepticus in childhood. Brain 125:1951-1959.

Scott RC, King MD, Gadian DG, Neville BG, Connelly A (2003). Hippocampal abnormalities after prolonged febrile convulsion: a longitudinal MRI study. Brain 126:2551-2557.

Scott RC, King MD, Gadian DG, Neville BG, Connelly A (2006). Prolonged febrile seizures are associated with hippocampal vasogenic edema and developmental changes. Epilepsia 47:1493-1498.

Setkowicz Z, Majcher K, Janicka D, Sulek Z, Skorka T, Jasinski A, Janeczko K (2006). Brains with different degrees of dysplasia show different patterns of neurodegenerative changes following pilocarpine-induced seizures. Histologic evidence of tissue damage correlated with MRI data. Neurol Res 28:453-460.

Shih TM, Scremin OU (1992). Cerebral blood flow and metabolism in soman-induced convulsions. Brain Res Bull 28:735-742.

Shorvon S (1994) Status Epilepticus. Cambridge University Press.

Siesjo BK, Wieloch T (1986). Epileptic brain damage: pathophysiology and neurochemical pathology. Adv Neurol 44:813-47.:813-847.

Sims RJ, III, Reinberg D (2006). Histone H3 Lys 4 methylation: caught in a bind? Genes Dev 20:2779-2786.

Sloviter RS (2002). Apoptosis: a guide for the perplexed. Trends Pharmacol Sci 23:19-24.

Sloviter RS (2005). The neurobiology of temporal lobe epilepsy: too much information, not enough knowledge. C R Biol 328:143-153.

Sloviter RS, Zappone CA, Harvey BD, Frotscher M (2006). Kainic acid-induced recurrent mossy fiber innervation of dentate gyrus inhibitory interneurons: possible anatomical substrate of granule cell hyper-inhibition in chronically epileptic rats. J Comp Neurol 20;494:944-960.

Smith PD, McLean KJ, Murphy MA, Turnley AM, Cook MJ (2005). Seizures, not hippocampal neuronal death, provoke neurogenesis in a mouse rapid electrical amygdala kindling model of seizures. Neuroscience 136:405-415.

Sperk G, Furtinger S, Schwarzer C, Pirker S (2004). GABA and its receptors in epilepsy. Adv Exp Med Biol 548:92-103.

Statler KD, Alexander H, Vagni V, Holubkov R, Dixon CE, Clark RS, Jenkins L, Kochanek PM (2006). Isoflurane exerts neuroprotective actions at or near the time of severe traumatic brain injury. Brain Res 1076:216-224.

Tanaka S, Sako K, Tanaka T, Nishihara I, Yonemasu Y (1990). Uncoupling of local blood flow and metabolism in the hippocampal CA3 in kainic acid-induced limbic seizure status. Neuroscience 36:339-348.

Teplan M (2002). Fundamentals of EEG measurement. Measurement Science Review 2:1-11.

Tetich M, Dziedzicka-Wasylewska M, Kusmider M, Kutner A, Leskiewicz M, Jaworska-Feil L, Budziszewska B, Kubera M, Myint AM, Basta-Kaim A, Skowronski M, Lason W (2005). Effects of PRI-2191--a low-calcemic analog of 1,25-dihydroxyvitamin D3 on the seizure-induced changes in brain gene expression and immune system activity in the rat. Brain Res 1039:1-13.

Theodore WH, Porter RJ, Albert P, Kelley K, Bromfield E, Devinsky O, Sato S (1994). The secondarily generalized tonic-clonic seizure: a videotape analysis. Neurology 44:1403-1407.

Thomas DL, Lythgoe MF, Gadian DG, Ordidge RJ (2002). Rapid Simultaneous Mapping of T2 and T2* by Multiple Acquisition of Spin And Gradient Echoes using Interleaved Echo Planar Imaging (MASAGE-IEPI). Neuroimage 15:992-1002.

Thomas DL, Lythgoe MF, Pell GS, Calamante F, Ordidge RJ (2000). The measurement of diffusion and perfusion in biological systems using magnetic resonance imaging. Phys Med Biol 45:R97-R138.

Timofeev I, Steriade M (2004). Neocortical seizures: initiation, development and cessation. Neuroscience 123:299-336.

Tokumitsu T, Mancuso A, Weinstein PR, Weiner MW, Naruse S, Maudsley AA (1997). Metabolic and pathological effects of temporal lobe epilepsy in rat brain detected by proton spectroscopy and imaging. Brain Res 744:57-67.

Traub RD, Contreras D, Whittington MA (2005). Combined experimental/simulation studies of cellular and network mechanisms of epileptogenesis in vitro and in vivo. J Clin Neurophysiol 22:330-342.

Treiman DM (1995). Electroclinical features of status epilepticus. J Clin Neurophysiol 12:343-362.

Trevelyan AJ, Sussillo D, Watson BO, Yuste R (2006). Modular propagation of epileptiform activity: evidence for an inhibitory veto in neocortex. J Neurosci 26:12447-12455.

Trevelyan AJ, Sussillo D, Yuste R (2007). Feedforward inhibition contributes to the control of epileptiform propagation speed. J Neurosci 27:3383-3387.

Tsukita S, Yonemura S (1997). ERM (ezrin/radixin/moesin) family: from cytoskeleton to signal transduction. Curr Opin Cell Biol 9:70-75.

Turrin NP, Rivest S (2004). Innate immune reaction in response to seizures: implications for the neuropathology associated with epilepsy. Neurobiol Dis 16:321-334.

Uchida Y, Ohshima T, Sasaki Y, Suzuki H, Yanai S, Yamashita N, Nakamura F, Takei K, Ihara Y, Mikoshiba K, Kolattukudy P, Honnorat J, Goshima Y (2005). Semaphorin3A signalling is mediated via sequential Cdk5 and GSK3beta phosphorylation of CRMP2: implication of common phosphorylating mechanism underlying axon guidance and Alzheimer's disease. Genes Cells 10:165-179.

Ueda Y, Yokoyama H, Nakajima A, Tokumaru J, Doi T, Mitsuyama Y (2002). Glutamate excess and free radical formation during and following kainic acid-induced status epilepticus. Exp Brain Res 147:219-226.

Urbanska EM, Czuczwar SJ, Kleinrok Z, Turski WA (1998). Excitatory amino acids in epilepsy. Restor Neurol Neurosci 13:25-39.

Ure J, Baudry M, Perassolo M (2006). Metabotropic glutamate receptors and epilepsy. J Neurol Sci 247:1-9.

van der Weerd L, Thomas DL, Thornton JS, Lythgoe MF (2004). MRI of animal models of brain disease. Methods Enzymol 386:149-177.

van Eijsden P, Notenboom RG, Wu O, de Graan PN, van Nieuwenhuizen O, Nicolay K, Braun KP (2004). In vivo (1)H magnetic resonance spectroscopy, T(2)-weighted and diffusion-weighted MRI during lithium-pilocarpine-induced status epilepticus in the rat. Brain Res 1030:11-18.

Vanheel B, Van d, V (2000). EDHF and residual NO: different factors. Cardiovasc Res 46:370-375.

VanLandingham KE, Heinz ER, Cavazos JE, Lewis DV (1998). Magnetic resonance imaging evidence of hippocampal injury after prolonged focal febrile convulsions. Ann Neurol 43:413-426.

Velisek L (2006). Models of Chemically-Induced Acute Seizures. Models of Seizures and Epilepsy. p. 111-126.

Vezzani A (2005). Inflammation and epilepsy. Epilepsy Curr 5:1-6.

Vezzani A, Granata T (2005). Brain inflammation in epilepsy: experimental and clinical evidence. Epilepsia 46:1724-1743.

Viviani B, Bartesaghi S, Gardoni F, Vezzani A, Behrens MM, Bartfai T, Binaglia M, Corsini E, Di Luca M, Galli CL, Marinovich M (2003). Interleukin-1beta enhances NMDA receptor-mediated intracellular calcium increase through activation of the Src family of kinases. J Neurosci 23:8692-8700.

Voutsinos-Porche B, Koning E, Kaplan H, Ferrandon A, Guenounou M, Nehlig A, Motte J (2004). Temporal patterns of the cerebral inflammatory response in the rat lithium-pilocarpine model of temporal lobe epilepsy. Neurobiol Dis 17:385-402.

Wait R, Chiesa G, Parolini C, Miller I, Begum S, Brambilla D, Galluccio L, Ballerio R, Eberini I, Gianazza E (2005). Reference maps of mouse serum acute-phase proteins:

changes with LPS-induced inflammation and apolipoprotein A-I and A-II transgenes. Proteomics 5:4245-4253.

Walker MC, Perry H, Scaravilli F, Patsalos PN, Shorvon SD, Jefferys JG (1999). Halothane as a neuroprotectant during constant stimulation of the perforant path. Epilepsia 40:359-364.

Walker MC, White HS, Sander JW (2002). Disease modification in partial epilepsy. Brain 125:1937-1950.

Wall CJ, Kendall EJ, Obenaus A (2000). Rapid alterations in diffusion-weighted images with anatomic correlates in a rodent model of status epilepticus. AJNR Am J Neuroradiol 21:1841-1852.

Warner DS, McFarlane C, Todd MM, Ludwig P, McAllister AM (1993). Sevoflurane and halothane reduce focal ischemic brain damage in the rat. Possible influence on thermoregulation. Anesthesiology 79:985-992.

Wasterlain CG, Mazarati AM, Naylor D, Niquet J, Liu H, Suchomelova L, Baldwin R, Katsumori H, Shirasaka Y, Shin D, Sankar R (2002). Short-term plasticity of hippocampal neuropeptides and neuronal circuitry in experimental status epilepticus. Epilepsia 43 Suppl 5:20-29.

Waxman EA, Lynch DR (2005). N-methyl-D-aspartate receptor subtypes: multiple roles in excitotoxicity and neurological disease. Neuroscientist 11:37-49.

White HS (2002). Animal models of epileptogenesis. Neurology 59:S7-S14.

Williams PA, Wuarin JP, Dou P, Ferraro DJ, Dudek FE (2002). Reassessment of the effects of cycloheximide on mossy fiber sprouting and epileptogenesis in the pilocarpine model of temporal lobe epilepsy. J Neurophysiol 88:2075-2087.

Wilson CL, Khan SU, Engel J, Jr., Isokawa M, Babb TL, Behnke EJ (1998). Paired pulse suppression and facilitation in human epileptogenic hippocampal formation. Epilepsy Res 31:211-230.

Wilson JV, Reynolds EH (1990). Texts and documents. Translation and analysis of a cuneiform text forming part of a Babylonian treatise on epilepsy. Med Hist 34:185-198.

Wolf OT, Dyakin V, Patel A, Vadasz C, de Leon MJ, McEwen BS, Bulloch K (2002). Volumetric structural magnetic resonance imaging (MRI) of the rat hippocampus following kainic acid (KA) treatment. Brain Res 934:87-96.

Wolfensohn S, Lloyd M (1998) Handbook of laboratory animal management and welfare. Blackwell Publishing.

Woolley CS, Gould E, McEwen BS (1990). Exposure to excess glucocorticoids alters dendritic morphology of adult hippocampal pyramidal neurons. Brain Res 531:225-231.

Wu CL, Huang LT, Liou CW, Wang TJ, Tung YR, Hsu HY, Lai MC (2001). Lithium-pilocarpine-induced status epilepticus in immature rats result in long-term deficits in spatial learning and hippocampal cell loss. Neurosci Lett %19;312:113-117.

Yaari Y, Beck H (2002). "Epileptic neurons" in temporal lobe epilepsy. Brain Pathol 12:234-239.

Yang JW, Czech T, Yamada J, Csaszar E, Baumgartner C, Slavc I, Lubec G (2004). Aberrant cytosolic acyl-CoA thioester hydrolase in hippocampus of patients with mesial temporal lobe epilepsy. Amino Acids 27:269-275.

Yuzlenko O, Kiec-Kononowicz K (2006). Potent adenosine A1 and A2A receptors antagonists: recent developments. Curr Med Chem 13:3609-3625.

Zhao H, Xu H, Xu X, Young D (2007). Predatory stress induces hippocampal cell death by apoptosis in rats. Neurosci Lett 421:115-120.

Zhong J, Petroff OA, Prichard JW, Gore JC (1993). Changes in water diffusion and relaxation properties of rat cerebrum during status epilepticus. Magn Reson Med 30:241-246.

Zhong J, Petroff OA, Prichard JW, Gore JC (1995). Barbiturate-reversible reduction of water diffusion coefficient in flurothyl-induced status epilepticus in rats. Magn Reson Med 33:253-256.